Tailor-made cellulose graft copolymers by controlled radical polymerization techniques

TECHNISCHE UNIVERSITÄT DARMSTADT

Vom Fachbereich Chemie

der Technischen Universität Darmstadt

zur Erlangung des akademischen Grades eines

Doktor-Ingenieurs (Dr.-Ing.)

genehmigte

Dissertation

vorgelegt von

Dipl.-Ing. Marcus Werner Ott

aus Langen

Referent:	Prof. Dr. Markus Biesalski
Korreferent:	Jr. Prof. Dr. Annette Andrieu-Brunsen
Tag der Einreichung:	07. November 2016
Tag der mündlichen Prüfung:	19. Dezember 2016

Darmstadt 2017

D17

Teile dieser Arbeit wurden bereits veröffentlicht oder auf Tagungen präsentiert:

Veröffentlichungen

I. M. Ott, M. Biesalski, *Defined cellulose-polymer hybrid materials by synthesis under homogeneous conditions*, Cellulose materials doctoral students summer conference 2014, PaPSaT, **2014**, Helsinki: Aalto University publication series – ISBN: 978-952-60-5817-7, 2014.

II. M. Ott, M. Biesalski, *Cellulose graft copolymers with mixed grafts by combination of grafting-from and grafting-to techniques*, Cellulose materials doctoral students summer conference **2015**, PaPSaT, 10/2015, Helsinki: Aalto University publication series – ISBN: 978-952-60-4896-5, 2015.

III. M. Ott, M. Graf, H. Herbert, M. Biesalski, *Cellulose-graft-polystyrene bottle-brush copolymers by homogeneous RAFT polymerization of soluble cellulose macro-CTAs and "CTA-shuttled" R-group approach*, Polymer, **2016**, 98: p.505-525.

Vorträge

IV. FPRIC-PaPSaT – Cellulose materials doctoral students summer conference 2014 (Ebernburg, Germany)

V. American Chemical Society Division of Cellulose and Renewable Materials, 249th ACS National Meeting, Denver, CO, 2015.

VI. FPRIC-PaPSaT – Cellulose materials doctoral students summer conference 2015 (Autrans, France)

Danksagung

Zuerst möchte ich Prof. Dr. Markus Biesalski für seine Unterstützung, spannende fachliche Diskussionen, den wissenschaftlichen Freiraum für eigene Ideen und die Möglichkeit an einem spannenden Thema forschen zu dürfen, danken. Des Weiteren möchte ich Jr. Prof. Dr. Annette Andrieu-Brunsen für die freundliche Übernahme des Korreferates danken, sowie den Fachprüfern Prof. Dr. Markus Busch und Prof. Dr. Gerd Buntkowsky für die schnelle und unkomplizierte Zusage.

Ein weiterer großer Dank gilt Michael Graf, Sonja Wendenburg, Sebastian von Gradowski und Julian Ott für die Korrektur meiner Arbeit.

Im Allgemeinen möchte ich den Kollegen aus dem Arbeitskreis Biesalski für die Gegenseitige Unterstützung und das angenehme Umfeld danken. Insbesondere möchte ich Jennifer Dietz, Andreas Geissler, Alexander Böhm, Heike Herbert, Simon Trosien, Conny Golla und Vanessa Schmidt sowie Dr. Tobias Meckel und Marcel Krause danken. Mein ganz besonderer Dank gilt meinen „Zuhörladies“ Melanie Gattermeier und Martina Ewald. Ferner möchte ich meinen Praktikanten Dominik Ohlig, Kevin Vogel, Max Nau und Roberto Dipalo für ihren Fleiß und ihren Forschungseifer danken. Mein weiterer Dank gilt den Menschen, die mich während meines Studiums und meiner Promotion begleitet und unterstützt haben; meine guten Freunde Simon Kokolakis, Christian Pfeiffer, Henning Curtze, meine Studienkollegen Sascha Knauer, Steffi Luckhart, Ali Shayegi und Carina Vogel, desweiteren Dr.-Ing. Hans-Jürgen Bär, Prof. Dr.-Ing. Alfons Drochner und Prof. Dr. Jürgen Brickmann.

Meinen Eltern Johanna und Werner Ott, meinen Brüdern Julian und Alexander, meiner Oma Sara meiner Tante Inge und meinem Onkel Michael sowie meinem Taufpaten Thomas Könitzer möchte ich für die stetige Unterstützung und Begleitung auf meinem Lebensweg danken, denn erst ihr habt mich zu demjenigen gemacht, der ich bin.

Table of Contents

Abbreviations

^{13}C-NMR	carbon nuclear magnetic resonance
^{1}H-NMR	proton nuclear magnetic resonance
AGU	anhydroglucose unit
AIBN	Azobis(isobutyronitrile)
ARGET ATRP	Activator ReGenerated by Electron Transfer
ATRP	atom transfer radical polymerization
BiB	bromo isobutyl
BiBB	bromo isobutyryl bromide
BpB	2-bromopropionyl bromide
CDI	*N,N*-carbonyldiimidazole
CPPA	4-cyano-4-(phenylcarbonothioylthio) pentanoic acid
CRP	controlled radical polymerization
DCC	dicyclohexyl carbodiimide
DCU	dicyclohexylurea
DMAc	*N,N*-dimethylacetamide
DMAP	*N,N*-dimethylaminopyridine
DMF	*N,N*-dimethylformamide
DMSO	dimethyl sulfoxide
EMIMC	1-ethyl-3-methyl-imidazolium chloride
kDa	kilo dalton [kg/mol]
LAM	less activated monomer
MA	methylacrylate
MAM	more activated monomer
MCC	microcrystalline cellulose
NiPAM	*N*-isopropylacrylamide
NMP	nitroxide mediated polymerization
PDI	poly dispersity index
PDMAA	polydimethylacrylamide
PEG	poly(ethylene glycol)
PHA	polyhydroxyalkanoate
PLA	poly lactic acid
PMMA	poly methylmethacrylate
RAFT	reversible addition fragmentation chain transfer
SEC	size exclusion chromatography
$SOCl_2$	thionyl chloride
TBAF	tetra butyl ammonium fluride
TEA	triethylamine
TES	tetraethyl silane
TFA	trifluoroacetic acid
Trt-Cl	triphenylmethyl chloride

1. Introduction

Biopolymers are defined as macromolecules produced in a natural way by biosynthesis in living organisms. Like synthetic polymers they consist of covalently bond monomer units to form large molecules. Depending on the chemical nature of the repeating units, they can be classified in groups such as polypeptides, polynucleotides or polysaccharides. Biopolymers have manifold vital functions in living species such as signal transmission, transport, digestion, energy storage, or carrier of genetic information [1]. A prominent example is the polysaccharide cellulose, which typically has a structural function as part of lignified cell walls such as wood fibers. Furthermore it can be found in seed fibers (cotton) bast, grasses, algae (*Valonica ventricosa*) and bacteria (*Acetobacter xylinum*) [2]. Cellulose from different origin is globally available in large quantities with an estimated annual natural production of $1.5 \bullet 10^{12}$ t per year, which makes it an almost inexhaustible source of raw material for ecological and biocompatible products [3].

Due to the high availability of cellulose-containing materials it has been used for more than two thousand years for different purposes like as energy source and as building material (wood), as material for textiles (cotton) or for paper (papyrus, hemp or linen fibers). Alternatively, cellulose fibers can be isolated from the biomaterial (e.g. wood) by delignification processes such as chemical pulping. These fibers are used for the production of tissue, paper and cardboard or become chemically modified to yield cellulose derivatives.

Cellulose has been first isolated and characterized with elemental analysis by Anselme Payen in 1838 [4]. For this, different plant tissues were treated with acids and bases followed by extraction of the soluble residues with different solvents to yield pure cellulose fibers. During the following decades chemical modification of cellulose molecules lead to the development of new materials featuring versatile properties. These cellulose derivatives are referred to as semi-synthetic or bio-based polymers since they are synthetic materials based on a renewable and natural material. The first synthesized cellulose derivative was cellulose nitrate, which was used as an explosive (smokeless gun powder), as thermoplastic material (celluloid) or for clothing (artificial silk). Other cellulose derivatives like cellulose acetate, ethyl cellulose, hydroxyl ethyl cellulose or carboxymethyl cellulose are produced in industrial scale today. These cellulose derivatives play an important role in our modern lifestyle and are used for coatings, laminates, optical films or sorption media, as well as for property-determining additives in building materials, pharmaceuticals, foodstuffs, and cosmetics [5]. However, with the up rise of the petrochemical industry and the plastics industry in the late 1940s, synthetic polymers emerged as a strong competition to cellulose-based plastics for many applications due to cheap oil prices and the high versatility. But with growing awareness of limited oil resources and environmental pollution the scope of research has been increasingly put on the development of ecological friendly alternatives to well established synthetic polymers. Various strategies have been pursued during the

last decades including the implementation of biodegradability into synthetic polymers [6], synthetic polymers derived from renewable biomass sources (e.g. PLA, PHA, starch plastics) [7] and biopolymers produced by biotechnology [8]. But not only ecological issues have driven the focus of research more towards the development of new cellulose-based materials. Composites containing biopolymers are lightweight, robust and can exhibit excellent mechanical properties, for instance in cellulose fiber-reinforced plastics [9], adhesive/ compatibilizer of wood/polymer blends [10], or nano-composites consisting of synthetic polymers and biopolymers [11].

As an alternative to the chemical transformation or physical blending of fibers with synthetic polymer, the covalent attachment of synthetic polymers (e.g. polystyrene, PMMA) to biopolymers (e.g. chitin, chitosan, starch, cyclodextrine or cellulose) produces bio-based graft copolymers with different chemical and physical properties [12]. These materials are far more versatile, since they are not limited in the improvement of mechanical properties as they may combine the advantages of both synthetic and biopolymers. Thus they may be used as high-performance material. In this context, cellulose is most frequently applied due to its high availability, cheap price, biocompatibility as well as mechanical and heat resistance. The synthesis of hybrid materials consisting of cellulose and synthetic polymers and their properties and applications has already been subject of various review articles [13-16].

More advanced and defined hybrid materials may be obtained by application of modern polymerization techniques. Especially the development of controlled radical polymerization (CRP) techniques during the last two decades the field of cellulose-based hybrid materials evolved towards tailor-made, well-defined materials. Some review articles focus exclusively on the design and properties of these new materials [17-20]. Here, we have to distinguish between homogenous and heterogeneous reaction conditions and between the application of native cellulose and pre-processed organo-soluble cellulose derivatives as starting materials. In this context, reversible addition fragmentation chain transfer (RAFT) and atom transfer radical polymerization (ATRP) are most frequently applied methods in homogenous and in heterogeneous reaction media. Today the ATRP technique has been adapted successfully on cellulose materials and many synthetic protocols are described in literature [21-25]. However, concerning RAFT polymerization on cellulose less work has been published. Especially the kinetics of the RAFT polymerization process on cellulose and optimal homogenous reaction conditions have not been investigated in detail. There are only few publications in this field such as the report from Barner-Kowollik et al. [26] or Lucia et al. [27]. These publications show a proof of concept of homogenous polymer grafting from cellulose via the RAFT technique but lack detailed analytic and mechanistic investigation. Potentially the RAFT process using cellulose as a starting material should offer a high potential for the synthesis of well-defined, tailor-made, cellulose-based hybrid materials. Therefore the purpose of this thesis is to investigate synthetic procedures and kinetic aspects which will finally serve as a “toolbox” for the design of cellulose graft copolymers.

The following sections will provide the reader with fundamental knowledge of cellulose chemistry, CRP techniques and with state-of-the-art methods regarding the synthesis of well-defined hybrid materials consisting of cellulose and synthetic polymers.

1.1. Cellulose chemistry

The chapters 1.1.1-.1.1.3 have been adapted and summarized from the book "Comprehensive Cellulose Chemistry" by D. Klemm et al. [28]. Passages from different origin are marked with the corresponding source.

Structure and properties of cellulose

Cellulose is a linear syndiotactic homopolymer composed of D-anhydroglucopyranose units (AGU) linked by ß-(1,4)-glycosidic bonds, as displayed in **Figure 1**. Each cellulose chain bears a non-reducing and a reducing end group, where the latter may be used for the selective modification of the aldehyde functionality.

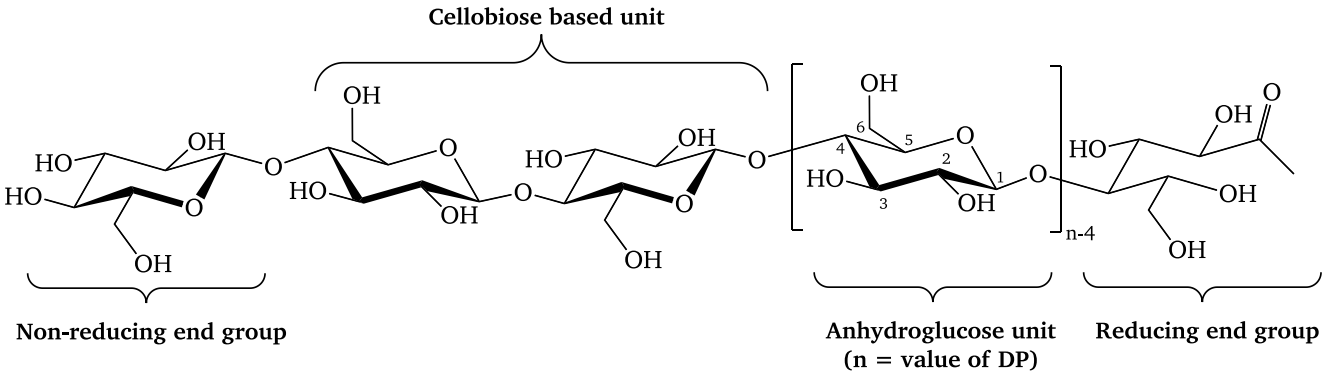

Figure 1. Illustration of the chemical structure of cellulose. Image redrawn with permission from [28].

Cellulose can also be considered as an isotatic polymer of the monomer cellobiose, consisting of two AGUs with each second unit rotated by 180° along the molecular axis, as shown in **Figure 2**. The molecular size of cellulose molecules is expressed by the average degree of polymerization, thus the number of repeating units. The DP can vary from small to huge molecules and depends on the source and the treatment of the natural material. Cellulose molecules from cotton fibers have DP values of up to 12,000 whereas micro crystalline cellulose (obtained by acidic hydrolysis) typically features DP values of about 100-200.

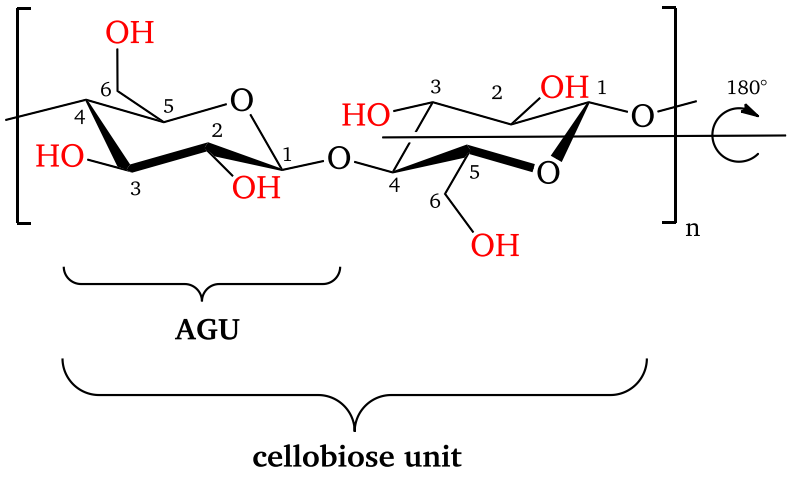

Figure 2. Chemical structure of cellobiose as a repeating unit of the polymer "cellulose". The cellobiose repeating unit is a dimer, consisting of two anhydroglucose units, where every second unit is rotated by 180°. Each anhydroglucose repeating unit carries hydroxyl groups at the carbon positions C-2, C-3 and C-6.

Each AGU has three hydroxyl groups on the C-2, C-3 and C-6 position. The functions can interact with other hydroxyl groups from the same molecule or with hydroxyl groups from another cellulose molecule, leading to intra- and intermolecular hydrogen bonding, as displayed schematically in **Figure 3**. These interactions have a significant effect on the properties and the physical structure of cellulose, such as the strong tendency of cellulose molecules to aggregate in ordered, semi-crystalline regions. These aggregates result in the formation of super-molecular structures, i.e. cotton fibers, as shown in **Figure 4**. These fibers show various valuable properties such as biocompatibility, low thermal and electrical conductivity or mechanical and thermal resistance; on the other hand they exhibit limited elastic properties and no thermoplastic behavior. Furthermore, cellulose shows high hydrophilicity and lacks of antimicrobial properties, which makes it unsuitable for certain applications [17]. Cellulose fibers are swellable but insoluble in water and common organic solvents and only few substances are able to disintegrate cellulose fibers to yield dissolved cellulose molecules. Swellability and solubility of the fibers has an important impact on the chemical accessibility of the functional groups of cellulose. Therefore the reaction conditions have to be adapted to the targeted product, as we will discuss in the next section.

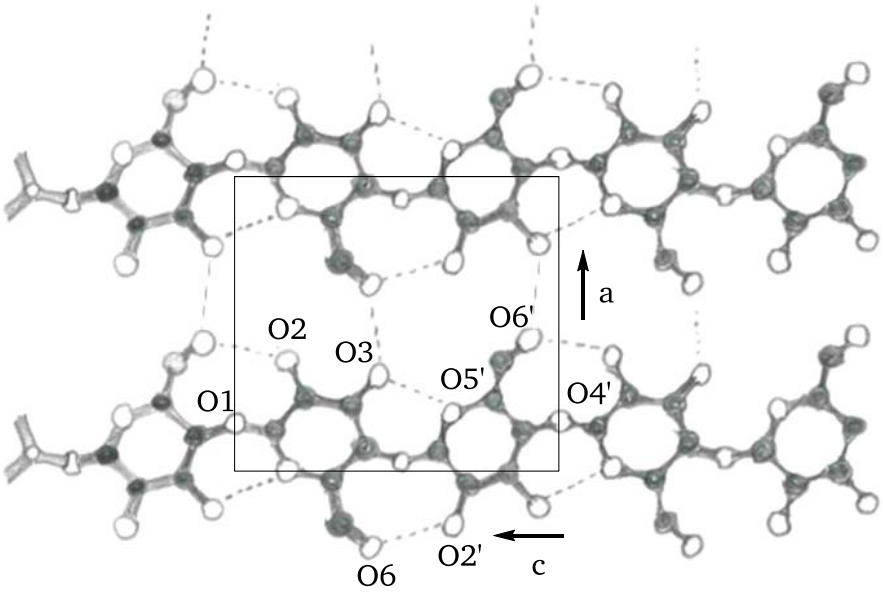

Figure 3. Schematic illustration of intramolecular and intermolecular hydrogen bonding in native cellulose, which has a cellulose I structure. Image redrawn from [28].

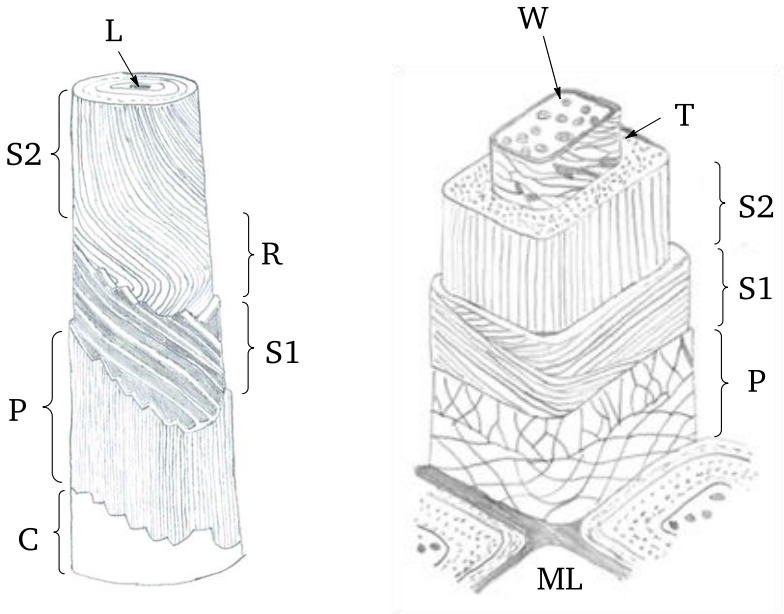

Figure 4. Schematic image of cotton fiber (left) and a wood fiber (right) structure. Denotation: C (cuticle), L-lumen, ML-middle lamella, P-primary wall, R-reversal of the fibril spiral. S1-secondary wall (winding layer), S2- secondary wall (main body), T-tertiary wall, W-wart layer. Image redrawn from [28].

Modification of cellulose

In order to expand the area of potential applications for cellulose-based polymeric materials, the chemical and physical properties have to be versatile. For this, the cellulose chains can be modified by chemical reactions of the hydroxyl functions, e.g. by esterification of etherification, grafting, cross linking or oxidation of cellulose [5]. The chemical modification of cellulose, analysis and application of cellulose derivatives are part of the field of cellulose chemistry. Today, various cellulosic products such as carboxymethyl cellulose [29-31] or cellulose acetate [32-34] can be found many products of daily life. However, with advent of CRP techniques in polymer synthesis, graft copolymers based on cellulose have been in focus of research during the last two decades. New routes for the modification of cellulose with synthetic polymers allow the design of new functional and sustainable materials [17].

Cellulose in homogeneous and heterogeneous reaction media: influence on the accessibility for chemical modification

As mentioned before, native cellulose derived from plants exhibits a fibrillar structure on the macroscopic level featuring both amorphous and crystalline regions. The fiber cell walls show inhomogenities of the structure including pores, capillaries, void and interstices [28]. This is why the total surface area (“inner surface”) of a cellulose fiber is much larger than its geometric outer surface, assuming a cylinder. The choice of the solvent for cellulose derivatization has a major impact on the extent of chemical modification. If a solvent is capable of breaking hydrogen bonds between the cellulose fibrils it enhances the availability of cellulose hydroxyl functionalities. This swelling effect is quantified by the “liquid retention value”, which basically represents the percentage of weight increase of a dry cellulose sample after immersion in a liquid. If more liquid is retained, the fibers are more swollen, thus more cellulose functionalities are available for chemical modification [28].

If solid cellulose fibers are dispersed in the beginning of a chemical modification and the latter occurs mostly or at the beginning at the interface between fiber and fluid, the reaction is referred as “heterogeneous”. If the cellulosic product remains solid over the whole process one can define the reaction as surface modification. With the right choice of solvent and reactants it is also possible to conduct a heterogeneous reaction which leads to soluble cellulosic products. For example, various industrial processes for the synthesis of cellulose derivatives (e.g. Viscose process, methyl cellulose) use sodium hydroxide solution as reaction media and swelling agent. Heterogeneous reactions are the simplest way of cellulose modification. However, heterogeneous reaction conditions have several limitations regarding the control of the degree of substitution and typically show an inhomogeneous distribution of functional groups along the biomacromolecules. If a better control is desired homogeneous reaction conditions are required. In order to conduct a reaction in homogeneous media, dissolution of the cellulose polymer has to be performed prior to the chemical modification.

Dissolution systems for homogeneous cellulose modification

Dissolution of cellulose cannot be performed in organic solvents which are typically used in organic chemistry. The process requires special mixtures which are capable of breaking the intra- and intermolecular hydrogen bonds that connect the individual cellulose chains. This topic is of high significance in the field of cellulose chemistry, thus various articles, reviews and books feature the evolution of dissolution systems for homogeneous cellulose modification [35-39]. A brief summary of cellulose dissolution systems is presented in the following section:

Derivatizing solvents and soluble transient intermediates: A solvent/reactant mixture which transforms the cellulose into a well soluble transient intermediate is called a derivatizing solvent. Due to the limited chemical stability of the substituents, the intermediate moieties can be exchanged in-situ with other functional groups in order to synthesize the final product. If necessary, soluble cellulose transient intermediates (e.g. cellulose nitrite, trimethyl silyl cellulose), can be produced in a separate step, isolated and then further modified in a different organic solvent. Prominent examples of intermediates and derivatizing solvent systems are nitrates (*DMF*/N_2O_4), acetals (DMSO/paraformaldehyde) or silylethers (DMF/trimethylsilylchloride). Further subsequent homogeneous reactions include oxidation, alkylation, acetylation or sulfation of the cellulose intermediates [35].

Aqueous, protic solvents: Aqueous systems which contain transition metal complexes (Cu, Ni, Zn,…) combined with amine or ammonium ligands are also suitable for cellulose dissolution. In this case the dissolution process results from deprotonation and complexation of the hydroxyl functionalities of the cellulose. This class of solvents was used for cellulose regeneration (production of fibers and dialysis membranes), for investigation of the macromolecular structure of cellulose (Hermann Staudinger, Nobel prize 1953) as well as for chemical modification [35].

Non-aqueous, non-derivatizing solvents: Certain ionic liquids like 1-ethyl-3-methyl-imidazolium chloride (EMIMCl) can dissolve cellulose. Viscosity is controlled by the cellulose concentration and dilution with low viscous, polar organic solvents like DMF. In literature, ionic liquids are presented as “green” solvents, however they are expensive and difficult regarding recycling/purification [35].

Polar organic solvent + salt: The most frequently applied system in the field of homogenous cellulose chemistry is *N,N*-Dimethylacetamide/LiCl. Since its development by McCormick in 1979 it has been utilized for analysis of cellulose and for the synthesis of a wide variety of cellulose derivatives [35]. The interactions of the DMAc/LiCl system with cellulose are still under investigation, but proposed interactions are illustrated in **Figure 5**. The cleavage of the cellulose hydrogen bonds is

provided by interaction of the hydroxyl function of cellulose with the lithium and chloride ions as well as the solvent. The DMAc/LiCl system exhibits several convenient properties for cellulose modification: Only negligible degradation of the cellulose polymer is observed, the solvent shows inert behavior for most chemical reactions and is also thermally stable. The only major drawback is that the dissolution process requires thermal or chemical activation, which is tedious when prepared in lab-scale. Nonetheless, due to its versatility, we consider DMAc/LiCl as a suitable solvent system for this work.

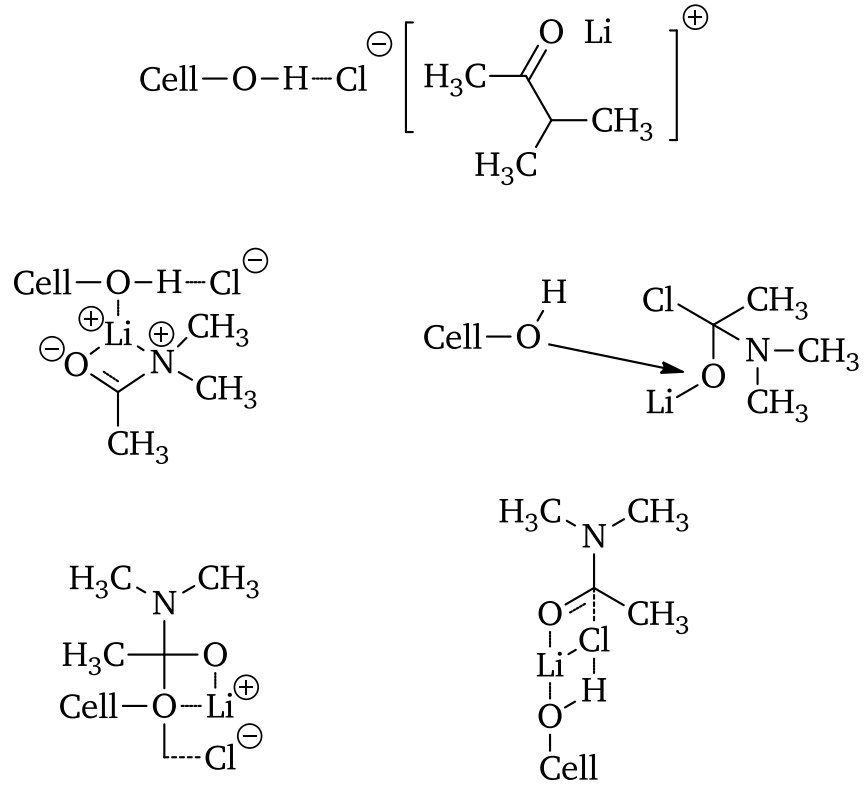

Figure 5. Illustration of the interactions of DMAc/LiCl with cellulose which break cellulose hydrogen bonding. Image redrawn from [39].

1.2. Methods for the synthesis of cellulose graft copolymers

In general, a graft copolymer consists of a long linear molecule, referred to as the polymer backbone, which features polymer branches, so called grafts, that are attached onto the linear structure (as shown in **Scheme 1**). Resulting structures are described as comb polymers or as brush polymers, depending on the density and the length of the polymer grafts.

Having polymer grafts attached onto a substrate, one can consider the structure as brush polymer when the average distance D between two grafts is less than radius of gyration R_G of each individual graft, hence $D \leq R_G$, otherwise the structure is considered a comb. Three different strategies may be pursued in order to obtain these polymeric architectures, as described in the following section.

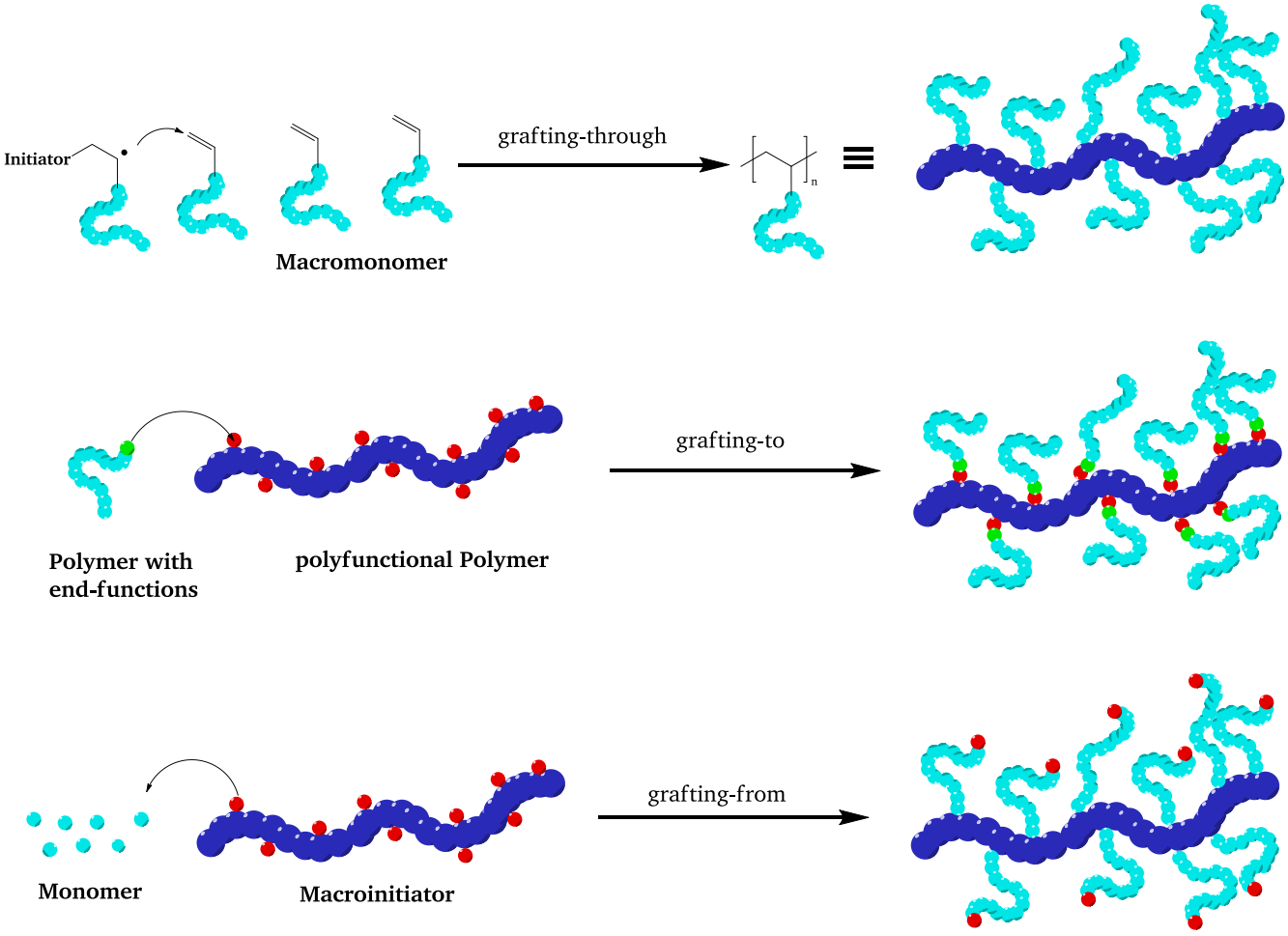

Scheme 1. Synthetic strategies for the synthesis of graft copolymers.

Grafting-through: The formation of bottlebrush structures via the grafting-through method is performed by (co)polymerization of a macro monomer, containing typically a polymerizable group at the end of each molecule, and another (typically small) monomer. In case of synthetic end-functionalized macro monomers, well defined bottlebrush and comb structures can be synthesized in a controlled fashion [40]. However, limited overall graft length and low reaction rates are observed due to steric hindrance during the polymerization process.

When grafting-through is applied on cellulose, typically vinyl monomers are immobilized on the cellulose macromolecule, leading to a poly-functionalized macro monomer (as shown in **Figure 6**). In the subsequent step a copolymerization with small monomer is conducted. This technique usually offers poor control over graft density, graft length and molar mass distribution but is simple to conduct. This is why it has been one of the first techniques applied in order to generate cellulose based graft copolymers [41, 42].

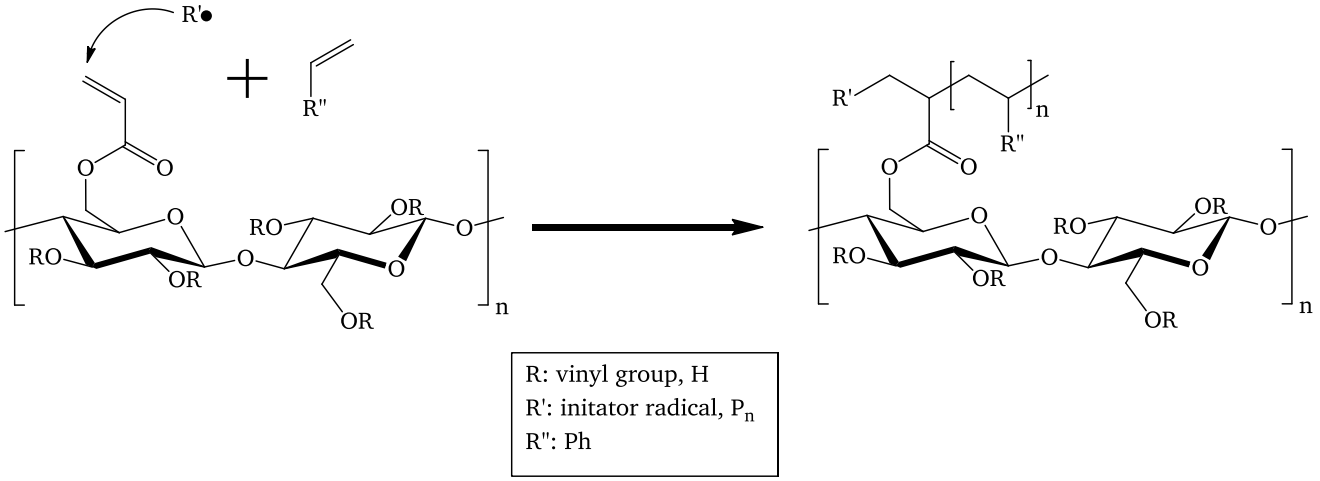

Figure 6. Illustration of grafting-through polymerization using vinyl functionalized cellulose and small monomer.

Grafting-to: This method uses preformed polymers with a functional end group for the modification of a polymeric backbone. In case of cellulose graft copolymers, polymer grafts can be synthesized by living polymerization or by CRP with subsequent modification of the polymeric end group into a reactive species with the ability to attach covalently onto the hydroxyl sites of the cellulose molecule, typically via esterification and etherification reactions. By modification of the cellulose with other functional groups like azide moieties other types of covalent attachment can be obtained, e.g. copper(I)-catalyzed azide-alkyne-cycloaddition, as shown by Hansson [43]. The advantage of the grafting-to method is the variety of the polymer grafts that can be attached onto the backbone, as long as suitable end functionalities are chosen. On the other hand, the major drawback is the limited amount of polymer grafts that can be attached due to steric hindrance [43].

Grafting-from: For this method the polymerization is initiated on the polymer backbone and polymer chains grow from the backbone molecule by addition of monomer. Grafting-from is the most frequently used grafting technique and has been successfully performed utilizing various polymerization techniques including living polymerization, CRP, radical polymerization and ring opening polymerization. In case of graft copolymers based on cellulose and vinyl monomers, early approaches date back to the early 1950s. In the past they were often based on free radical polymerization on solid cellulose fibers. Radicals were generated by diazotation of the cellulose fibers, by chain transfer reactions, redox reactions and photochemical initiation or by radiation. These rather simple methods for graft copolymerization from cellulose have been subject of a review article by Rajani et al. [44]. All these early strategies showed limited control of the grafting process itself, but resulted in significant changes of the properties of the modified cellulosic products. The strategies for polymer grafting from cellulose have been on focus of various reviews and books [16, 17, 45]. The next section will look at CRP techniques on cellulose in a grafting-from approach, because they have been most relevant for this work.

1.3. Controlled radical polymerization (CRP) techniques

The features of the CRP techniques including their advantages and limitations have been summarized by Matyjaszewski and Müller [46]. Until today a large number of CRP techniques have been developed, most of them based on one of the three well-established CRP techniques NMP, ATRP and RAFT. The oldest CRP technique, NMP, shows low reaction rates and is not suitable for methacrylates, the choice of solvents is limited to organic systems, end-functionalization is difficult and moderators must be used in stoichometric amounts. Both ATRP and RAFT techniques are newer and more versatile methods; they are variable in the choice of monomers, solvent, reaction temperature and allow simple functionalization of the chain ends. However, ATRP typically features slow reaction rates due to its deactivation equilibrium and obtained polymers are limited in the maximum degree of polymerization due to ß-H abstraction as side reaction. Furthermore, the transition metal catalyst has to be removed completely, especially when biomedical applications are targeted. On the other hand, RAFT polymerizations may not be suitable for alkaline polymerization conditions such as the polymerization of primary and secondary amine containing monomers. Furthermore, thio-containing end-groups may be considered difficult due to color and smell; therefore these groups have to be eventually removed by chemical conversion. It can be concluded, that none of the prominent CPR techniques is superior to the other systems in all aspects, therefore the choice of the techniques rather depends on the requirements of the target structure and its properties. Also it should be noted that with the advent of these techniques some individual intrinsic limitations have been overcome by the development of these systems. For example ATRP techniques are very sensitive against oxygen and are

limited in the synthesis of large polymers, but sensitivity could be lowered and also a significant increase in the DP of polymers could be managed by evolving the ATRP technique, using reduction agent such a ascorbic acid “ARGET ATRP” [47].

Cellulose graft copolymers by CRP techniques

Most of the relevant publications concerning CRP technique on polysaccharides have been presented in review articles during the last few years [17, 18, 20]. Today, the design of cellulose graft copolymers synthesized by CPR techniques via a grafting-from approach is clearly dominated by application of ATRP [20]. Many publications in the field of well-defined cellulose graft copolymers via CRP techniques leave open questions, because experimental results concerning graft ratio, initiation efficiency and graft length deviate from the expected (calculated) values [48]. Note, the terms “graft ratio” (relative mass of polymer grafts to the mass of the backbone) and “initiation efficiency” (percentage of active CRP functionalities) are explained in detail in chapter 3.3.2.
In this context it should be noted that in 2011 Raus et al. [49] published a comparative study, where they investigated the influence of reaction parameters on the resulting polymer grafts. Using 2-bromoisobutyro-functionalized cellulose derivative without sacrificial initiator, the authors were able to estimate the relative amount of active initiator with respect to the total amount of immobilized initiator, the so-called initiation efficiency. For this, they determined the average molar masses of the polymer grafts with SEC and compared the data with the calculated average molar mass (**Table 1**). With this approach the authors could show that well-defined, densely packed cellulose graft copolymers were obtained by optimization of the reaction conditions. As summarized, initiation efficiency values of up to 100 % indicate a well-controlled polymerization reaction, where termination reactions play an insignificant role.

Table 1. Analytical data of graft copolymerization experiments using a grafting-from approach via ATRP with styrene as model monomer. Reaction conditions: 100 °C, solvent: DMSO. Initiation efficiencies between 90 % and 100 % indicate excellent control over the polymerization process. Reprinted with permission from [49].

Entry	DS[a]	[M]/[I]/[Cu(I)]/[Cu(II)]/[PMDETA]	Conversion (%)	M_n (grafts) Theor.[b]	M_n (grafts) SEC[c]	M_w/M_n	Initiation Efficiency (%)
1	0.11	863/1/1/0.5/1	13	11,400	11,000	1.38	100
2	0.11	1726/1/1/0.5/1	11	19,000	21,200	1.28	90
3	0.52	806/1/1/0.5/1	12	9,700	12,200	1.35	80
4	0.52	1207/1/1/0.5/1	13	15,900	16,500	1.36	96
5	0.52	1207/1/1/0.5/1	21	26,900	27,200	1.24	99
6[d]	1.04	665/1/1/0.5/1.5	16	11,300	11,200	1.18	100
7	1.04	1140/1/1/0.5/1	13	14,900	15,700	1.42	95
8	1.04	1140/1/1/0.5/1	19	22,100	24,100	1.32	92

[a] Degree of substitution of the macroinitiator (number of initiation groups per one anhydroglucose unit).
[b] Theoretical M_n estimated from the monomer conversion and DS of the macroinitiator.
[c] M_n of released polystyrene grafts measured by SEC.
[d] Experiment was carried out in DMAc.

Tizotti et al investigated and analyzed the publications in this field within a review article [18]. This analysis clearly shows that the number of publications concerning synthesis of hybrid materials using carbohydrate backbones such as cellulose and RAFT polymerization is significantly smaller than the amount of publications concerning carbohydrate backbones and ATRP mediated polymerization (**Figure 7**).

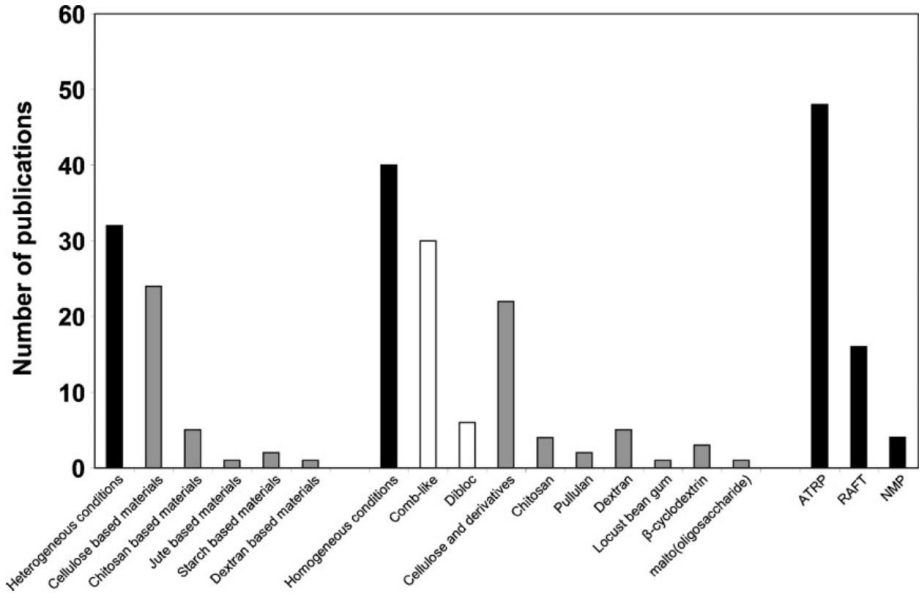

Figure 7. Analysis of the number of publications concerning CRP techniques on polysaccharides until the year 2010. Image reprinted with permission from [18].

When the focus is put on RAFT polymerization on cellulose, the publications known to the author typically focus on the design of cellulose-based hybrid materials by use of functional, “smart” polymer grafts or focus on the application of cellulose graft copolymers as new materials. However, most of the relevant literature in this field does not investigate the control and optimization of RAFT polymerization process from cellulose or from any other cellulosic material. Furthermore it should be

noted, that in all publications the amount of polymer grafts on the backbone was reported much lower then what would be expected when multiplying the number of active sites on the backbone with the average molar mass of the polymer grafts. In none of the author known sources the initiation efficiency reached 10 %, meaning more than 90 % of the immobilized functionalities remain inactive during the polymerization process, indicating significant difficulties in the process. Not much work, which investigates mechanistic and kinetic aspects in this field, has been presented yet, although this should help to understand the origin of these difficulties.

Motivation: RAFT polymerization on cellulose

As discussed in chapter 3.2.1, a RAFT agent has a R-group and a Z-group, defined as the fragmenting and the non-fragmenting group. Thus, when a RAFT agent is immobilized onto a substrate such as cellulose, it can be attached by both, the R-group and the Z-group respectively. For this, some functionality on the RAFT agent for binding onto the hydroxyl moieties on the cellulose have to be provided, typically a carboxylic function for esterification. Depending on the binding site of the RAFT agent on the substrate, the graft copolymerization takes place under a distinct reaction mechanism. This is illustrated in **Scheme 2**, where a RAFT agent is attached on cellulose with its R-site, leading to a graft copolymerization via a so-called “R-group approach”. In this case the graft copolymerization on cellulose is initiated by a reversible chain transfer, where a propagating polymer chain adds to the dithioester functionality, which is bound to the cellulose. The reaction expels the RAFT agent from the cellulose, leaving a radical located at the cellulose. Then graft copolymerization starts by monomer addition. Ideally, the polymerization process proceeds in an equilibrium state where reversible chain transfer ensures an equal rate of polymer growth from all CTA functionalities (shown on the bottom). Finally, the polymerization ends when propagating chains are terminated.

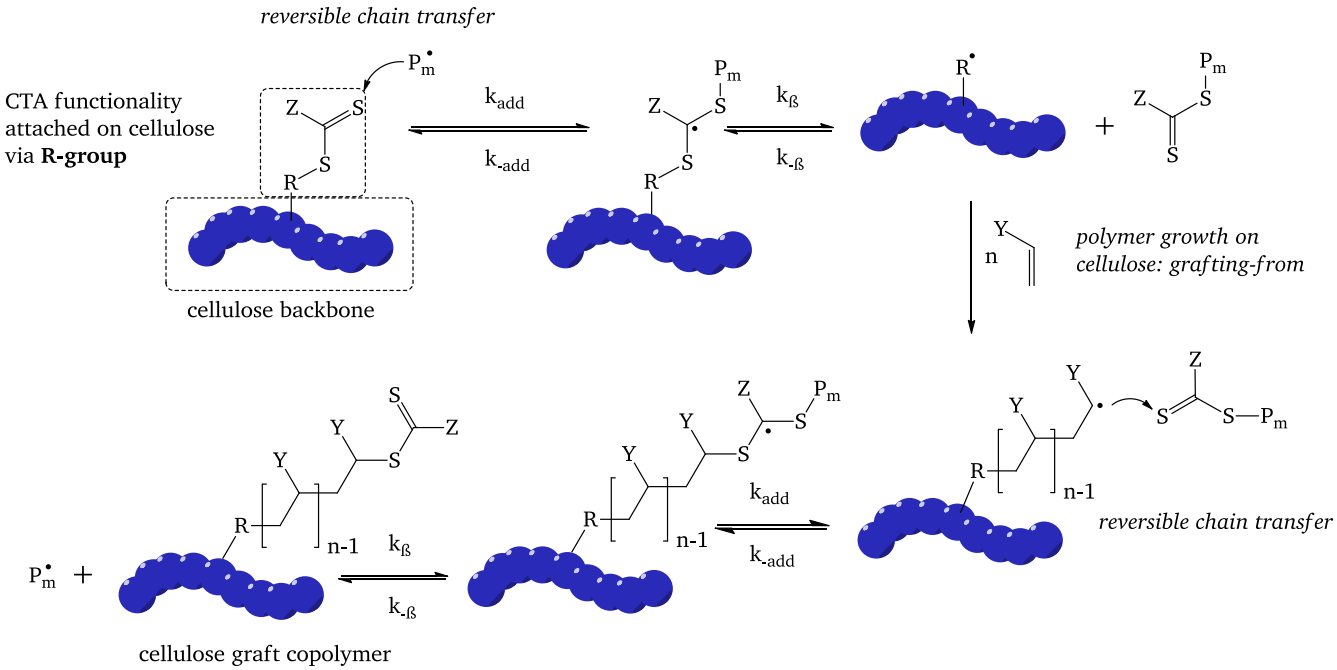

Scheme 2. Illustration of the synthesis of cellulose graft copolymers via RAFT polymerization from cellulose macro-CTA via R-group approach.

Alternatively to the R-site the RAFT agent may also be immobilized by its stabilizing Z-group. Stenzel et al. have presented first RAFT agents attached on the organo-soluble cellulose derivative HPC, using carboxyl functionalized RAFT agent and standard esterification protocols [50]. A brief schematic image, shown in **Scheme 3**, illustrates the very different nature of the polymer grafting process, when the RAFT agent is attached on the cellulose with its Z-group. In this case, no radicals are formed on the cellulose backbone and chain propagation does not occur at the cellulose backbone but only on growing linear homopolymer-derived radicals. This is why polymer grafts are only obtained when propagating homopolymer chains attach to the thiocarbonyl moiety, which is bound to the cellulose. Therefore the polymerization mechanism via the Z-group is a grafting-onto method, thus including features and limitations of grafting-onto, as explained in chapter 1.2. The properties of both R- and Z-group approach are summarized in **Table 2**.

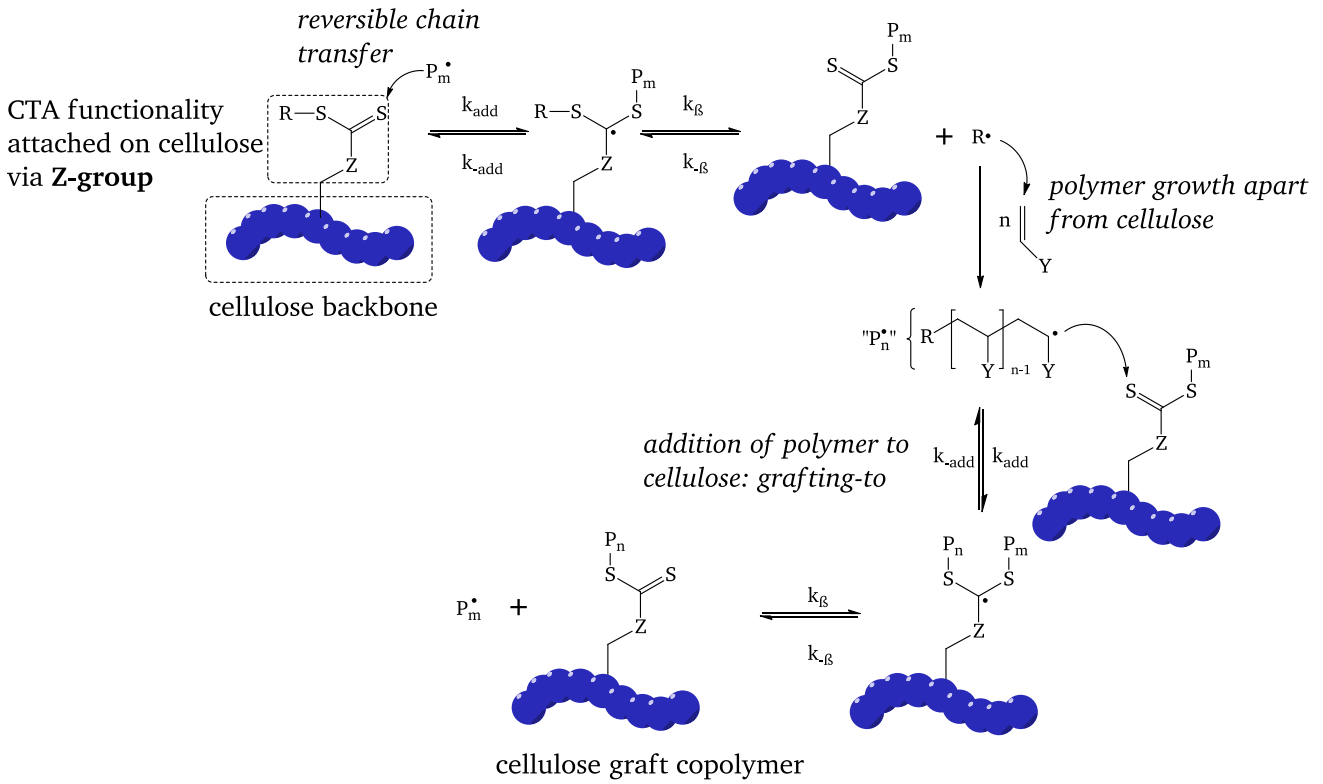

Scheme 3. Illustration of the synthesis of cellulose graft copolymers via RAFT polymerization from cellulose macro-CTA via Z-group approach.

Table 2. Features of R- and Z-group approach.

R-group approach	Z-group approach
End group modification of polymer grafts	No end group modification
No shielding effect at high conversions	Assumed shielding effect even at low conversions
Low restrictions of molecular weight for polymer grafts	Threshold of molecular weight of polymer grafts; lack of variability in chain length
Potentially higher dispersity of polymer grafts	Very narrow dispersity of polymer grafts throughout the whole process
Strong linkage between graft and cellulose	Weak thiocarbonyl linkage between grafts and cellulose
High local radical concentration	Low radical concentration of cellulose
Increased radical-radical termination	Dead chains to not attach to the cellulose, thus no dead polymer grafts

As can be inferred from **Table 2** the R-group approach offers many desirable features for the grafting process, but also inhibits some significant limitations originated by the high local radical concentration, leading to dead chains and increased dispersity of the polymer grafts. This intrinsic property of the R-group approach is the main reason why most publications in this field use the Z-group approach.

A more advanced R-group approach, the so-called “CTA-shuttled R-group approach” has recently been investigated by Zheng et al [51]. The authors aimed for the synthesis of well-defined polymer bottlebrush structures based on fully synthetic material. For this, the author used poly (4-vinylbenzyl chloride) as polymer backbone, which was then modified by transfer of the chlorine moiety into a CTA, resulting in the synthesis of a macro-CTA. Subsequent graft copolymerization of macro-CTA with styrene revealed high dispersity and thus indicated limited control over the RAFT polymerization. This phenomenon was attributed to an “entrapment” of active free radicals attached to the polymer backbone, originated by an insufficient addition-fragmentation equilibration. To overcome this problem, another graft copolymerization of macro-CTA with styrene was performed according to the “CTA shuttled” approach, where free, “sacrificial” was added. Here, significant improvement of the control of the process was gained, leading to narrow disperse graft copolymers.

The differences between conventional R-group approach and CTA-shuttled R-group approach as proposed is shown in **Scheme 4**; in the conventional process (shown in the middle) active radicals can only transfer intermolecular or intramolecular to neighboring CTA-groups. Considering that the CTA groups are restricted in their movement because of their attachment to a macromolecule a sufficient equilibration cannot be provided. In the other case (bottom), added free “sacrificial” CTA significantly supports the equilibration of all propagating chains, thus leading to a well-controlled process. It should be noted that the use of “sacrificial” CTA forms linear polymer as a side product, thus using this method an additional purification step is needed, which may be tedious when the solubility behavior of graft copolymer and linear homopolymer is similar. The CTA-shuttled R-group approach on a cellulosic material has been first performed by Perrier et al. [52]. For this, hydroxypropyl cellulose was modified with RAFT agent on its R-site via esterification, followed by a graft copolymerization of NiPAM. The authors observed no polymer grafts on the cellulosic material, but only linear homopolymer. Polymer grafting was only successful when additional RAFT agent was added. However this observation was not further investigated or discussed by the authors in more detail.

Although the CTA-shuttled R-group approach has shown a high potential for the synthesis of cellulose based graft copolymers it has not been well analyzed yet. Various questions remain: Which ratio of macro-CTA and free CTA delivers good control without producing too much linear polymer as waste material? Do propagating polymer grafts inhibit the same kinetics like free propagating polymer chains? Do all CTA groups on macro-CTA participate in the polymerization or do other effects like steric hindrance still play a significant role? Does the approach still work at high monomer conversions and high degrees of polymerization, respectively?

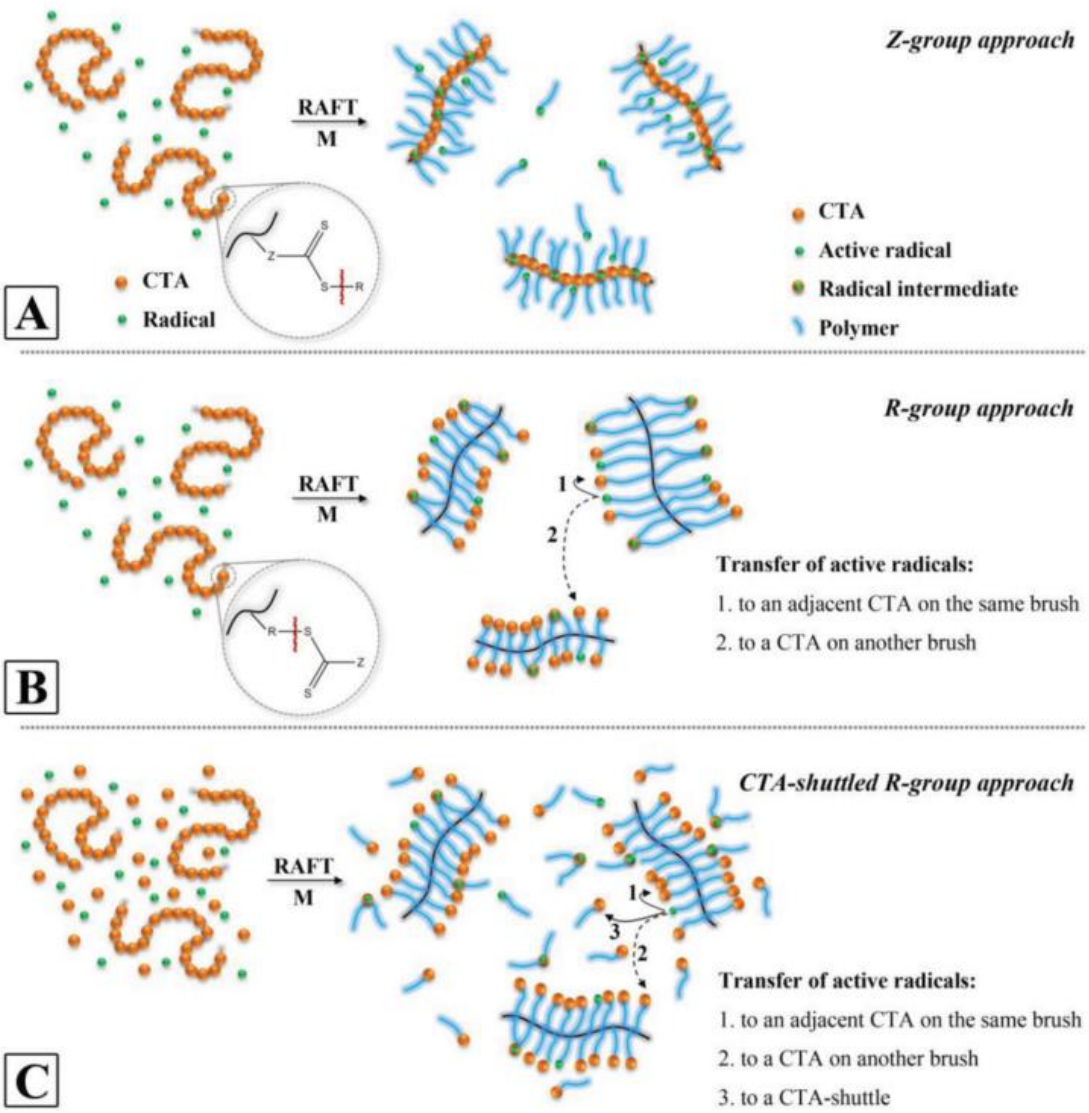

Scheme 4. Proposed mechanisms of the Z-group approach (A), the R-group approach (B) and the "CTA-shuttled" R-group approach (C) to synthesize CPBs. The red wavy line indicates where monomer will be inserted. Reprinted with permission from [51].

It is concluded, that much progress in this field of research may be achieved by identifying the limitations of previous graft copolymerization protocols and analyzing their origin. Then, new synthetic strategies and suitable analysis procedures have to be developed and investigated in order to overcome these limitations. The main goal of this work is to improve the grafting-from process via RAFT polymerization on cellulosic materials. Furthermore, the synthesis of more complex cellulose-based polymer architectures such as cellulose with mixed grafts is targeted in order to enhance the versatility of tailor-made, cellulose-based hybrid materials.

2. Goals and Strategy

2.1. Goals

GOAL 1: The scope of the work presented here is to develop and validate new synthetic protocols for the well-controlled synthesis of cellulose based graft copolymers by the application of RAFT on cellulose material. Here, the term "well-controlled" refers to the control of graft density (i.e. the average distance d between two individual grafts), the number average molar mass of polymer grafts (M_n) and their corresponding molar mass distribution, as illustrated in **Scheme 5**.

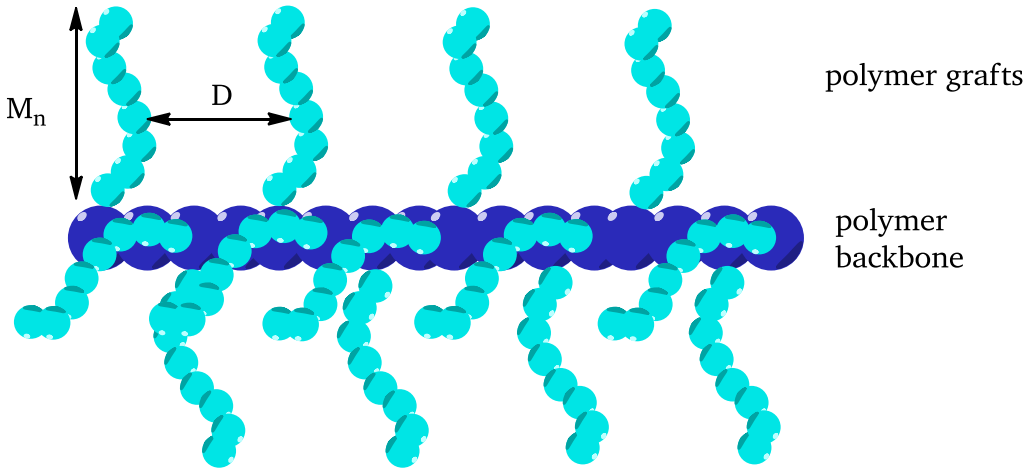

Scheme 5. Illustration of a cellulose based, semi-synthetic graft copolymer. This polymer architecture is based on a cellulose backbone (blue) with synthetic polymer grafts tethered to the backbone (bright blue). Control of the average distance D between two individual grafts and the control of the M_n of the polymer grafts is targeted.

In order to characterize and understand the controlled modification of cellulose with synthetic polymer grafts, we have to establish a system, where the polymerization can be conducted in a homogenous fashion in a variety of typical solvents for RAFT polymerization. In order to analyze the graft copolymers, reliable, quantitative and convenient analytical methods are needed, which typically include dissolved products. Finally, we like to develop synthetic protocols for cellulose macro-CTAs which act as a "toolbox" for tailor-made cellulose-based graft copolymers, thus cellulose macro-CTAs should be suitable for the polymerization of a variety of typical monomers, such as acrylates, methacrylates and styrene.

Main targets of goal 1 are summarized as follows:

- Synthesis and characterization of well-defined cellulose macro-CTAs
- Identification of reaction conditions for graft copolymerization
- Development of characterization protocols for graft copolymers
- Optimization of graft copolymerization parameters with respect to M_n, Đ, graft-ratio and graft efficiency

GOAL 2: The synthesis of more complex polymer architectures has to be investigated in order to enhance versatility and potential applications as "smart" materials. Examples for these more complex architectures include synthetic mixed grafts or block copolymer grafts. Theoretically, these structures can be obtained by any combination of two different grafting techniques or by combination of two different polymerization techniques using the same grafting mechanism. However not all polymerization and grafting techniques are compatible and for this reason the synthetic strategy has to be chosen carefully.

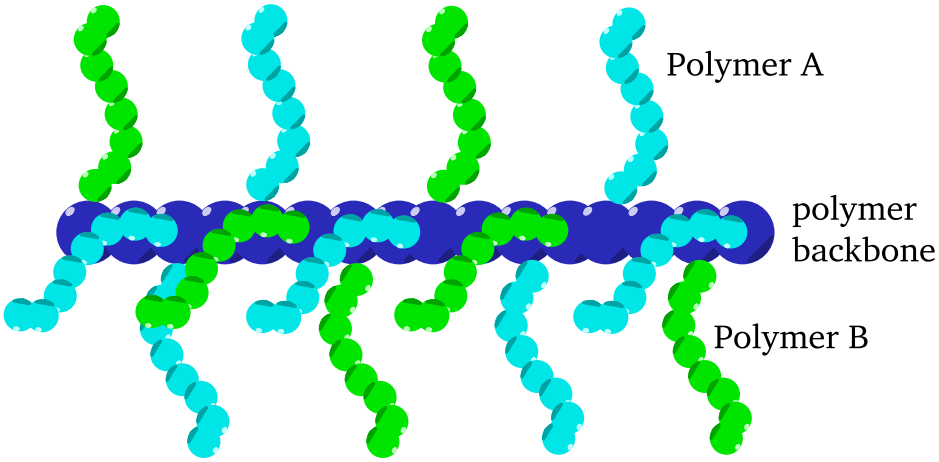

Figure 8. Illustration of a cellulose based, mixed graft copolymer. Here, the cellulose backbone (blue) is connected with two different types of synthetic polymer, denoted as polymer A and polymer B.

Main targets of goal 2 are summarized as follows:

- Validation of existing synthetic procedures for polymer grafting, followed by the implementation into a novel synthesis protocol regarding mixed grafts on a cellulose backbone
- Synthesis, characterization and comparison of the resulting mixed graft copolymers originated from different strategies for mixed graft synthesis
- First optimizations of the synthetic strategies (reduction of required steps, identification and overcoming limitations) as basis for future projects

2.2. Strategy

Two different strategies were identified for goal 1, as presented in **Figure 9**.

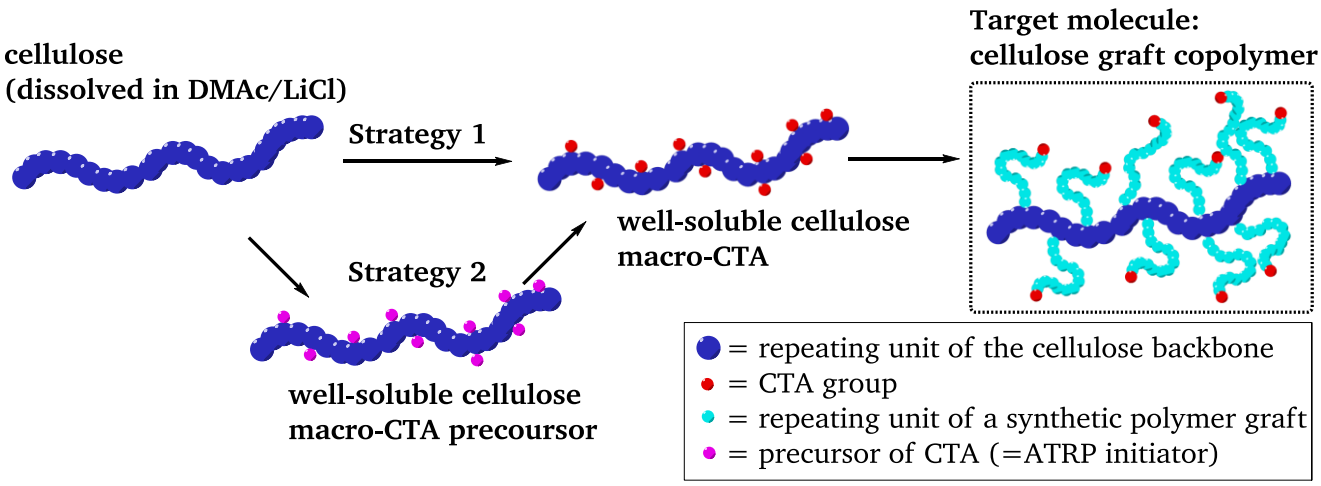

Figure 9. Illustration of the two different synthesis strategies used for the design of well-defined cellulose graft copolymers.

Strategy 1: Synthesis is based on the derivatization of cellulose with a two-step one pot reaction. For this, a carboxyl terminated CTA will be attached to the hydroxyl functions of the cellulose via esterification in the first step. The carboxyl group on the CTA has to be activated for the esterification process, therefore activation agents such as carbodiimides, thionylchloride and *N,N'*-carbonyldiimidazole will be tested for the compatibility with the CTA. The activated CTA should efficiently attach to the cellulose and side reactions such as the decomposition of the CTA should be avoided. In the subsequent step, the complete esterification of remaining hydroxyl functions using propionic acid anhydride will be performed in order to gain organo-soluble cellulose macro-CTAs, which allows the determination of DS values and CTA content via ^{1}H-NMR. A set of graft copolymerization- and homopolymerization experiments using the monomer *N,N*-dimethyl acryl amide (DMAA) or styrene will be conducted in order to identify optimal reaction conditions for the grafting process. Analysis of the polymer content on the cellulose backbone ("graft ratio") will be performed by ^{1}H-NMR or SEC.

Strategy 2: As an alternative route to strategy 1, all intermediate cellulose derivatives can be isolated and characterized. This strategy aims to generate CTA-functionalities on the cellulose in a step-wise fashion with a CTA precursor (bromine-functionalized ester) attached to the cellulose, followed by complete esterification with propionic acid anhydride and the partial transformation of bromine groups into trithiocarbonate groups.

The performance of these trithiocarbonate-based cellulose macro-CTAs will be tested and optimized by a set of graft copolymerization- and homo-polymerization experiments. Various parameters (monomer concentration, CTA/initiator ratio…) will be modified with focus on high amounts of polymer grafts (graft ratio), a low dispersity of the polymer grafts and a high percentage of CTA groups participating in the RAFT polymerization (initiation efficiency). For this, homopolymer, graft copolymer and cleaved polymer grafts will be analyzed quantitatively using ^{1}H-NMR and SEC.

Strategies for GOAL 2:

Two different strategies were identified for goal 2, as presented in **Figure 10**.

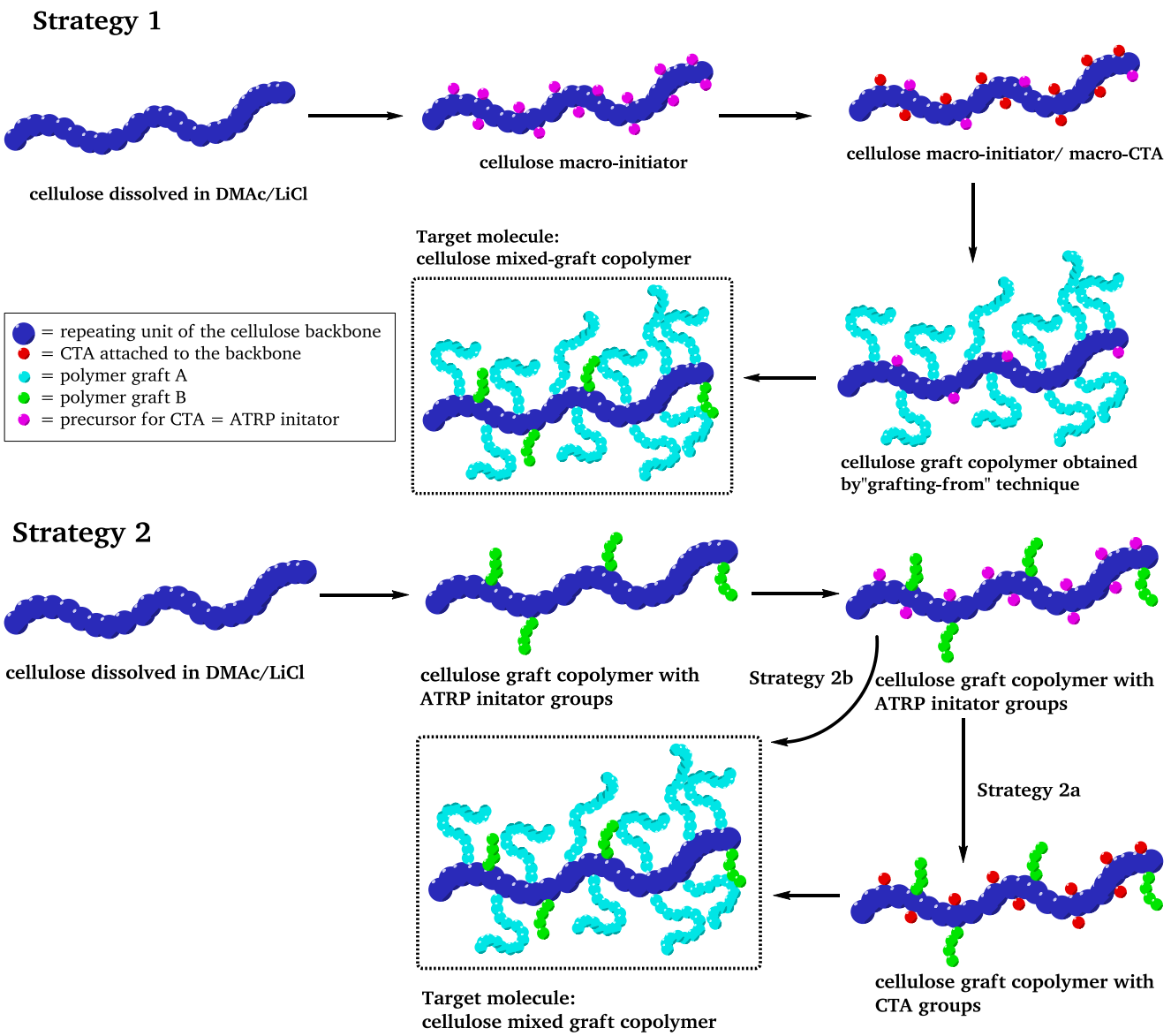

Figure 10. Synthesis strategies planned for the design of cellulose mixed graft copolymers. Strategy 1 is based on the combination of a grafting-to with a grafting-from approach, while strategy 2 is based on two individual grafting-from approaches by combination of RAFT and ATRP.

Strategy 1: First, we immobilize bromine functionalities on the cellulose, which serve as ATRP initiator and as RAFT precursor respectively. A subsequent propionylation reaction of residual hydroxyl moieties ensures good solubility of the cellulose derivative in organic solvents. The bromine functionalities are then partially transferred into CTA groups. The mixed grafts will be obtained by a sequence of a RAFT polymerization, followed by an ATRP, both via a grafting-from approach. Quantitative analysis of the polymers and the intermediates will be performed using ^{1}H-NMR and SEC.

Strategy 2: This strategy includes a combination of two different grafting methods. For this, preformed, end-functionalized polymer grafts are attached via a grafting-to method. This technique may or may not include regioselective modification of the cellulose with polymer grafts. Further modification follows with the attachment of CTA-groups or bromine functionalities, which then allow RAFT polymerization (strategy 2a) or polymer grafting via ATRP (strategy 2b), both in a "grafting-from" approach.

3. Methods

3.1. Methods for the homogenous modification of cellulose

Various solvent systems for cellulose have been developed and investigated during the last decades, however only few of them showed good compatibility for controlled esterification reactions. A good summary of cellulose solvent systems has been provided by Liebert et al. [35]. A cellulose solvent should not just show good properties in the dissolution behavior of cellulose; it should also show low toxicity, low volatility and should be inert with respect to the reaction conditions. The solvent should be versatile for various reaction conditions, easy to handle and cellulosic products should not precipitate during the reaction process in order to ensure homogenous modification. Having all these factors in mind, only a limited number of promising candidates remain. In the following section we explain briefly the process of finding a suitable reaction media.

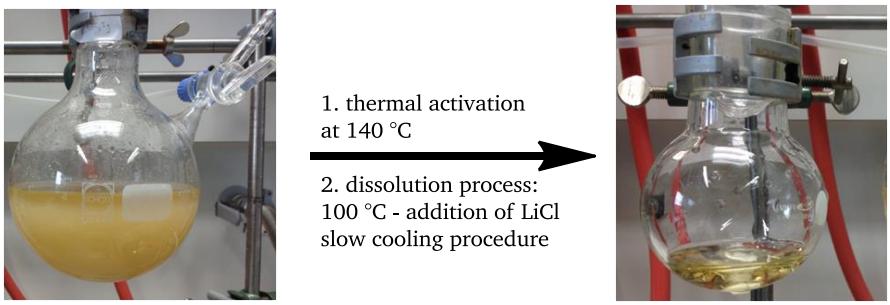

Figure 11. Typical photographs of a cellulose dispersion before and after dissolution. Reaction conditions include thermal activation of the cellulose fibers, followed by a slow dissolution process, and are outlined in detail in the experimental section.

In order to ensure homogenous distribution along the cellulose chains, substituted celluloses must not precipitate during the reaction. Hence, the solvent must dissolve the non-substituted as well as the substituted cellulose. Furthermore, modification is planned as esterification reaction of stoichiometric amounts of carboxylic acids with the hydroxyl moieties of the cellulose. This excludes for instance all aqueous solvent systems or systems that include water like the recently introduced, efficient and easy-to-handle solvent system DMSO/TBAF*3H_2O. Having this system, every equivalent of TBAF bears three

equivalents of crystal water which may hydrolyze reagents like active esters, anhydrides or acid chlorides. Thus excess of activated carboxylic acids would be necessary for the modification of cellulose. Furthermore strong and effective chlorination agents like thionyl chloride or oxalyl chloride may not be used, due to their reactivity with DMSO (Swern oxidation).

Thus, we define the following requirements on the solvent system:

- good control of DS and homogenous distribution of substituents along the cellulose backbone
- solvent should be versatile regarding the acylating agent: esterification via acyl anhydrides, acyl chlorides or activation in-situ with agents like DCC, DIC, EDC, CDI, $SOCl_2$, should be possible.
- high esterification efficiency, compatibility with the reactants

The solvent system *N,N*-dimethylacetaamide/lithium chloride was first used for esterification of cellulose by McCormick [53]. Among all solvent systems for cellulose, this one has become the most widely applied for various reasons, such as dissolution of cellulose under mild conditions, reducing polymer degradation by depolymerization. Also, this system shows good compatibility for many reactants and is versatile regarding the reaction conditions. Nonetheless working with DMAc/LiCl requires some level of caution due to its high hygroscopic behavior, thus inert and water free storage and reaction conditions are needed. Furthermore the dissolution process may turn out tedious, because the cellulose polymer does not always dissolve spontaneously but needs eventually several heating/cooling cycles until complete dissolution is obtained. In order to improve the dissolution process of cellulose in DMAc/LiCl, several activation methods have been established like thermal or chemical activation of the polymer prior to the dissolution process [54, 55]. In both cases, thermal and chemical activation the cellulose fibers undergo a swelling process which facilitates the dissolution.
It should be noted that cellulose derivatives synthesized under homogenous reaction conditions do not always show good solubility in organic solvents. This effect can be observed if low DS values are obtained or if the substituents are incompatible with organic media. This is why in this work the system DMAc/LiCl is used, but the synthetic protocols are modified in order to gain fully substituted cellulose derivatives during polymer analogous reactions. This procedure ensures a high solubility of cellulosic products in a variety of organic solvents, which facilitates subsequent derivatization steps in homogenous fashion.

Alternatively, soluble cellulose intermediates may be used for chemical modification as long as functional groups on the cellulose backbone are available. For this, one has to distinguish between temporary and permanent substituents in cellulose intermediates. If a permanent substituent is attached to the cellulose, only remaining functionalities may be modified, which may lead to

limitations regarding the extent of modification. For example 2.5-acetyl cellulose has 0.5 remaining hydroxyl functions per AGU on average, thus this value cannot be exceeded when another chemical group is introduced.

If a temporary substituent is introduced, one may gain organo-soluble intermediates such as silylethers, acetals, chloro acetates and formates of cellulose. Depending on the reaction conditions, these substituents can be exchanged e.g. via trans-esterification or remaining hydroxyl groups on the cellulose are substituted. In the latter case, after cleavage of the temporary substituent, an inverse pattern of substitution on the cellulose is obtained [35]. This synthetic concept may be also used for the design of regioselective substituted cellulose derivatives [56]. For this, regioselective introduction of protecting groups onto the cellulose hydroxyl functionalities has to be performed. After isolation of the cellulose intermediate, further modification can be performed homogenously after dissolving the macromolecules in a suitable solvent (typically DMF or DMSO), which then transforms all remaining hydroxyl functionalities. Then, the protecting groups may be removed (as exemplarily shown in **Figure 12**), followed by another substation process of the recovered hydroxyl moieties.

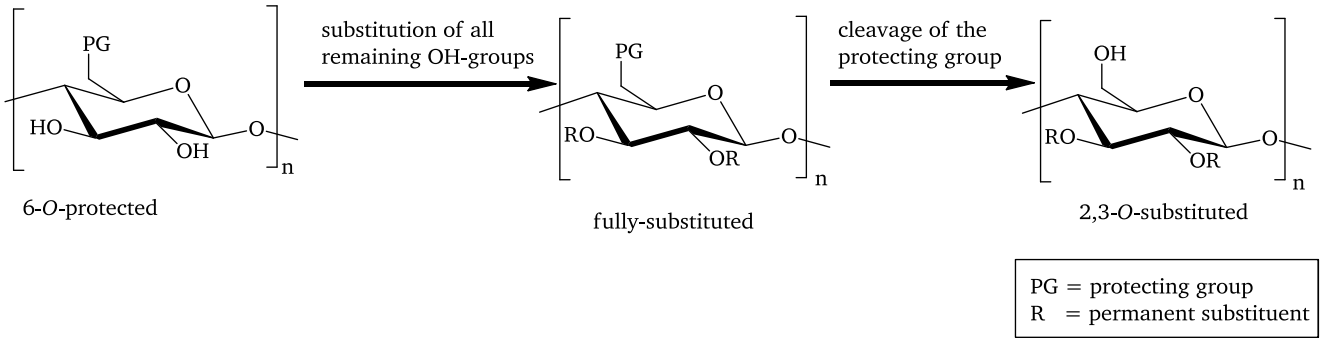

Figure 12. Exemplary synthetic pathway for the synthesis of a 2,3-*O*-substituted cellulose.

Commonly used protecting groups in cellulose chemistry are the triphenyl methane “trityl” group which blocks the 6-O position and the thexyldimethylsilyl “TDMS” group which blocks the 2-*O* and 6-*O* position of the anhydroglucose repeating units [57, 58]. The strategy of regioselective protection will be used for the synthesis of cellulose macro-CTA as described in chapter 9.3.

3.2. CRP techniques and RAFT polymerization

In the following subchapter properties and features of RAFT polymerization will be explained. For this purpose, it is necessary to consider the mechanistic aspects of the radical polymerization first. In free radical polymerization the polymer chains are formed in a chain-growth reaction of monomer started by radicals, which are formed by a radical source such as a thermal initiator. The propagation of each polymer chain proceeds by monomer addition of the radical site until chain termination occurs. In the free radical polymerization process individual chains are continuously formed, propagated and terminated until depletion of monomer or radicals. The obtained molar mass of the polymer chains depends on the monomer concentration and thus changes with reaction time and conversion, respectively. Furthermore the molecular weight distribution depends on statistic factors like propagation and termination probability, leading to broad distribution, as expressed by dispersity. Free radical polymerizations can be easily performed with a low demand on the purity of the reactants. On the other hand this technique does not allow the synthesis of well-defined polymer architectures. With the advent of so-called “controlled radical polymerization” techniques such as ATRP, NMR and RAFT, radical polymerizations with features of living polymerizations (e.g. low dispersity, polymer architectures and control of molecular weight) could be conducted, as explained in the next section.

3.2.1. Mechanism of RAFT polymerization

In order to conduct a controlled radical polymerization, irreversible termination reactions of propagating chains have to be suppressed. In case of RAFT polymerization this is achieved by addition of a chain transfer agent (CTA) to the reaction mixture. The CTA can interact with radicals in a reversible fashion, basically leading to the transfer of a radical from a propagating chain to a dormant chain. A simplified mechanism of RAFT polymerization, including a reversible chain transfer, has been suggested by Chiefari et al. [59] and is shown in **Scheme 6**.

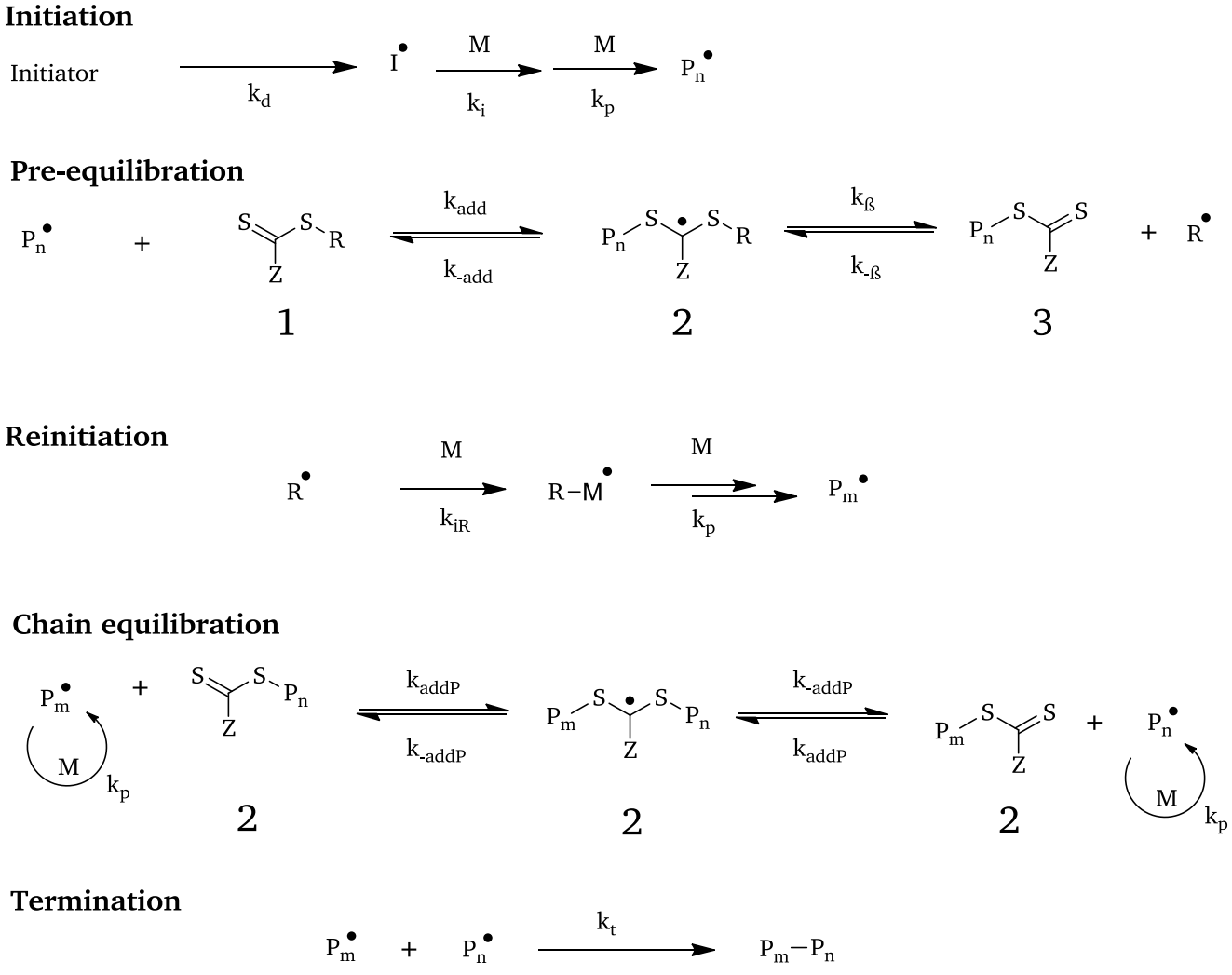

Scheme 6. Schematic illustration of the reaction mechanism of a RAFT polymerization. Scheme redrawn from [60].

The process is started and maintained by a radical source, typically by decomposition of an azo- or peroxy initiator. During the initiation phase the free radicals add vinyl monomers until the process is interrupted by reaction with a chain transfer agent **1**. Addition of the propagating polymer chain to the CTA leads to the formation of an intermediate **2**, which than may fragment into dithioester **3** and a

radical bearing the R-group of the RAFT agent, which then acts as a new active site for monomer addition (re-initiation). The process of the pre-equilibration and re-initiation ends when all RAFT agents have expelled their R-group and bear a polymer chain instead. In this phase, a rapid chain equilibration provides that all polymer chains have the same probability of propagation. Chain propagation ends when radicals get irreversibly terminated. In order to conduct a well-controlled radical polymerization via RAFT various aspects have to be taken into consideration:

Choice of the RAFT agent

As shown in **Figure 13**, all RAFT agents have a thiocarbonylthio structure in common. The performance of RAFT polymerization is based on the choice of the substituents R and Z. The stabilizing group Z controls the addition rate k_{add} of radicals on the C=S double bond (**1** and **3**), as well as the fragmentation rate of the radical intermediate **2**. Depending on the chemical nature of Z, the RAFT agents can be classified as dithioesters, trithiocarbonates, xanthates and thiocarbamates.

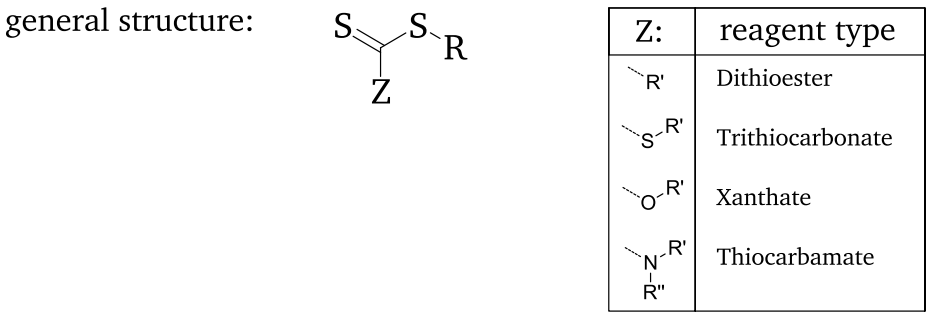

Figure 13. General structure of a RAFT agent and classification of RAFT agents.

The other substituent is called R-group, which is the fragmenting site during the reversible chain transfer process of intermediate **2** shown in **Scheme 6**. Generally, the S-R single bond should be weak and the expelled radical R• must be able to reinitiate polymerization. Guidelines for the choice of the substituents R and Z, which have been presented by Graeme et al. [61] are shown in **Figure 14**. Here it can be seen that phenyl moieties and thio-moieties as Z-groups are well suitable for the polymerization of various monomers like MMA, MA and styrene. Suitable R-groups consist typically out of a secondary or tertiary carbon atom with adjacent stabilizing groups like phenyl or nitrile groups. As mentioned before, intermediate **2** can expel the radical R• or the radical P_n•. Thus a good leaving group R must have the ability to fragment preferably. This is required because a short initialization phase is needed in order to ensure the equal chain propagation of all RAFT agents.

The relative ability of a moiety R to fragment is described by the partition coefficient φ and is defined as follows [60]:

$$\varphi = \frac{k_ß}{k_{-add} + k_ß} \quad (1)$$

Here $k_β$ is the rate constant of the transformation of intermediate 2 into species 3, whereas k_{-add} is the rate constant of the transformation of intermediate 2 into species 1, as shown in **Scheme 6**. Thus the R-group should have a partition coefficient of $\varphi > 0.5$ in order to prepare polymers with narrow dispersity.

The overall activity of a RAFT agent is defined by the chain transfer coefficient C_{tr} [60]:

$$C_{tr} = \frac{k_{tr}}{k_p} \quad (2)$$

With:

$$k_{tr} = \varphi * k_{add} \quad (3)$$

Here k_{tr} is the transfer rate constant, which is defined by the partition coefficient φ and the rate constant k_{add} of the transformation of 1 into intermediate 2, as shown in **Scheme 6**. For a well-controlled RAFT polymerization, C_{tr} should be at least 10, most active RAFT agents have C_{tr} values above 100 [60]. In order to obtain high C_{tr}, a high k_{tr} (thus a high addition rate k_{add} and a high partition coefficientφ) are required. These factors directly depend on the R- and the Z-group, therefore the right choice of the RAFT agent is crucial for the control of the polymerization. Furthermore, it can be seen in **Figure 14** that the chemical identity of the Z-moiety has an important influence on the control depending on the chemical nature of the monomer. For instance a Z-moiety is a phenyl group delivers good control over the polymerization process of MMA, MA and styrene, but is not well suitable for the polymerization of VAc. The phenomenon is explained by the electronic situation of the vinyl function. If a electron rich atom is adjacent to the carbon-carbon double bond, the monomer is classified as lesser activated monomer (LAM). Typical examples for LAMs are vinyl amide and vinyl esters such as *N*-vinylpyrollidon and vinyl acetate. On the other hand, so-called “more activated monomers” (MAMs) have neighboring functions such as carbonyl groups or an aromatic ring, like acrylates, acryl amide or styrene, respectively.

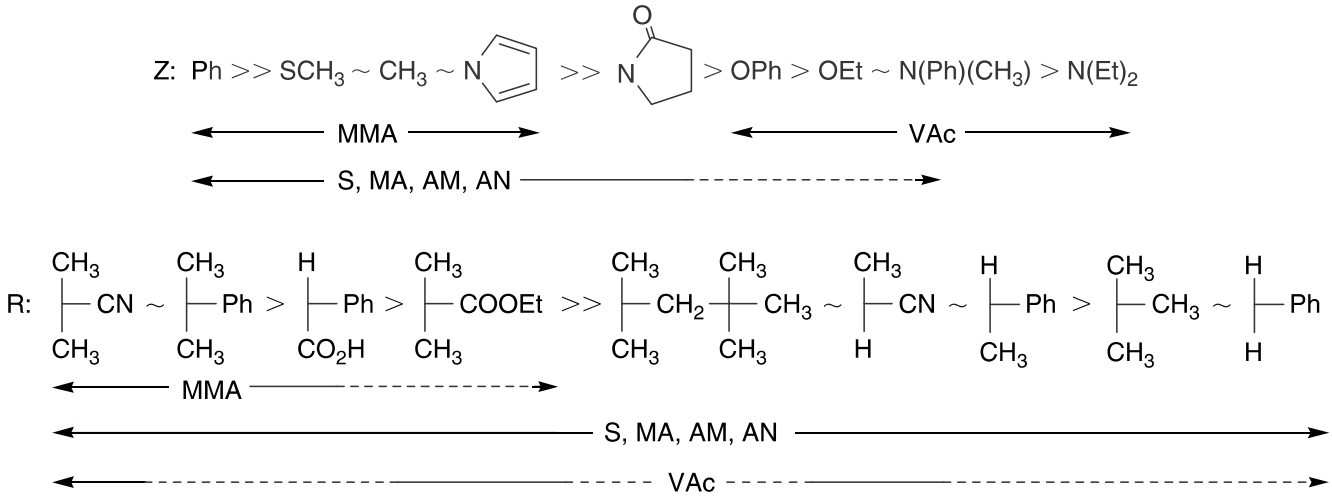

Figure 14. Guideline for the choice of the RAFT agent for various monomers. **Top:** Depending on the substituent Z the addition rate decreases from left to right and the fragmentation rate increases. **Bottom:** R must be a good leaving group (high fragmentation rates) by having a weak C-S bond; however the expelled radical still must be able to reinitiate polymerization. Here the fragmentation rate decreases from left to right. A full line indicates good compatibility with the monomer whereas the dashed line indicates limited control (regarding dispersity and control of molecular weight). Image redrawn from [61].

Generally MAMs are more reactive towards radical polymerization, however not only the reactivity of the vinyl function has to be considered, but also the steric situation and the electronic stabilization of the corresponding macro-radicals have also to be kept in mind. For example a propagating radical derived from methyl methacrylate is more stabilized than a corresponding VA (vinyl acetate) radical, as shown in **Figure 15**. Having a less stabilized, hence more active radical such as (c), leads to an increased addition rate to the CTA along with a decreased fragmentation rate, which may result in complete inhibition of the polymerization reaction.

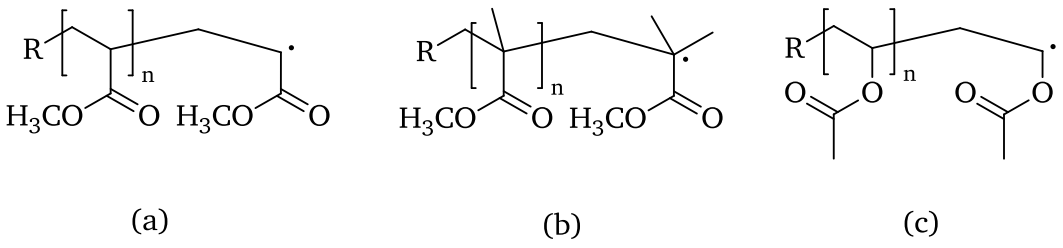

Figure 15. Chemical structure of propagating radicals of methyl acrylate (A) , methyl methacrylate (B) and vinyl acetate (C). Image redrawn from [60].

This can be circumvented by the use of less active RAFT agents, carrying electron rich Z-groups such as *N*-alkyl (dithiocarbamates) or *O*-alkyl groups (xanthogenates), as shown in **Scheme 7**. These groups donate electrons into the thiocarbonyl group, which makes these functionalities less active towards addition of radicals, thus reducing addition rate constants and increasing fragmentation rate constants.

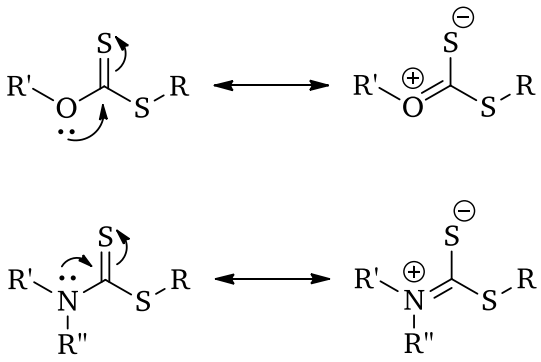

Scheme 7. Zwitterionic resonance contributors of xanthates and dithiocarbamates. Image redrawn from [60].

It can be summarized that polymerization of MAMs produces less reactive macro radicals, thus requiring more reactive RAFT agents. The polymerization of LAMs forms more reactive macro radicals, which favor the reaction with active RAFT agents in comparison to polymerization. This is why in case of polymerization of LAMs less reactive RAFT agents like xanthogenates and dithiocarbamates have to be used. Thus reference [60] comes to the conclusion: *"Understanding the reactivity of the propagating radical formed from a given monomer is key in the selection of an appropriate RAFT agent for control over its polymerization"*.

Prediction of the number average molecular weight

One feature of CRP techniques is the control of the molecular weight of the resulting polymers by the monomer/CTA ratio and by the monomer conversion. The average molecular weight can be predicted by the following equation:

$$M_n(theo.) = \frac{[M]_0 - [M]_t}{[RAFT]_0 + df([I]_0(1 - e^{k_d t}))} * M_{Monomer} + M_{RAFT} \quad (4)$$

Here M_n(theo.) is the theoretical number average molar mass, k_d the rate constant of the dissociation of initiator, d is the average number of chains formed by radical-radical termination. In an event of recombination d = 1 and in an event of disproportionation d = 2, thus d has a value of between 1 and 2 and is determined by the relative probability of recombination and disproportionation. [M] and [I] is

the monomer concentration and the initiator concentration, respectively. The factor f is the initiator efficiency. In a typical RAFT polymerizations $[RAFT]_0 >> df([I]_0(1 - e^{k_d t})$, therefore $[RAFT]_0 + df([I]_0(1 - e^{k_d t}) \approx [RAFT]_0$. This leads to the more simplified and frequently used equation:

$$M_n(theo.) = \frac{[M]_0 - [M]_t}{[RAFT]_0} * M_{Monomer} + M_{RAFT} \quad (5)$$

Here $M_{Monomer}$ is the molar mass of a monomer unit and M_{RAFT} is the molar mass of a RAFT agent.

Deviation of the ideal RAFT mechanism.

Similar to a living polymerization, an ideal controlled radical polymerization by RAFT offers low dispersity, linear correlation of degree of polymerization and conversion, polymer architectures (e.g. block-copolymers) and reactive end groups for post modification. The requirements for ideal conditions have been discussed in literature [61]: RAFT agents should have a very high transfer constant, providing a fast exchange between dormant and living chains, therefore the probability of chain propagation is identical for all chains. RAFT agents should be transformed fast into macro-RAFT agents (fast pre-equilibrium) and expelled radicals R• should reinitiate polymerization quickly. Furthermore, the radical concentration should be similar to a free radical polymerization, meaning no retardation occurs and the radical concentration should remain constant over the whole polymerization process. Termination reactions should be suppressed and side reactions of the RAFT agent should not occur. However, during application of RAFT, various phenomena may be observed, which will be discussed in the following subchapter.

a) Retardation/inhibition

Deviation of ideal polymerization kinetics can be observed as a consequence of retardation or inhibition, as shown in **Figure 16**.

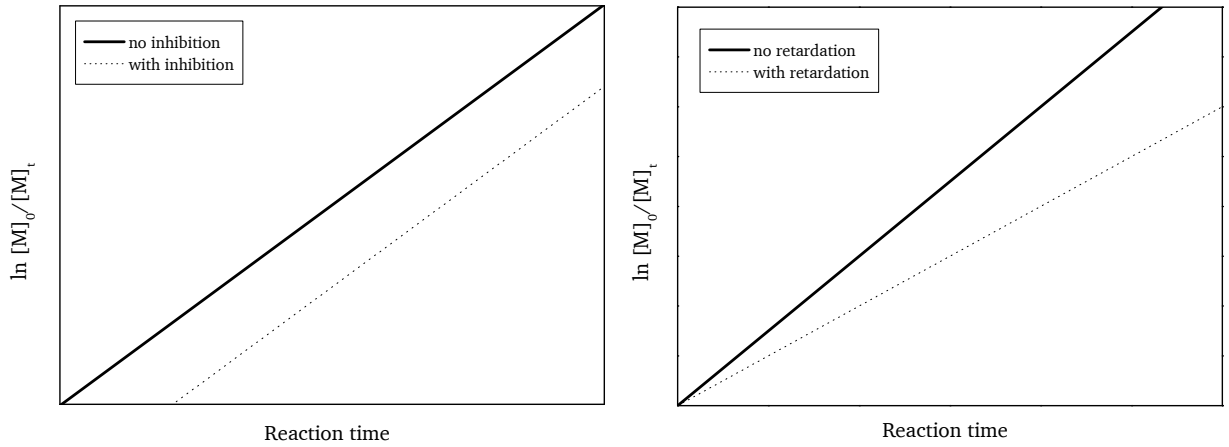

Figure 16. Deviation of ideal RAFT polymerization. Left: A induction period causes the reaction to start with a time delay. Right: Conversion of monomer is slowed down due to the influence of the RAFT agent on the polymerization reaction.

In case of inhibition no polymerization occurs in the beginning of the process (induction time). This phenomenon was attributed to slow formation of macro-RAFT agents during the pre-equilibrium. This theory was supported by subsequent experiments, where no inhibition was observed when polymeric RAFT agents were used, thus skipping the pre-equilibrium step [62]. The other phenomenon, retardation, causes decreased rates of polymerization in comparison to a free radical polymerization under identical reaction conditions.

Both phenomena, retardation and inhibition, depend on the chemical structure of the RAFT agent and on the structure of the used monomer. The addition-fragmentation-mechanism is shown in **Figure 17**. Inhibition may be originated from low transfer constants C_{tr}, leading to slow pre-equlibration of the RAFT agent **2** into macro-RAFT agent **4** or from slow re-initiation of the expelled radical **5** (low k_{iR}), retardation may result from slow fragmentation of the RAFT intermediate **3** or **6** ($k_{ad} > k_{\beta}$). An increased concentration of these intermediate radicals leads to lower concentration of propagating polymer chains since the total amount of all radicals is stationary by reaching the main equilibrium.

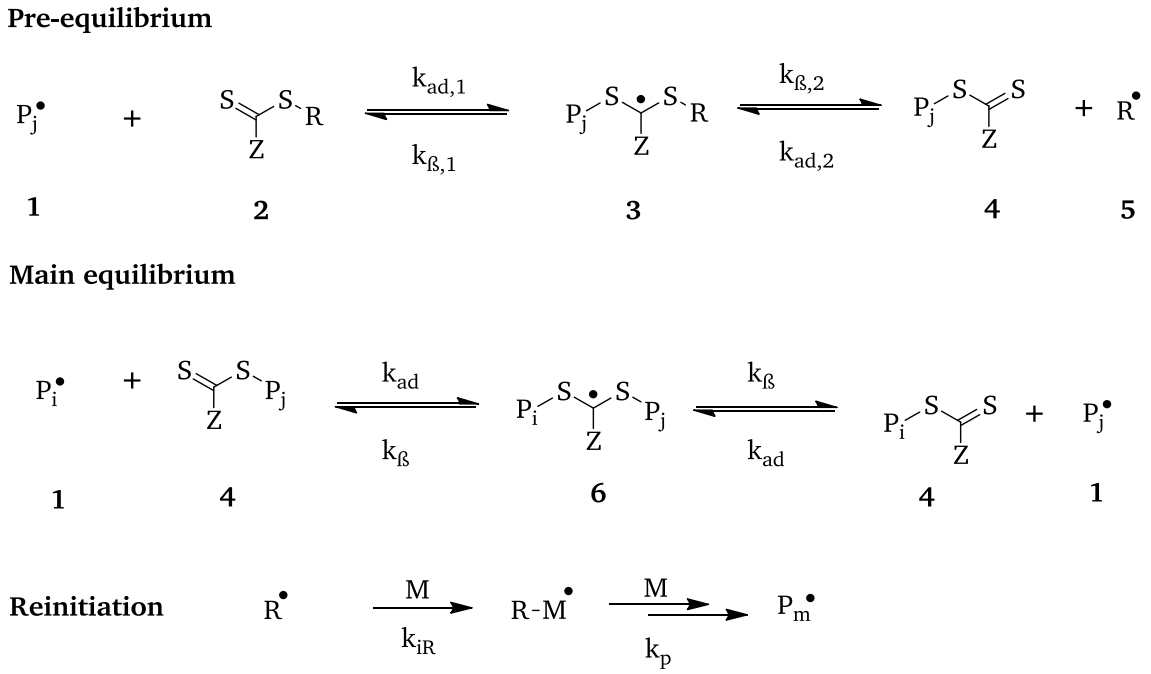

Figure 17. RAFT agent intermediates **3** and **6** before and after transformation of RAFT agent into macro RAFT agent. Image adopted from [62].

The extent of retardation depends also on the RAFT agent concentration and has been investigated experimentally by Kwak et al. [63], as shown in **Figure 18**. From the data plot it can be concluded that the increase of RAFT agent concentration leads to decreased reaction rates of the polymerization process.

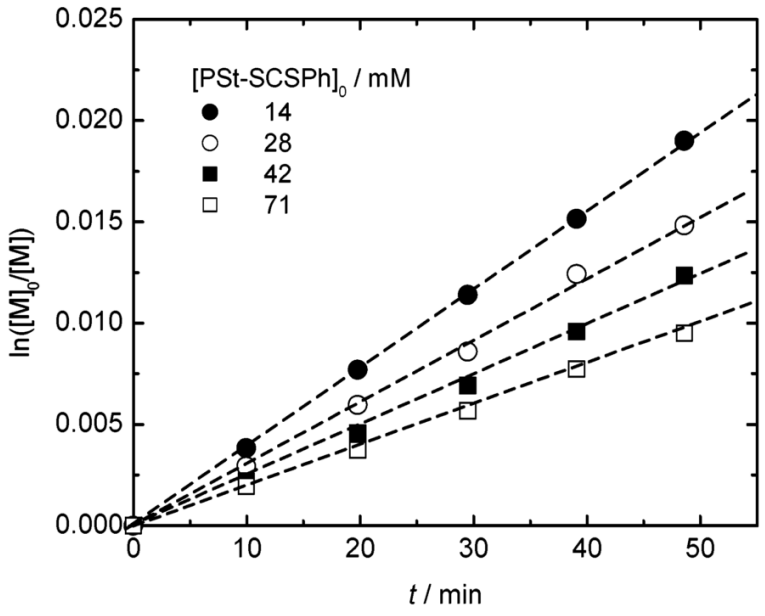

Figure 18. Kinetic plot for the polymerization of styrene, using linear polystyrene with RAFT agent end-functionalization (macro RAFT-agent). By application of different initial concentrations of macro RAFT-agent (varying from 14 mM to 71 mM) a retardation effect is observed. Reprinted with permission from [63]. Copyright (2004) American Chemical Society.

Another source for retardation effects is the resonance stabilization of RAFT intermediate radical and cross-termination, as shown in **Figure 19** or in **Figure 20**, respectively. Both of these effects can decrease the concentration of active radicals, thus causing retardation.

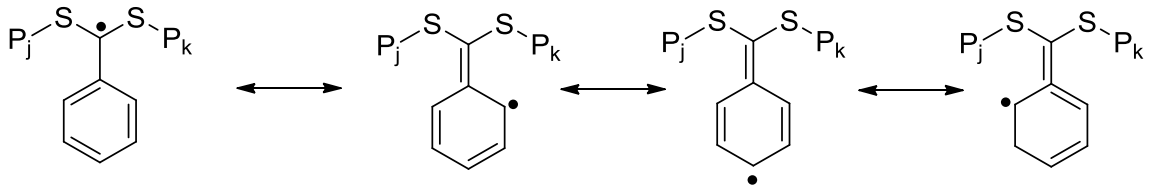

Figure 19. Resonance stabilization of intermediate radical **6** derived from dithiobenzoate RAFT agents. Image redrawn from [62].

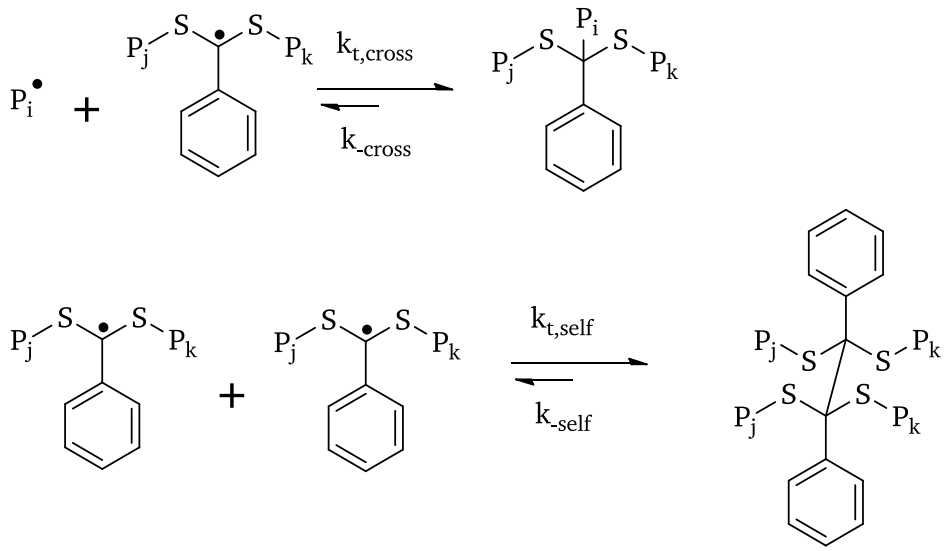

Figure 20. Retardation of a RAFT polymerization as a consequence of (reversible) cross termination of macro-RAFT agent with a propagating polymer chain (A) and (reversible) self-termination of two individual macro-RAFT agent radicals (B). Note: this is only a selection of potential reaction products. Image redrawn from [62].

Note, various mechanisms for retardation/inhibition such as (reversible) cross-termination are still under debate and contradictory conclusions can be found in literature. More detailed information about kinetic aspects of RAFT polymerization and deviation from ideal polymerization kinetics can be found in literature, such as reports from Barner-Kowollik et al. [62], Ting et al. [64], Chernikova et al. [65], Ranieri et al [66] or Sidoruk et al. [67]. However, it is commonly accepted that the choice of the RAFT agent and the monomer as well as the concentration of RAFT agent has a significant influence on retardation/inhibition and thus should be always be taken into consideration when conducting a RAFT polymerization.

b) Side reactions of RAFT agent

Unwanted side reactions of RAFT agent with the reaction media have been investigated by Thomas et al. [68]. RAFT agents are prone to hydrolysis or aminolysis, the products of these side reactions don't serve as RAFT agent anymore and thus the concentration of active species is diminished over time, leading to increased molar mass and higher dispersity of the polymer. For this reason the synthesis of cellulose macro-CTA and polymerization experiments described in this work was performed mostly during absence of water (exception: purifying procedures like extraction or precipitation).

c) Termination and dead chains: influence of the ratio [CTA]/[Initiator]

The initiator concentration and the rate of dissociation of initiator k_d control both, the polymerization rate and the extend of bi-radical termination. Thus the effective radical concentration has to be chosen as a compromise between polymerization rate and control over molar mass and dispersity of the chains. RAFT polymerization of styrene and other standard monomers have been well investigated, thus suitable reaction conditions for well-defined polymers are provided in literature (e.g. [59]). In general RAFT polymerizations are performed with an excess of CTA in relation to the initiator concentration ($[RAFT]_0 > [Initiator]_0$) in order to ensure sufficient control of the polymerization process, typically having a ratio of about 5 to 10. The percentage, and thus the extent of termination reactions, may be estimated by use of the following equation:

$$fraction\ of\ dead\ chains\ [\%] = \frac{[dead\ chains]}{[living\ chains] + [dead\ chains]} \tag{6}$$

assumption:

$$[living\ chains] = [RAFT]_0 \tag{7}$$

$$[dead\ chains] = (1+q) f [I]_0 (1 - \exp(-k_d t)) \tag{8}$$

Here, the termination parameter q is defined as $q = k_{t,d}/k_t$ $(0 \leq q \leq 1)$, where $k_{t,d}$ is the termination rate constant by disproportion and k_t the total termination rate constant. The initiator efficiency f is defined as the fraction of radicals generated from the initiator, which induce a polymerization process and thus may not exceed 1. Furthermore the initial initiator concentration is defined as $[I]_0$.

The combination of the equations (6), (7) and (8) leads to the following equation:

$$fraction\ of\ dead\ chains\ [\%]\ =\ \frac{(1+q)f[I]_0(1-\exp(-k_d t))}{[RAFT]_0+\ (1+q)f[I]_0(1-\exp(-d_d t))} \tag{9}$$

Equation (9) can be simplified by accumulation of all constant values into a constant "C":

$$fraction\ of\ dead\ chains\ [\%]\ =\ \frac{C*[I]_0}{[RAFT]_0+\ C*[I]_0} \tag{10}$$

The constant C cannot exceed a value of 2, therefore the requirement on the reaction conditions for a minimal amount of dead chains (hence a living process) is $[RAFT]_0 >> [I]_0$. More details can be found in [69]. However, one has to keep in mind, that the concentration of RAFT agent correlates with the molecular weight of the polymers with $DP \propto [CTA]^{-1}$, thus the concentration RAFT agent cannot be increased without decreasing the degree of polymerization. This is why the synthesis of polymers with low dispersity and high average molar mass at the same time has limitations. It may be concluded that the [CTA]/[Initiator] ratio has to be chosen carefully, depending on the requirements of the targeted polymers.

d) Hybrid behavior

Depending on the chemical nature of the Z-group, the complete transformation of RAFT agent to macro-RAFT agent may be slow in comparison to the monomer addition of propagating polymer chains. This is the case when k_{tr} is not high enough in comparison to k_p, thus if C_{tr} is too small. In this case, a hybrid behavior consisting of free radical polymerization and RAFT polymerization is obtained, leading to deviation of ideal RAFT kinetics, as shown in **Figure 21**.

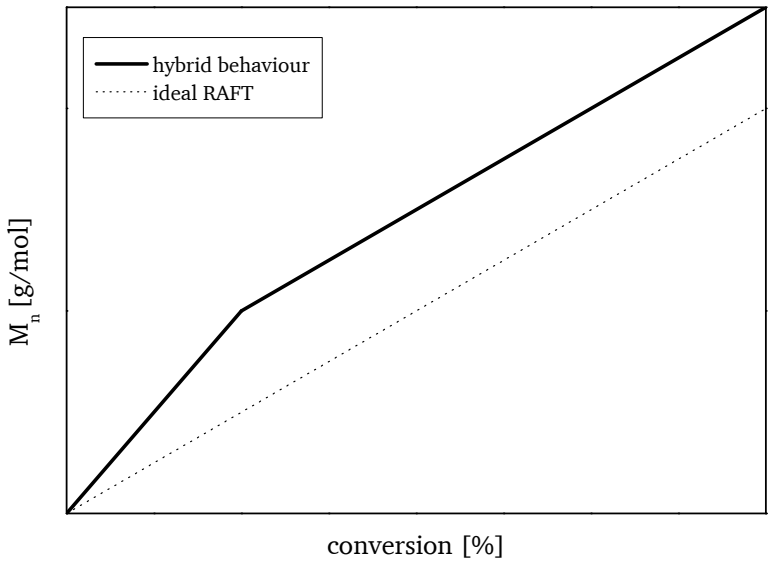

Figure 21. Deviation of M_n from theoretical values due to hybrid behavior.

As consequence, the molar mass of the polymers exceeds the predicted values during the early stages of polymerization, followed by a linear increase of molecular mass over conversion during the polymerization process. As an example, this phenomenon has been investigated by Barner-Kowollik et at. [70] for the RAFT polymerization of MMA and styrene with RAFT agent cumyl phenyldithioacetate. In order to avoid hybrid behavior, it is suggested to choose the RAFT agent depending on the monomer in order to obtain high transfer constants C_{tr}.

3.3. Characterization of cellulose graft copolymers

As described in chapter 2.1 one aim of this work is to investigate synthetic strategies for the fabrication of well-defined, “tailor-made” graft copolymers based on cellulose. Here, the term “well-defined” includes the control of graft-density and molar mass of each individual graft. For this, suitable methods for the characterization of cellulose precursor and graft copolymers have to be found, as described in the following sections.

3.3.1. Analysis of degree of substitution (DS) on cellulose

In general, grafting density can be defined as the average distance of two individual grafts along a polymer backbone. Having a polymer backbone carrying an averaged number of polymer grafts per repeating unit, the average distance may be calculated by the degree of functionalization (i.e. how many polymer grafts per repeating unit) and the size of each repeating unit. Regarding cellulose graft copolymers using RAFT polymerization, the average distance between polymer grafts can be controlled by the degree of substitution of CTA groups, which allow the controlled growth of polymer chains on the backbone in a subsequent polymerization step.

For this, DS values of cellulose macro-CTA were precisely determined by ^{1}H-NMR spectroscopy as analytical method. A precise analysis requires the CTA to bear protons at distinct chemical shifts with baseline separated signals in the spectra. This is why we chose CTAs having aromatic protons which appear at a chemical shift which is typically not interfering with protons of cellulose or common substituents of cellulose, such as propionic ester protons. Using the proton signals of the cellulose backbone as reference, the DS values for all substituent can be determined easily, as exemplary shown for cellulose macro-CTA “MCC-CTA14”, which is carrying three different substituents, as shown in **Figure 22**. Note, the determination of the DS values of the cellulose macro-CTA has been adopted from [71].

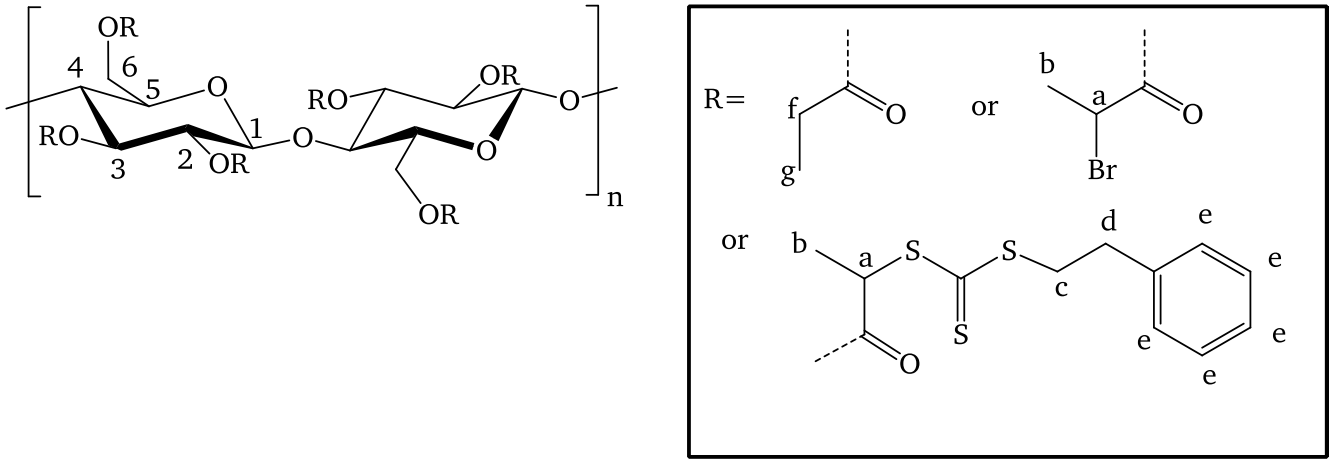

Figure 22. Chemical structure of a cellulose macro-CTA (sample: MCC-CTA14). Note, that the calculated values for the substituents only refer to the monomer anhydroglucose unit, not to the corresponding dimer cellobiose.

The corresponding ^{1}H-NMR- spectra of the cellulose macro-CTA and its precursor substance 2-bromopropionyl/propionyl cellulose esters are displayed in **Figure 23**.

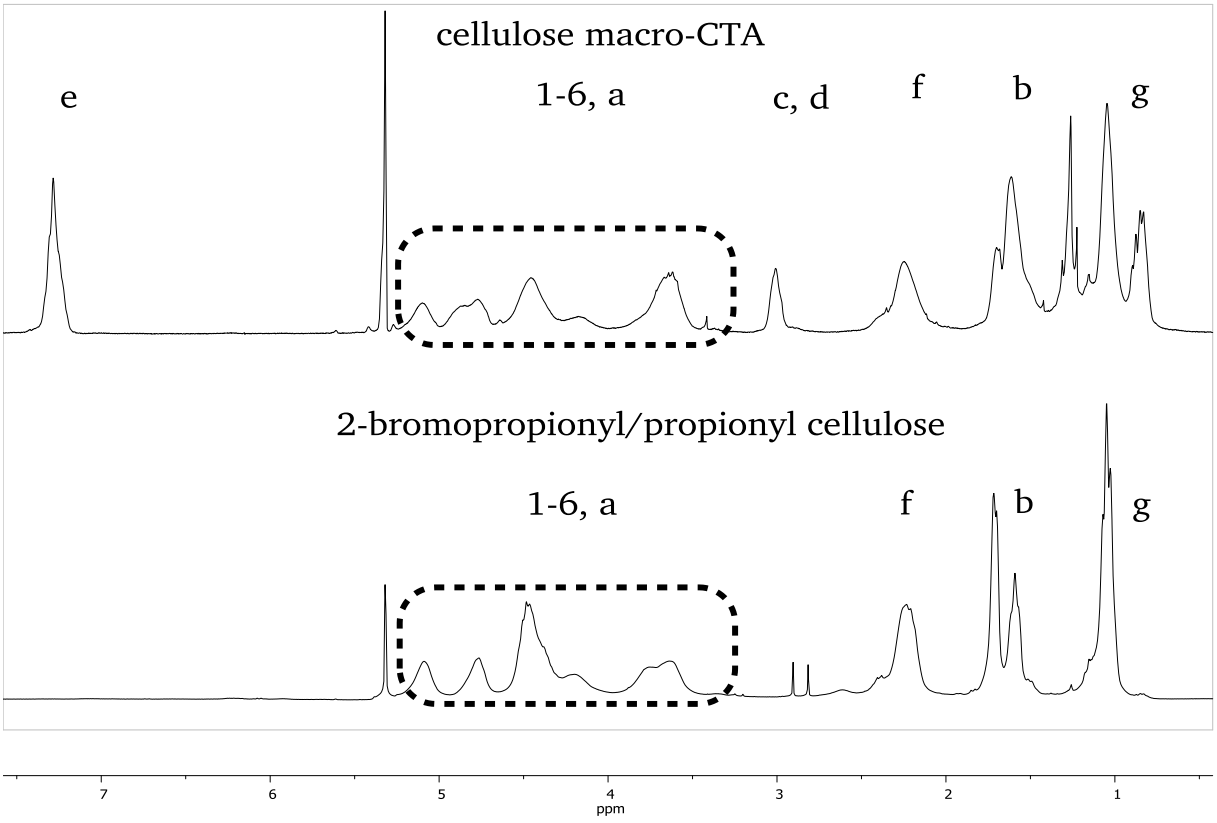

Figure 23. ^{1}H-NMR spectra of cellulose-CTA (top) and the precursor 2-bromopropionyl/propionyl cellulose (bottom) in CD_2Cl_2 (5.32 ppm). The DS(CTA) was determined by comparison of the cellulose backbone protons (7 H, 3.5 ppm – 5.2 ppm) with the protons of the CTA (4 H, 2.9 ppm and 5 H, 7.2 ppm). The denotation corresponds to **Figure 22**. Reprinted with permission from [71].

First, the precursor of cellulose macro-CTA was characterized by means of DS values for 2-bromopropionyl (Bp) and propionyl (Pr) moieties, using the following equations:

$$DS(Pr) = \left(\frac{\frac{\int(f+g)}{5}}{\frac{\int(1-6)}{7} + \frac{\int(a)}{1}} \right) \quad \text{with } \int(a) = \frac{\int b}{3} \; and \; \frac{\int b}{3} + \frac{\int(f+g)}{5} = 3 \tag{11}$$

$$DS(Bp) = \left(\frac{\frac{\int(b)}{3}}{\frac{\int(1-6)}{7} + \frac{\int(a)}{1}} \right) = 3 - DS(\mathrm{Pr}) \tag{12}$$

From the ^{1}H-NMR data we determined DS(Pr) = 1.5 DS(Bp) = 1.5

Note: for this calculation a complete substitution of the cellulose, i.e. DS(total) = 3 was assumed. This assumption could be validated by ATR-IR spectroscopy, where no residual OH-groups could be detected (see chapter 4.2.2). After partial transfer of 2-bromopropionyl functionalities into CTA groups, the DS values for all functionalities on the cellulose macro-CTA were determined using the following equations:

$$DS(CTA) = \left(\frac{\frac{\int(e)}{5}}{\frac{\int(1-6)}{7}} \right) = 0.54 \tag{13}$$

$$DS(Pr) = \left(\frac{\frac{\int(f+g)}{5}}{\frac{\int(1-6)}{7} + \frac{\int(a)}{1}} \right) = 1.5 \tag{14}$$

$$DS(Bp) = 3 - DS(\mathrm{Pr}) - DS(CTA) = 0.96 \tag{15}$$

The CTA content in cellulose macro-CTA was calculated from the DS values of the precursors. For better comprehension a schematic illustration of a cellulose repeating unit, bearing all different types of substituents is shown in **Figure 24**.

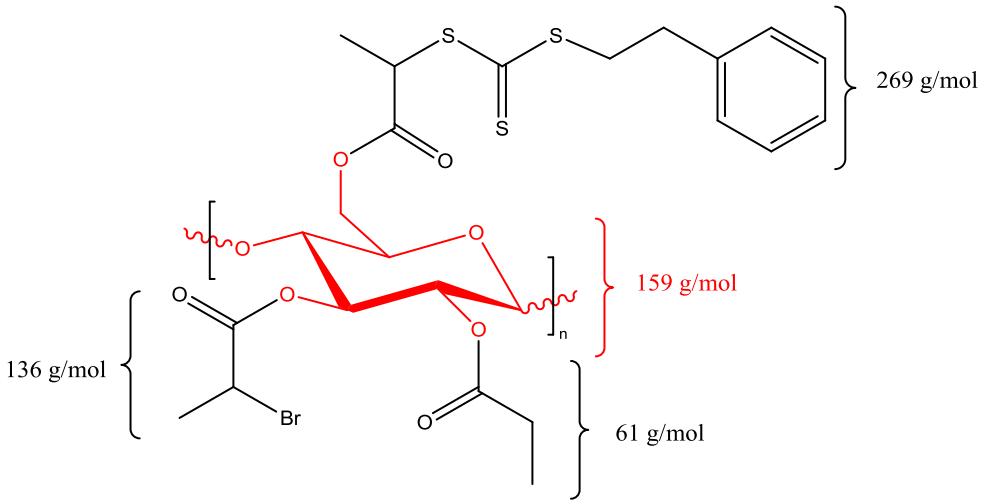

Figure 24. Schematic segment of a cellulose macro-CTA containing all three different types of substituents used in this work. Note, this structure does not represent the real distribution of the substituents, it is rather supposed to guide the reader how the DS values were calculated. Figure reprinted with permission from [71].

$$M_{Cellulose-CTA} = M_{AGU} - 3 * M_H + DS(\mathrm{Pr}) * M\_\mathrm{Pr} + DS(Bp) * M_{Bp} + DS(CTA) * M_{CTA} \tag{16}$$

$$\begin{aligned} M_{Cellulose-CTA} &= 162\frac{g}{mol} - 3 * 1\frac{g}{mol} + 1.5 * 61\frac{g}{mol} + 0.96 * 136\frac{g}{mol} + 0.54 * 269\frac{g}{mol} \\ &= 526\frac{g}{mol} \end{aligned} \tag{17}$$

$$CTA\ content\ on\ cellulose\ macro - CTA\ \left[\frac{mmol}{g}\right] = \frac{1}{M_{Cellulose-CTA}} * DS(CTA) = \mathbf{1.03} \tag{18}$$

Result: 1 g of cellulose macro-CTA "MCC-CTA14" contains 1.03 mmol CTA groups.

Standard error:

It should be kept in mind that the quantitative analysis of the cellulose samples with ^{1}H-NMR technique inherits some limitations regarding sample preparation, analysis of the samples and interpretation/processing of the analytical data. The first issue refers to the chemical modification of cellulose via polymer analogous conversion. According to the experience of the author it was not trivial to synthesize well soluble and pure cellulose samples. Having sometimes (partially) insoluble samples and/or remaining traces of impurities (reactants or solvents), causes problems during the quantitative analysis of the samples via NMR technique. The second issue refers to the analysis of polymeric materials. Depending on the parameters chosen during ^{1}H-NMR spectroscopy (temperature, solvent, number of scans, relaxation time, ect.) signal intensity and peak shape may vary [72].

The third issue refers to the processing and interpretation of the NMR data. The analytical data was interpreted using MestReNoVa as software. The cellulose derivatives that we analyzed typically showed broad signals in the NMR spectra from about 3.5 ppm to about 5.2 ppm. Having broad proton signals leaves uncertainties in the determination of the integral signal intensity depending on the choice of the baseline correction, as exemplary shown in **Figure 25**.

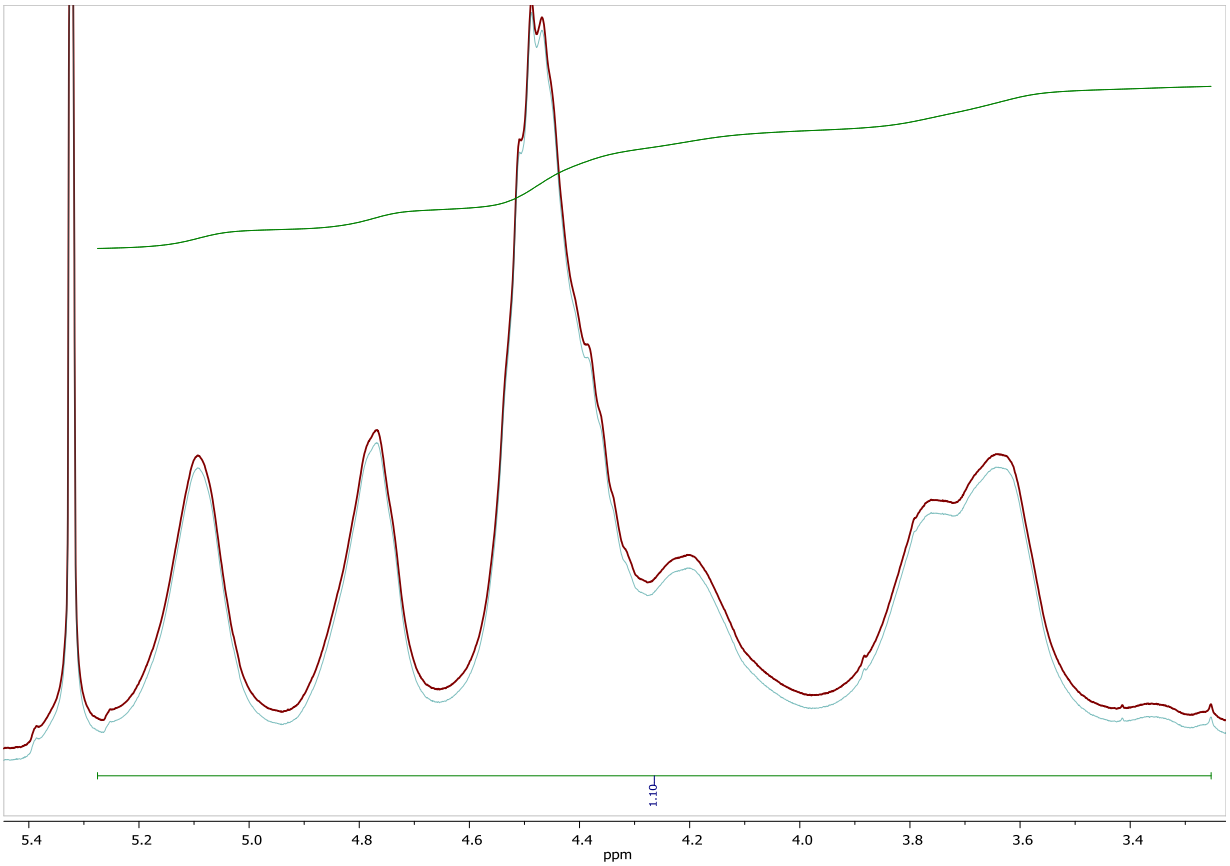

Figure 25. Integral signal intensity of a cellulose sample ("MCC-BpB4-Pr") using the baseline correction "Whittacker Smoother" (blue curve) with a normalized value of 1.00 or a baseline correction "polynomial fit" with a normalized value of 1.10. These two methods of baseline correction lead to a relative difference of about 10 %, indicating the significant effect of data processing on the analytical results. Note, MestReNova (version 9.1.0-14011) was used for processing the NMR data.

Having all these factors that affect the accuracy of the quantitative analysis of the polymer samples, the determination of the standard error for each individual analysis is not trivial. This is why the author estimated the relative error of ± 5 %, which is a value provided from literature[1]. Note that this value should be considered a rough estimation.

[1] www.analytik.ethz.**ch**/vorlesungen/biopharm/Spektroskopie/**NMR**.pdf , *19.08.2016.*

3.3.2. Analysis of the graft ratio and the initiation efficiency of cellulose graft copolymers

As described in the previous section, the grafting density of cellulose graft copolymers may be controlled by the DS(CTA) of the corresponding cellulose macro-CTA. However, it is pointed out that the hypothesis is only valid for the ideal assumption, that all CTA functionalities on the cellulose are actually transferred into polymer grafts. In the non-ideal case, not all CTA-functionalities on the cellulose are chemically available and some of the propagating polymer grafts may undergo termination reactions. This is why other parameters like graft ratio and initiation efficiency have to be carefully monitored. Especially determination of the initiation efficiency provides information how close a graft copolymerization system (including concentration of reactants, reaction temperature and conversion) approaches ideal conditions.

It should be noted, that in literature various terms and various definitions concerning polymer architectures can be found, such as graft yield [41], initiation efficiency [49], graft ratio [27], grafting degree [73] or degree of functionalization [74]. Therefore the definitions used in this work are described in the following section.

a) Graft ratio

We define the graft ratio as the relative amount of polystyrene attached to the cellulose macro-CTA.

$$graft\ ratio\ [\%] = \frac{m(polystyrene\ grafts)}{m(cellulose\ macro-CTA)} * 100\ \% \tag{19}$$

Here, the resulting product is always a mixture of linear homopolymer from free CTA and cellulose graft copolymer. Therefore it is not possible to determine the mass of the polymer grafts directly via gravimetry. The graft ratios were calculated from the total amount of polymer, determined by conversion (with ^{1}H-NMR) and the fraction of polymer grafts relative to the total amount of polymer (analyzed by SEC with UV-Vis detection). For this, the following equations were used:

$$x(PS\ on\ Cellulose) = \frac{\int S\ (cellulose-graft-PS)}{\int S\ (cellulose-graft-PS) + \int S(linear\ PS)} \tag{20}$$

x = mass fraction [%], S = detector signal (baseline corrected)

The total amount of polystyrene was calculated:

$$m(PS, total) = m_0(styrene) * conversion\ [\%] \tag{21}$$

With m_0 as initial monomer mass. Finally, the graft ratio could be calculated:

$$graft\ ratio\ [\%] = \left(\frac{x(PS\ on\ cellulose) * m(PS, total)}{m(cellulose\ macro - CTA)}\right) * 100\ \% \tag{22}$$

b) Initiation efficiency

The initiation efficiency is described as the percentage of chemically active CTA groups on the cellulose backbone with respect to the total amount of cellulose-bound CTA groups.

$$I_{eff}[\%] = \frac{N(CTA_{cellulose})_{active}}{N(CTA_{cellulose})_0} * 100\ \% \tag{23}$$

Since the amount of active CTA groups cannot be determined directly, we assumed the following: In order to have an active CTA group, it needs to be accessible during the polymerization process and thus carries a polystyrene graft after the reaction. Therefore initiation efficiency can also be described with the following equation:

$$I_{eff}[\%] = \frac{n(PS\ grafts)}{n(CTA\ groups\ on\ Cellulose)} * 100\ \% \tag{24}$$

The molar amount of polystyrene grafts could be estimated by calculation of the polymer graft mass and the number average molar mass, whereas the molar amount of CTA groups could be directly calculated from the amount of cellulose macro CTA, the molar mass and the DS(CTA) values. Note, this assumption is only valid if the polymerization kinetics of free CTA and CTA groups on cellulose are identical. Alternatively, having UV-Vis detection coupled to the SEC, the initiation efficiency can be determined using the following equation:

$$I_{eff}[\%] = \frac{[CTA_{free}]}{[CTA_{cellulose}]} * \frac{x(PS\ on\ cellulose)}{x(PS\ homopolymer)} * 100\ \% \tag{25}$$

Here, the mass fractions of homopolymer and graft copolymer were calculated from the relative integral signal intensities in the elugrams, determined by SEC with UV-Vis detection. According to the Lambert-Beer-Law, there should be a direct correlation between the integral intensity of the signal and the concentration of light-absorbing species (in our case the phenyl group of the polystyrene at 254 nm wavelength). In order to validate the reliability of the SEC measurements, several reference analyses were made in order to prove the relation between the detector response and polymer concentration. All of the following polymerization experiments were analyzed in the concentration range, where a linear correlation of the detector signal was provided.

4. Synthesis of cellulose macro-CTA

The nomenclature of the experiments and general remarks

Since cellulose derivatives were generated in a sequence of chemical transformations the following nomenclature was used:

Example: MCC-CPPA16-Pr-PDMAA_2

As cellulose material microcrystalline cellulose (MCC) was first esterified with 4-Cyano-4-(phenylcarbonothioylthio)pentanoic acid (CPPA), which was the 16th approach of attaching CPPA to a cellulose. Then the product was modified with propionic ester groups (Pr). In the subsequent copolymerization with DMAA for the second time (PDMAA_2), graft copolymers were generated.

DS values were always referred to one anhydroglucose repeating unit (AGU). Note, in the reaction schemes always the cellobiose repeating unit is shown, with every unit containing two AGUs.

4.1. Synthesis of dithioester-modified cellulose macro-CTA

As described in chapter 2.2, the initial strategy for immobilization (Goal 1, Strategy 1) of CTA onto cellulose was based on the activation of a functional group on a preformed CTA, as shown in **Figure 26**. For this we chose 4-cyano-4-(phenylcarbonothioylthio) pentanoic acid (CPPA), which is a CTA carrying a carboxylic moiety. We used CPPA because its carboxylic function allows the covalent attachment onto cellulose via esterification **(1)**. Furthermore is CPPA a well known and often used CTA and typically shows a good polymerization performance [75]. Then the remaining OH-groups were completely esterified using propionic acid anhydride **(2)**, to yield a well soluble cellulose macro-CTA.

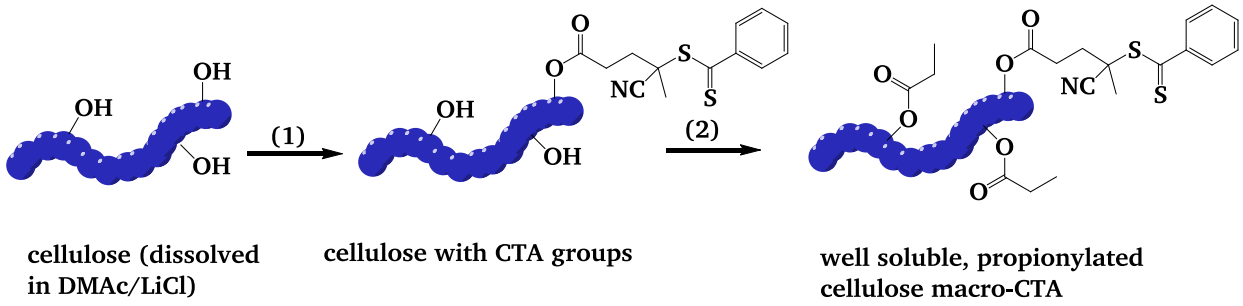

Figure 26. Schematic image of the initially targeted cellulose macro-CTA.

Before the immobilization of CPPA on cellulose was performed, various stability tests were carried out in order to avoid side reactions or transformation of the dithioester-functionality during the activation procedure, as described in the following sections.

Validation of the chemical and thermal stability of CPPA in the cellulose solvent DMAc/LiCl.

As described in chapter 3.1 the solvent system DMAc/LiCl was chosen for homogenous cellulose modification. Thus, the stability of the CTA was tested using DMAc/LiCl as solvent at 60 °C, which is typical reaction temperature for esterification reactions on cellulose (**Figure 27**).

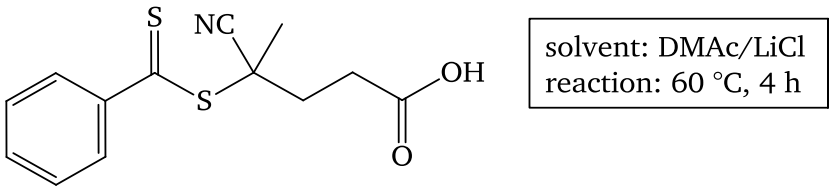

Figure 27. The chemical structure of CPPA and the reaction conditions, which were applied for the stability test.

After a reaction time of 4 hours at 60 °C, the CTA was recovered by extraction, using chloroform and water. The organic phase was dried with $MgSO_4$ and all volatiles were removed by evaporation. The chemical stability was monitored by comparison of the ^{1}H-NMR spectra before and after treatment. The corresponding spectra of the CTA are displayed in **Figure 28**; they clearly show that the signal pattern does not change, indicating that treatment does not affect the chemical structure of the CTA. The only new signals correspond to remaining DMAc residues.

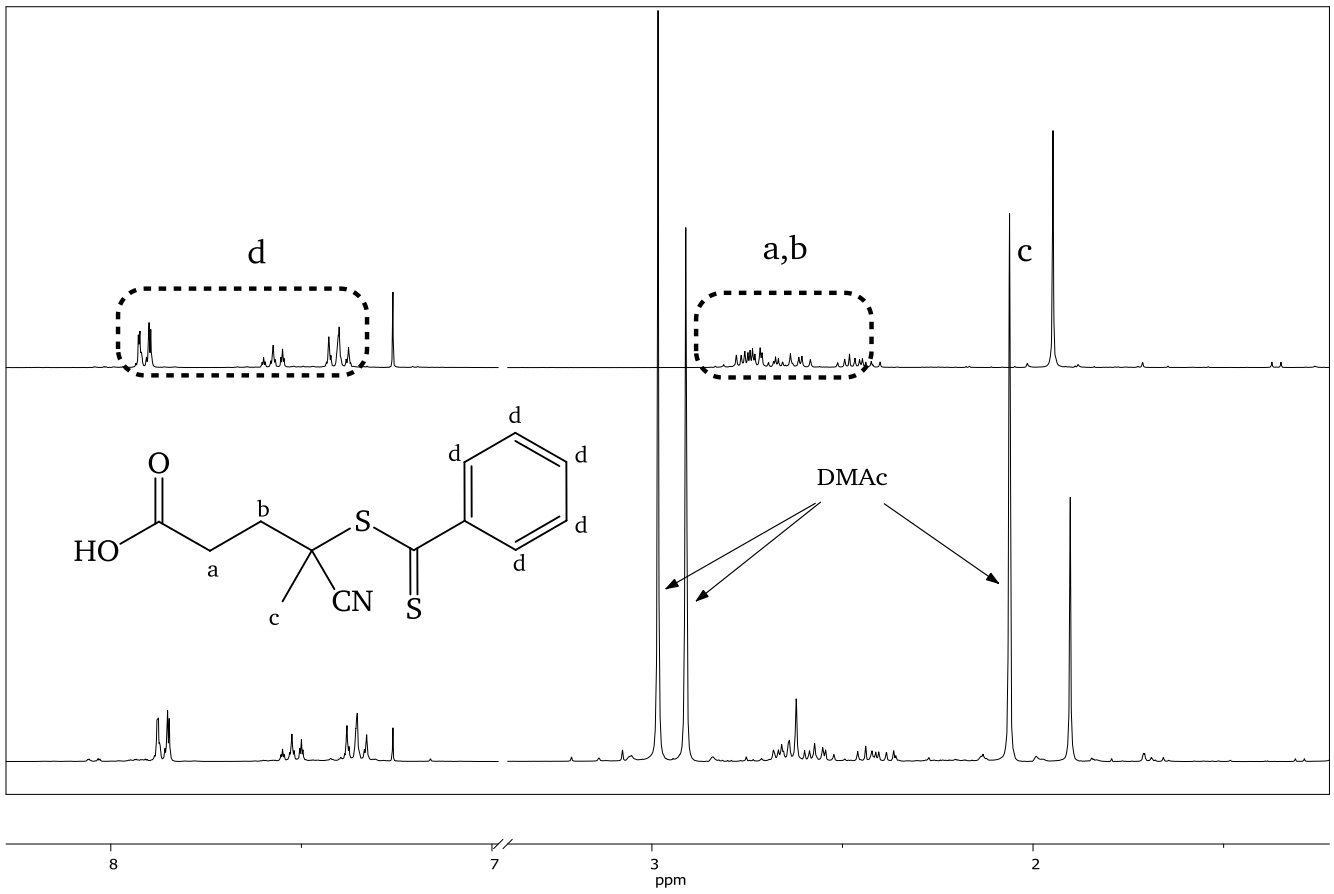

Figure 28. ^{1}H-NMR Spectra of the CTA before (top) and after treatment in DMAc/LiCl at 60 °C (bottom), referenced against $CDCl_3$ (7.26 ppm).

Activation with dicyclohexyl carbodiimide (DCC)

The chemical stability of CPPA was tested by application of activation agent DCC and catalyst *N,N*-dimethylaminopyridine (DMAP), which are reactants of a typical Steglich esterification [76]. The reaction conditions and the activated CPPA are shown in **Figure 29**.

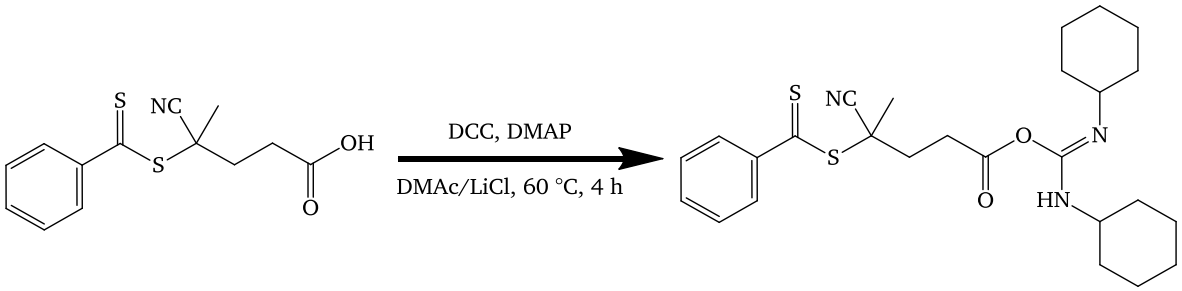

Figure 29. Reaction scheme of the activation of a RAFT agent with DCC.

After a reaction time of 4 hours at 60 °C, the product was isolated by extraction, using chloroform and water. The organic phase was dried with $MgSO_4$ and all volatiles were removed by evaporation. Subsequent analysis via ^{1}H-NMR (**Figure 30**) reveals additional signals especially in the region 7.0-8.0 ppm (aromatic protons), which may only originate from phenyl ring of CPPA or CPPA-derived side product.

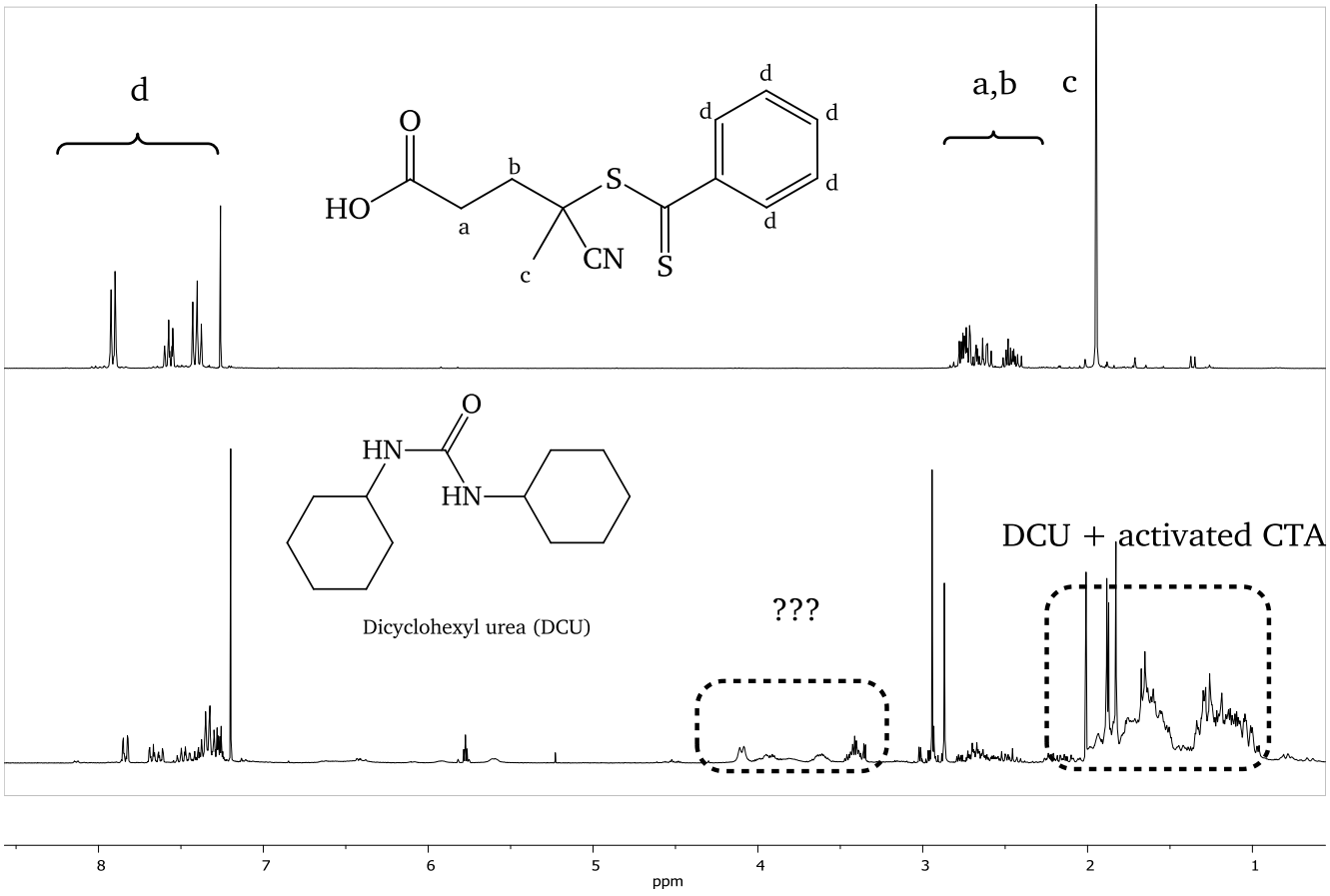

Figure 30. ^{1}H-NMR spectra of the stability test of CPPA. Before reaction (top) and after reaction with DCC (bottom). Various new signals do not originate from CPPA, DCC or DCU (dicyclohexylurea), which is considered an indication for side reactions.

Since the original signal pattern of the aromatic protons (denoted as d) was not conserved after the reaction, this was considered an indication for side reactions, transferring the dithioester functionality at least partially into a different chemical species. Therefore we concluded that DCC may not be a suitable choice as coupling agent for CPPA. Interestingly, this observation is in direct contrast to publications, where carbodiimides were used for heterogeneous esterification of CTA onto cellulosic surfaces [77] or homogeneous on HPC [52]. Barsbay et al. showed that the resulting surface-modified cellulose fibers were capable of subsequent RAFT polymerization, leading to very small graft ratios, indicating that only a small amount of intact CTA functionalities had been immobilized. However, no reference experiments concerning the stability of CTA against carbodiimides were conducted within these reports [52, 77]. It thus may be assumed that a side reaction destroying the dithioester functionality is occurring at the same time like the esterification reaction. In the case of heterogeneous reaction conditions the destroyed CTA groups do not attach onto the cellulosic surface, thus being removed easily by extraction [77]. It should be also be noted that reports about homogenous RAFT polymerization on cellulose often do not use quantitative methods for the analysis of the amount of grafted polymer and deviations between expected and resulting polymer loadings onto the cellulose are not discussed [26, 52].

Activation with thionyl chloride ($SOCl_2$)

Another possible activation method for CPPA is the conversion of the carboxylic function into the corresponding acid chloride by the use of thionyl chloride, as performed on cyclodextrin and carboxyl functionalized RAFT agent by Stenzel et al. [78]. Starting from the synthesis protocol, the stability of the CTA against thionyl chloride at typical reaction conditions was investigated (reaction conditions provided in **Figure 31**).

Figure 31. Reaction scheme for the esterification of CPPA with IPA, using thionyl chloride for activation of the carboxyl group.

The isolation of acid chlorides is not trivial due to their high reactivity; therefore the intermediate was directly esterified by addition of isopropyl alcohol under the reaction conditions of an esterification protocol, which is also described by Stenzel et al. [78]. In the first step the carboxylic function reacted

with an excess of thionyl chloride under anhydrous conditions and reflux. Then remaining thionyl chloride was removed by distillation, followed by the addition of anhydrous isopropyl alcohol.

The product was isolated by removal of all volatiles, dissolved in chloroform, followed by extraction with hydrogen carbonate solution and water. Subsequent analysis with ^{1}H-NMR (see **Figure 32**) revealed many new signals from unknown origin. It was concluded that activation of CPPA with thionyl chloride was an unsuitable method.

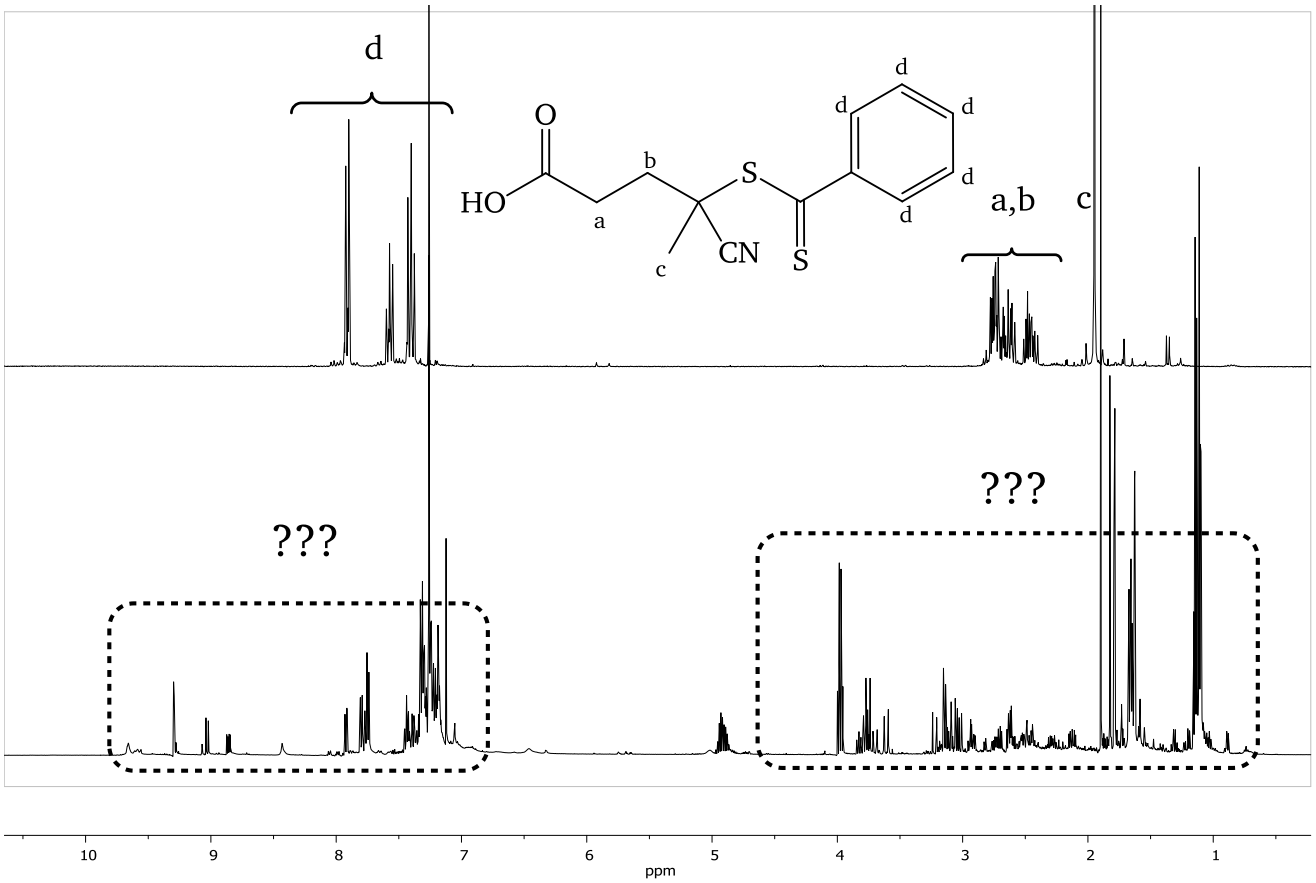

Figure 32. ^{1}H-NMR spectra of CPPA before (top) and after esterification with isopropyl alcohol (bottom), referenced against $CDCl_3$ (7.26 ppm). Even though the product was purified before analysis via extraction, the spectrum contains many signals from unknown functionalities which don't belong to any of the reactants or solvent.

Activation with *N,N`*-carbonyldiimidazole (CDI)

Esterification of aliphatic carboxylic acids with cellulose can be performed in a mild and efficient fashion by use of the coupling agent *N,N`*-carbonyldiimidazole (CDI), as presented by Heinze et al. [79]. Since this method has not been applied on RAFT agents, a reference experiment was performed in order to validate the compatibility of the RAFT agent with the activation agent (reaction conditions are described in **Figure 33**).

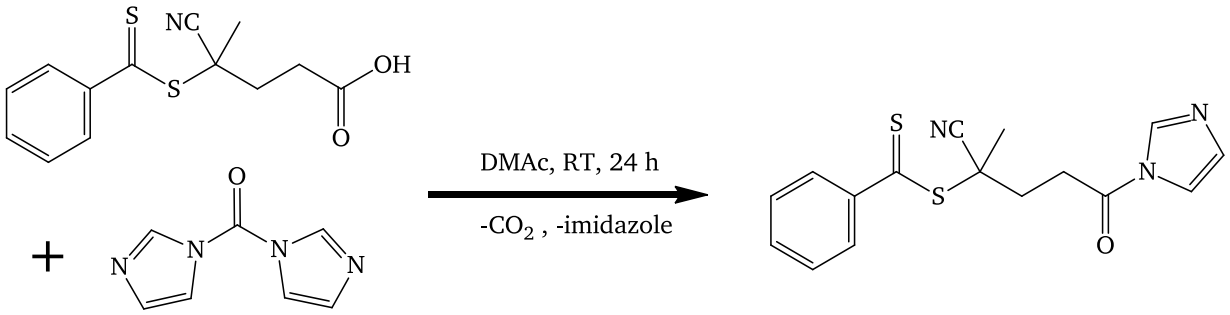

Figure 33. Typical reaction conditions for the activation of CPPA using CDI.

After the reaction, the product was isolated and ^{1}H-NMR analysis was performed, as shown in **Figure 34**.

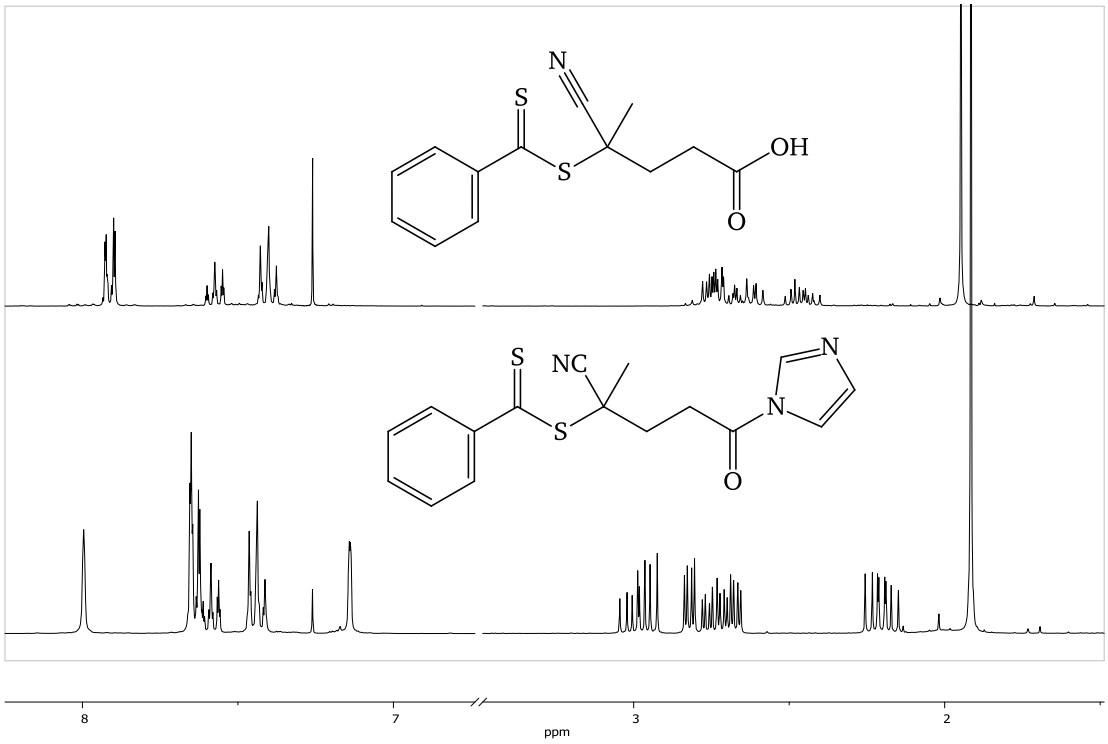

Figure 34. ^{1}H-NMR spectra of the stability test of CPPA against activation with CDI. The spectrum of CPPA is shown at the top and the spectrum of CPPA after activation with CDI at room temperature overnight is shown in the bottom, both referenced against $CDCl_3$ (7.26 ppm). The signals at 7.15 and 8.0 ppm belong to the imidazole, whereas the other signals belong to the phenyl ring of CPPA.

A chemical shift of a signal at about 2.2 ppm is observed, which can be attributed to a different chemical environment of the neighboring CH_2-group after coupling with CDI. Besides that, a chemical shift of a phenyl proton from about 8.0 ppm to 7.6 ppm is observed. Nonetheless the signal pattern and the relative integral intensity of the signals indicate an intact chemical structure after conversion with CDI. Thus, we decided to start first sets of experiments for cellulose esterification using CDI.

Cellulose macro-CTA by esterification of CPPA

Heinze et al. [80] reported that cellulose derivatives produced with CDI as activation agent were found to be only partially substituted, which often lead to insoluble substances after precipitation and drying of the product. Therefore, Heinze suggested suspending the insoluble cellulose derivatives, followed by heterogeneous esterification reaction of the remaining hydroxyl functions using propionic acid anhydride. During this esterification process, the insoluble cellulose turned soluble with progressing reaction time. Finally well soluble, completely esterified cellulose mixed esters were obtained.In contrast to Heinze, we observed that isolated cellulose derivatives could typically not be turned organo-soluble by the heterogeneous esterification process. We found out that usually most of the cellulose derivative remained as insoluble gel. When only the organo-soluble fraction of the cellulose derivative was isolated, we received very low yields. Thus we decided to modify the protocol of cellulose derivatization. The partially substituted cellulose derivatives were not isolated and resuspended, but treated in a one-pot synthesis by addition of propionic acid anhydride, triethyl amine and DMAP to the reaction mixture. The chemical process is shown exemplary in **Figure 35**.

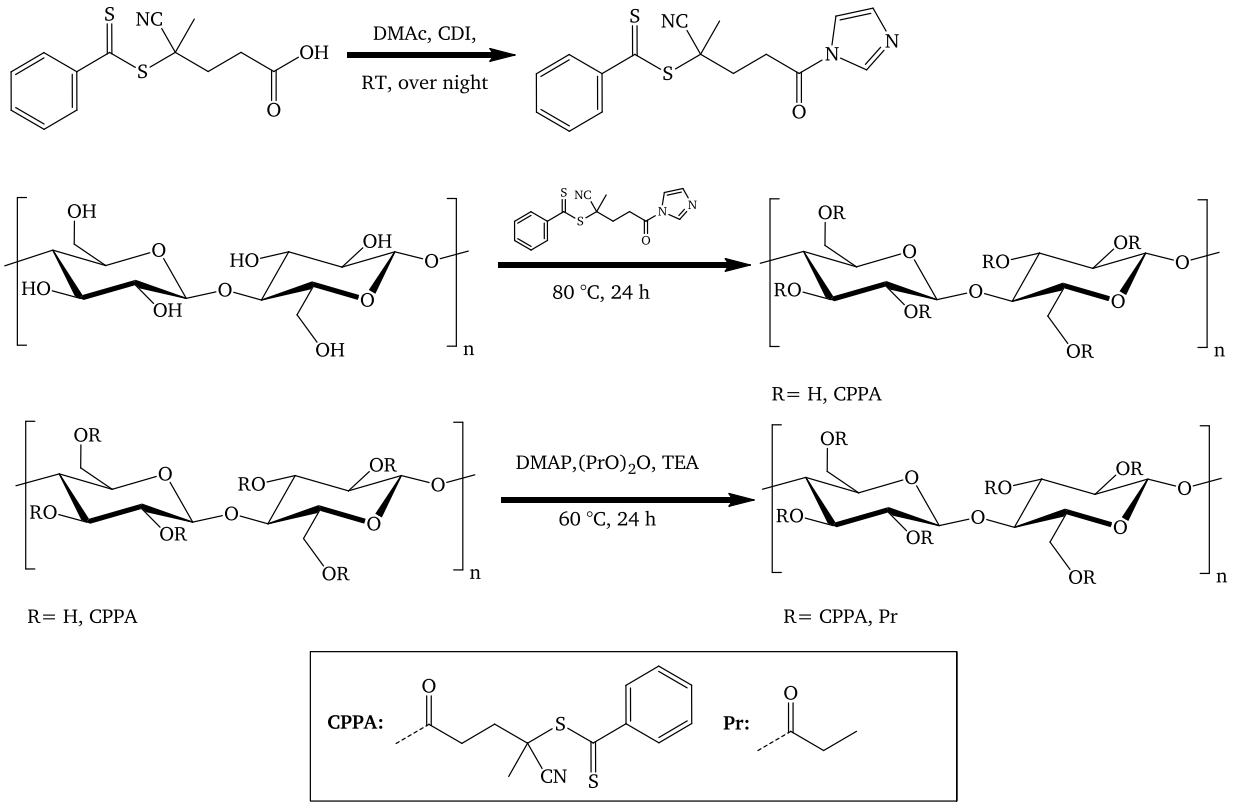

Figure 35. Reaction scheme for the synthesis of well-soluble cellulose macro-CTA, obtained by esterification of cellulose with CPPA and propionic acid anhydride. In the first step, the carboxyl group of CPPA is activated with CDI over night at room temperature, followed by esterification of dissolved cellulose for 24 hours at 80 °C in the second step. Finally, a total esterification of residual OH-groups is achieved by addition of an excess of propionic acid anhydride for 24 hours at 60 °C.

The highly substituted products were found to be well soluble in a variety of organic solvents including THF, dioxane, $CHCl_3$, DMF and DMSO. Subsequent analysis with ^{1}H-NMR (see **Figure 36**) showed pure substances with distinct signals of the cellulose protons (7H, 3.3-5.5 ppm) and therefore the cellulose derivatives could be well characterized with respect to DS values.

The DS value of propionic ester groups was determined by analysis of the integral intensity of the CH_2 and CH_3 group, while the DS value of CPPA was estimated by the integral intensity of the aromatic protons of the phenyl group. Furthermore ^{1}H-NMR analysis of various samples showed that a DS value for CPPA never exceeded 0.3 regardless of the molar feed of CPPA/CDI or extension of the reaction time. Therefore this value was considered an intrinsic threshold, eventually due to steric hindrance of the bulky CPPA moiety, which limits accessibility of the respective OH-groups.

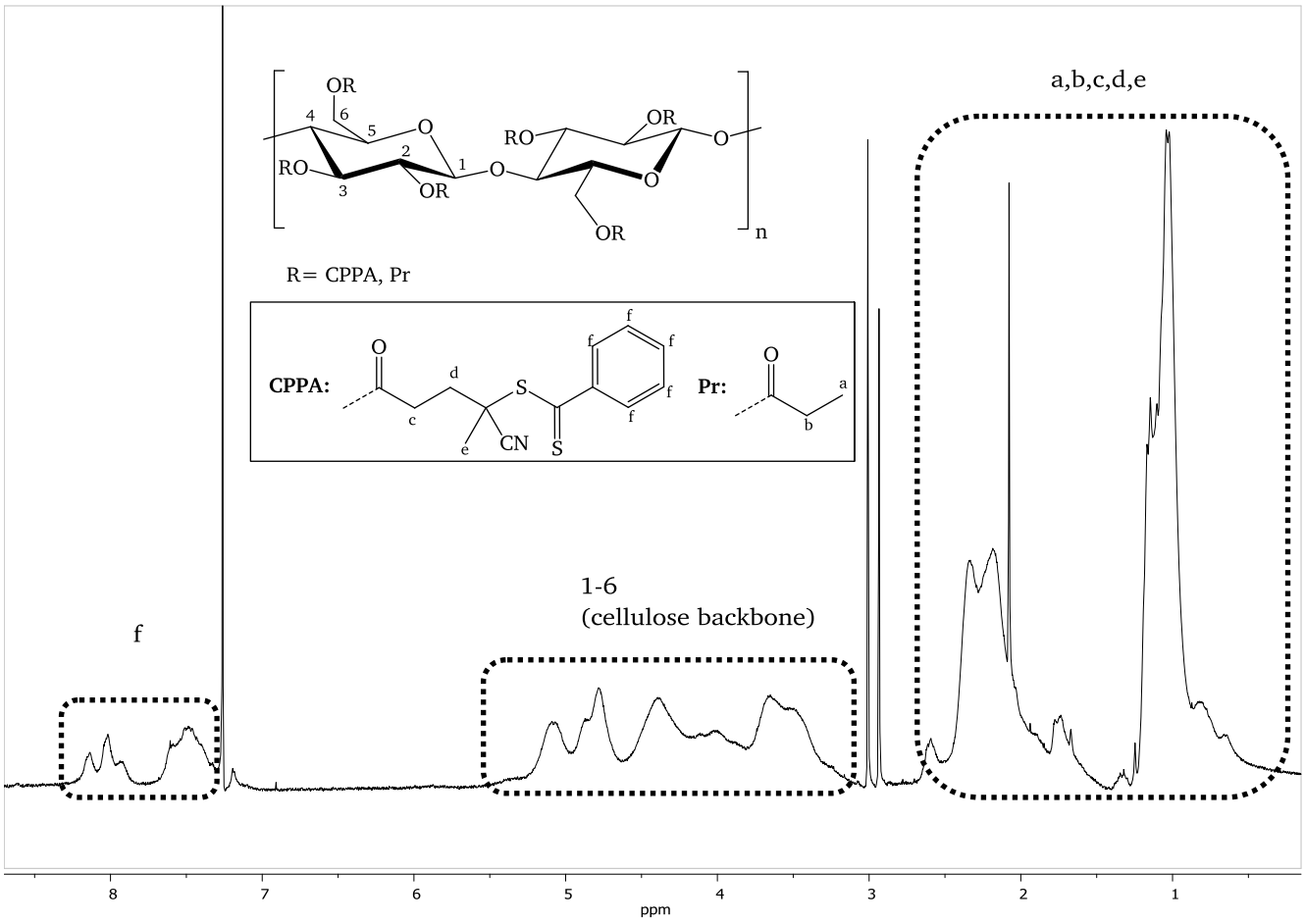

Figure 36. ^{1}H-NMR spectrum of cellulose macro-CTA (experiment MCC-CPPA16-Pr), referenced against $CDCl_3$ (7.26 ppm). The DS values of propionic ester groups and immobilized CTA were calculated from the integers relative to the cellulose backbone. DS(CTA) = 0.3, DS(Pr) = 2.7.

The cellulose macro-CTAs were next used for several graft copolymerization experiments with DMAA and styrene (chapter 9.1 and 5.1). Strong deviations in the amount of grafted polymer in comparison to theoretical (calculated) values indicated problems with the reaction conditions of the cellulose graft copolymerization. We assumed that the reaction conditions (monomer concentration, Initiator/CTA ratio, ect.) needed to be optimized in order to gain more reproducible results. We investigated several reaction conditions for the polymerization. For this, a set of RAFT polymerization experiments was performed using free CTA, resulting in well-defined homopolymers (chapter 5.1). However, the problem of insufficient control of RAFT polymerization on cellulose macro-CTA could not be solved.

We assumed limitations in the applied macro-CTA system originated from side reactions resulting in deactivation of CTA immobilized on the cellulose backbone. This is why attention was paid to the analysis of the typical functional groups of the CPPA on the cellulose macro-CTAs, especially the nitrile group and the dithioester group. Thus, the samples were analyzed via RAMAN IR-spectroscopy by Krasimir Kantchev in the working group of Prof. Dr.-Ing. Vogel, with focus on the nitrile (**Figure 37**), C=S (**Figure 38**) and C-S (**Figure 39**) bands.

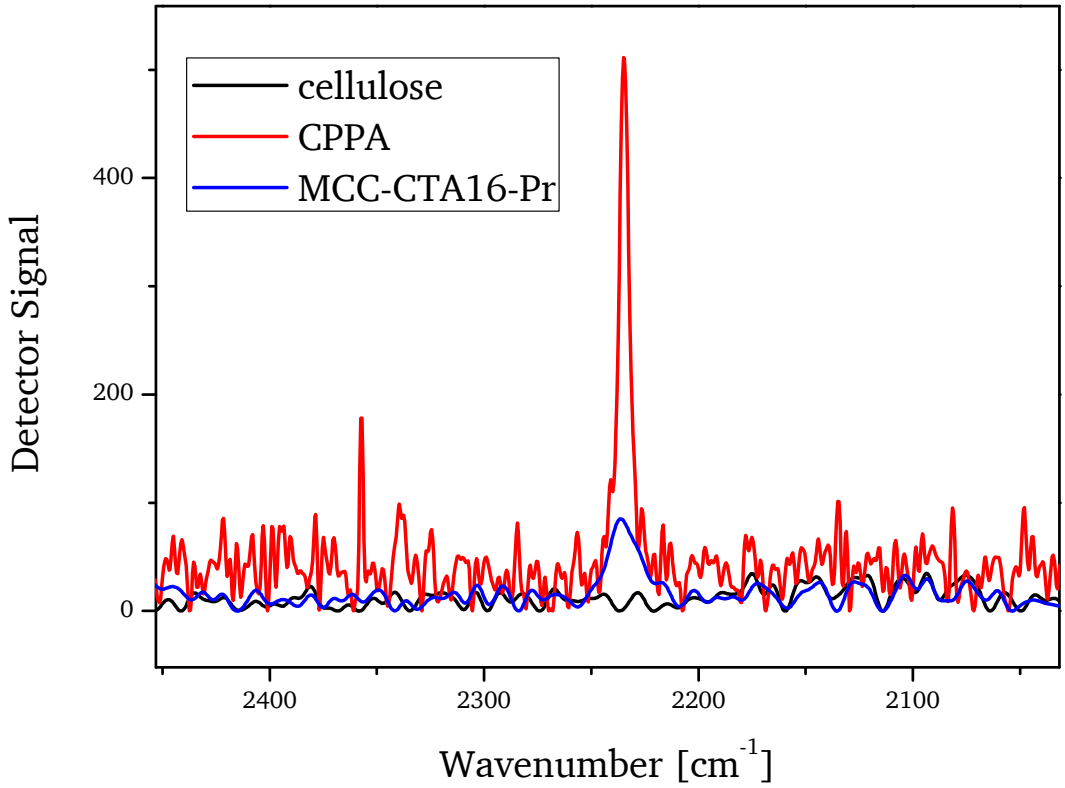

Figure 37. RAMAN spectra for the comparison of pure MCC, pure CPPA and cellulose macro-CTA "MCC-CPPA16-Pr". The signals at 2240 cm^{-1} is attributed to the nitrile functionality on the CTA.

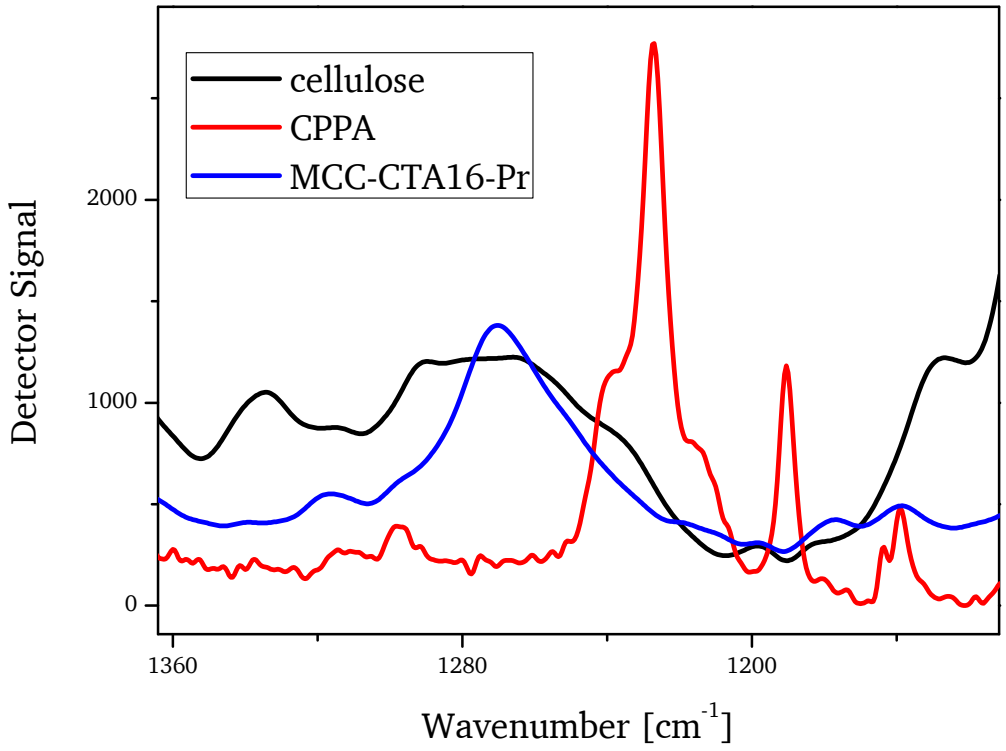

Figure 38. RAMAN spectra for the comparison of pure MCC, pure CPPA and cellulose macro-CTA "MCC-CPPA16-Pr". The signal at 1230 cm^{-1} is attributed to the C=S functionality on the CTA. However the cellulose macro-CTA does not clearly show a distinct signal in this range. Thus the existence of dithioester groups may not be definitely confirmed by this method.

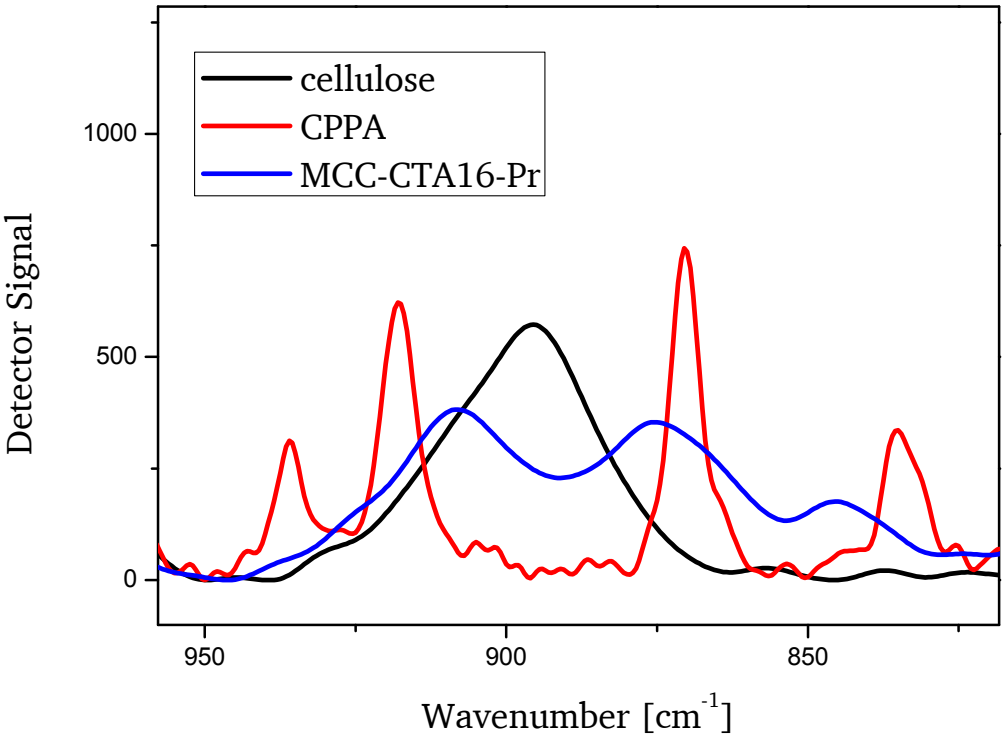

Figure 39. RAMAN spectra for the comparison of pure MCC, pure CPPA and cellulose macro-CTA "MCC-CPPA16-Pr". The signals at 870 cm^{-1} and 920 cm^{-1} are attributed to the C-S functionality on the CTA.The cellulose macro-CTA sample shows a similar signal pattern. This may be taken as indication for the existence of C-S single bond containing species such as dithioester functionality.

The spectroscopic analysis revealed that nitrile bands and the C-S bands were observed, but not the C=S band belonging to the CTA. This contradictory observation was not clear from first view. Therefore an additional reference experiment was carried out, where the existence of a C=S band should be validated via ^{13}C-NMR. A reaction of CPPA with CDI was performed and subsequently analyzed with ^{13}C-NMR. The corresponding spectrum is shown in **Figure 40**. When the product is compared with the spectrum of CPPA, the typical signal for the dithio-carbon atom at 222.3 ppm disappeared after reaction with CDI. Instead a new signal at 202.5 ppm appeared. Incremental calculations supports the assumption, that the dithioester functionality was transformed into another chemical species (denoted a “2”), which is also shown in the figure as insert scheme.

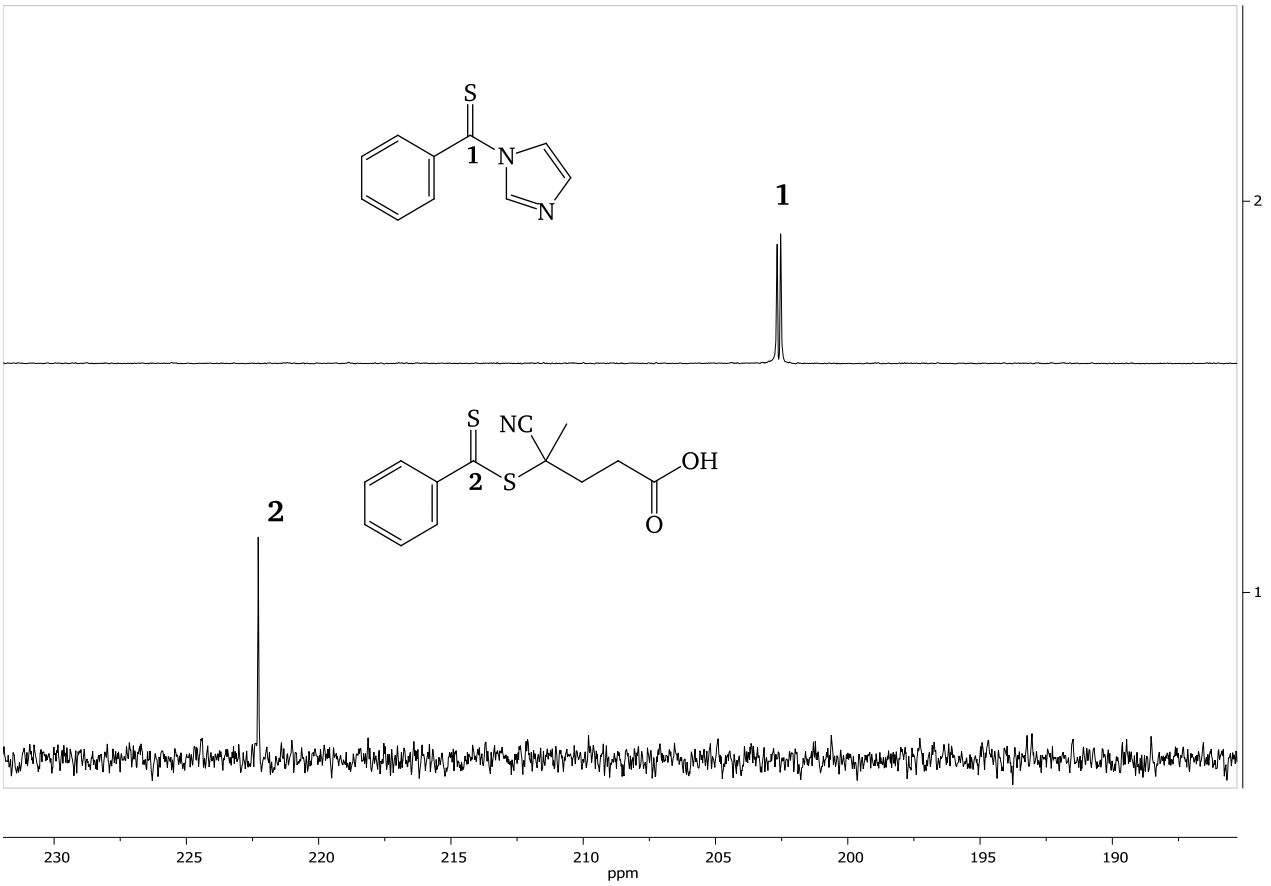

Figure 40. ^{13}C-NMR spectra of CPPA and after the reaction with CDI at room temperature (top) and CPPA before the reaction as reference (bottom). Note: the assignments of the C=S carbon atoms were validated by incremental calculations with ChemDraw.

If all analytical results of ^{13}C-NMR, ^{1}H-NMR, SEC and RAMAN are compared, we can conclude that the cellulose macro-CTAs are assumed to consist out of different substituents, of which are some RAFT active and others RAFT inactive. We assume the following structures, which are displayed in **Figure 41**.

- Thioalcohol species **(A)** originated from cleavage of the dithioester after successful esterification of the CTA onto cellulose (verified via RAMAN)
- When the species 2 in **Figure 40** reacts with the hydroxyl moieties of cellulose, we would expect the formation of a thionester (verified with ^{13}C-NMR)**(B)**.
- CTA functionality on cellulose macro-CTA (verified by successful grafting , chapter 9.1) **(C)**

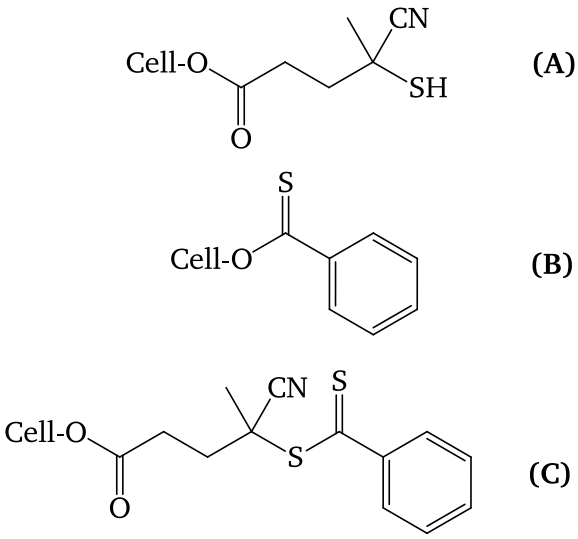

Figure 41. Observed chemical moieties on cellulose macro-CTA originated by side reactions of CPPA with CDI. Nitrile containing species **(A)** (verified with RAMAN), aromatic species **(B)** (verified with ^{1}H-NMR, C-NMR), immobilized CPPA **(C)** (verified with SEC via molar mass increase after graft copolymerization; see chapter 9.1)

Having a mixture of all these different chemical species, quantitative characterization is not trivial. Even more important, due to side reactions of the CTA on the cellulose, the cellulose macro-CTA has limitations in its grafting density because of RAFT-inactive chemical species blocking the hydroxyl sites for active CTA groups. Thus, this approach for CTA immobilization was not further investigated and subsequent experiments focused on an alternative route for cellulose functionalization using trithiocarbonate-based CTA, as presented in the following chapter.

4.2. Synthesis of trithiocarbonate modified cellulose macro-CTA

The functionalization of cellulose using activation agents and dithioester included side reactions (as shown in the previous chapter), thus an alternative approach, such as a step-wise synthesis of CTA on cellulose, had to be found. The stepwise build-up of a dithioester on cellulose as reported by others typically includes metal organic chemistry such as Grignard reactions on cellulose, which is not trivial for the synthesis of cellulose derivatives and which has been shown to have limited success [81, 82]. A different class of CTA, trithiocarbonate, was chosen instead because it requires synthetic protocols that have been applied successfully on cellulose like the modification of cellulose with halogen alkanes as precursor for ATRP reactions, as described by Raus et al. [49]. Furthermore the synthesis of small-molecule trithiocarbonate based CTA has shown nice features like convenient synthesis with high conversions and easy purification [83], thus we tried to transfer these protocols to the application on cellulose, as schematically shown in **Figure 42**.

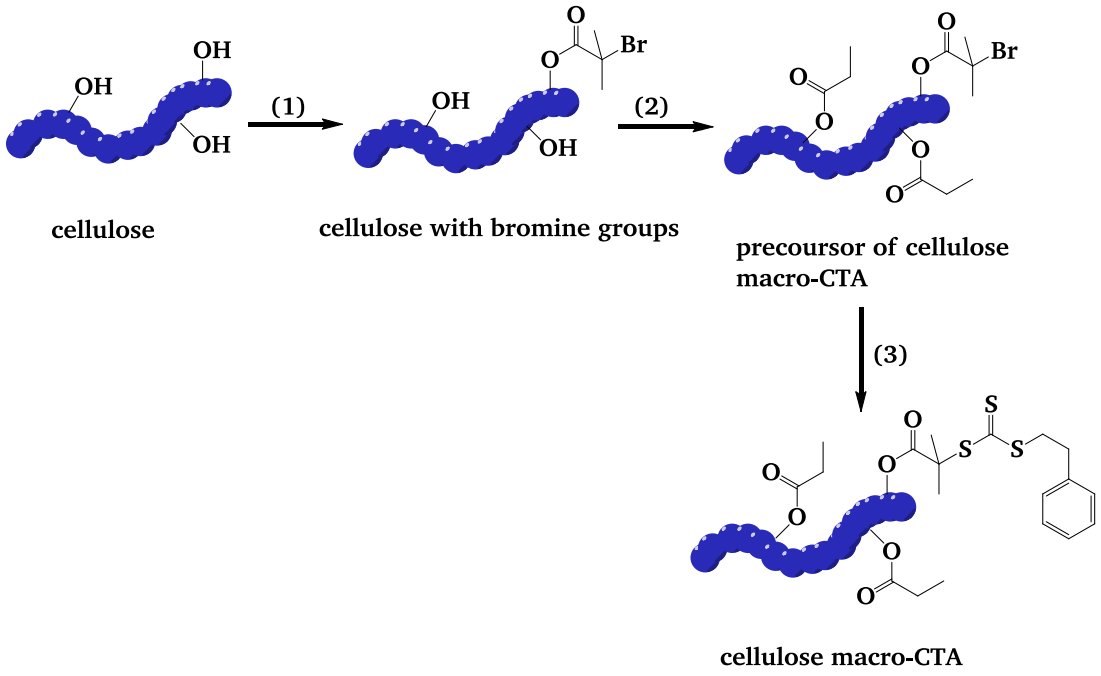

Figure 42. Synthesis strategy of the transformation of cellulose into cellulose macro-CTA.

The following synthesis protocols, presented in chapter 4.2.1 based on a three step procedure, involving the attachment of bromine containing esters **(1)** as precursor of the CTA functionality and the complete esterification of remaining hydroxyl groups **(2)**, followed by partial transformation of bromine functionalities into CTA **(3)** in a third step. We modified cellulose with bromo-isobutyro ester (BiB) as CTA precursor because CTAs which carry a tertiary carbon atom on the trithiocarbonate function typically show excellent performance during the RAFT polymerization and feature fast equilibration and low dispersity.

4.2.1. Cellulose macro-CTA with bromo-isobutyro moiety as R-group

Synthesis of free CTA ("PE-BiB-Me-TTC")

Free CTA was synthesized under similar reaction conditions as described by O'Reilly et al.[83]. The reaction is displayed in **Figure 43**.

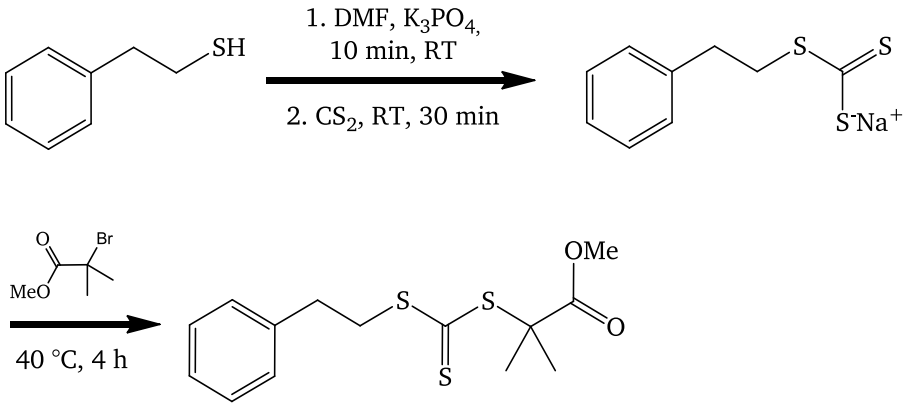

Figure 43. Reaction conditions of the synthesis of free trithiocarbonate-based CTA (experiment "PE-BiB-Me-TTC").

In the first step, trithiocarboxylate was generated in-situ by reaction of phenylethyl mercaptane with carbon disulfide, followed by a nucleophilic displacement reaction on 2-bromo-isobutyric acid methyl ester. After purification by extraction yields of about 80 % were obtained. Subsequently the chemical identity and purity were confirmed using ^{1}H-NMR.

Synthesis of the cellulose macro-CTA precursor ("MCC-BiB-Pr")

The modification of cellulose with bromo-isobutyro functionalities was performed according to a protocol from Raus et al. [49]. The application of this procedure included a reaction temperature of 50 °C after addition of the bromo-isobutyro bromide (BiBB). When these reaction conditions were used, coloration/blackening of the reaction mixture was observed within minutes. This indicates side reactions and degradation of the cellulose. Thus, a temperature of about 5 °C was used during addition BiBB and then the reaction continued overnight at room temperature, as shown in **Figure 44**.

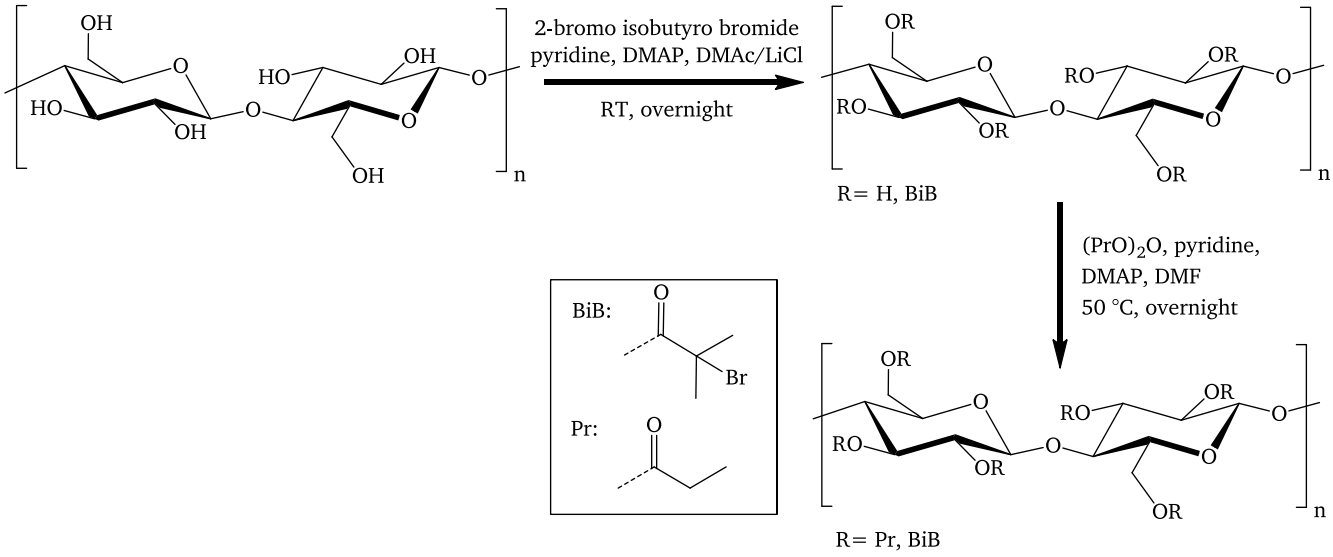

Figure 44. Schematic illustration of a two-step synthesis of well soluble cellulose mixed ester containing 2-bromo-isobutyro and propionic ester groups.

This modification of the reaction conditions minimized the coloration of the reaction mixture and was further reduced when BiBB was diluted in DMAc and added slowly to the cellulose solution. After the reaction the product was isolated by precipitation and washing with water followed by drying. The resulting pale orange solid was swellable in $CHCl_3$, insoluble in THF, ethyl acetate or toluene but soluble in acetone, DMF and DMSO. In a second step, the cellulose was dissolved in DMF and remaining hydroxyl functions were completely esterified with propionic acid anhydride. This procedure was supposed to enhance solubility (in solvents such as toluene and THF) and avoid formation of xanthates in later reaction steps when CS_2 is applied for the transformation of bromo-isobutyro moieties into CTA.

^{1}H-NMR analysis (**Figure 45**) showed a clean product with distinct signals of isobutyric ester groups and propionic ester groups. DS values were estimated by comparison of the respective integral intensities with the cellulose backbone protons (7H, 3.5-5.3 ppm). DS(BiB) = 2.2; DS(Pr) = 0.8

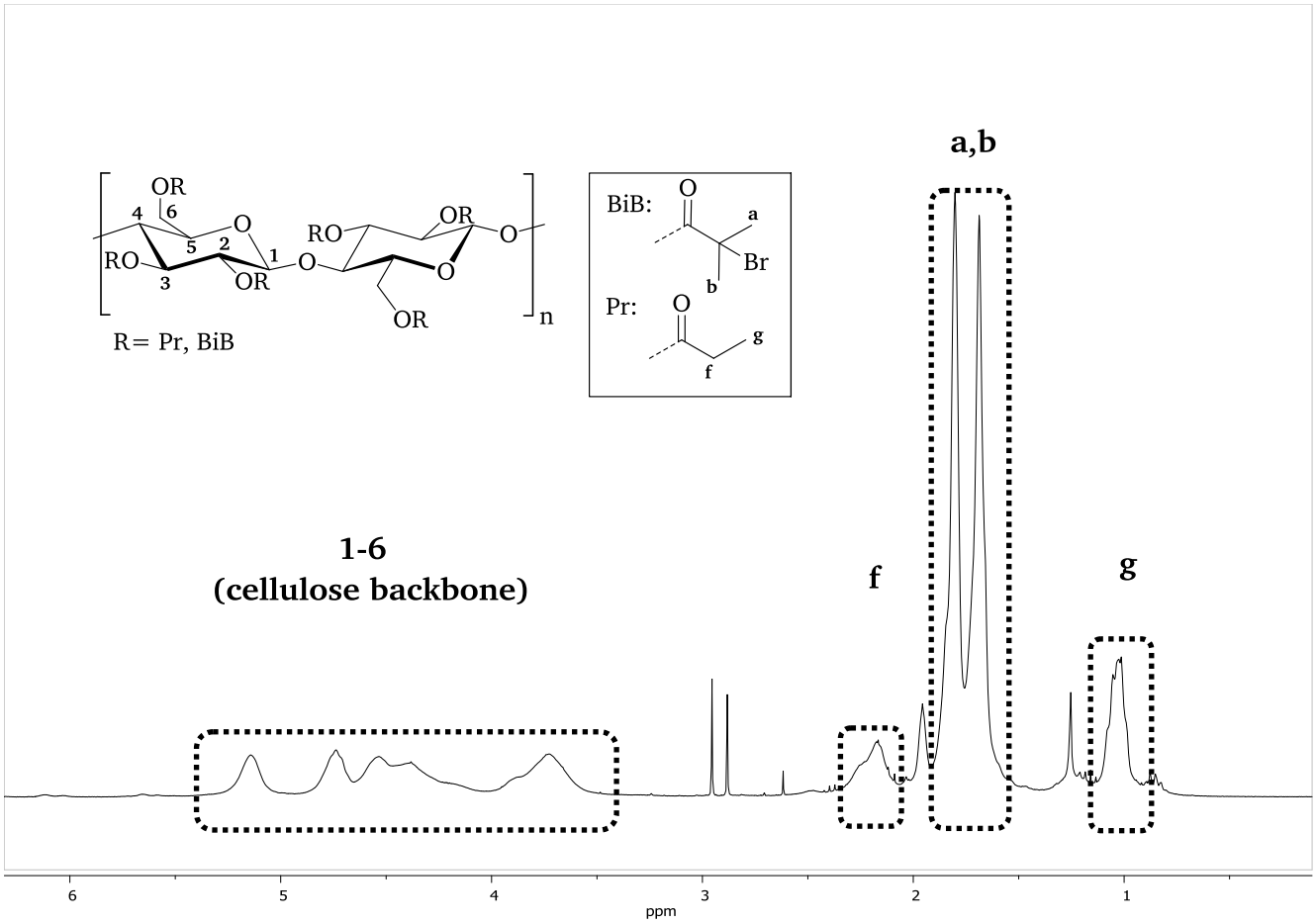

Figure 45.[1]H-NMR spectrum of cellulose mixed ester containing 2-bromo propionic and propionic ester functionalities, measured in $CDCl_3$ (7.26 ppm).

Synthesis of the cellulose macro-CTA ("MCC-CTA3" – "MCC-CTA5")

The halogen functionality of BiB was next transformed into the corresponding thiocarbonate. The corresponding thiocarboxylate was synthesized in-situ prior to the modification of cellulose, as displayed in **Figure 46**.

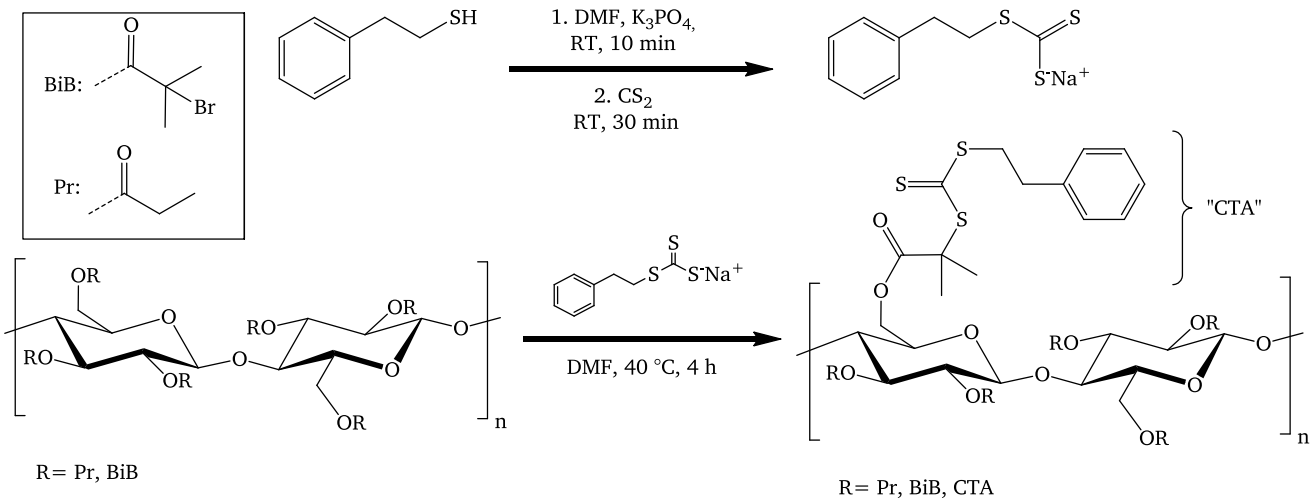

Figure 46. Reaction conditions for the transformation of the bromine functionality on cellulose into CTA.

Phenylethyl mercaptane was coupled with CS_2 in absolute DMF as organic solvent under basic conditions to generate a thiocarboxylate, which than reacts with the bromine functionalities of the cellulose. DS values of CTA were determined via ^{1}H-NMR by the ratio of the aromatic protons and the cellulose protons (**Figure 47**).

The DS(CTA) of the products varied between 0.08 and 0.13, regardless of the molar feed of thiocarboxylate (see **Table 3**). A relative standard error of 5 % of the integral intensity was assumed, which is a typical value for ^{1}H-NMR analysis[2].

Table 3. Dependence of the DS(CTA) in respect to the molar ratio of carboxylate relative to anhydroglucose units.

Experiment	equiv. PE-SH/CS_2/K_3PO_4	DS(CTA)
MCC-CTA3	3/9/3	0.09 ± 0.0045
MCC-CTA4	0.4/1.2/0.4	0.13 ± 0.0065
MCC-CTA5	10/30/10	0.08 ± 0.0040

[2] www.analytik.ethz.**ch**/vorlesungen/biopharm/Spektroskopie/**NMR**.pdf , *19.08.2016.*

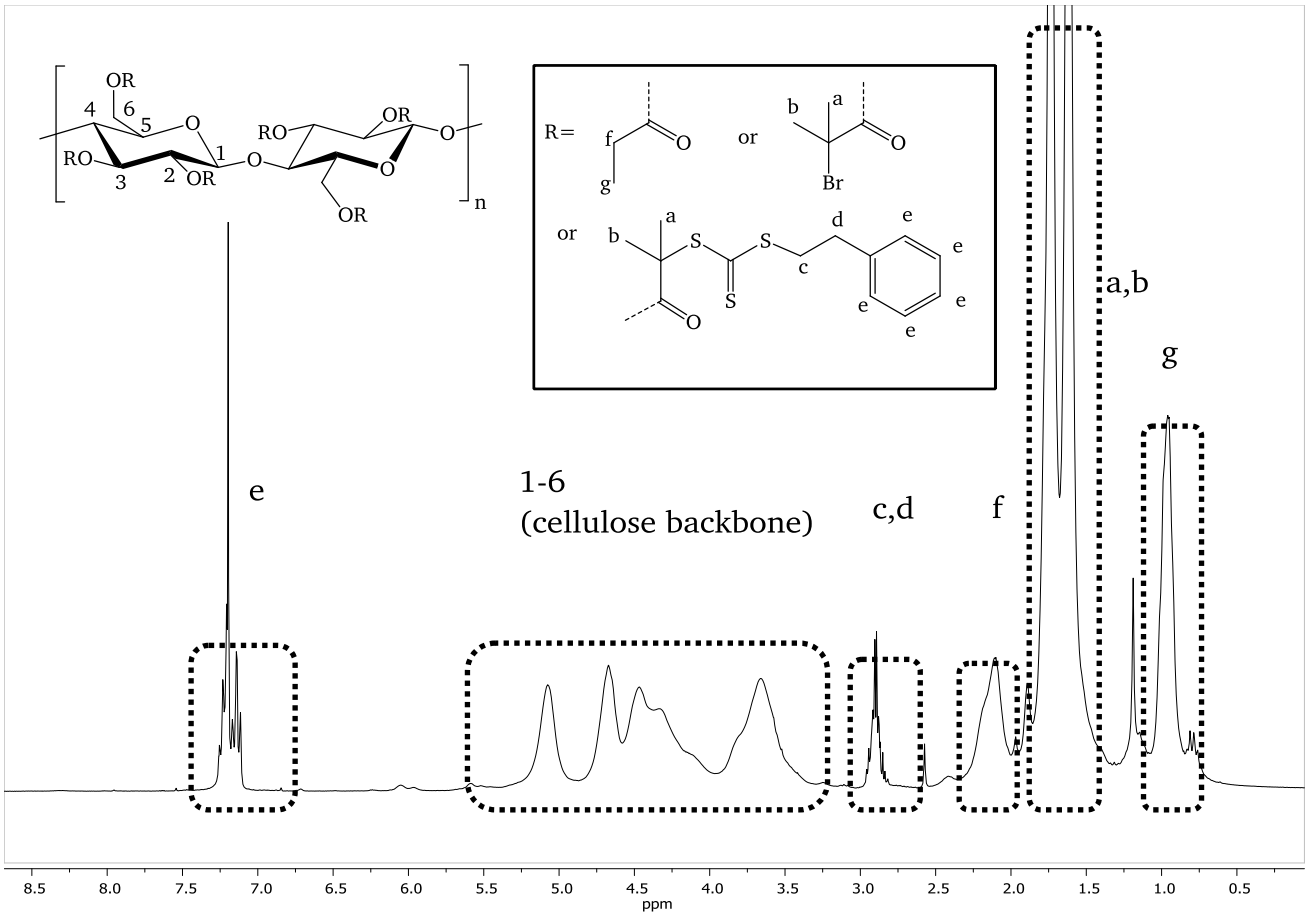

Figure 47. Typical ^{1}H-NMR spectrum of a cellulose macro-CTA derived from bromoisobutyo-functionalized cellulose, measured in $CDCl_3$ (7.26 ppm).

It was assumed that low DS values could originate from a limited chemical availability resulting from the covalent attachment of the 2-bromo-isobutyl group onto the cellulose polymer. As consequence further experiments for cellulose modification were performed with 2-bromopropionic ester groups as functional group. This molecule features a secondary halogen carbon, which presumably should be more reactive towards chemical transformation.

4.2.2. Cellulose macro-CTA with 2-bromo-propionyl moiety as R-group

Synthesis of the cellulose macro-CTA precursor ("MCC-BpB4-Pr")

To validate the hypothesis, that low CTA contents on 2-bromoisobutyro-modified cellulose are caused by steric hindrance, the bromo-containing moiety was changed. The new synthesis followed the same protocol described in chapter 4.2.1, but BpB (2-bromopropionyl bromide) was used instead of 2-bromoisobutyro bromide.

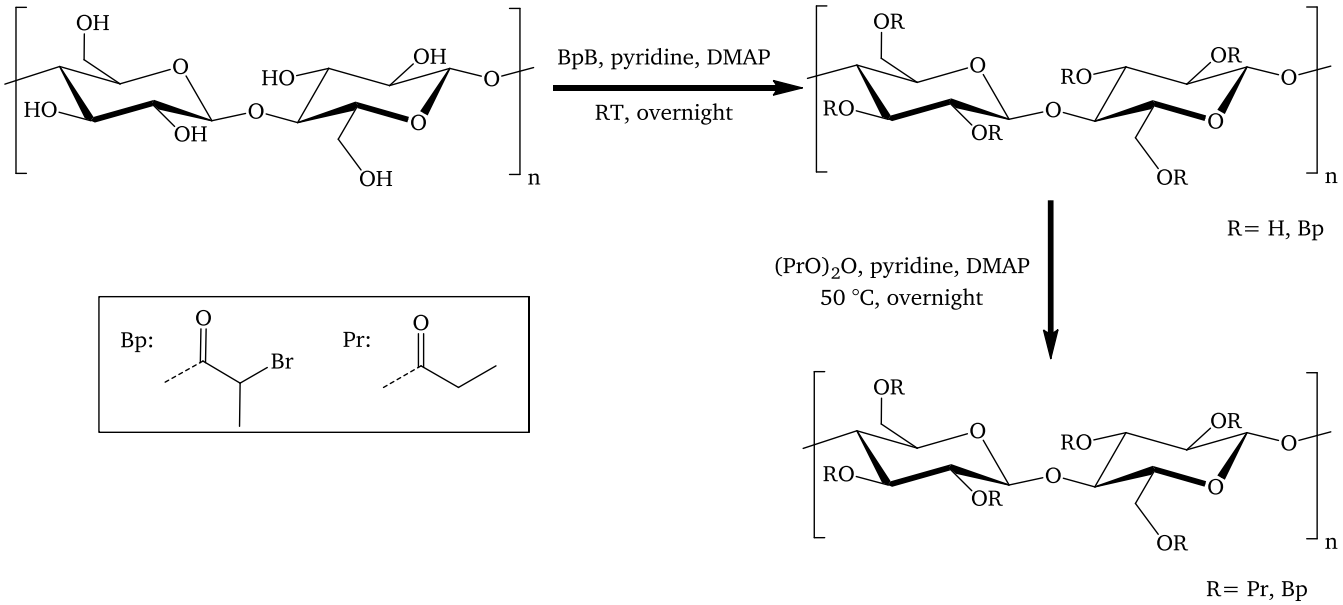

Figure 48. Two-step synthesis of well soluble bromo-functionalized cellulose mixed ester.

After esterification with propionic acid anhydride the DS values of 2-bromopropionyl and propionyl groups were calculated from ^{1}H-NMR data, the spectrum is shown in **Figure 49**. The ratio of the integers was 1:1 with a DS(total) = 3.2, which, of course is chemically not possible, but originates from various factors during sample preparation, analysis and interpretation of the spectra, as discussed in chapter 3.3.1.

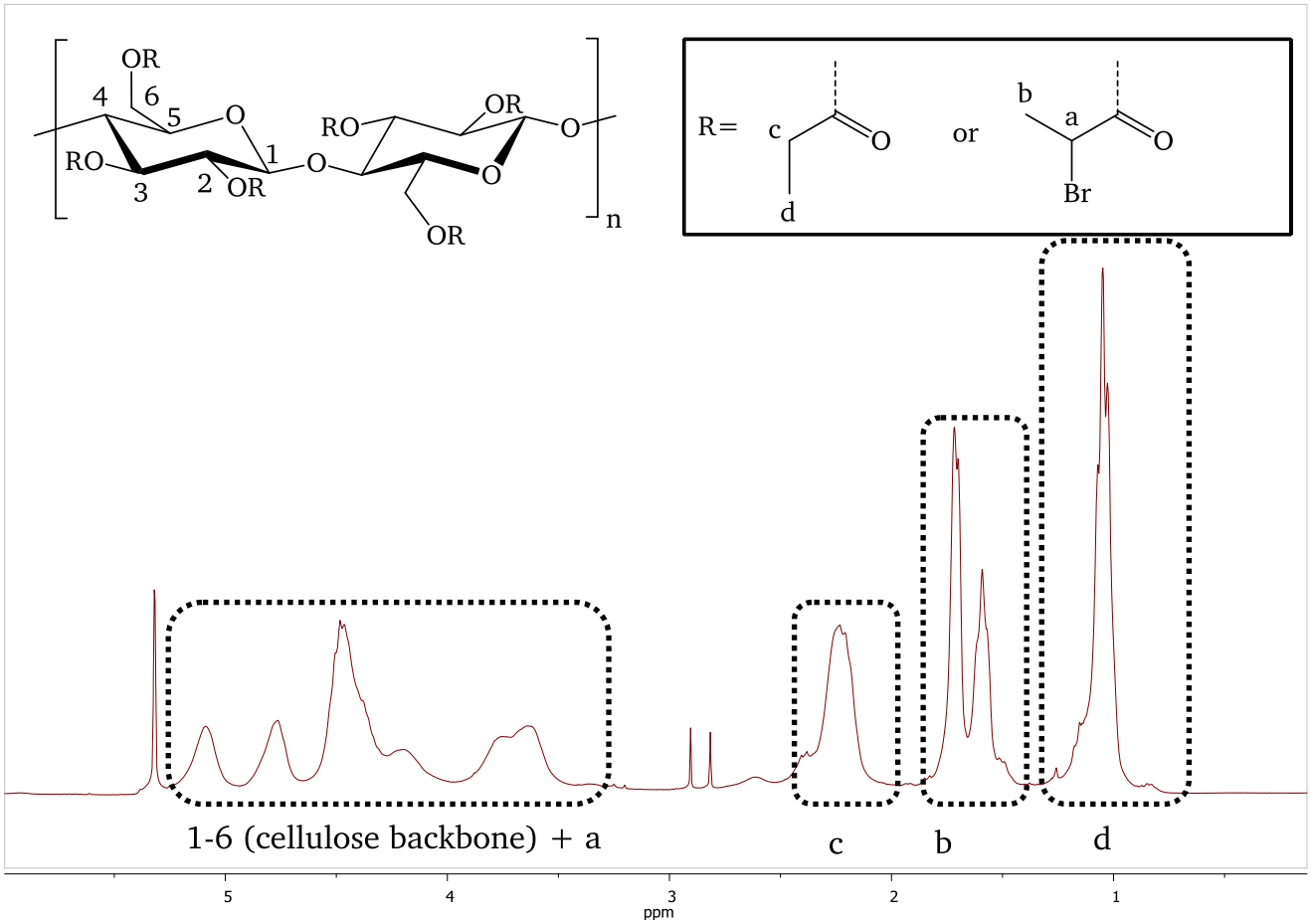

Figure 49. ^{1}H-NMR spectrum and the assignment of the signals of the cellulose macro-CTA precoursor "MCC-BpB4-Pr".

A complete esterification was assumed with a DS(total) = 3, leading to DS(Pr) = 1.5, DS(Bp) = 1.5. The complete esterification of the cellulose was verified by ATR-IR, where no remaining hydroxyl groups could be detected (**Figure 50**).

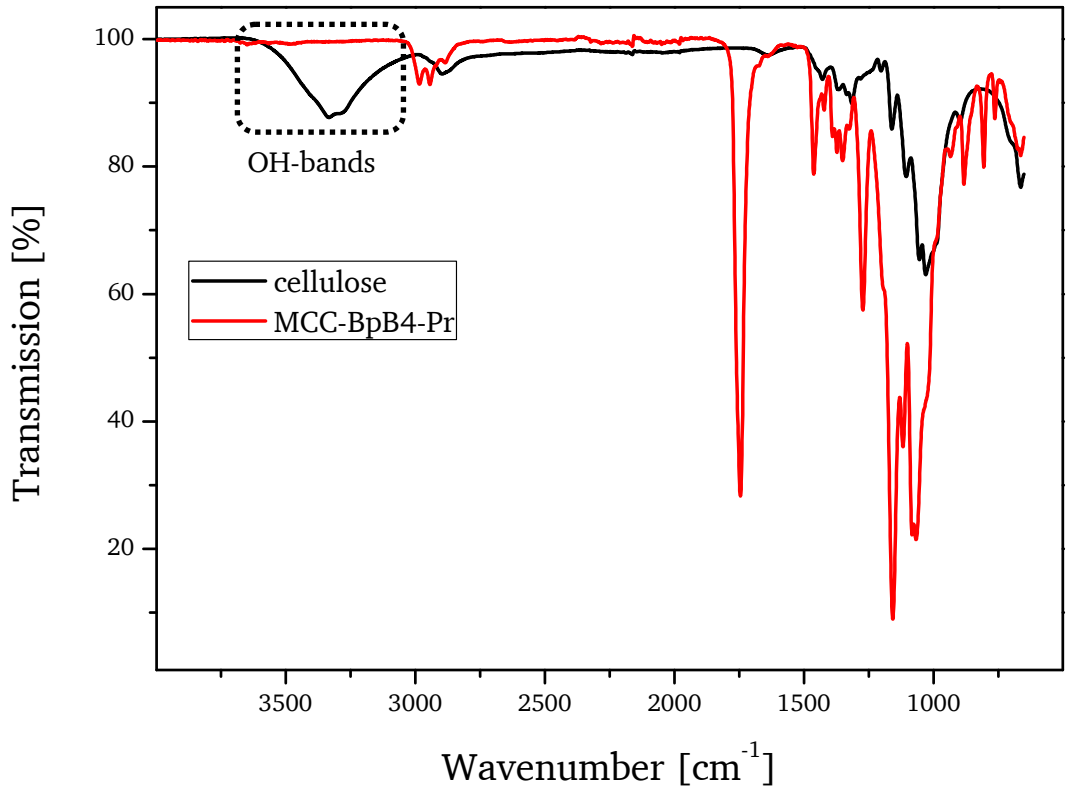

Figure 50. Exemplary ATR-IR spectra of cellulose and of a cellulose derivative containing 2-bromopropionyl and propionyl moieties. As concerning for the cellulose derivative, no absorption at wave numbers >3000cm^{-1} indicates no remaining hydroxyl groups and thus a complete substitution of the cellulose.

Synthesis of the cellulose macro-CTA (MCC-CTA12 – MCC-CTA16)

The transformation of bromine functions into the corresponding CTA groups was performed as a two-step one pot reaction, as shown in **Figure 51**.

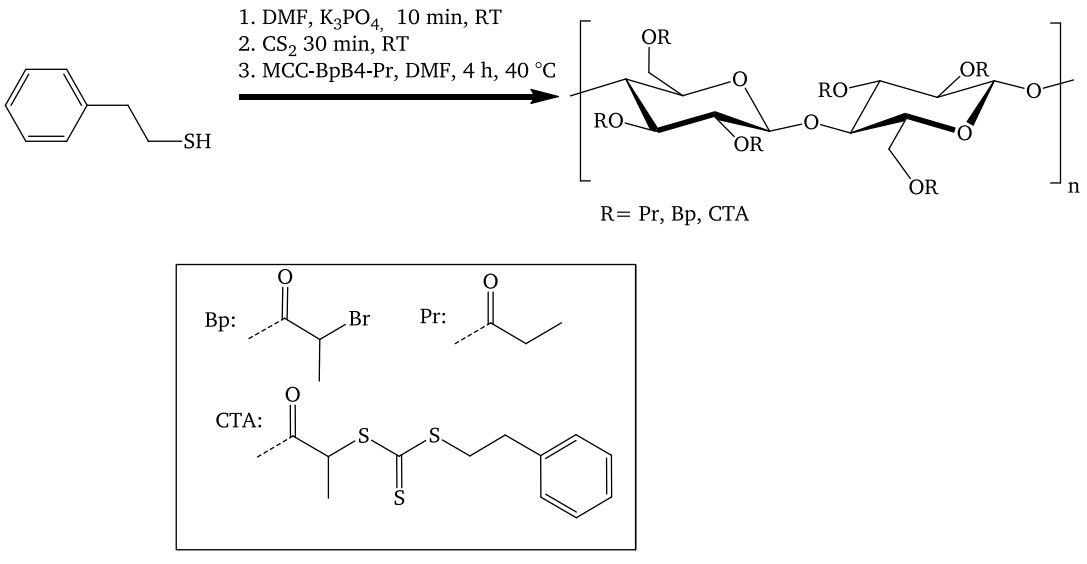

Figure 51. Synthesis of cellulose macro-CTA derived from 2-bromopropionyl moieties.

The synthesis was performed under the same reaction conditions as described in chapter 4.2.1. The DS(CTA) values were determined with ^{1}H-NMR, the corresponding spectrum is displayed in **Figure 23**, see chapter 3.3.1. Determination of the DS was done according to chapter 3.3.1. The results were validated by sulfur elemental analysis. The analytical data is summarized in **Table 4**. Here it can be seen that DS(CTA) values obtained by ^{1}H-NMR and elemental analysis were very similar, proving the suitability of ^{1}H-NMR analysis for the determination of the DS(CTA). Note, a relative error of about 5% was assumed, which is typically obtained in standard ^{1}H-NMR analysis.[3] The elemental analysis measurements and the relative error were provided by the "Forschungszentrum Jülich". By variation of the molar feed of thiocarboxylate (generated in-situ in the first step), the DS(CTA) could be adjusted between 0.25 and 0.56. All attempts to convert bromine completely into CTA groups failed because insoluble products were generated (experiments MCC-CTA8 and MCC-CTA11B). However, it was not further investigated up to which DS(CTA) the cellulose macro-CTAs remained soluble. Instead, the cellulose sample MCC-CTA14, which contained the highest amount of CTA, was used for subsequent graft polymerizations (chapter 5.3).

Table 4. Comparison of the DS(CTA) values calculated from ^{1}H-NMR and EA analysis.

sample	M_{AGU}	DS(CTA, ^{1}H-NMR)	DS(CTA, sulfur EA)
MCC-CTA15	484	0.25± 0.013	0.23± 0.002
MCC-CTA12	507	0.36± 0.018	0.40± 0.004
MCC-CTA14	528	0.54± 0.027	0.56± 0.011

[3] www.analytik.ethz.**ch**/vorlesungen/biopharm/Spektroskopie/**NMR**.pdf , *19.08.2016.*

5. Graft copolymerizations using cellulose macro-CTAs

5.1. Graft copolymerization of styrene with dithioester-modified cellulose macro-CTA

Initially, the graft copolymerization of cellulose macro-CTA with DMAA was pursued because of the convenient removal of water soluble PDMAA homopolymer from water insoluble graft copolymer. Further details regarding graft copolymerization with DMAA are discussed in the appendix. However, after several experiments it was concluded from the analytic data that the polymerization process had a low performance regarding kinetic control. This is why subsequent experiments were performed with styrene as model monomer, which offers advantages over DMMA also during the characterization of the corresponding polymers, i.e. commercially available polystyrene standards for SEC calibration.

Model experiments: RAFT polymerization of styrene using CPPA

Prior to graft copolymerization, the reaction conditions for the polymerization of styrene with free CTA "CPPA" were investigated in bulk and in solution, the general reaction scheme and the reaction conditions are displayed in **Figure 52**.

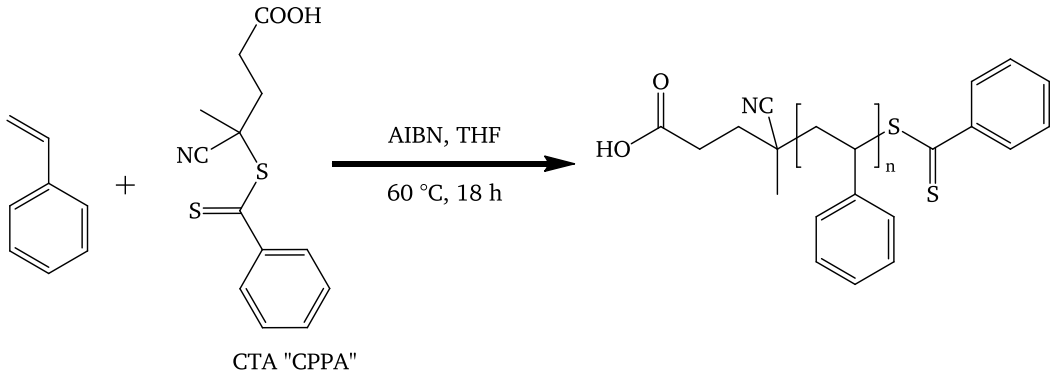

Figure 52. Reaction scheme with the reaction conditions which were used for RAFT mediated polymerization of styrene.

In several sets of experiments we investigated the effect of monomer concentration, the initiator concentration and the CTA concentration independently. We started with the variation of the monomer concentration, as presented in the next section.

A) Effect of monomer concentration on M_n and dispersity

The styrene concentration was varied by replacing defined amounts of monomer with THF. The total volume was kept constant at 10 ml. For example, the sample with 20 % partial volume of styrene was prepared by addition of 2 ml styrene into a Schlenk-flask. Then, stock solutions of CTA and AIBN in THF were added, followed by the addition of THF to gain a total volume of 10 ml. The reaction mixture was then deoxygenated by three pump-freeze-thaw cycles. The reaction vessel was then put into a preheated oil bath for a preset reaction time. The reaction was stopped by pouring the reaction mixture into methanol, where the polymer precipitated. Then the polymer was dried under vacuum. The resulting polymer was then analyzed with SEC. The average molar mass was determined by calibration against polystyrene standards (**Figure 53**).

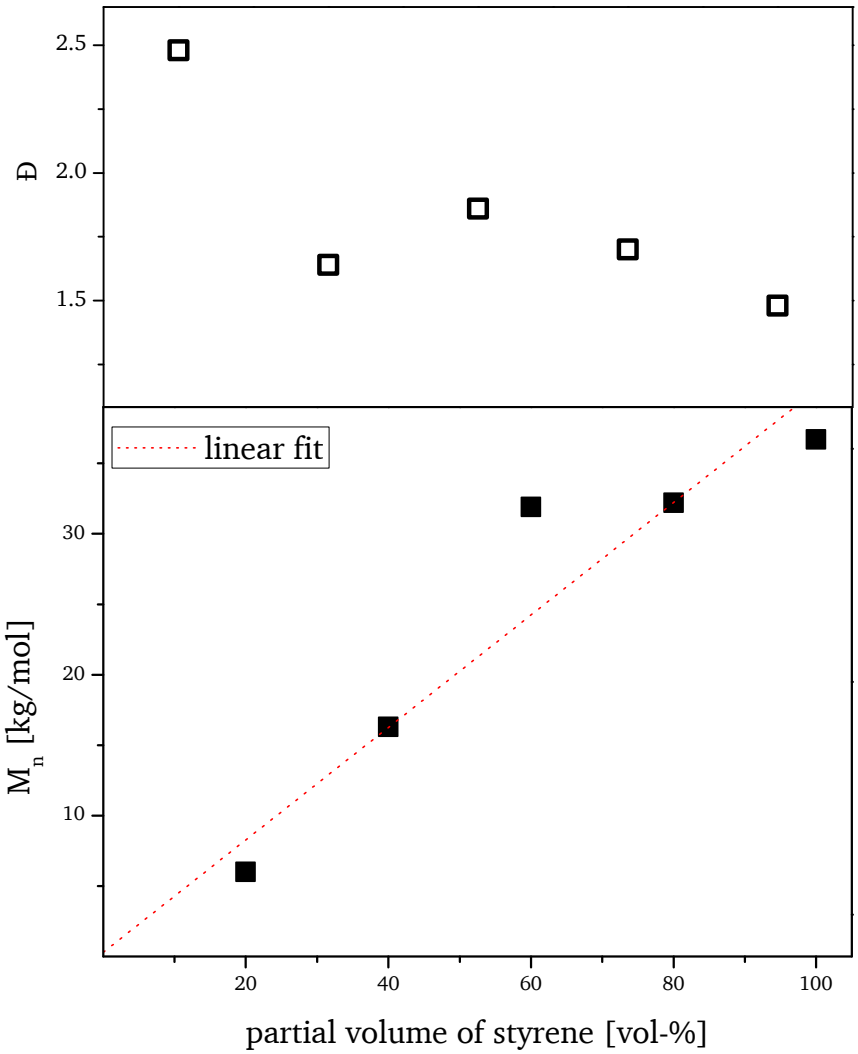

Figure 53. RAFT polymerization of styrene using CPPA. The concentration styrene was varied, whereas the other parameters were kept constant. [AIBN] = 2 mmol/L; [CTA] = 4 mmol/L; V(total) = 10 ml; T = 60 °C; t = 18 h; solvent: THF.

The outcome of this first polymerization series indicates a good correlation of the molar mass of PS with the initial monomer concentration in a linear fashion. However, there is no clear effect of the monomer concentration on the dispersity. The high dispersity values can be an indication for difficulties in the control of the process. A lower dispersity was obtained in bulk polymerization; thus the next set of experiments was conducted as bulk polymerization under the same reaction conditions.

B) Effect of initiator concentration on M_n and dispersity

In the next set of experiments the impact of the initiator concentration on M_n and Đ of the polymers was investigated. The polymerization was carried out in bulk, the CTA concentration was kept constant at 8.74 mmol/L, whereas the initiator concentration was varied between 2 and 10 mmol/L. The synthesis, purification and analysis were performed in the same way as described in the previous section. The analytical results are displayed in **Figure 54**.

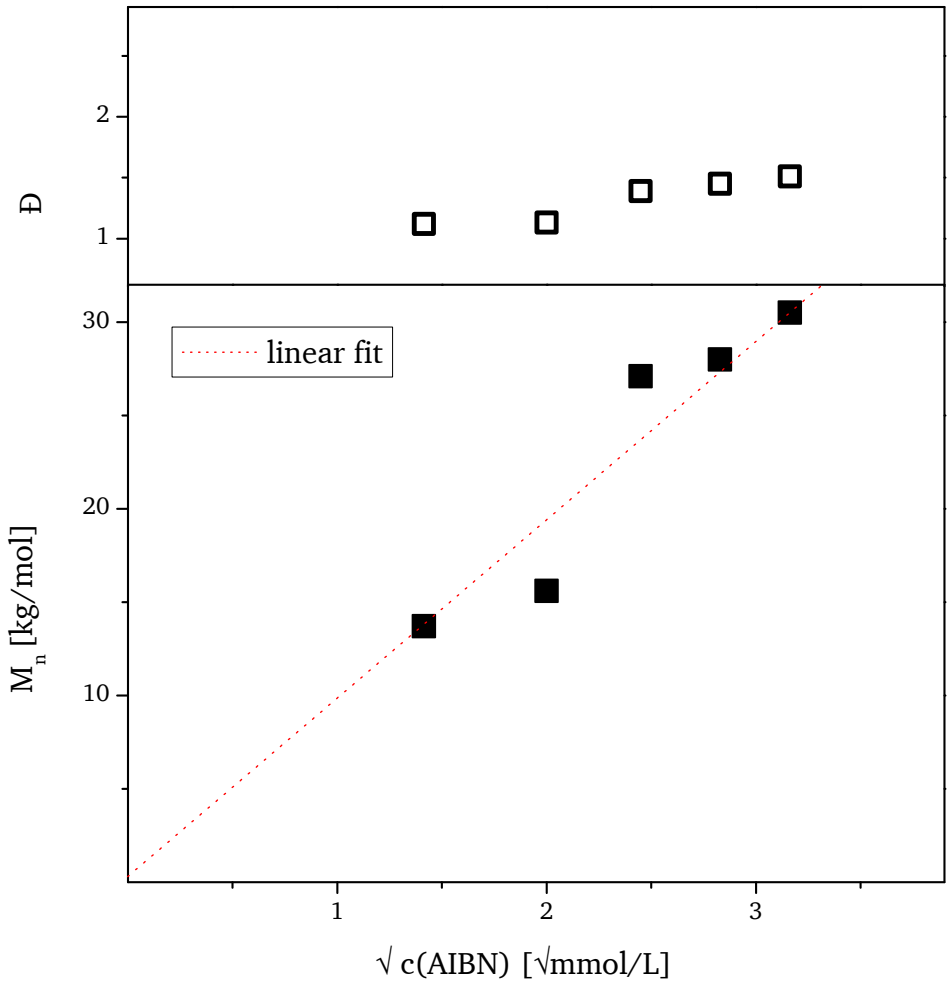

Figure 54. RAFT polymerization of styrene using CPPA. The concentration of initiator was varied; the other parameters were kept constant. Reaction conditions: [styrene] = 8.74 mol/L (bulk polymerization); [CTA] = 8.74 mmol/L; V(total) = 10 ml; T = 60 °C; t = 18 h.

From the presented data it can be concluded that increasing initiator concentrations lead to higher molar masses in a linear fashion with respect to the square root of the initiator concentration. As concerning for the kinetics of a RAFT mediated polymerization we consider the rate of chain propagation for a free radical polymerization defined as:

$$r_p = \frac{d[M]}{dt} = k_p\,[M] * \sqrt{[AIBN]} \tag{26}$$

When a constant rate of chain propagation is assumed (which is valid e.g. for low conversions, otherwise it's an approximation), the following equation may be taken:

$$\frac{[M]_0 * X_M}{\Delta t} = k_p\,[M] * \sqrt{[AIBN]} \tag{27}$$

With X_M as monomer conversion. The linear correlation between M_n and X_M has been discussed in the chapter *Mechanism of RAFT polymerization* (Eq. (5)). In brief, it can be defined as:

$$M_n \propto X_M \tag{28}$$

By inserting Eq. (28) into Eq. (27), a correlation between molar mass and initiator concentration is provided:

$$M_n \propto \sqrt{[AIBN]} \tag{29}$$

This is why we conclude that the analytic results are in good agreement to theoretical considerations. Furthermore, all resulting polymers had dispersity values lower than 1.5, indicating that the polymerization was much more controlled, if compared to the processes carried out in THF. Using AIBN concentrations of 4 mmol/L or less resulted in even lower dispersity of about 1.1. This phenomenon was attributed to the initial [CTA]/[AIBN] ratio of > 2:1, since it is well known from literature that the [CTA]/[AIBN]-ratio has a crucial effect on the dispersity of the polymer [84].

C) Effect of CTA concentration on M_n and dispersity

In the next set of experiments the impact of the CTA concentration on M_n and Đ of the polymers were investigated. The samples were synthesized under the same reaction conditions as described before. The CTA concentration was varied between 2-10 mmol/L, whereas the AIBN concentration was kept constant at 2 mmol/L and styrene as bulk. After 18 hours reaction time at 65 °C the polymers were isolated by precipitation in methanol with subsequent analysis with SEC. The resulting data is presented in **Figure 55**.

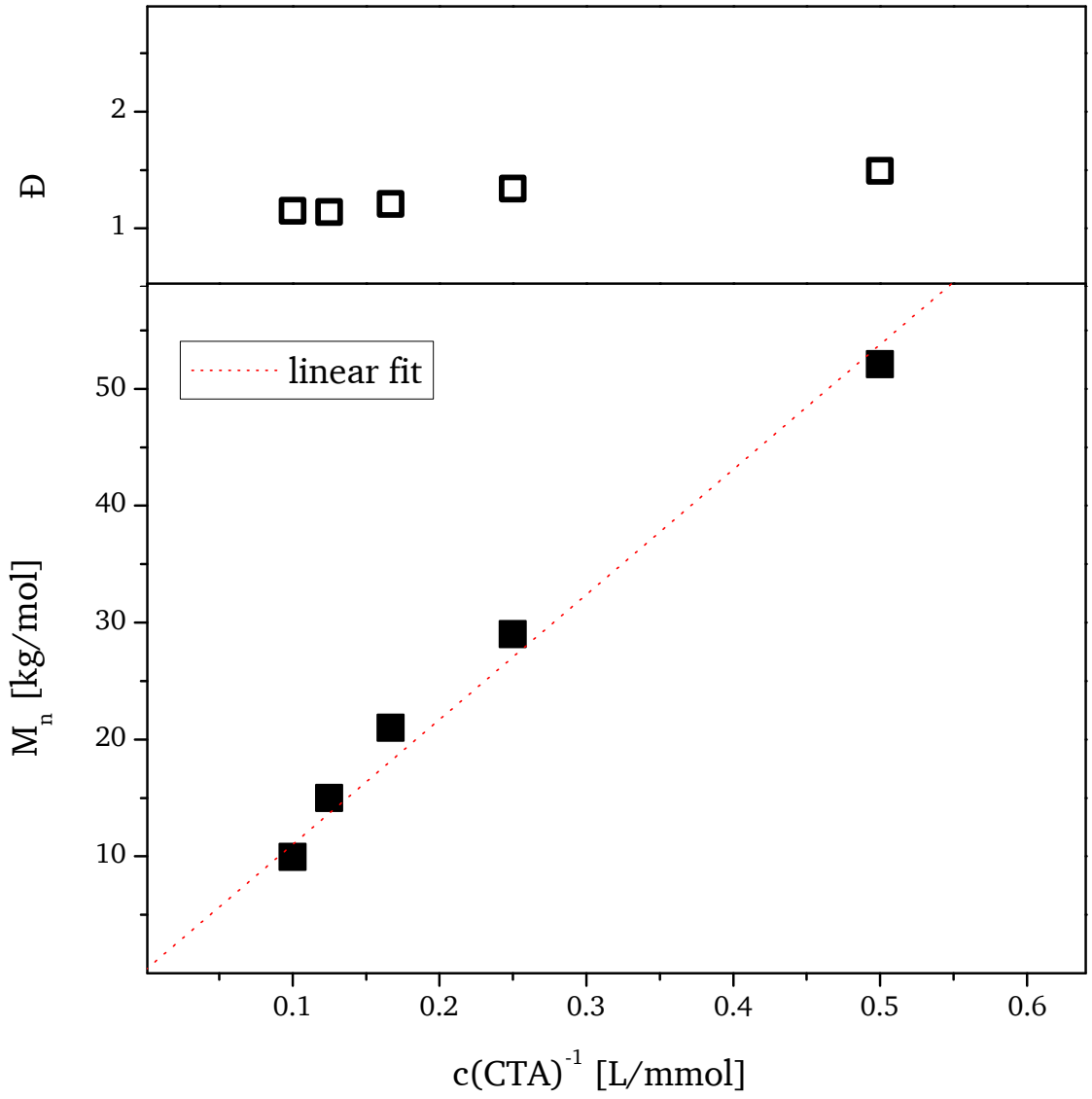

Figure 55. RAFT polymerization of styrene using CPPA. The concentration of initiator was varied; the other parameters were kept constant. Reaction conditions: [styrene] = 8.74 mol/L (bulk polymerization); [AIBN] = 2.0 mmol/L; V(total) =10 ml; T= 60 °C; t = 18h. Note, that polymer samples with low dispersity (<1.5) were obtained in all experiments. Especially low dispersity was observed when [CTA]/[AIBN] >2:1, which is provided for all datapoints with a reciprocal CTA concentration of <0.25.

For a better comprehension the molar mass was plotted against the reciprocal CTA concentration. The analytical data with SEC shows the expected behavior, where M_n and dispersity decrease with increasing CTA concentration. A linear regression with $R^2>0.99$ confirms the quality of the obtained data, since the data follows the theoretical correlation of molar mass and CTA concentration, as described by Eq. (5) in chapter 3.2.1:

$$M_n \propto \frac{1}{c(CTA)} \tag{30}$$

As concerning for the dispersity of the polymers, the variation of the CTA concentration agrees with the observations of the experimental setup B) with varying initiator concentrations, where narrow molar mass distributions were obtained, when the applied ratio [CTA]/[AIBN] exceeded 2:1.

From the three sets of experiments we concluded, that bulk polymerization at 65 °C for 18 hours reaction time with [CTA]/[AIBN] ratios > 2:1 should deliver good control for a RAFT polymerization of styrene. This finding is in agreement with a publication from Li et al [85] where CPPA anchored silica nano-particles showed excellent control of the graft copolymerization of styrene was obtained when low AIBN concentrations and high [CTA]/[AIBN] ratios were applied.

Graft copolymerization on cellulose macro-CTA using styrene and free, "sacrificial" CTA

Further experiments for graft copolymerization on cellulose were performed under optimized reaction conditions as described in the previous section. For the experiments, the "CTA-shuttled R-group"-approach (described in chapter 3.3.2) was applied by the addition of one molar equivalent (referring to the amount of free CPPA) of cellulose-immobilized CPPA groups from cellulose macro-CTA. The general reaction and the corresponding reaction conditions are described in **Figure 56**.

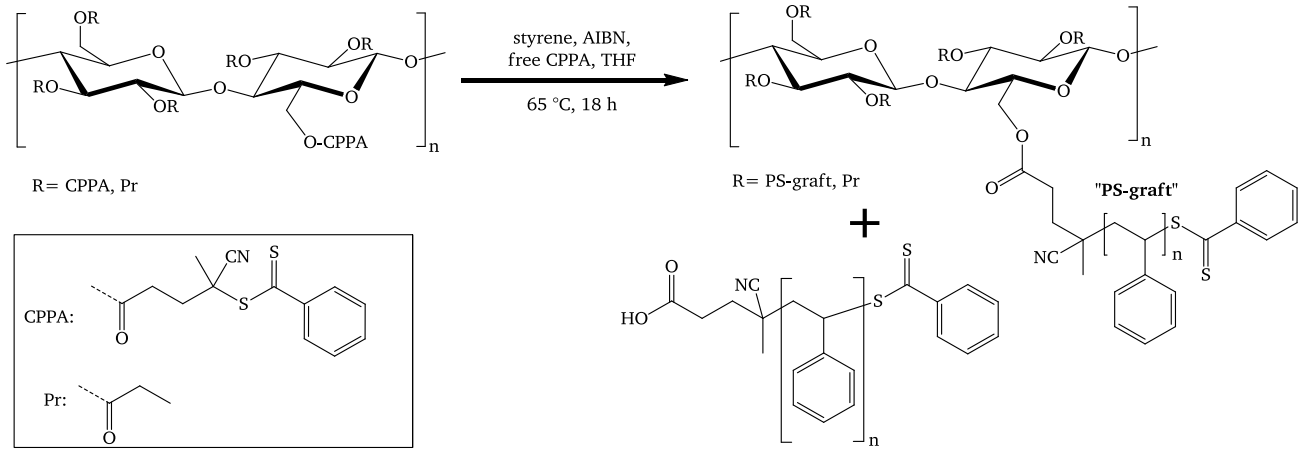

Figure 56. Graft copolymerization of cellulose macro-CTA "MCC-CPPA16-Pr" with styrene during the presence of free "sacrificial" CTA (free CPPA). [styrene] = 8.74 mol/L (bulk polymerization); [AIBN] = 0.3 mmol/L; [free CTA]= 2.5 mmol/L; [CTA on cellulose macro-CTA] = 2.5 mmol/L; V(total) = 3 ml; T = 60 °C; t = 18h.

In first experiments we realized high viscosity of the reaction mixture under the reaction conditions described in the previous section. Therefore the initiator concentration was lowered from initially 2 mmol/L to 0.3 mmol/L, whereas the total CTA concentration was kept at 5.0 mmol/L. Problems with high viscosity were circumvented by high [CTA]/[AIBN] ratio and low AIBN concentration (i.e. reduced monomer conversion). After a polymerization time of 18 hours the reaction was stopped by precipitation of the polymer in methanol and reprecipitation from THF in methanol. Analysis of the product with SEC (**Figure 57**), using THF as eluent, shows a bimodal distribution, originated from graft copolymer and homopolymer. When compared with the cellulose macro-CTA, the cellulose graft copolymer shows a shift towards smaller elution volumes from about 7.7 ml to 7.2 ml (signal peak maximum), indicating a higher apparent hydrodynamic radius and therefore a successful grafting process.

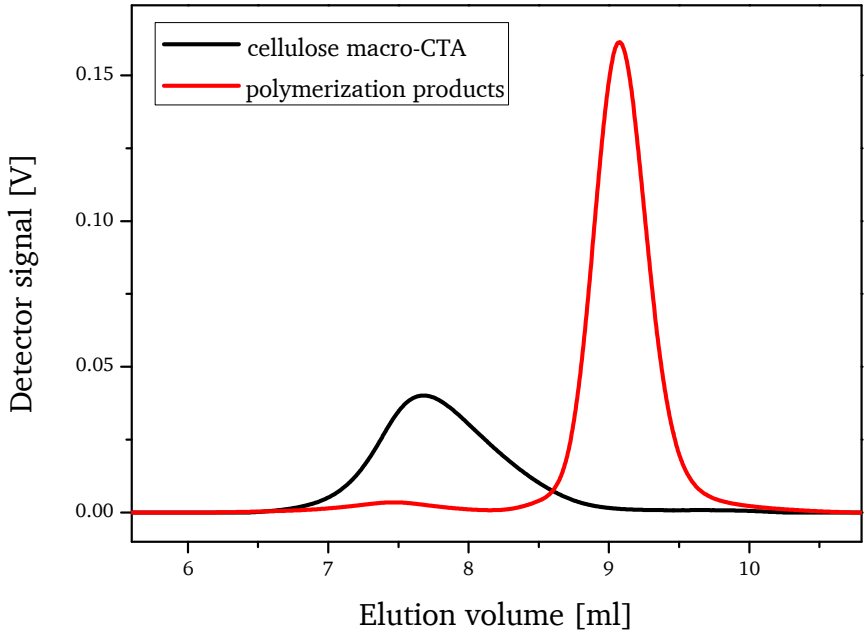

Figure 57. SEC traces of cellulose macro-CTA before (black) and after graft polymerization (red) with styrene. The bimodal distribution after graft copolymerization results from homopolymer polystyrene and cellulose graft copolymer. The cellulose graft copolymer shows low signal intensity in comparison to the polystyrene homopolymer.

By use of narrow disperse PS-standards apparent molar mass distribution of homopolymer and graft copolymer was determined, as shown in **Figure 58**.

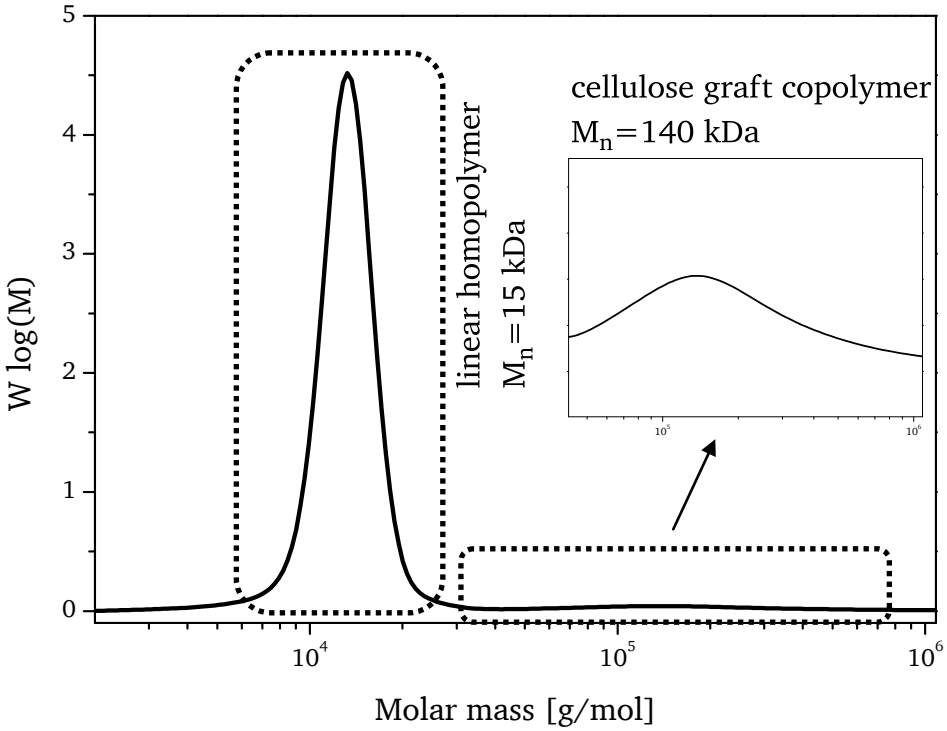

Figure 58. Molar mass distribution of the polymer mixture, containing cellulose graft copolymer and free homopolymer. The signal of cellulose graft copolymer and homopolymer are highlighted with dashed squares.

The generated homopolymer has a M_n = 15 kDa and a Đ of 1.1. The cellulose graft copolymer has a M_n = 140 kDa. Since the cellulose macro-CTA had a M_n = 52 kDa before polymerization, there is a significant increase in the apparent average molar mass.

However, the relative signal of the graft polymer is very small in comparison to the signal of the homopolymer (see insert in **Figure 58**). Since equal amounts of free CTA and immobilized CTA were used, the ratio of the integral signal intensity was expected to be approximately 1:1 using a UV-Vis detector coupled with the SEC column. This leads to the hypothesis that the polymerization reaction on the cellulose backbone might be somehow constrained and that the kinetics of the polymerization on the backbone could be different from homopolymerization due to diffusion effects and an increased local viscosity. In addition, the availability of the immobilized CTA groups might be diminished due to steric hindrance in direct comparison with free “sacrificial” CTA. A second hypothesis based on possible side reactions of the CTA groups such as hydrolysis of the dithioester function might eventually result in the transformation of CTA into inactive species. Therefore further investigation was focused on potential side reactions that might impair the activity of the CTA groups (chapter 4.1). In order to understand the above findings in more detail and in order to question the raised hypothesis, further experiments and analysis of the resulting polymers and cellulose precursors were conducted. It was

observed that the covalent attachment of CPPA onto cellulose with the activation agent CDI led also to various side reactions and therefore to significant deactivation of the CTA attached to the cellulose. Hence, the attachment of dithioester containing RAFT functionalities via activation and esterification of carboxyl functions lead to (partial) destruction of the RAFT agent. This may explain why only limited amounts of polystyrene grafts can be achieved with the cellulose macro-CTA, even if optimal reaction conditions for a well-controlled RAFT polymerization are used. Therefore trithiocarbonate-functionalized cellulose macro-CTAs were used instead for the synthesis of cellulose graft copolymers, as described in the next section.

5.2. Graft copolymerization of styrene with cellulose macro-CTAs based on BiB-derived trithiocarbonates

Model experiments: RAFT polymerization of styrene with CTA "PE-BiB-Me-TTC"

Before starting with the graft copolymerization of trithiocarbonate modified cellulose macro-CTA, a set of two experiments was performed as test polymerizations of styrene with free CTA "PE-BiB-Me-TTC" in order to validate the performance of the reaction system. Reaction conditions are summarized in **Figure 59**.

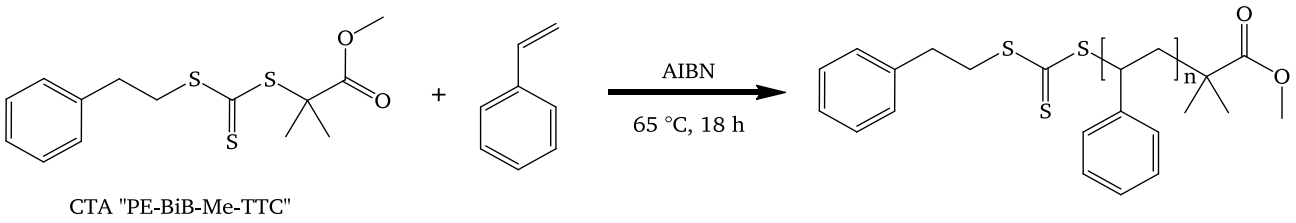

Figure 59. RAFT polymerization of styrene with trithiocarbonate based CTA. Reaction parameters: t = 18 hours, T = 65 °C, [AIBN] = 0.3 mmol/L, [styrene] = 8.74 mmol (bulk), variation of the concentration of CTA: [PE-BiB-Me-TTC] = 2.5 mmol/L or 5.0 mmol/L.

In brief, two separate model polymerizations were performed using the above introduced system. In both cases the temperature and polymerization time were kept constant at T = 65 °C and t = 18 hours, respectively. The polymerization only varied in the amount of added CTA (2.5 mmol/L; 5.0 mmol/L). After polymerization the resulting polymers were analyzed by SEC. Molar mass distributions are shown in **Figure 60**.

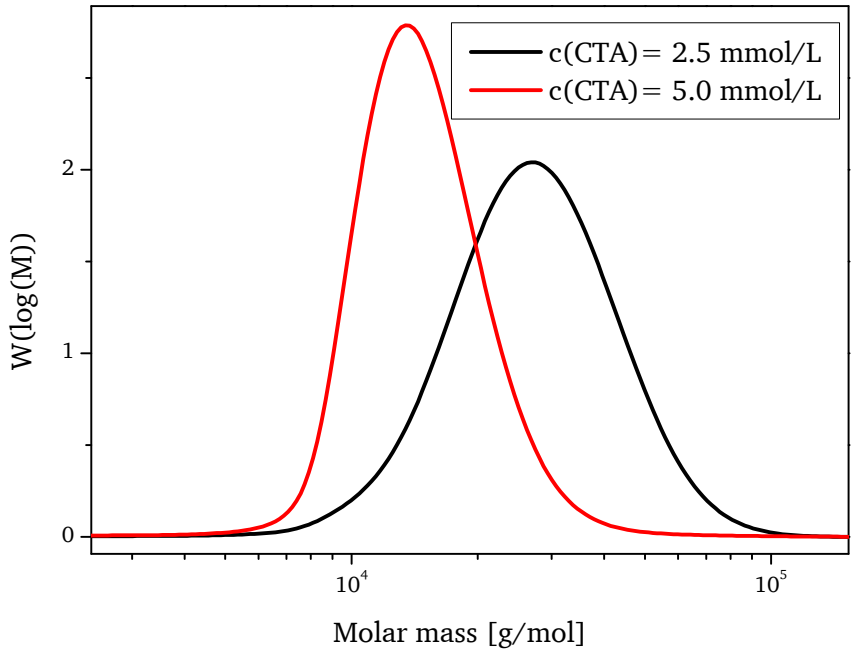

Figure 60. Molar mass distribution of polymer samples, using two different concentrations of CTA "PE-BiB-Me-TTC". Samples were analyzed by SEC with THF as eluent and referenced with polystyrene standards.

In both experiments a low dispersity (Đ < 1.3) was obtained, indicating good control of the polymerization process and suitable reaction conditions for subsequent graft copolymerization experiments.

Graft copolymerization of styrene with cellulose macro-CTA "MCC-CTA4"

In the next step, the reaction conditions of the model polymerizations were adapted for the synthesis of cellulose graft copolymers, as shown in **Figure 61**.

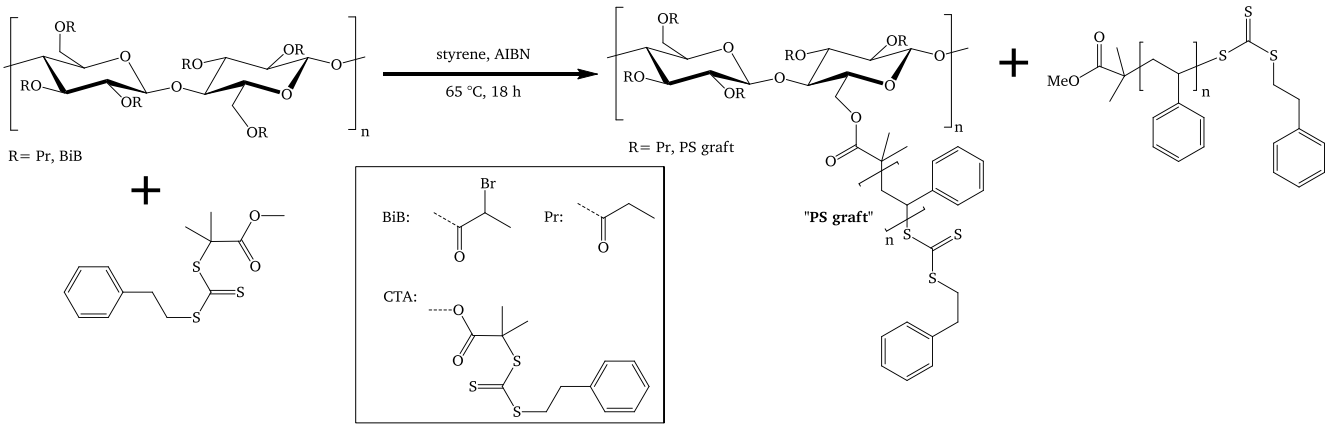

Figure 61. Synthesis of cellulose graft copolymers using cellulose macro-CTA. RAFT polymerization of styrene with trithiocarbonate based CTA. Constant reaction parameters: [AIBN] = 0.3 mmol/L, [styrene] = 8.74 mmol (bulk), [PE-BiB-Me-TTC] = 5.0 mmol/L. The amount of cellulose macro-CTA was varied: MCC-CTA4-PS_1: [CTA groups on MCC-CTA4] = 1.72 mmol/L and MCC-CTA4-PS_2: [CTA groups on MCC-CTA4] = 3.44 mmol/L.

Cellulose macro-CTA ("MCC-CTA4") based on cellulose 2-bromoisobutyro esters (see chapter 4.2.1) was used for a set of two graft copolymerization experiments with styrene, denoted as "MCC-CTA4-PS_1" (having 25 mol-% CTA-groups bond to cellulose and 75 % free CTA with respect to the total amount of CTA) and "MCC-CTA4-PS_2" (with 40 mol-% CTA-groups bond to cellulose and 60 % free CTA with respect to the total amount of CTA). Regardless of the ratio of immobilized CTA and free CTA, polymerizations were leading to well soluble graft copolymers, which were than analyzed with SEC (**Figure 62**).

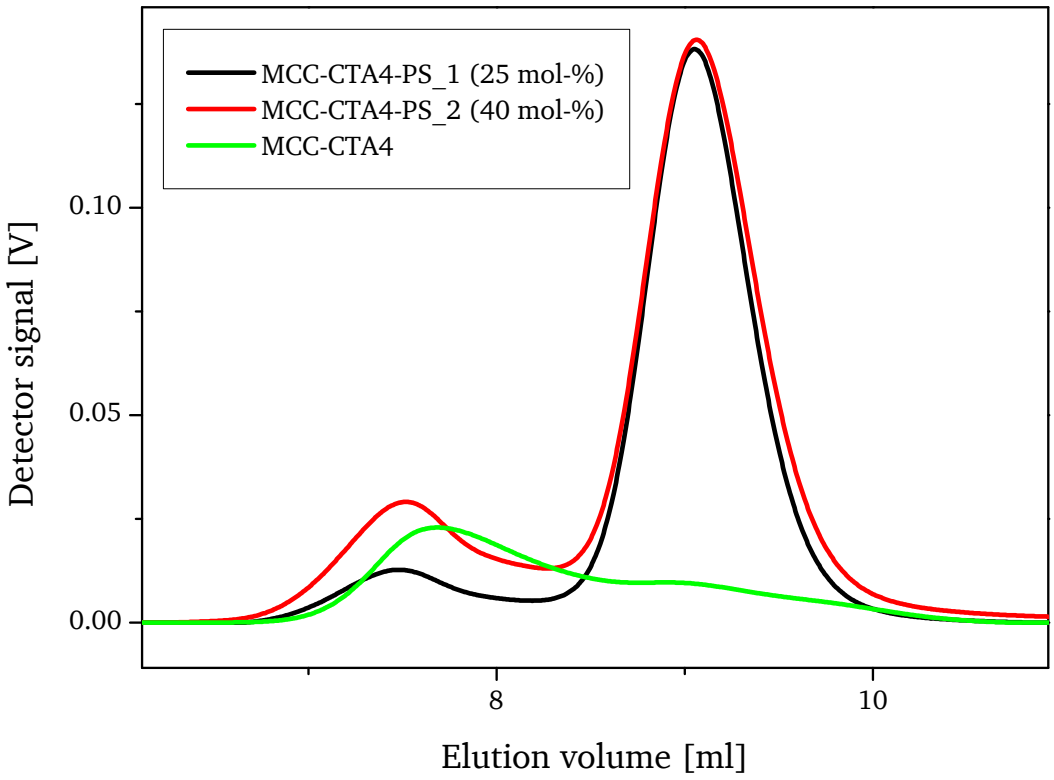

Figure 62. SEC traces of cellulose macro-CTA (MCC-CTA4) compared to graft copolymerization experiments MCC-CTA4-PS_1 and MCC-CTA4-PS_2 graft copolymerization, using THF as eluent. Note, the SEC traces at elution volumes of about 8 to 10 minutes originate from homopolymer, originated from free, "sacrificial" CTA.

The signal maximum of cellulose macro-CTA shifts towards smaller retention volumes after graft copolymerization, which indicates an increase in the apparent hydrodynamic radius and therefore an increase of the average molar mass. Furthermore, when the SEC traces of both graft copolymerization experiments are compared, an increase of the signal intensity of the graft copolymer trace (at elution volumes of about 7 to 8 ml) for "MCC-CTA4-PS_2" indicates a higher amount of (UV-Vis visible) polystyrene attached onto the cellulose-CTA. This observation is in good agreement to the theory that a higher amount of cellulose bound CTA-functionalities relative to free, "sacrificial" CTA should result in a higher relative amount of grafted polymer chains (chapter 5.1).

Concerning the experiments MCC-CTA4-PS_1 and –PS_2, in the SEC analysis, the signal at elution volumes of about 9 minutes originates from the corresponding linear homopolymer, which is a side product from the added free CTA. Analysis of the homopolymer reveals a M_n = 12 kDa with Đ = 1.1, which suggests a pseudo-living character of the polymerization. The product was also quantitatively analyzed with SEC (THF, PS standards) using a UV-Vis detector.

For this, the elugrams of the samples "MCC-CTA4-PS_1" and "MCC-CTA4-PS_2" were used to determine the relative integral signal intensities of both curves, i.e. for the homopolymer signal and for the graft copolymer signal. The result is shown in **Table 5**.

Table 5. Summary of the results of SEC analysis.

Experiment	M_n	M_w	Đ	relative signal area
MCC-CTA4-PS_1	kDa	kDa		%
cellulose graft copolymer	140	303	2.1	12.1 ± 0.12
homopolymer	12	13	1.1	87.9 ± 0.88
MCC-CTA4-PS_2				
cellulose graft copolymer	123	214	1.7	19.5 ± 0.2
homopolymer	10	13	1.3	80.5 ± 0.8

The relative detector signal areas of graft copolymer and homopolymer allow an estimation of the graft-ratio and the initiation efficiency, hence the performance of the cellulose-CTA. The method for calculation is described in detail in chapter 3.3, the determination of the relative detector areas and the standard error is described in chapter 5.3.4. For the experiment MCC-CTA4-PS_1 a graft ratio of **113 %** and an initiation efficiency of **41 %** is calculated. For experiment MCC-CTA4-PS_2 the yield could not be determined because of yield loss during precipitation, but we could determine an initiation efficiency of **36 %** using SEC.

In conclusion, the analytical data from SEC indicated promising first results for a successful graft copolymerization process. However, due to the limitation in the DS(CTA) (chapter 4.2.1), we decided to develop the cellulose macro-CTAs by means of higher DS(CTA) values in order to gain more versatility of the grafting density. Further experiments focused on cellulose macro-CTAs based on cellulose 2-bromopropionyl esters (chapter 4.2.2). It was hypothesized that a secondary carbon atom carrying a bromine functionality might be better available for nucleophilic displacement reactions, such as the transformation from a 2-bromopropionyl functionality into a trithiocarbonate.

5.3. Graft copolymerizations of styrene with cellulose macro-CTA based on Bp-derived trithiocarbonates

First we performed several pre-experiments in order to evaluate the optimal conditions for a well-controlled RAFT polymerization with the CTA "PE-BpB-Me-TTC". The corresponding reaction conditions are displayed in **Figure 63**.

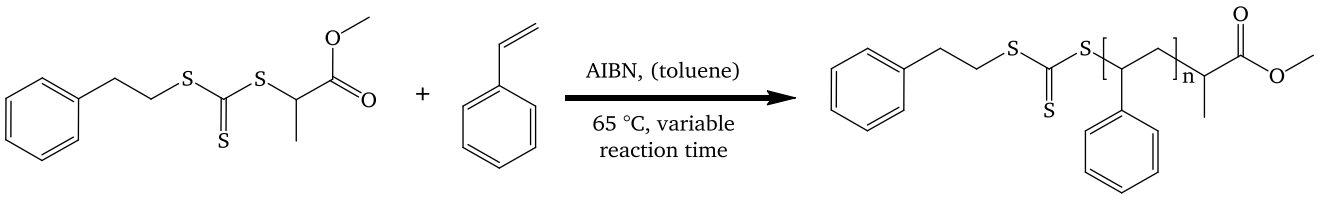

Figure 63. RAFT polymerization of styrene with trithiocarbonate based CTA.

First approaches (experiments PE-BpB-Me-PS_1 to PE-BpB-Me-PS_3) were performed as bulk polymerization ([styrene] = 8.73 mol/L) with variation of the initiator concentration followed by solution polymerization in absolute toluene ([styrene] = 4.36 mol/L and below) in order to circumvent high viscosity. The monomer conversion was determined by ^{1}H-NMR and the polymers were characterized by SEC (using THF as eluent and polystyrene standards for calibration). The results are summarized in **Table 6**.

Table 6. Results of the RAFT polymerization of styrene in bulk and in solution.

experiment	solvent: toluene	[styrene]/[CTA]/[AIBN]	conv.	M_n	$M_{n,\,theo.}$	Đ	remarks
	vol-%	[mmol/L]	[%]	[kDa]	[kDa]		
PE-BpB-Me-PS_1	0	8,730/10/1	19	10	17	1.3	bulk polym.
PE-BpB-Me-PS_2	0	8,730/10/5	43	24	39	1.2	bulk polym. high viscosity
PE-BpB-Me-PS_3	0	8,730/10/10	57	28	52	1.8	bulk polym. gelation
PE-BpB-Me-PS_4	50	4,360/5/5	27	15	25	1.2	
PE-BpB-Me-PS_5a	50	4,360/10/2	18	8	8	1.2	t = 16 h
PE-BpB-Me-PS_5b	50	4,360/10/2	26	11	12	1.1	t = 22 h
PE-BpB-Me-PS_5c	50	4,360/10/2	38	15	17	1.1	t = 40 h

The first three experiments “PE-BpB-Me-PS_1”, “PE-BpB-Me-PS_2” and “PE-BpB-Me-PS_3” were performed as bulk polymerization, using different AIBN concentrations ranging from 1 mmol/L to 10 mmol/L. It was observed that increasing initiator concentrations resulted in high conversions which finally lead to high viscosities/gelation of the reaction mixture, high dispersity of the polymers and strong deviation of the molar mass from theoretical, calculated values.

Subsequent polymerizations (PE-BpB-Me-PS_4 and following experiments) were continued as solution polymerization. By addition of one volume equivalent of toluene to the reaction mixture, the viscosity could be kept low, resulting in a reduced monomer conversion and low dispersity of the polymers. However, a strong deviation from experimental the theoretical M_n values still remained. In the polymerization experiment “PE-BpB-Me-TTC-PS_5” the CTA/AIBN ratio was raised, because it was assumed that a better control could be achieved this way. The resulting polymers showed low dispersity and excellent agreement of experimental the theoretical M_n values. Furthermore, the kinetics of monomer consumption was investigated (sample 5a = 16 h, 5b = 22 h, 5c = 40 h, see (**Figure 64**). The data indicates first order kinetics regarding the consumption of monomer styrene, which is typical for a radical polymerization.

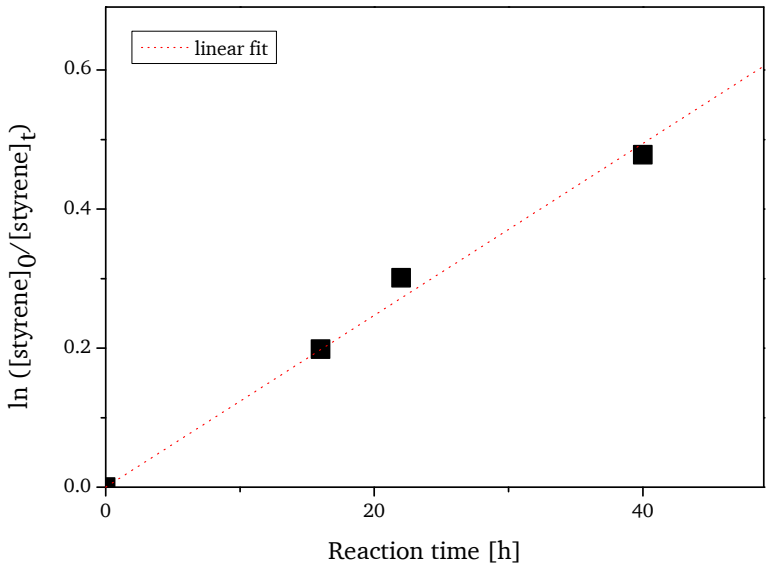

Figure 64. Dependance of the monomer conversion from the reaction time for the experiment “PE-BpB-Me-TTC-PS_5”. Here, the logarithm of the ratio $[styrene]_0/[styrene]_t$ is plotted against the reaction time. A linear fit of the data with a $R^2 > 0.99$ suggests, that the data fits well to a first order kinetic.

In **Figure 65** the dependence of M_n on conversion is presented. Additionally the dispersity of the polymer samples is provided in the top part of the illustration.

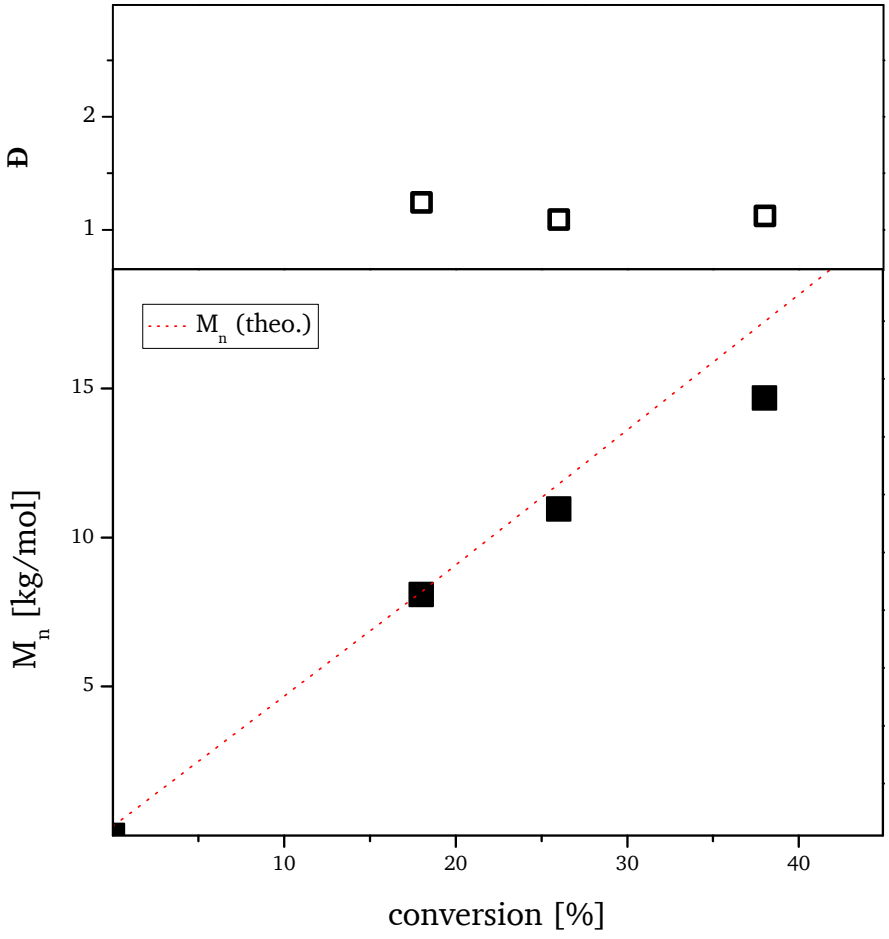

Figure 65. Dependence of M_n and Đ on conversion for solution polymerization of CTA with styrene in toluene for the experiments "PE-BpB-Me-TTC-PS_5a" to "PE-BpB-Me-TTC-PS_5c"). The linear relation of molar mass and conversion is very similar to the theoretical, calculated values. Furthermore the Đ values are very low; therefore the homopolymerization works in a well-controlled manner. Note, the molar mass of the initiator (i.e. 0 % conversion) has been calculated.

The molar mass of the polymer increases from about 8 kDa to 15 kDa if the monomer conversion increases from about 15 % to about 40 %. If we compare the experimentally observed data to the theoretically expected molar mass (red line in **Figure 65**, see also equation (5)), we can conclude that molar masses of styrene polymers in this series can be well controlled. The latter is supported by reasonable narrow dispersity between 1.1 and 1.2, respectively.

Reference-experiment: Graft copolymerization on cellulose 2-bromopropyl/propionyl mixed ester (experiment "MCC-BpB4-Pr-PS_1") by radical transfer

After the modification of cellulose 2-bromopropionyl esters into cellulose macro-CTA a large number of the 2-bromopropionyl moieties remain unmodified. In order to exclude that polymer-grafting might not originate from the RAFT process but from radical transfer, we conducted a reference experiment outlined in **Figure 66**.

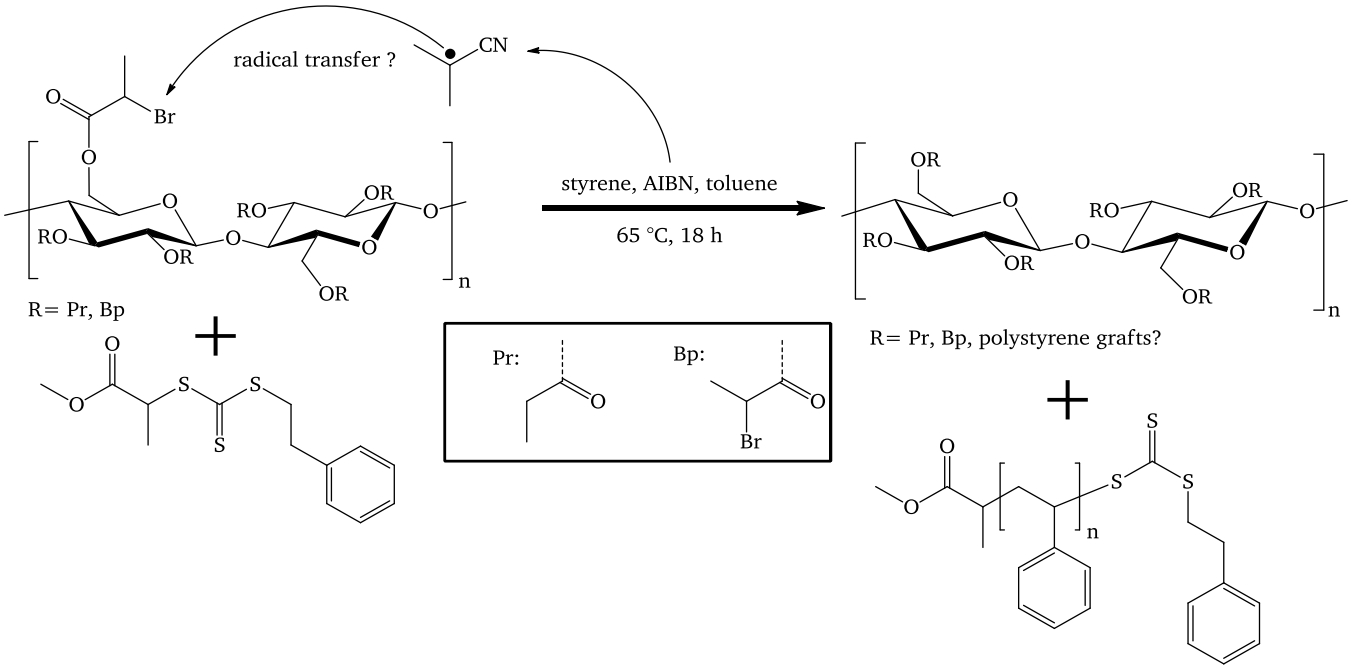

Figure 66. Hypothetical reaction mechanism, which would lead to polymer grafts on cellulose due to radical transfer.

In brief, the 2-bromopropionyl modified cellulose precursor "MCC-BpB4-Pr", which carries no CTA groups was used under similar conditions as for the RAFT polymerizations described before. Under such conditions only PS homopolymer is expected due to the RAFT polymerization with the added small-molecule free CTA, but no graft copolymer should be detected. After the polymerization for 18 hours at 65 °C, the resulting polymer was analyzed with SEC. In this analysis no signal of a graft copolymer was observed. Thus polymer grafting in RAFT processes originating from radical transfer could be excluded.

Reference-experiment: R-approach without free CTA:

As discussed in chapter 1.3, it has been shown by others [51] that the addition of free CTA is crucial for the control of the RAFT "CTA-shuttled R-group approach". If such results can be transferred to our system and in order to learn about the effect of free CTA added to the reaction, first a reference experiment was conducted without addition of free CTA, as displayed in **Figure 67**.

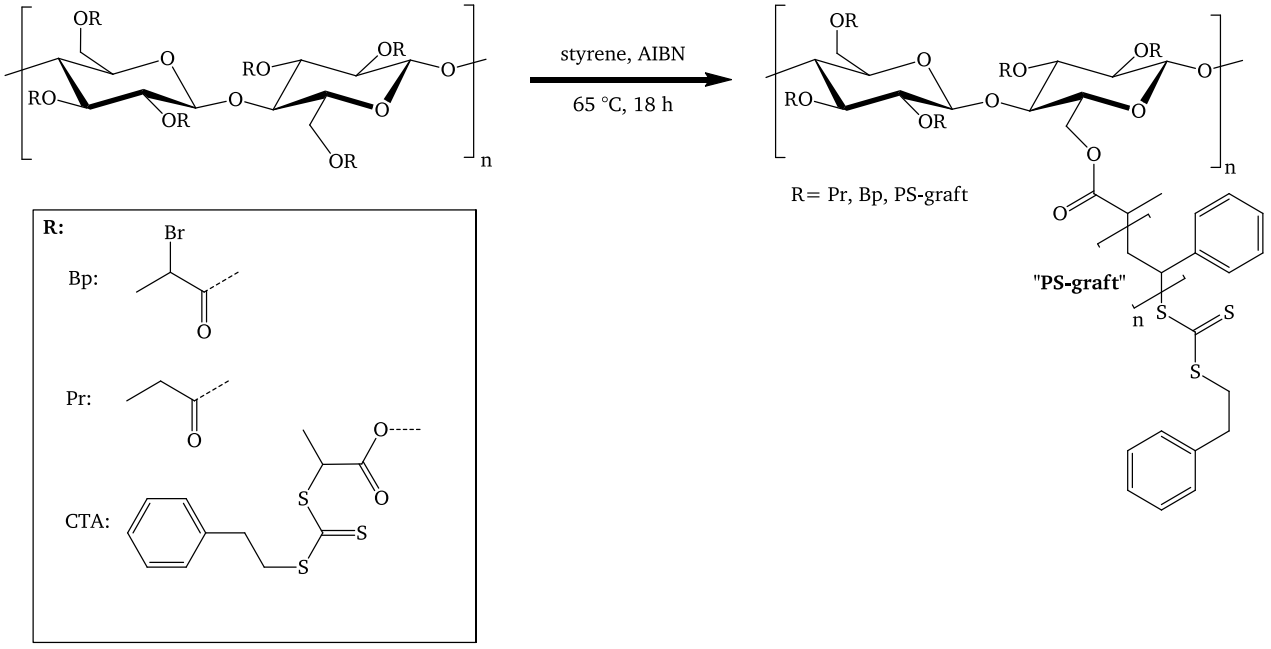

Figure 67. Reaction scheme of a graft copolymerization of styrene using cellulose macro-CTA without additional free CTA.

For the experiment "MCC-CTA14-PS_1" 57 mg cellulose macro-CTA was dissolved in a mixture containing 3 ml styrene and 3 ml toluene. After the polymerization at 65 °C for 18 hours, the initial solution had turned into a gel. The resulting gel was insoluble in THF and was therefore discarded without further analysis. In order to exclude that high concentrations of macro-CTA caused the formation of gel, another experiment was performed, where the cellulose macro-CTA was diluted with toluene (experiment "MCC-CTA14-PS_6": 28 mg cellulose macro CTA in 3 ml styrene and 9 ml toluene). After again 18 hours at 65 °C, the resulting polymer was analyzed by SEC. Note, only some parts were dissolved in THF, other parts of the product remained insoluble. A sample from the insoluble fraction was further processed by cleavage of the polymer grafts and also analyzed by SEC (**Figure 68**).

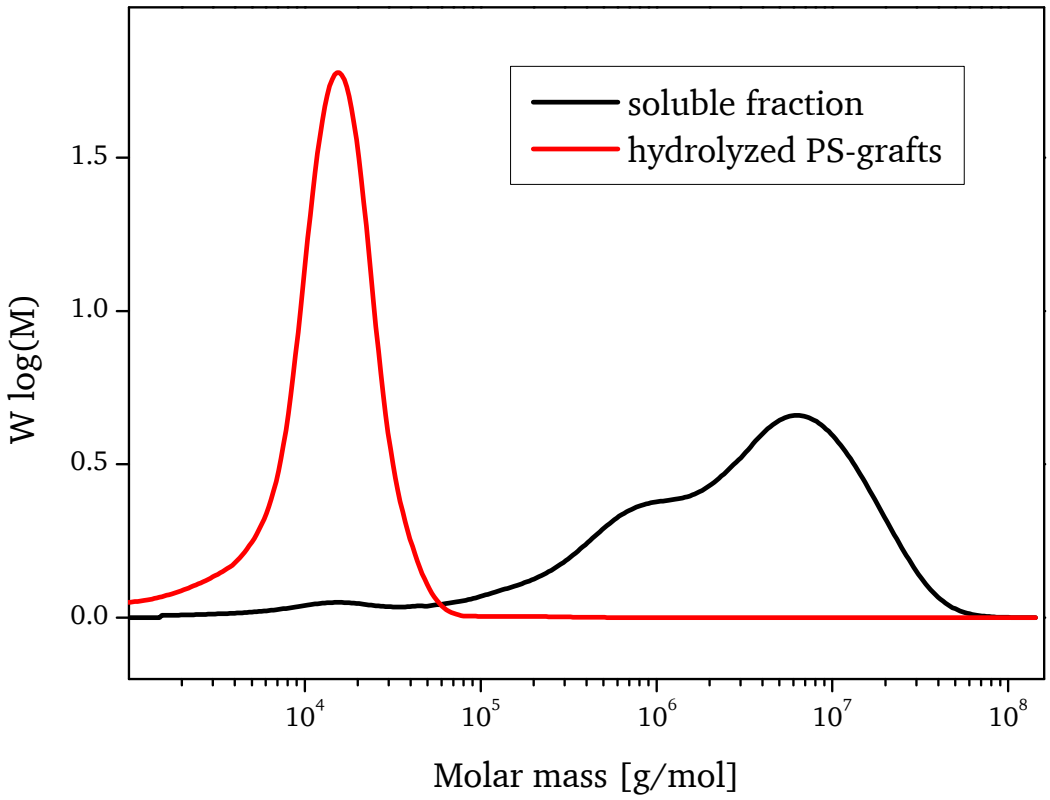

Figure 68. Molar mass distribution of cellulose graft copolymer and hydrolyzed polystyrene grafts. The soluble fraction shows traces of small polymer (≈ 10 kDa). However the total amount of free radical polymerization induced homopolymer is negligible (<<1 %). Isolated polymer grafts after hydrolysis have a dispersity of Đ = 1.8 and no remaining graft copolymer, indicating limited control and a successful cleavage by hydrolysis.

Using linear polystyrene standards as reference, the soluble fraction with cellulose-g-PS showed a high apparent molar mass of cellulose graft copolymer; only traces of homopolymer with low molar mass were observed. It was concluded, that the polymerization predominantly took only place on the cellulose macro-CTA, although generated radicals are more likely surrounded by monomer instead of cellulose macro-CTA molecules. This observation can be considered as an indication of high transfer constants and therefore for the suitability of the cellulose macro-CTA for RAFT polymerization.

The product containing cellulose graft copolymer showed very high molar mass, probably due to agglomeration or cross linking of individual cellulose chains due to radical recombination. The cleaved-off polystyrene grafts had a disperisity of Đ = 1.8, which supports the assumption, that the polymerization process without free CTA has a diminished control compared to an ideal CRP, where a dispersity Đ < 1.5 is typically obtained. In order to exclude that cross-linking events between cellulose macro-CTAs are originated from concentration effects (such as exceeding the overlap concentration), cellulose macro-CTA was further diluted in a subsequent polymerization experiment (28 mg cellulose macro CTA in 24 ml styrene/toluene; experiment “MCC-CTA14-PS_7”). Because of the lower concentrations of all reactants the polymerization time was prolonged to 66 hours, resulting again in a

gel as reaction product. It was also observed, that addition of more toluene to the gel only partially dissolved the crude product. For further characterization, the remaining insoluble gel-fraction was suspended and washed several times with methanol to remove impurities such as non-reacted monomer. After purification the product was suspended in THF and hydrolyzed with potassium t-butanolate to yield a well soluble white powder. The subsequent analysis with SEC revealed cleaved off polystyrene grafts with M_n = 8 kDa and Đ = 1.35, indicating a pseudo-living character, even though no sacrificial CTA was added.

In the next set of experiments, cellulose macro-CTA and free CTA were added to the reaction mixture in different ratios ranging from 60 mol-% cellulose-macro CTA (and 40 mol-% free CTA) to 10 mol-% cellulose macro-CTA (and 90 mol-% free CTA), whereas the total amount of CTA was kept constant at 10 mmol/L.

For the experimental setup a defined amount of cellulose macro-CTA and free CTA was dissolved in a mixture containing 3 ml water-free styrene and 3 ml water-free toluene, followed by the addition of AIBN to yield an initiator concentration of 2 mmol/L. After time intervals of 18 hours, 38 hours and 48 hours, small samples of the reaction mixture were removed with an argon-flushed syringe and the resulting polymers were precipitated with methanol, followed by the analysis with SEC.

The results are summarized as follow: When experiments were performed with l0 mol-% and 25 mol-% of cellulose macro-CTA, the reaction mixtures remained as solution up to 48 hours reaction time, whereas a reaction mixture with 50 mol-% cellulose macro-CTA and 50 mol-% free CTA showed a high viscosity after a reaction time of 18 hours but was still completely soluble in THF or toluene. However, another reaction mixture containing 60 mol-% cellulose macro-CTA and 40 mol-% free CTA resulted in an insoluble gel after a reaction time of 18 hours. The same is true for all experiments using 100 % cellulose macro-CTA regardless of the dilution of the reaction mixture. This conclusion sets the boundary conditions of further grafting experiments described in the upcoming sections of this work. Furthermore the reaction mixtures which contained 10 mol-% and 25 mol-% cellulose macro-CTA are discussed in detail in the next section.

5.3.1. Graft copolymerization with styrene ("Procedure A")

The subsequent polymerization reactions were all carried out using the same cellulose macro-CTA (MCC-CTA14 with DS(CTA) = 0.56). Various parameters such as concentration of educts, conversion and educt ratios ([monomer]/[cellulose macro-CTA]/[free CTA]/[initiator]) were varied. From the resulting SEC analysis the reaction conditions were optimized in an iterative process. A general reaction scheme for these graft copolymerization experiments is displayed in **Figure 69**.

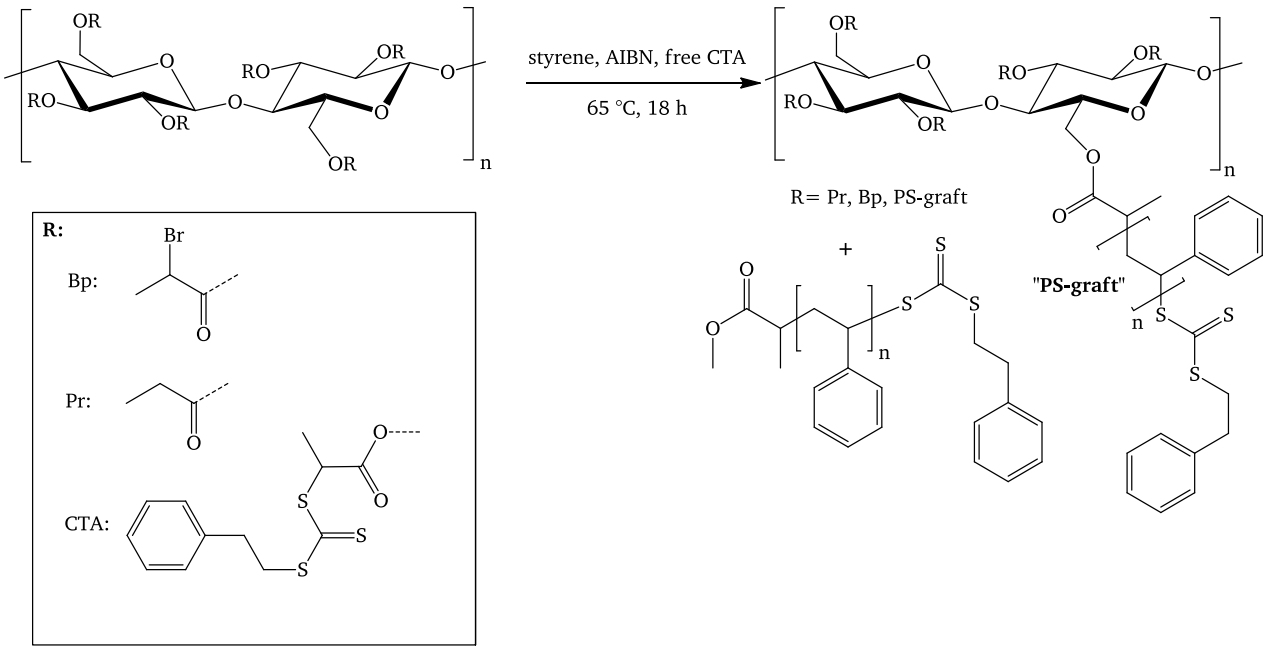

Figure 69. Reaction scheme of a graft copolymerization using cellulose macro-CTA "MCC-CTA14" and styrene as monomer.

A set of polymerization experiments was performed under the conditions described in **Table 7**. The experiments are denoted as "MCC-CTA14-PS_2" to "MCC-CTA14-PS_4", the initial experimental setup (hence the ratio: $[styrene]_0/[CTA, total]/ [AIBN]_0$) of all these first experiment is denoted as "Procedure A"

Table 7. Reaction conditions for the polymerization experiments.

experiment name	$[styrene]_0$	[CTA on cellulose]	[free CTA]	$[AIBN]_0$	$[styrene]_0/[CTA, total]/[AIBN]_0$
	[mol/L]	[mmol/L]	[mmol/L]	[mmol/L]	
MCC-CTA14-PS_2	4.36	5.0 (50 mol-%)	5.0	2.0	2180/5/1
MCC-CTA14-PS_3	4.36	2.5 (25 mol-%)	7.5	2.0	2180/5/1
MCC-CTA14-PS_4	4.36	1.0 (10 mol-%)	9.0	2.0	2180/5/1

The total amount of CTA groups was kept constant at 10 mmol/L, but the relative amounts of free CTA and cellulose macro-CTA were varied:

$$[CTA\ on\ cellulose] + [free\ CTA] = [CTA, total] = 10\ mmol/L \quad (31)$$

Furthermore the amounts of monomer, CTA and initiator (hence the $[monomer]_0/[CTA]_0/[initiator]_0$-ratios) were kept constant. The relative amounts of CTA on cellulose and free CTA was varied between 10 mol-% and 50 mol-%. The experiment MCC-CTA14-PS_2 with 50 mol-% of cellulose macro-CTA showed high viscosity after polymerization time of 18 hours and was therefore discarded. The other two experiments were continued up to two days reaction time, samples of the reaction mixtures were removed and analyzed after time intervals of 18 hours 38 hours and 48 hours. Conversions were determined with ^{1}H-NMR, molar mass distribution and dispersity with SEC. A typical elugram, analyzed with UV-Vis detection, is displayed in **Figure 70**. The signal of graft copolymer at low elution volume is separated from the homopolymer signal at high elution volume. This allows the quantitative determination of relative abundance of grafts and homopolymer. Using linear polystyrene standards for calibration, also average molar mass of the homopolymer was determined (as exemplary shown for one sample in **Figure 71**) from the corresponding homopolymer signal in SEC.

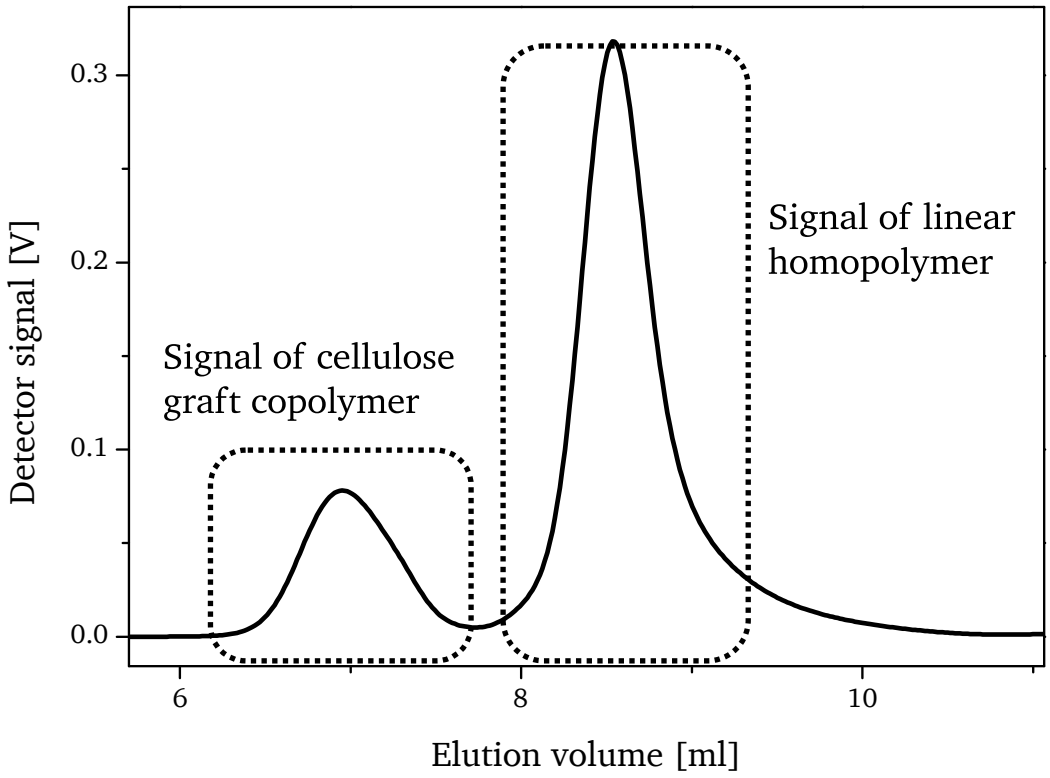

Figure 70. Typical SEC traces of a graft copolymerization experiment. A polymer mixture containing graft copolymer and free homopolymer is obtained due to the addition of free CTA to the reaction mixture.

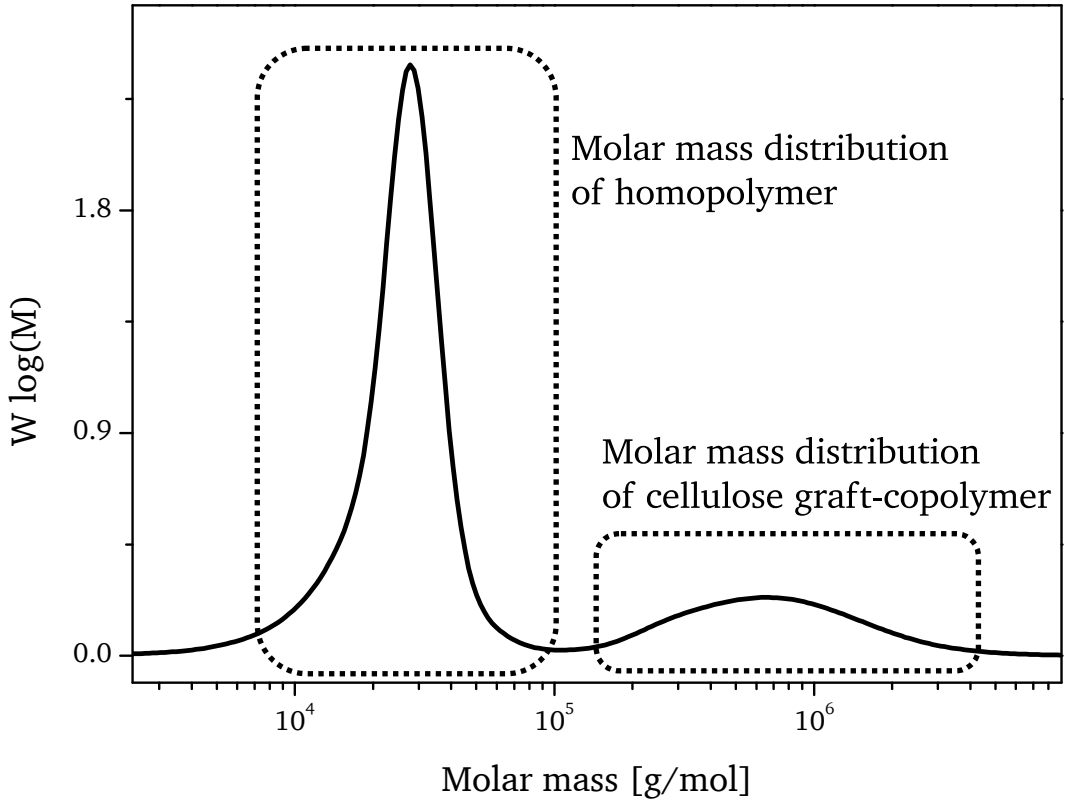

Figure 71. Molecular weight distribution of a graft copolymer / homopolymer mixture.

The number average molar mass derived from SEC measurements of the homopolymers is presented in **Figure 72**. Note, the average molar mass of the corresponding cellulose graft copolymers is not quantitatively discussed due to its different structural nature in comparison to the linear polystyrene standards used for calibration. However, the obtained graft copolymers have shown significantly larger values of the apparent molar mass than their corresponding precursors, thus confirming qualitatively the success of the graft copolymerization.

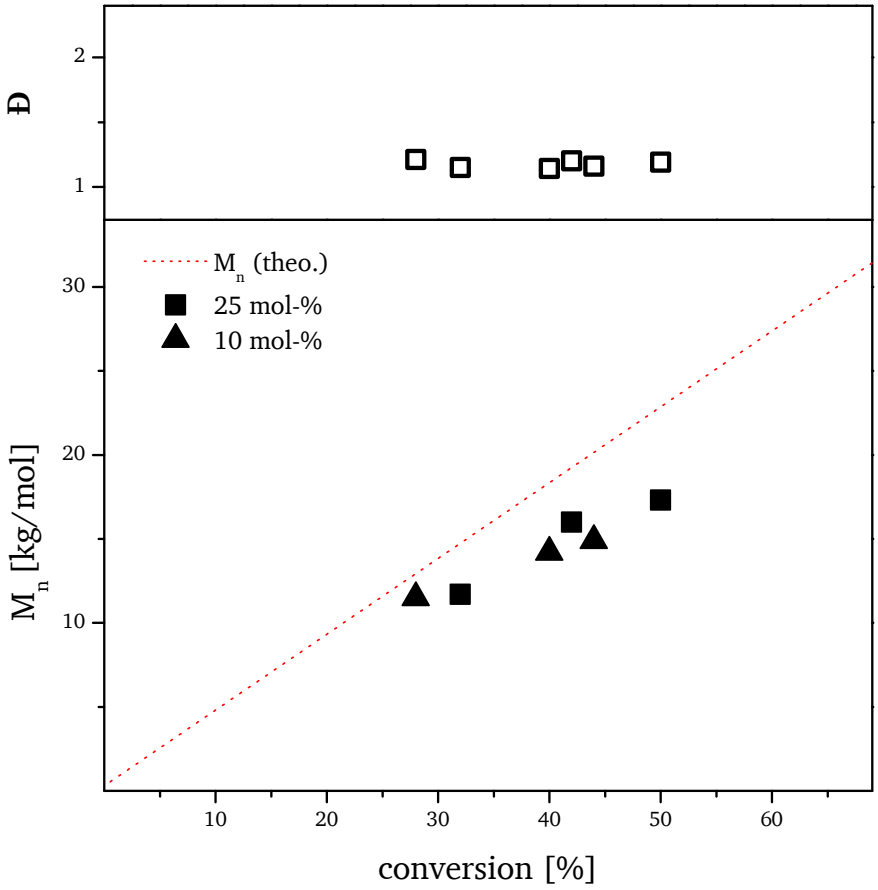

Figure 72. Dependence of Đ and M_n on monomer conversion. The data refers to linear homopolymer generated in the polymerization experiments MCC-CTA14-PS_3 and MCC-CTA14-PS_4, which was then analyzed with SEC relative to polystyrene standards. The denoted mol-% refers to the amount of CTA functionalities on cellulose macro-CTA relative to the total amount of CTA in the polymerization.

It can be seen in **Figure 72** that M_n increases within the observed range of the reaction conversion (here: 25 % up to 50 %). The values obtained for M_n are close, however always slightly below the expected M_n, as calculated from RAFT kinetics. The dispersity of all samples is in the order of 1.2 which are typical values obtained for controlled RAFT reactions.

Characterization of the polymer-grafts

In order to gain more quantitative information about the cellulose graft polymers, the crude product of MCC-CTA14-PS_3c was exemplary further processed by purification and isolation of the polymer grafts by fractional precipitation, using methanol and THF, followed by the alkaline cleveage of the polymer grafts from the cellulose backbone using potassium tert.-butanolate as base and THF as solvent. The subsequent SEC analysis of crude product, isolated graft copolymer and cleaved polymer grafts in THF as eluent is summarized in **Figure 73**.

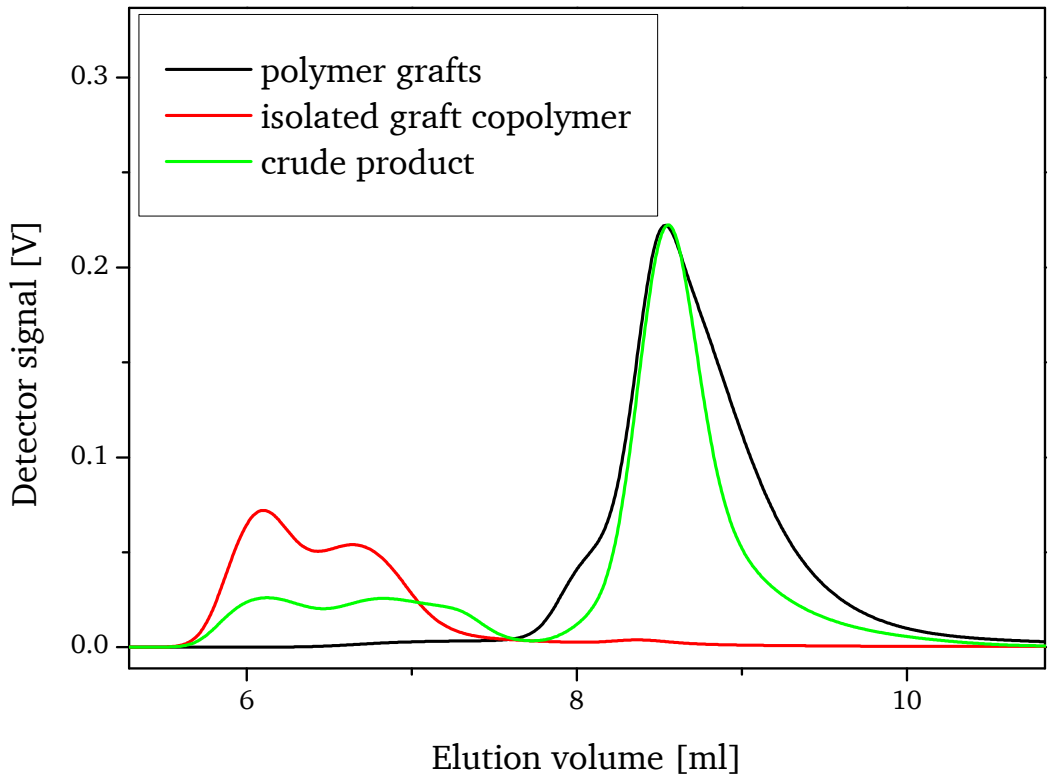

Figure 73. Crude product of experiment MCC-CTA14_3c contains homopolymer and graft copolymer. Exemplary purification of cellulose graft copolymer shows only remaining traces of homopolymer. Subsequent isolation of the polymer grafts by cleavage shows a signal maximum at the same retention time as free homopolymer, indicating a very similar kinetic behavior of graft copolymerization and free homo polymerization.

It should be noted, that the signal of the graft copolymer in the elugram shows a bimodal distribution. This may be attributed to agglomeration of graft copolymers, as this assumption was verified by treatment of graft copolymer solutions with ultrasonic sound for several hours, resulting in a mono modal distribution. The signal of cleaved polymer grafts appeared broader than the signal from the homopolymer, indicating an increased occurrence of termination reactions, but the signal maximum was observed at the same elution volume. The latter suggests that the reaction kinetics of the graft copolymerization and the homopolymerization under the chosen reaction parameters were similar. This allows the assumption that the molar mass of the polymer grafts may be estimated by knowledge of the molar mass of the free linear homopolymer.

5.3.2. Optimization of the graft length ("Procedure B")

Under ideal RAFT conditions the graft-length depends on the consumed monomer in relation to the amount of CTA groups:

$$M_n(theo.) = \frac{\Delta n(monomer)}{n(CTA)} * M(monomer) + M(CTA) \quad (32)$$

$$\Delta n(monomer) = [monomer]_0 * conversion\,[\%] \quad (33)$$

According to equation (32), longer grafts can be obtained by increase of the Δn(monomer)/n(CTA)-ratio: a higher $[monomer]_0$/[CTA] ratio or higher conversion of monomer lead to polymers with increased molar mass. In further experiments the total concentration of CTA was reduced, which increases the $[monomer]_0$/[CTA] ratio. The amount of initiator was slightly increased, thus diminishing the [CTA]/[AIBN] ratio, which can impair the control of the RAFT process but increases the monomer consumption. This modification of the reactant ratios is denoted as "Procedure B". The molar fraction of CTA on cellulose and free CTA was varied from 20 to 40 mol-%. The concentrations of all reactants are summarized in **Table 8**. All reactions were performed in Schlenk-tubes as solution polymerization with 6 ml styrene and 6 ml toluene with a total volume of 12 ml.

Table 8. Modified reaction conditions with the aim to obtain larger polymer grafts.

experiment name	$[styrene]_0$	[CTA on cellulose]	[free CTA]	$[AIBN]_0$	$[styrene]_0$/ [CTA, total]/ $[AIBN]_0$
	[mol/L]	[mmol/L]	[mmol/L]	[mmol/L]	
MCC-CTA14-PS_9	4.36	1.0 (20 mol-%)	4.0	2.5	1744/2/1
MCC-CTA14-PS_10	4.36	1.5 (30 mol-%)	3.5	2.5	1744/2/1
MCC-CTA14-PS_11	4.36	2.0 (40 mol-%)	3.0	2.5	1744/2/1

For the experiment "MCC-CTA14-PS_9", which uses 20 mol-% cellulose macro-CTA and 80 mol-% free CTA, polymer samples were taken in a time interval between 6 hours and 72 hours reaction time. For this we used every time a argon-flushed syringe. Then the polymer was isolated via precipitation in methanol and analyzed with SEC for the analysis of M_n and Đ. The conversion was determined by ^{1}H-NMR of the reaction mixture. The evolution of the molar mass distribution of linear polystyrene over reaction time is exemplary shown in **Figure 74** for the experiment "MCC-CTA14-PS_9".

In the image the molar mass distributions of the polymer samples after different polymerization times are shown. It can be seen that the distribution shift towards higher molar masses with increasing polymerization time, which agrees with the mechanism of RAFT kinetics.

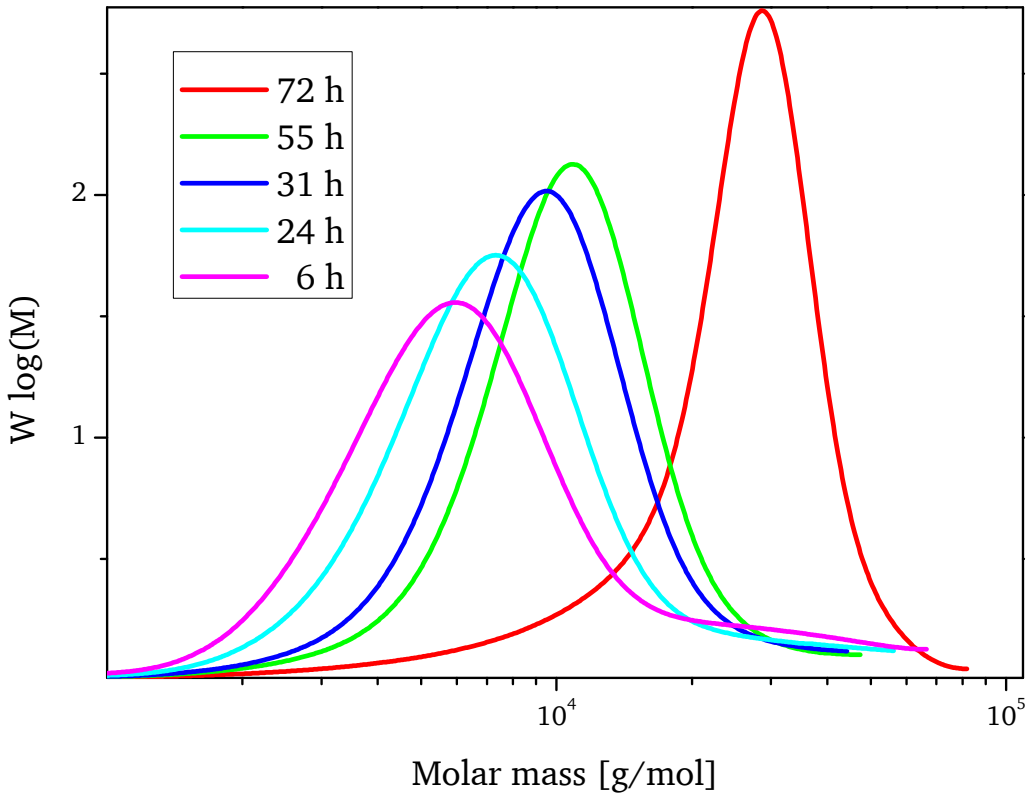

Figure 74. Molar mass distribution of free polystyrene chains by RAFT copolymerization of styrene with MCC-CTA14 and free CTA with AIBN in toluene (experiment MCC-CTA14-PS_9). Samples were taken after different reaction times from 6 up to 72 hours, denoted in the figure.

The sample with 40 mol-% cellulose macro-CTA showed gelation after 24.5 h reaction time (conversion 28 %) and therefore polymerization was stopped and polymer was purified by dissolution of the reaction mixture with toluene with subsequent precipitation of the polymer in methanol. After polymerization time of 31.5 hours the other two reaction mixtures with 20 mol-% and 30 mol-% also became viscous (conversion 35 %). Therefore it was decided to stop the reaction and to add another 6 ml of toluene. Oxygen was removed again by three pump freeze thaw cycles and the reactions were continued up to 100 hours reaction time (conversion = 50 %). Due to the dilution of the reaction mixtures the concentration of all reactants was changed, therefore the reaction rate was not analyzed. On the other hand that procedure also proved the livingness of the process due to its feasibility for reinitiation. The analysis of the polymer samples is summarized in **Figure 75**.

Note, that the analysis only refers to the number average molar mass of the homopolymers originated from free CTA, whereas the molar mass of the graft copolymers is not discussed here. From the data it can be seen for all three experiments that the M_n increases with conversion in a linear fashion and polymer grafts with up to almost 40 kDa can be obtained.

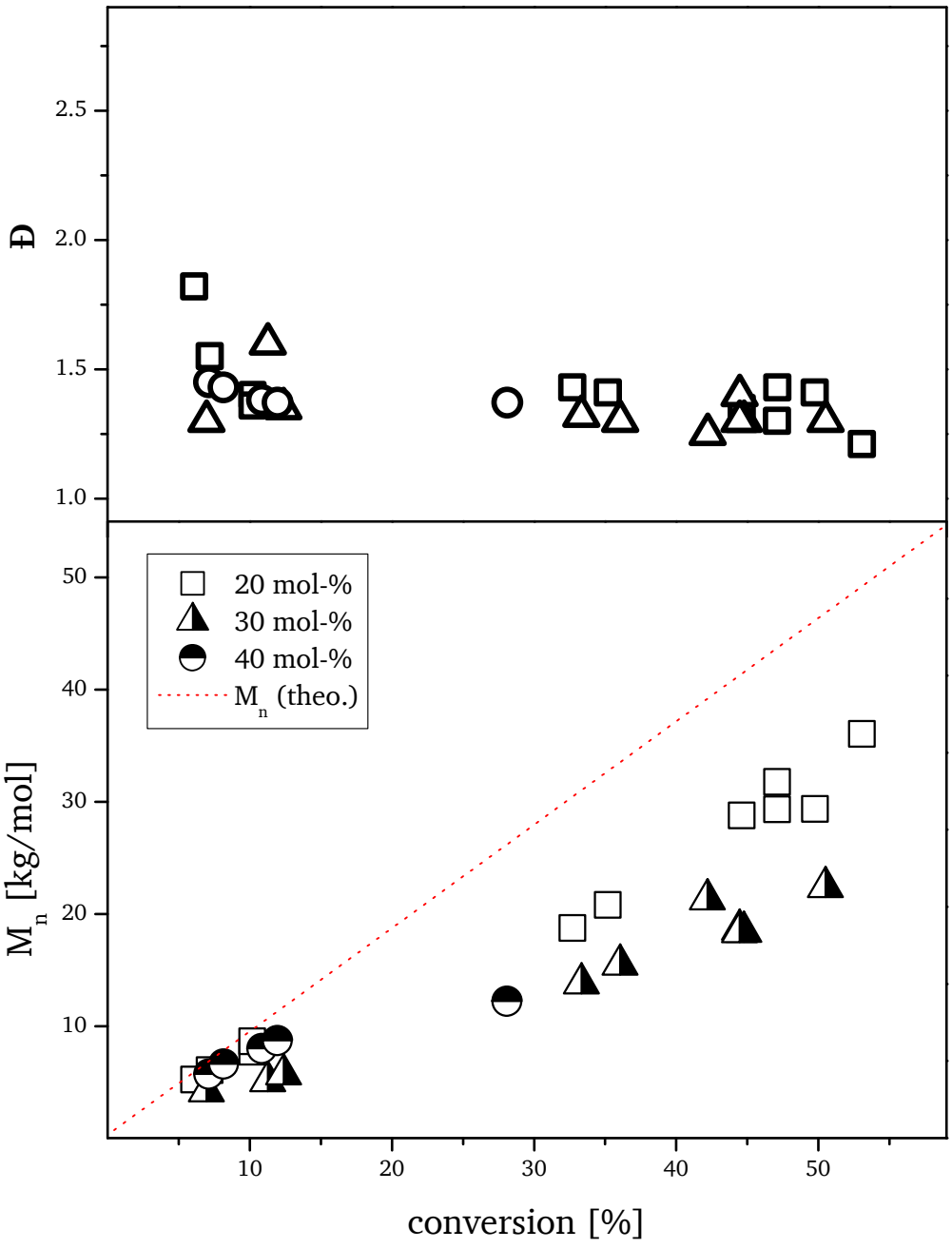

Figure 75. Evolution of the M_n and Đ with monomer conversion, determined by SEC in THF as eluent, calibrated with low disperse PS standards. All experiments were performed under the same reaction conditions but with variation of the relative amount of cellulose macro-CTA with respect to the total amount of CTA. Reaction conditions: T = 65 °C, V(total) = 6 ml, V(styrene) = 3 ml, V (toluene) = 3 ml, [styrene] = 4.36 mmol/L, [AIBN] = 2.5 mmol/L, [CTA,total]= 10 mmol/L. Square symbol: [CTA on cellulose] = 1.0 mmol/L (20 mol-%), [free CTA] = 4.0 mmol/L (80 mol-%); Triangle: [CTA on cellulose] = 1.5 mmol/L (30 mol-%), [free CTA] = 3.5 mmol/L (70 mol-%); Circle: [CTA on cellulose] = 2.0 mmol/L (40 mol-%), [free CTA] = 3.0 mmol/L (60 mol-%).

However, significant deviation of the M_n values from the theoretical M_n values (shown as red dashed line) especially at higher conversions as well as the dispersity values indicate that the control of the process seems to be lower than the previous experiments. It should be noted that the dispersity at conversions <10 % may be too high since the baselines of the homopolymer and the graft copolymer are not separated at that point.

From all these observations we conclude that the choice of the [CTA]/[AIBN] ratio is an optimization problem: high ratios lead to a well-controlled process and to short polymer grafts while low ratios result in less controlled conditions but larger polymer grafts.

5.3.3. Optimization of the graft ratio ("Procedure C")

For the subsequent experiment the concentrations of reactants were changed in order to target larger polymer grafts already at low conversions, thus avoiding high viscosity or gelation of the reaction mixture (experiment "MCC-CTA14-PS_12", **Table 9**)

Table 9. Experiment MCC-CTA14-PS_12: concentrations and ratios.

experiment name	$[styrene]_0$	[CTA on cellulose]	[free CTA]	$[AIBN]_0$	$[styrene]_0/[CTA_{total}]/[AIBN]_0$
	[mol/L]	[mmol/L]	[mmol/L]	[mmol/L]	
MCC-CTA14-PS_12	5.24	1.0 (25 mol-%)	3.0	1.0	5240/4/1

Besides concentrations and ratios of educts, reaction conditions and procedures were kept the same like prior polymerizations (temperature, degassing by pump freeze thaw and removal of samples via argon filled syringe). Once again an exemplary analysis of both, homopolymer and cleaved polymer-grafts was performed. The sample with the highest conversion was taken and the homopolymer and the graft copolymer were separated by fractional precipitation. Using the isolated graft copolymer, the polymer grafts were cleaved by hydrolysis, using potassium tert.-butanolate and THF as solvent. Then, the isolated graft copolymer, the polymer grafts and the homopolymer were analyzed with SEC (**Figure 76**). The almost identical shape of the signals of the homopolymer and the polymer grafts indicate very similar reaction kinetics of free CTA and cellulose macro-CTA. Having polymer grafts similar to free homopolymer, conclusions for the polymer grafts from the corresponding homopolymer regarding initiator efficiency can be made.

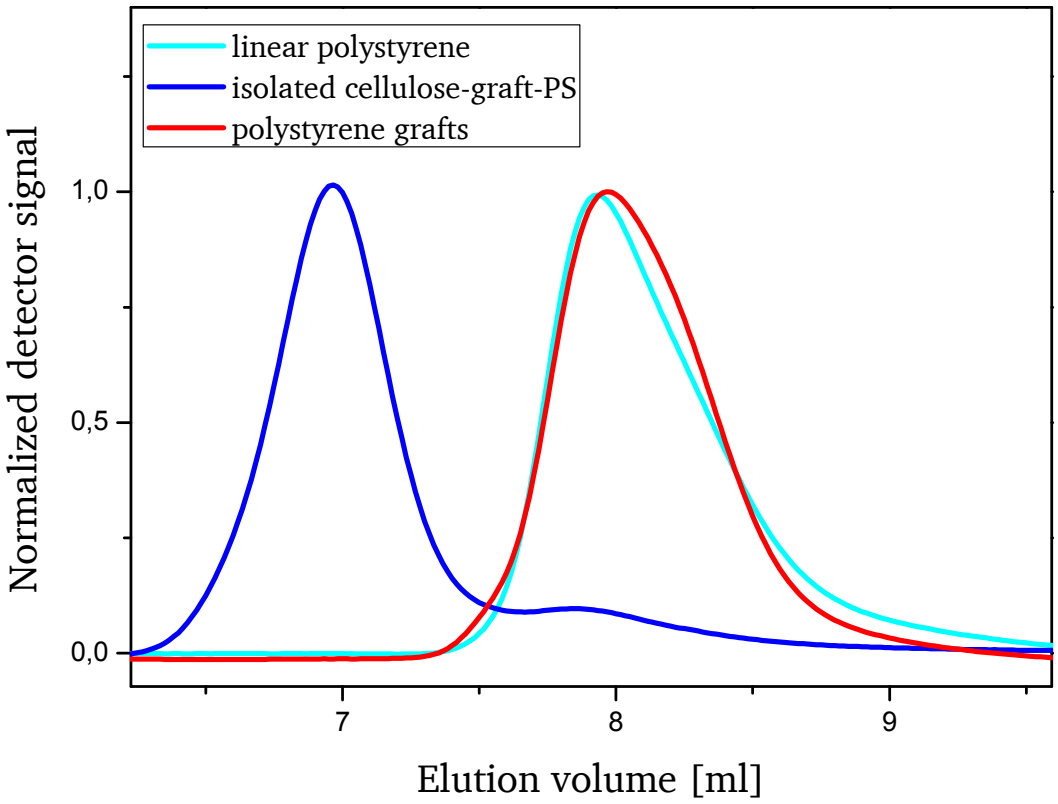

Figure 76. SEC traces of polymer from experiment MCC-CTA14-PS_12f: isolated graft copolymer (dark blue), isolated homopolymer (light blue), hydrolyzed polymer grafts after cleavage from isolated graft copolymer (red).

The samples were analyzed with SEC and the molar mass distribution of the homopolymer was investigated. The data presented in **Figure 77** shows a clear dependence of the molar mass on conversion. The obtained M_n values are close to the theoretical M_n values calculated from RAFT kinetics. Furthermore the dispersity is below 1.5 during the whole process. We conclude that the reaction seems to proceed in a well-controlled manner. The number average molar mass of linear polystyrene exceeded 40 kDa, therefore also the aim to generate large polymer grafts was successfully accomplished.

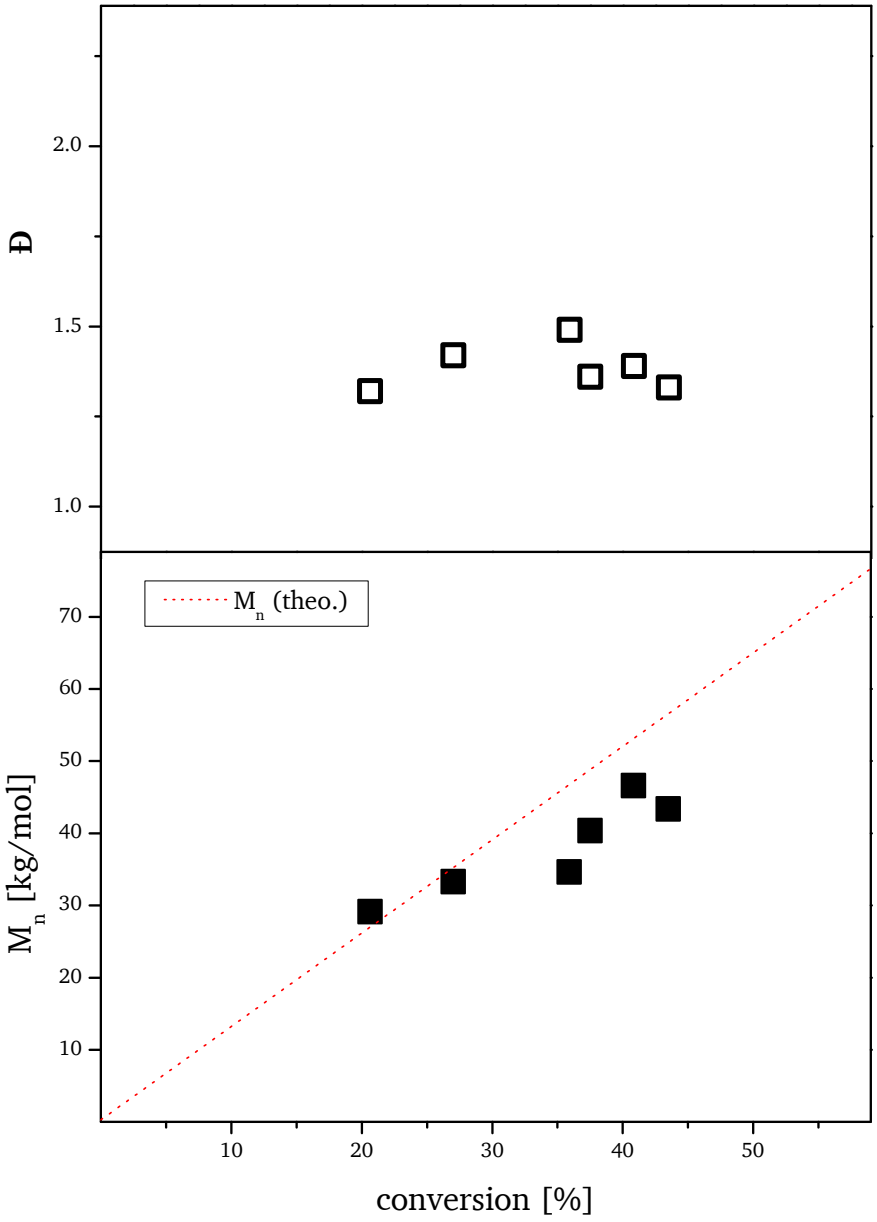

Figure 77. Number average molar mass of linear polystyrene originated from free CTA added to the reaction mixture, as a function of the reaction conversion. The M_n values were determined by SEC in THF as eluent and with a calibration using PS standards. The dotted line corresponds to the theoretically expected (calculated) values for M_n according to reaction kinetics of the RAFT process. Reaction conditions for procedure C: T = 65 °C, [styrene] = 5.24 mol/L, [CTA on cellulose] + [free CTA] = 4.0 mmol/L, [AIBN] = 1.0 mmol/L. Figure redrawn from [71].

After we gained insight into the optimization of the RAFT process by the analysis of the linear homopolymers, generated by the addition of free, "sacrificial" CTA, we wanted to learn more about the structure of the graft copolymers. In this context, we were especially interested in the polymerization performance of the cellulose-bound CTA groups. This is why the graft copolymers were quantitatively analyzed by SEC using UV-Vis detection. As measure of performance two significant parameters for graft copolymerization were analyzed as described in the following section.

5.3.4. Quantitative analysis of the cellulose graft copolymers: graft ratio and initiation efficiency

When SEC is coupled with a UV-Vis detector it should be possible to determine the concentration of both homopolymer and graft copolymer, therefore the ratio of linear polymer and cellulose-graft-polymer in the polymer mixture can be calculated.

a) Assumptions:

- absorption of UV-light is independent of polymer architecture or molar mass but only dependant of the molar amount of light absorbing species
- light absorption of the cellulose backbone and CTA is negligible in comparison to the absorption of the polymer grafts

b) Requirements:

- use the same wavelength for the analysis of all samples
- known correlation between detector signal and concentration, in best case a linear behavior
- separated signal for homopolymer and graft copolymer

The light source in the UV-Vis region is used with a wavelength of 254 nm, where the absorption maximum for polystyrene is provided. The linearity between concentration and detector response was first validated by a calibration using linear, narrow disperse polystyrene standards (see **Figure 78**). Furthermore, a relative standard error of the signal area of about 1 % was calculated using the standard error provided by the linear regression (**Figure 78**, top image).

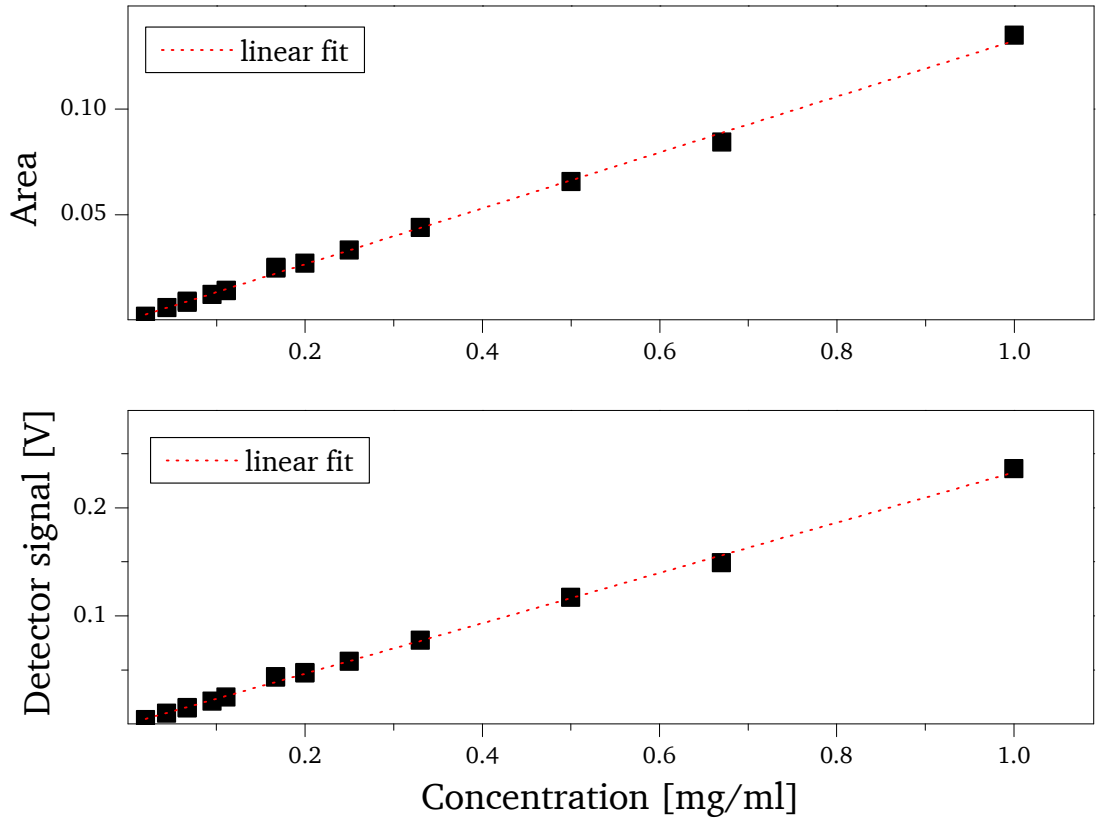

Figure 78. Validation of the linearity of the SEC UV-Vis detector signal and the corresponding area. Stock solutions of linear polystyrene standards in THF were used for analysis. R^2 >0.99 proofs the good correlation of the detector signal and die signal area in respect to the polymer concentration. Note, the relative standard error of about 1 % is too small to be displayed in this figure.

The areas of the corresponding detector signal were determined with suitable software (WIN GPC or Origin). Sometimes problems occurred, when graft copolymer samples with low monomer conversion were measured, because at early stages of the polymerization the curve of the graft copolymer overlaps with the homopolymer (an exemplary elugram, where quantification was not possible, is shown in **Figure 79**).

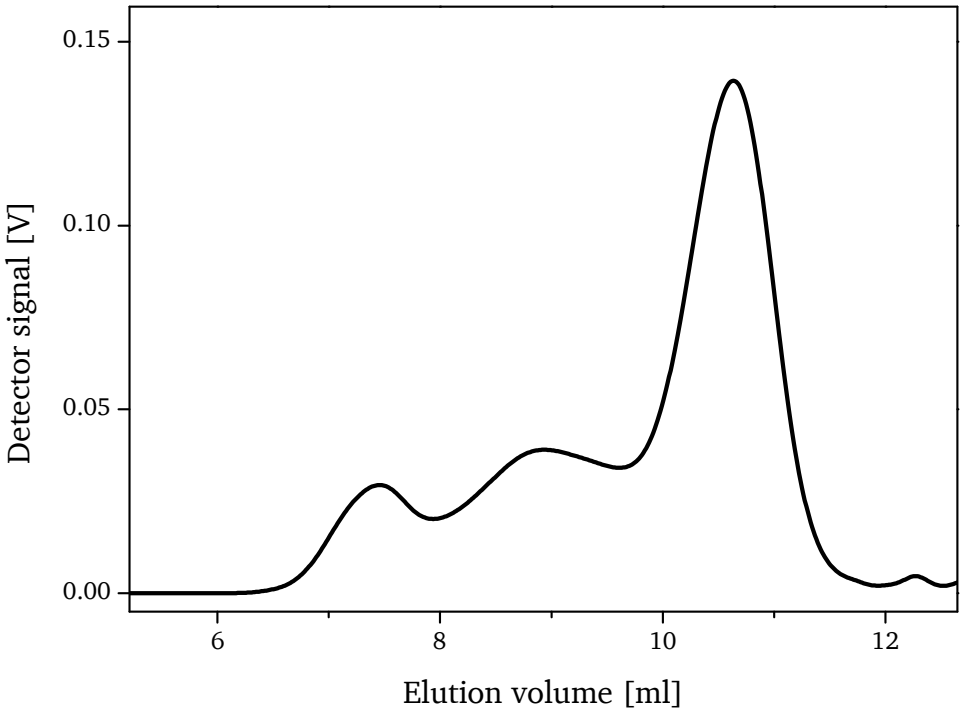

Figure 79. Exemplary SEC elugram ("MCC-CTA14-PS_10b", conversion = 4.5 %) which does not allow quantitative analysis. Homopolymer and graft copolymer signals cannot be clearly identified.

Therefore ambiguous data had to be discarded. An exemplary SEC elugram which allows quantitative analysis is displayed in **Figure 80**.

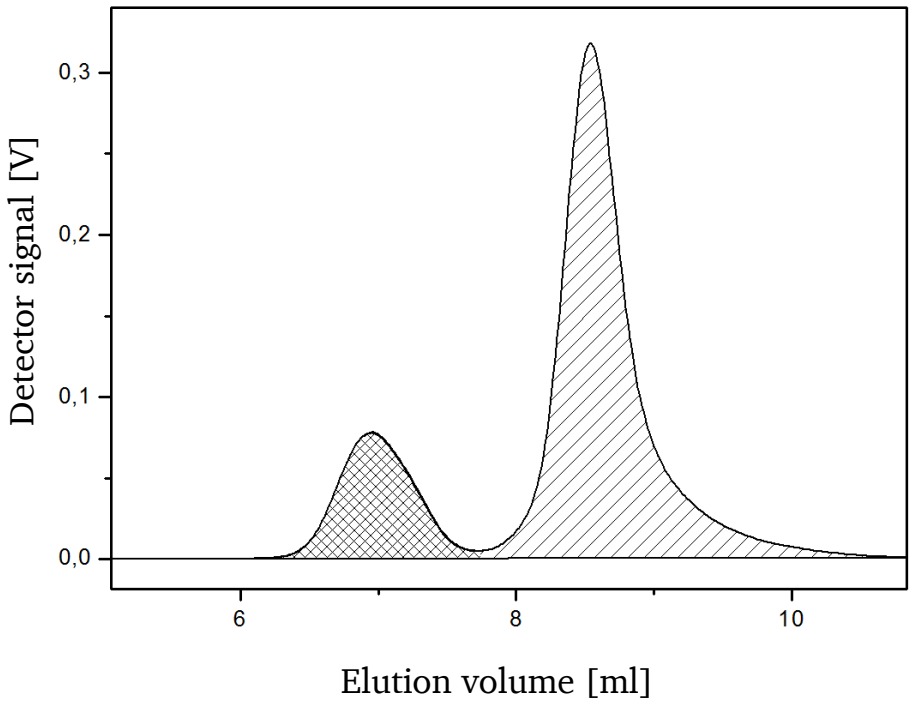

Figure 80. Typical SEC traces of a polymer mixture containing cellulose graft copolymer (left signal) and free, linear polystyrene (right signal) obtained by UV-Vis detection. Determination of the relative signal areas- here displayed as checkered and lined areas- allows calculation of the ratio of polymer grafts on the backbone with respect to free polymer and therefore the graft ratio and graft efficiency. Figure reprinted with permission from [71].

From this data the amount of polymer grafts, graft ratios and initiation efficiencies can be determined. Graft ratios and initiation efficiencies are regarded a measure of performance of the CTA groups attached to the cellulose in comparison to free CTA groups in solution. The initiation efficiency is defined in the following equation:

$$initiation\ efficiency\ [\%] = \frac{[CTA_{cellulose,active}]}{[CTA_{cellulose}]_0} \tag{34}$$

Since the amount of the cellulose-graft-PS was not determined by gravimetry but by the signal ratio of cellulose-graft-PS and linear PS with SEC, the following equation was used instead:

$$initiation\ efficiency\ [\%] = \frac{[CTA_{free}]}{[CTA_{cellulose}]} * \frac{A(PS\ on\ CTA_{cellulose})}{A(PS\ on\ CTA_{free})} * 100\ \% \tag{35}$$

A = Area of the corresponding UV-Vis signal in SEC analysis

The graft ratio describes the relative mass increase of cellulose macro-CTA due to the attachment of polymer grafts.

$$graft\ ratio\ [\%] = \left(\frac{m(Cellulose\ graft-copolymer)}{m(Cellulose\ macro-CTA)} - 1\right) * 100\ \% \tag{36}$$

For example, if 1 g cellulose macro-CTA is transformed into 11 g of cellulose graft copolymer a graft ratio of 1,000 % is reached. As long as the polymerization takes place in a controlled (ideal) fashion (all CTA groups activate and no termination reactions occur), high grafting densities and long polymer grafts result in high graft ratios. The control was quantified by the initiation efficiency. If the polymer grafts grow in the same fashion such as the free homopolymer, a value of 100 % would be reached, indicating ideal behavior of the macro-CTA. Incomplete activation of the CTA groups, incomplete solvatation, steric hindrance, termination reactions or other effects decrease the initiation efficiency and the graft ratio, respectively.

Analysis and comparison of the graft copolymers:

The graft copolymers, which were synthesized according to the procedures described in the chapters 5.3.1 to 5.3.4 were further analyzed using SEC with UV-Vis detection. In order to provide the reader a better overview about the performed experiments, the experimental data of the synthesis of the graft copolymers is summarized in table **Table 10**.

Table 10. Summary of the experimental conditions for the synthesis of graft copolymers. As inferred from the $[styrene]_0/[CTA, total]/[AIBN]_0$ ratio, the experiments can be separated into three groups, as described by procedure A, B and C, respectively.

experiment name	$[styrene]_0$	[CTA on cellulose]	[free CTA]	$[AIBN]_0$	$[styrene]_0/[CTA, total]/[AIBN]_0$
	[mol/L]	[mmol/L]	[mmol/L]	[mmol/L]	
Procedure A					
MCC-CTA14-PS_3	4.36	2.5 (25 mol-%)	7.5	2.0	2180/5/1
MCC-CTA14-PS_4	4.36	1.0 (10 mol-%)	9.0	2.0	2180/5/1
Procedure B					
MCC-CTA14-PS_9	4.36	1.0 (20 mol-%)	4.0	2.5	1744/2/1
MCC-CTA14-PS_10	4.36	1.5 (30 mol-%)	3.5	2.5	1744/2/1
MCC-CTA14-PS_11	4.36	2.0 (40 mol-%)	3.0	2.5	1744/2/1
Procedure C					
MCC-CTA14-PS_12	5.24	1.0 (25 mol-%)	3.0	1.0	5240/4/1

The analytic data obtained by SEC with UV-Vis detection was then further processed (by the method described in the previous section) to calculate the graft ratio and the initiation efficiency. The results are summarized in **Figure 81**.

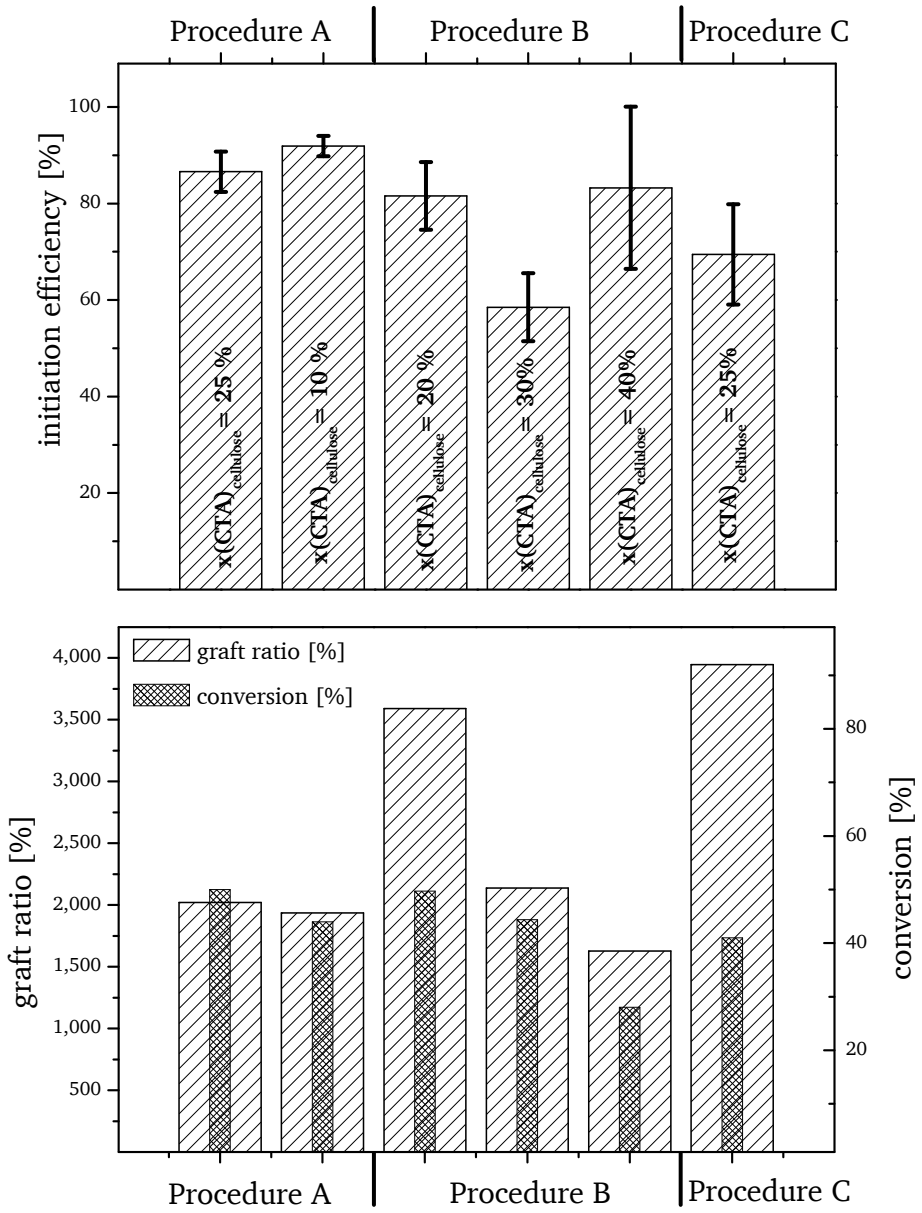

Figure 81. Top: Initiation efficiencies (I_{eff}) for the different polymerization procedures A , B and C, respectively. Note: this denotation of the procedures refers to the denotation provided in table Table 10. I_{eff} was calculated from the corresponding SEC analysis of the polymers. The percentage denoted in the individual columns refers to the amount of CTA groups immobilized on cellulose in comparison to the total amount of CTA groups set in the reaction. Errors given correspond to standard deviation. Bottom: Graft ratio for each polymerization with the longest reaction time (i.e. highest conversion). The graft ratio was calculated from the total amount of the polymer mixture and the relative amount of polymer grafts, respectively. The monomer conversion of individual reaction is plotted on the right y-axis. Image redrawn with permission from [71].

Graft copolymers from the experiments MCC-CTA14-PS_3, MCC-CTA14-PS_4 (procedure A), were obtained by application of a high [CTA]/[AIBN]-ratio of 5:1. The high initiation efficiencies of about 90 % indicate excellent control over the polymerization, but relative low graft ratios of about 2,000 % were obtained compared to the subsequent experiments, because of the relative short polymer grafts with average molar masses M_n< 20kDa, as discussed in chapter 5.3.1.

The graft copolymers obtained by the experiments MCC-CTA14-PS_9, MCC-CTA14-PS_10 and MCC-CTA14-PS_11 (procedure B) showed a reduced initiation between 60 % and 80 %, depending on the relative amount of cellulose macro-CTA to the overall amount of CTA. The graft ratio could be raised up to more than 3,500 % for the experiment MCC-CTA14-PS_9.

The graft copolymers obtained by the experiment MCC-CTA14-PS_12 (procedure C) showed the highest graft ratios, but the initiation efficiency and thus the control of the RAFT polymerization were still diminished in direct comparison to the polymers obtained by procedure A. It should be kept in mind, that the graft ratio depends on DS(CTA), initiation efficiency and molar mass of the polymer grafts. The DS (CTA) was constant because the same cellulose macro-CTA was used for all experiments, but initiation efficiencies varied on the reaction conditions and the molar mass of the grafts also varies with applied reactant ratios and conversion. Therefore comparisons of the graft ratios between the different experiments can be made only to a limited extend.

Samples MCC-CTA14-PS_3 and MCC-CTA14–PS_4 have a similar conversion and are only different in the applied cellulose [macro CTA]/[free CTA] ratio and show as expected a similar graft ratio. On the other hand, comparing sample MCC-CTA14–PS_9 with sample MCC-CTA14-PS_10 a similar graft ratio was expected because of similar conversion, but a strong deviation can be observed. The reason for this is the significant different initiation efficiency because of an increased viscosity which assumingly leads to termination reactions. Finally, sample MCC-CTA14-PS_12 shows the largest graft ratio of all samples, even though it had the second lowest initiation efficiency. This can be explained by the high molar mass of the polymer grafts which is larger than in all other samples. Furthermore an increased high viscosity had not been observed, eventually due to the low concentration of cellulose macro-CTA.

5.3.5. Control of the graft density

As explained in chapter 4.2.2 the DS(CTA) (hence the density of CTA groups) on the cellulose backbone were varied between 0.23 and 0.56. In the next step, cellulose graft copolymers with controlled graft density were investigated. The synthesis of graft copolymers based on cellulose macro-CTA “MCC-CTA12” and “MCC-CTA15”, having as DS(CTA) = 0.4 and DS(CTA) = 0.23 respectively. Besides that, typical reaction conditions (i.e. concentrations, solvent and temperature) were applied. After polymerization, the graft copolymers were isolated from homopolymer via fractional precipitation and analyzed with SEC (**Figure 82** and **Figure 83**).

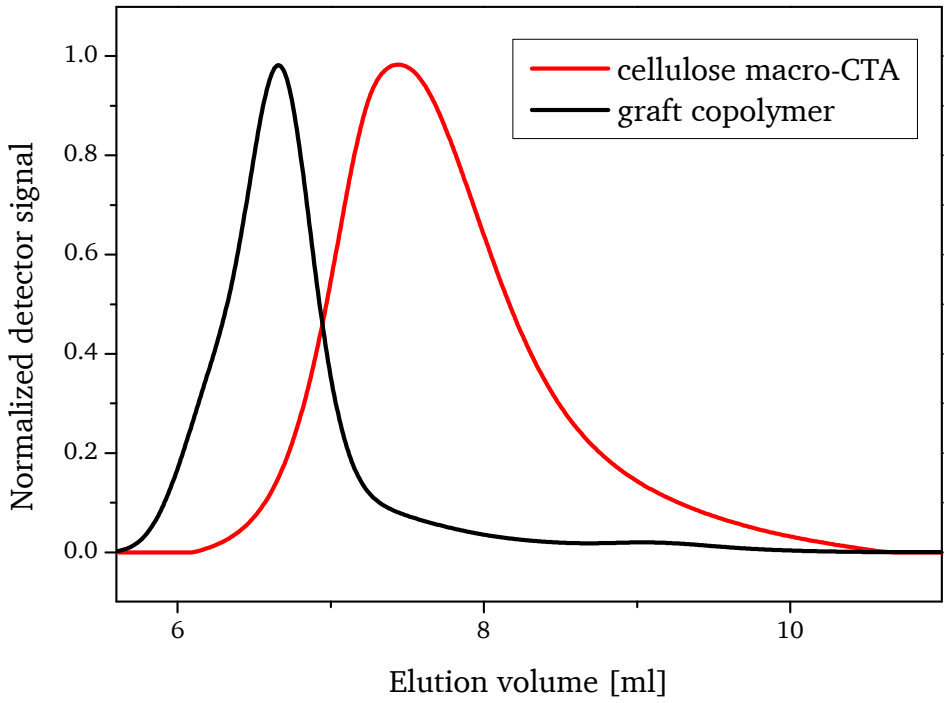

Figure 82. SEC traces of cellulose macro-CTA "MCC-CTA12", having a DS(CTA) = 0.40 before polymerization and isolated cellulose graft copolymer after polymerization.

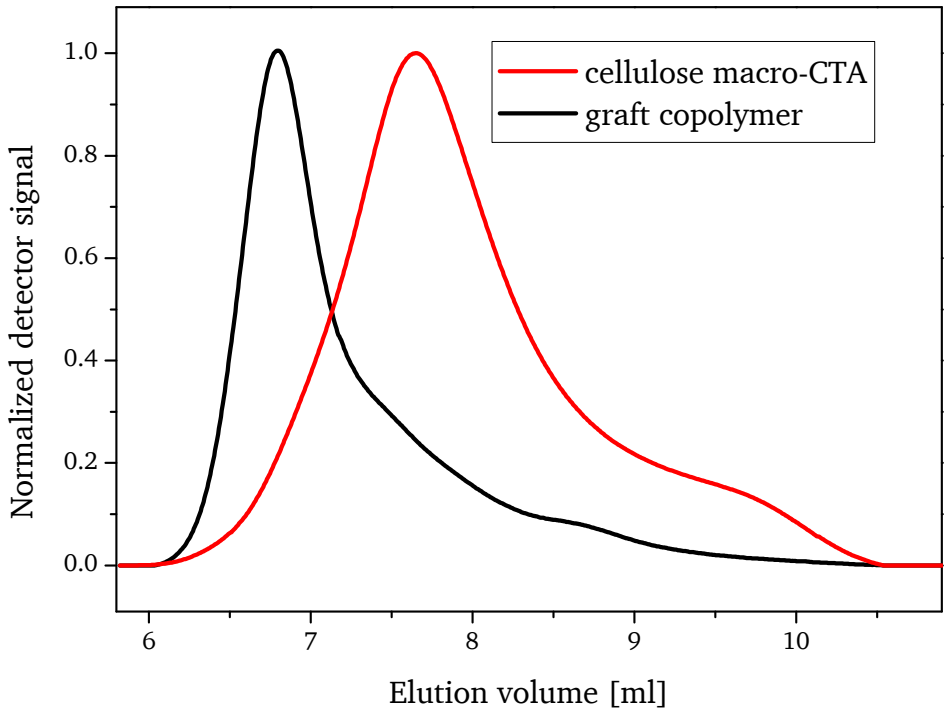

Figure 83. SEC traces of cellulose macro-CTA "MCC-CTA15", having a DS(CTA) = 0.23 before polymerization and isolated cellulose graft copolymer after polymerization.

In both elugrams, a shift towards smaller elution volumes indicates an increase in the apparent hydrodynamic radius, indicating an increased average molar mass and thus a successful graft copolymerization.

For chapter 5.3 we conclude that graft ratios of up to about 3,500 % and initiation efficiencies of about 90 % suggest a successful and efficient graft copolymerization process of polystyrene on cellulose macro-CTA. Polymer grafting from cellulose via RAFT techniques is predominantly performed in heterogeneous media such as cellulose fibers, nanocrystaline cellulose or cellulose nano-whiskers by other groups. There are only few reports regarding homogenous reactions for RAFT mediated graft copolymerization on cellulose (derivatives). In these reports yields, graft ratios and initiation efficiencies are often not analyzed, therefore a comparison with our results is difficult. Lucia and coworkers reported graft ratios of about 30 %, obtained by homogenous grafting of polystyrene in ionic liquid [27]. Perrier et al reports polymer grafting of NiPAM or EA , using hydroxypropyl cellulose derived cellulose macro-CTA [52], however the graft ratio was not provided. From the published experimental data, we estimated a graft ratio of up to 750 % using NiPAM, and a graft ratio of about 420 % using EA as monomer for Perrier's work. Comparison of this data with our data indicates an improvement of the RAFT mediated polymerization process from cellulose, using well-soluble cellulose macro-CTA and "CTA-shuttled R-group approach".

Finally we were addressing to the question, if the structure of the presented cellulose graft copolymers could be referred as brush polymers or as comb polymers. In brief, we define a graft copolymer a brush polymer, if individual polymer grafts interact with each other by means of repulsive forces which results in a stretching of the polymer graft away from the polymer backbone. This phenomenon is provided if $R_g > D$, where R_g is the radius of gyration of the polymer graft and D the average distance between two polymer grafts attached onto the polymer backbone. If this is not provided, hence if $R_g < D$, we consider the polymer architecture as a comb polymer. Taking the cellulose macro-CTA "MCC-CTA14" with as DS(CTA) = 0.54, we were able to calculate the average distance of about D = 1 nm. Then we calculated the radius of gyration of the polymer grafts of about Rg = 2.5 nm, by assuming a low molecular mass polymer graft with M_n= 10 kDa. From these values we can conclude, that the graft copolymers presented in chapter 5.3 can be considered as brush polymers. Details about the model calculations and the theory are described in the appendix, chapter 9.2.

6. Mixed brush copolymers with a cellulose backbone

Note, some of the data shown in the following section 6.1 concerning the ATRP reactions, were obtained in collaboration with the groups of Markus Gallei and Matthias Rehahn. ATRP reactions were performed together with Christian Rüttiger (PhD student).

6.1. Synthesis by combination of RAFT and ATRP

Since the graft copolymers based on cellulose macro-CTA showed very promising results regarding the control of the polymerization using a CTA-shuttled R-group approach, further experiments were performed in order to extend the concept to more complex architectures like cellulose mixed graft copolymers. The latter can be defined as graft copolymers having two different types of grafts attached to a single cellulose backbone, as exemplary displayed in **Figure 84**.

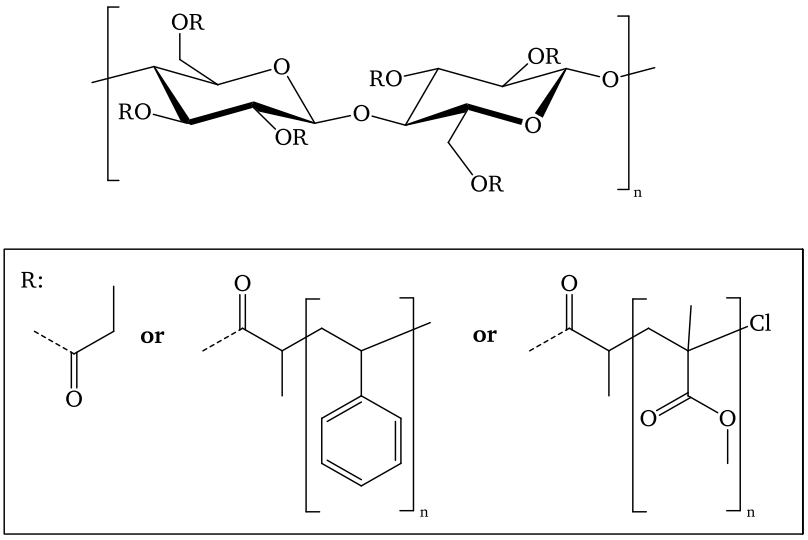

Figure 84. General structure of the target molecule.

We first followed a synthesis strategy for mixed grafts on cellulose, which was based on macro-CTAs and using sequential polymerization of two different monomers with two different techniques. There are different limitations and difficulties, which need to be considered when planning multi-step consecutive polymerizations, such as the choice of CPR techniques, the sequence of the polymerization steps, the choice of monomers and targeted DPs of the polymer grafts. It should be noted that the synthesis of complex polymers by combination of polymerization techniques is a wide field and therefore we refer to the review article from Bernaerts et al. [86] for more detailed information.

Considering all these important aspects, the following detailed strategy was chosen:

- Synthesis of a cellulose graft copolymer with short polymer grafts using RAFT polymerization
- subsequent removal of CTA groups from the graft copolymer
- second polymerization with a different monomer using ATRP technique
- cleavage of the polymer grafts from the cellulose backbone by hydrolysis followed by SEC analysis

The RAFT polymerization needs to be performed before the ATRP reaction because only this sequence allows the synthesis of mixed grafts. The application of ATRP before the RAFT polymerization leads to block copolymer grafts, because the propagating polymer grafts, initiated by the atom transfers of the 2-bromopropionyl groups can also react with the CTA groups attached to the cellulose by a reversible chain transfer mechanism. The resulting structure is schematically presented in **Figure 85**.

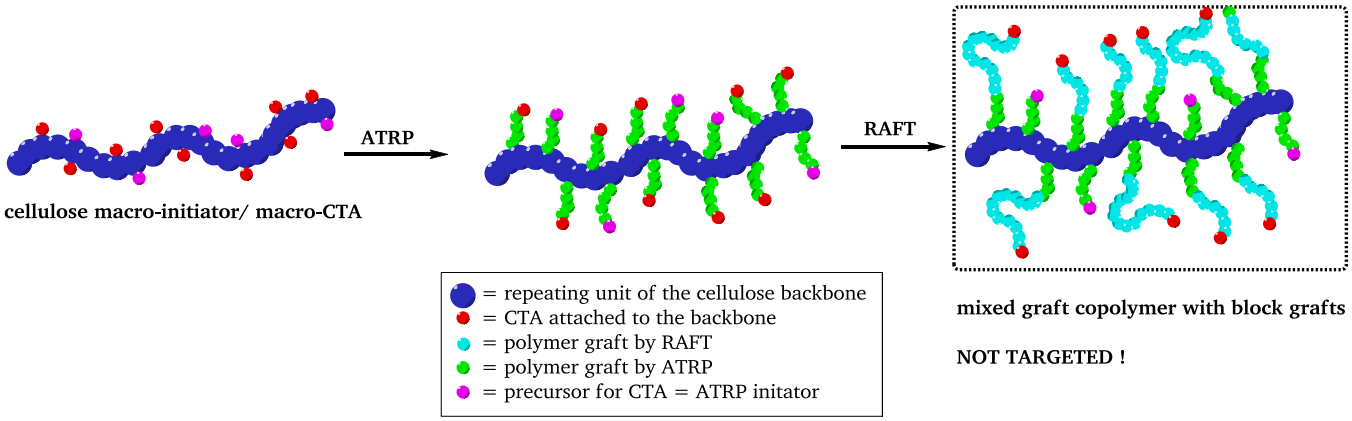

Figure 85. Schematic image of the synthesis of graft copolymer using ATRP before RAFT as sequence. The resulting structure exhibits a mixture of grafts and block copolymer grafts.

The polymerization via ATRP during the presence of CTA is also known as SET RAFT, as reported by Zhang et al.[87]. This method is convenient for the synthesis of well-defined block copolymers, however these polymer architectures were not targeted in this work.

The next aspect which needs to be considered is the removal of the CTA groups after the RAFT polymerization and before the ATRP. As explained above, the presence of CTA groups during the subsequent ATRP reaction leads to a SET RAFT reaction and to the undesired formation of block copolymer grafts.

The third aspect concerns the formation of two different types polymer grafts as we pursued the concept of more complex polymer architectures. For the proof of concept we chose the synthesis of PMMA and PS mixed grafts because both polymers are well established and are convenient in the characterization with SEC. The synthesis strategy is displayed in detail in **Figure 86**.

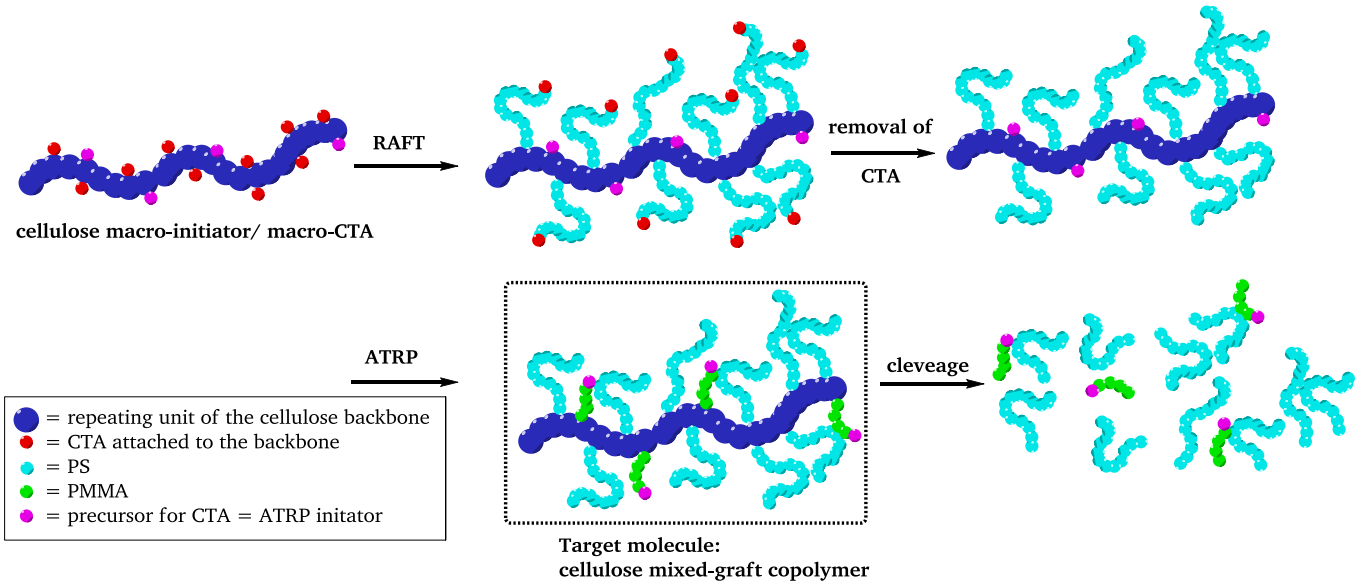

Figure 86. Synthesis strategy for the formation and the analysis of cellulose PS/PMMA mixed-graft copolymers.

Model experiment: Graft copolymerization of MMA by ATPR using 2-bromopropionyl cellulose mixed ester

Prior to the synthesis of the mixed graft copolymers, a set of model experiments was performed in order to validate the chosen reaction parameters. First attempts of ATRP on cellulose were performed with a cellulose macro-initiator carrying 2-bromopropionyl and propionyl functionalities ("MCC-BpB4-Pr", see chapter 4.2.2) but no further polymer grafts. It should be noted, that the same cellulose derivative was also used as a precursor of cellulose macro-CTAs. The reaction conditions of the ATRP reaction are displayed in **Figure 87**.

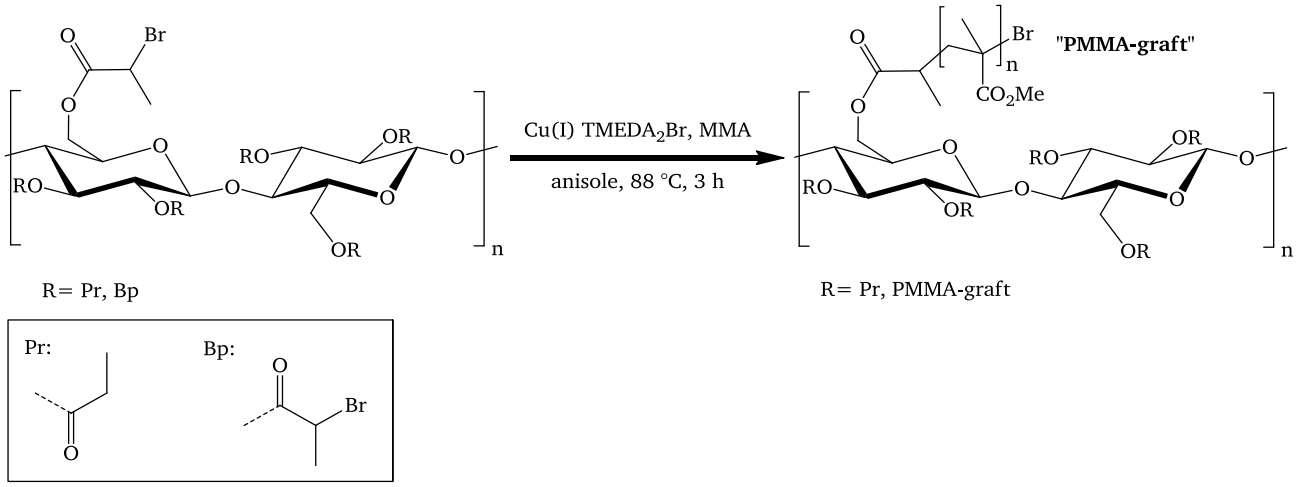

Figure 87. Graft copolymerization of a cellulose macro-initiator via ATRP using MMA as monomer.

The reaction was carried out in the absence of oxygen and water. The reactants were added in a Schlenk-tube, the reaction mixture was then degassed and the polymerization was started by heating with an oil bath. After the reaction the copper compounds were removed by filtration through a basic aluminum oxide column. The polymer was isolated by precipitation of the reaction mixture into methanol. A sample of the graft copolymer was hydrolyzed; the cleaved-off polymer-grafts were isolated. Note: After hydrolysis the remaining polymer became insoluble in THF, likely due to hydrolysis of the PMMA into poly methacrylic acid. Thus, for better comparison, all samples (including cellulose macro-initiator) were dissolved in DMF, and then analyzed by SEC (**Figure 88**) with DMF/LiCl as eluent.

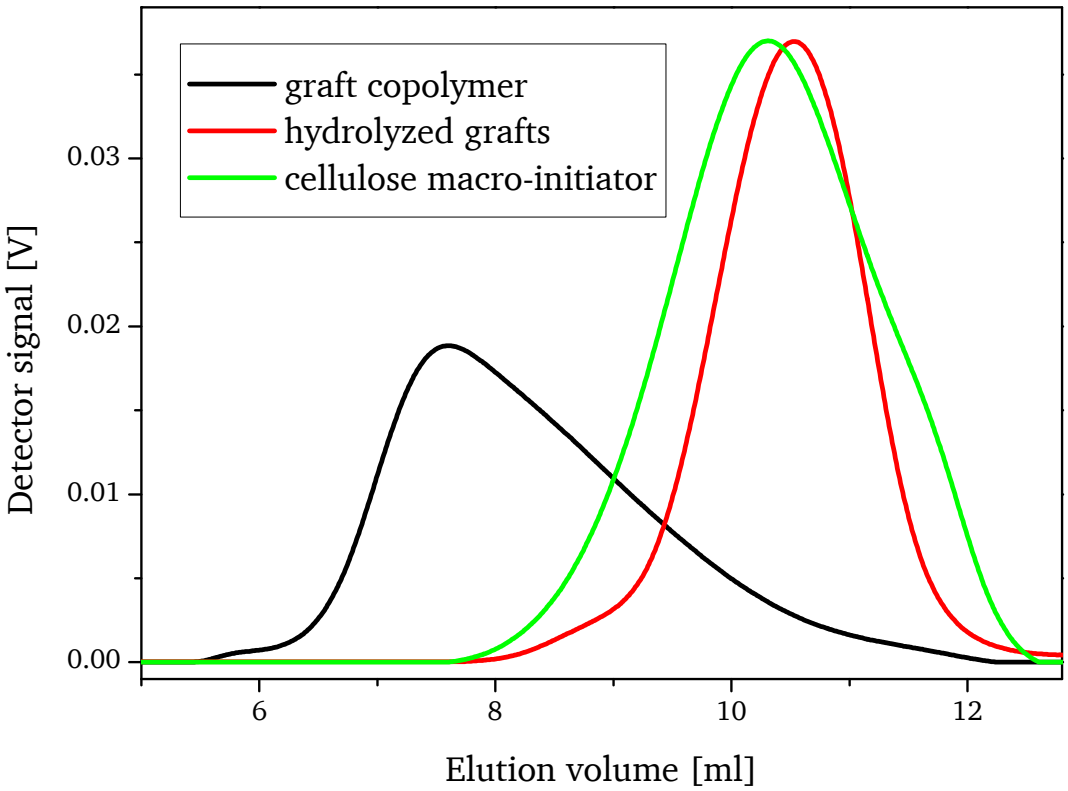

Figure 88. SEC traces of the polymer samples, using DMF/LiCl as eluent. The cellulose macro-initiator "MCC-BpB4-Pr" (green), after graft copolymerization (black) and after the cleavage of polymer grafts by hydrolysis (red). A shift of the signal towards higher elution volumes after treatment of the graft copolymer under strong alkaline conditions indicates successful cleavage of the polymer grafts from the cellulose backbone.

After the graft copolymerization the signal maximum of the elution volume of cellulose macro-initiator decreases from about 10 ml to about 8 ml, indicating a higher apparent hydrodynamic radius. After hydrolysis of the graft copolymer under strong alkaline conditions the isolated polymer grafts show a shift towards high elution volumes, confirming the cleavage of the cellulose backbone. These results indicate that graft copolymerization of MMA with ATRP can be successfully performed. This is why this method was considered promising for the synthesis of cellulose mixed graft architectures by combination of RAFT and ATRP techniques in subsequent experiments.

Synthesis of the mixed graft precursor, having short polymer grafts:
RAFT polymerization of styrene with cellulose macro-CTA

The RAFT polymerization was performed before the ATRP reaction as discussed above. The synthesis was conducted in the same fashion as described in chapter 5. In order to avoid physical blocking of polystyrene grafts in subsequent ATRP reaction, an average molar mass of about 5 kDa-10 kDa was targeted. The reaction scheme is presented in **Figure 89** and reactant concentrations are provided in **Table 11**.

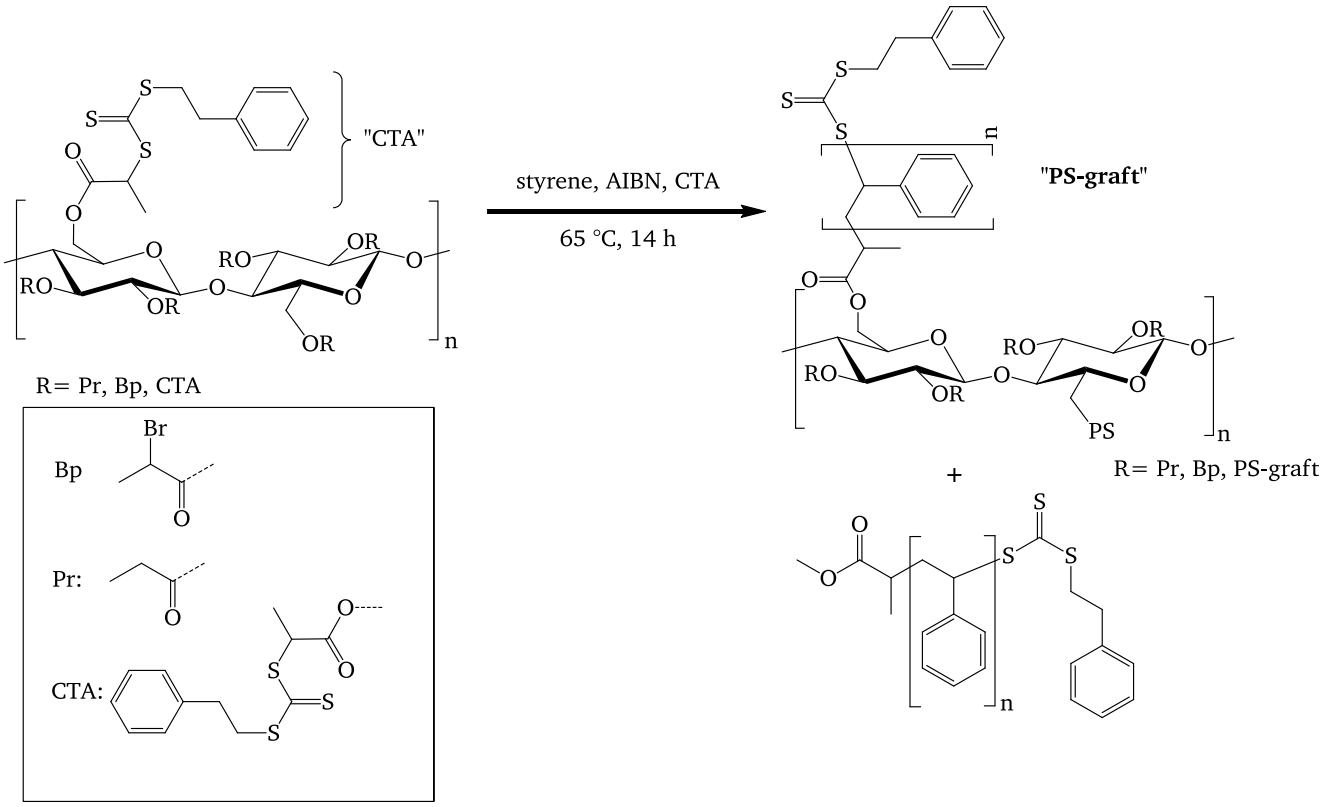

Figure 89. Reaction scheme of the graft copolymerization of cellulose macro-CTA with styrene.

Table 11. experimental parameters for the experiment "MCC-CTA14-PS_13".

experiment name	$[styrene]_0$	[CTA on cellulose]	[free CTA]	$[AIBN]_0$	$[styrene]_0$/ [CTA, total]/ $[AIBN]_0$
	[mol/L]	[mmol/L]	[mmol/L]	[mmol/L]	
MCC-CTA14-PS_13	4.36	4.0	6.0	2.0	2180/5/1

A monomer conversion of 17 % was determined with ^{1}H-NMR and a yield of about was 1.95 g was determined. Then the Mn and Đ of homopolymer and graft copolymer were determined by SEC, using THF as eluent and calibration with low disperse PS standards. M_n (homopolymer) = $8.0*10^3$ g/mol, Đ(homopolymer) = 1.2, M_n(graft copolymer) = $2.06*10^5$ g/mol.

The contents of polymer grafts and homopolymer in the product were analyzed by SEC coupled with UV-Vis detection, as shown in **Figure 90**.

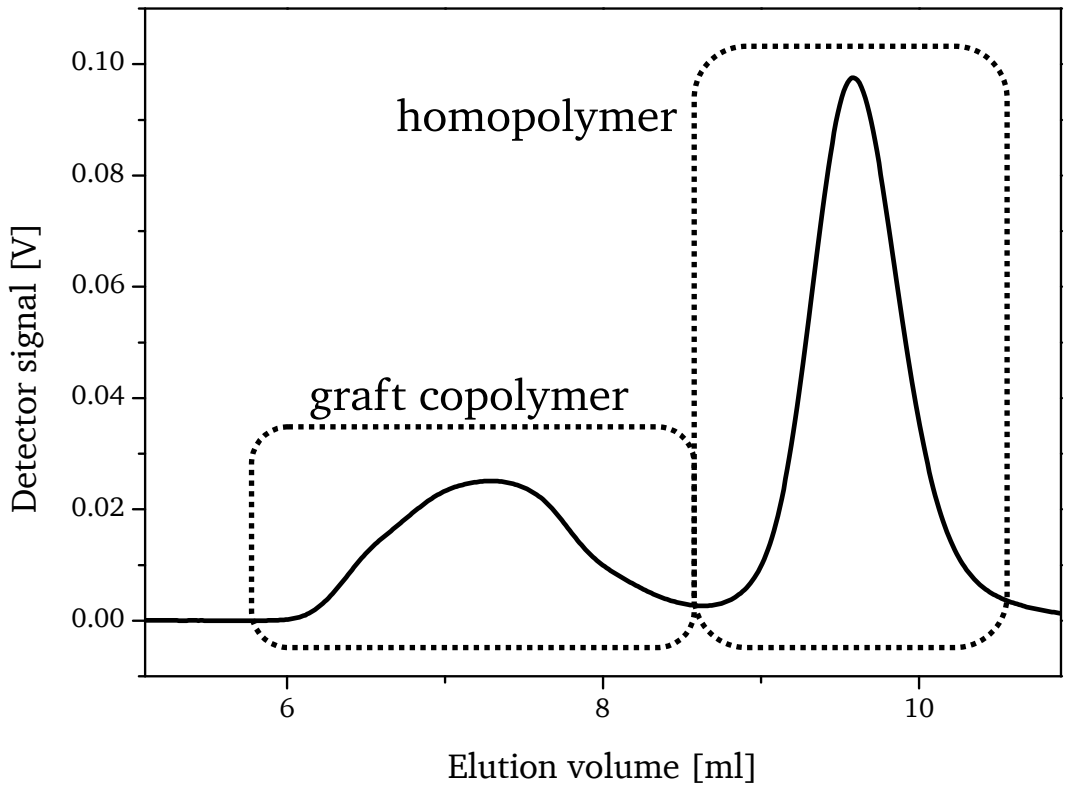

Figure 90. SEC traces of the polymer mixture containing graft copolymer and homopolymer from the experiment "MCC-CTA14-PS_13", using THF as eluent and UV-Vis detection. The signal at low elution volume is originated from the cellulose graft copolymer, whereas the signal at high elution volumes is originated from homopolymer. Since UV-Vis detection was used, the relative signal areas correlate with the content of graft copolymer and homopolymer, respectively. For the calculation of the integral signal intensities, the software Origin was used.

The relative amount of graft copolymer was then calculated by the relative integral signal intensities to be about 36 %. As the yield was about 1.95 g, it contained 1.86 g of polystyrene and 0.09 g of cellulose macro-CTA. Having 36 % of the total amount of polystyrene attached onto the cellulose macro-CTA, means that about 0.67 g of polystyrene is attached as grafts onto 0.09 g of cellulose macro-CTA, leading to a graft ratio of 740 %. Furthermore, by using equation **(25)**, an initiation efficiency I_{eff} of about 85 % was calculated from the SEC data. After successful synthesis of the cellulose polystyrene graft copolymer, all CTA functionalities had to be removed, in order to avoid chain transfer during the grafting initiated by ATRP using the remaining bromine functionalities left on the cellulose backbone, as shown in the next section.

Removal of the terminal CTA-groups on the cellulose graft copolymer

Removal of the terminal trithiocarbonate groups was performed by a recombination reaction of cellulose graft copolymer with a large excess of AIBN, as shown in **Figure 91**.

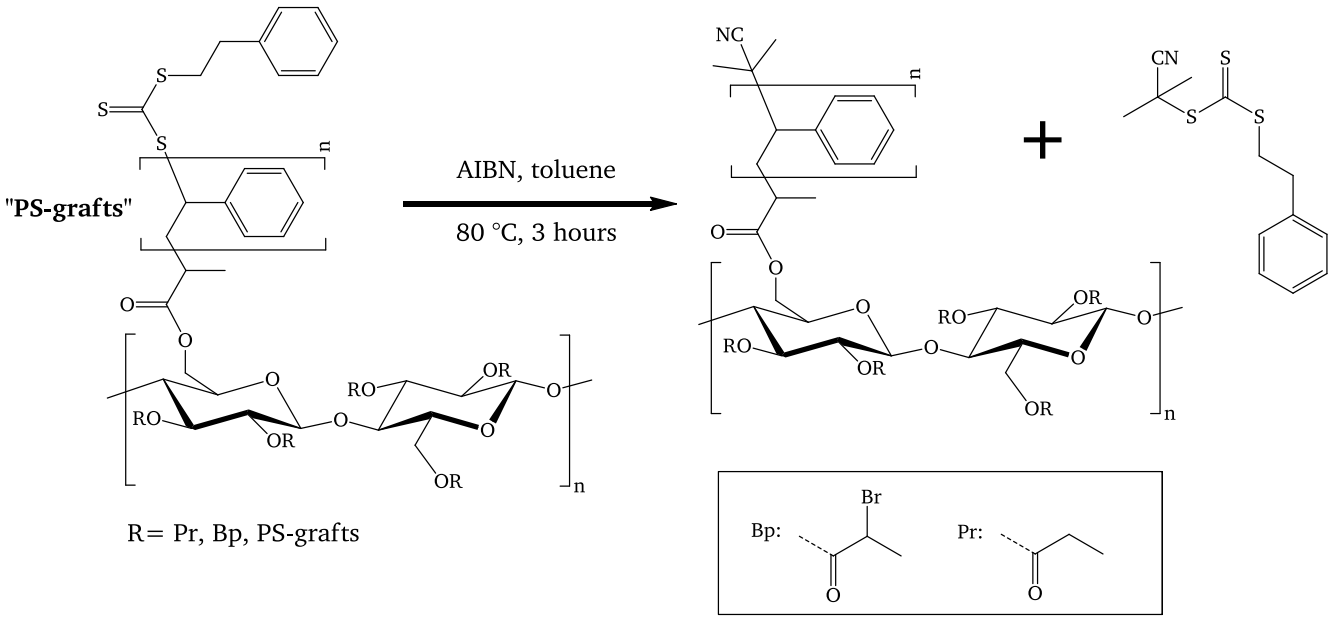

Figure 91. Schematic procedure for the removal of terminal CTA groups from cellulose graft copolymer and linear homopolymer by excess of AIBN in solution.

The reaction and the reaction conditions were adopted from literature [88]. For this, 1.0 g of polymer and 0.5 g AIBN were dissolved in toluene and added to a reaction vessel. The reaction mixture was stirred at 80 °C for three hours; the polymer was isolated by precipitation in methanol with subsequent drying. First attempts to monitor the removal of CTA groups from the polymer with UV-Vis were not successful because of strong light absorbance of the polystyrene (300 nm) and only weak characteristic absorbance of the thio-moiety at 450 nm wavelength. Therefore, the removal of the CTA groups was confirmed by other observations. For example, the product did not show its characteristic yellow color (which arises from the CTA functionalities), which is an indication for the removal of the CTA groups. This finding was further confirmed by analysis of the polymer with ^{1}H-NMR, since no remaining CTA-functionalities could be determined. Finally, the structure of the polymer was analyzed by SEC, where no degradation was observed, as shown in **Figure 92**.

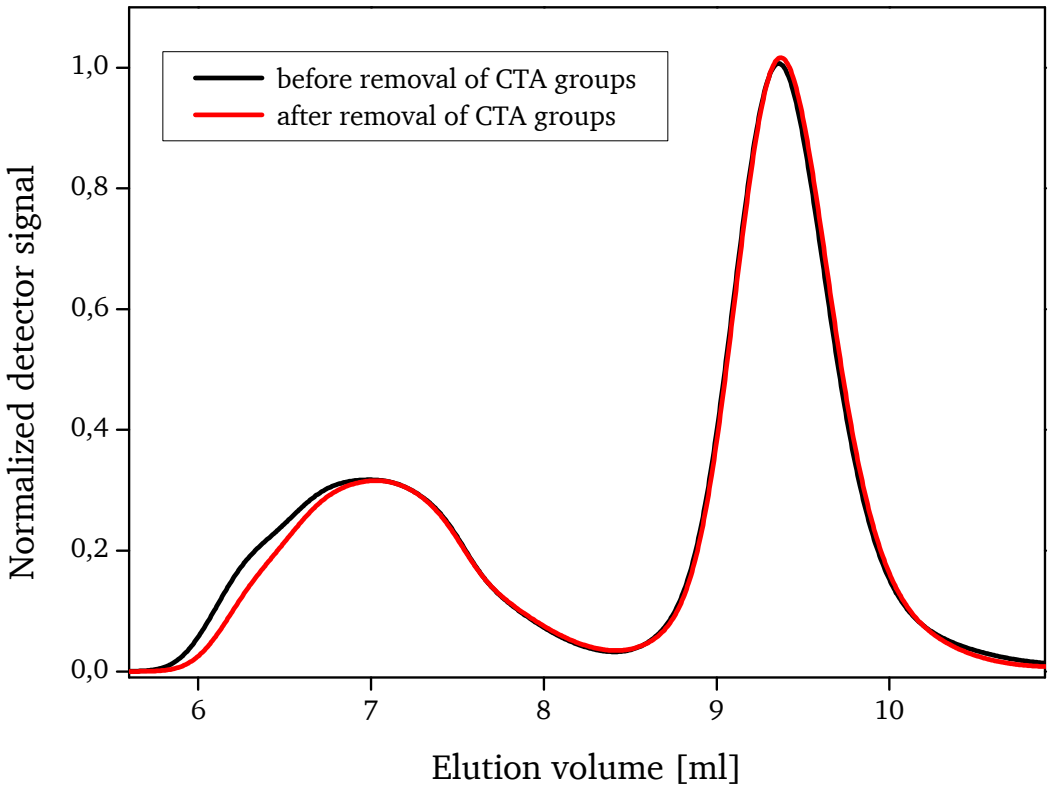

Figure 92. SEC traces of homopolymer and graft copolymer of experiment MCC-CTA14-PS_13 before and after removal of the terminal CTA groups, measured in THF as eluent and UV-Vis detection. The black line represents the graft copolymer and homopolymer before removal of the CTA functionalities, whereas the red line corresponds to the polymer mixture after the removal. The signals at low elution volumes (cellulose graft copolymer) and at high elution volumes (homopolymer) show a very similar pattern thus proving that no degradation occurred during the removal of the CTA groups.

Both elugrams have an almost identical signal shape of graft copolymer before and after treatment with AIBN, indicating that the polymers remained intact and did not undergo depolymerization processes. The analysis additionally shows that the CTA moieties are attached at the end of the polymer grafts (R-approach) rather than the position between the cellulose and the polymer graft (Z-approach). If graft copolymers would have been derived from a Z-approach, AIBN treatment at high temperatures would lead to a significant loss in grafted PS chains and hence a change in the outcome of SEC analysis.

After removal of the CTA groups, the graft copolymer MCC-CTA14-PS_13 was further modified by a graft copolymerization of MMA initiated through the remaining bromine functionalities. No additional “sacrificial” bromine containing initiator was added, thus polymerization should only occur at the cellulose backbone.

ATRP reaction of MMA with cellulose graft copolymer "MCC-CTA14-PS_13"

In brief, the ATRP reaction was carried out as follows. The cellulose graft copolymer was dissolved in anisole to yield a 12.5 wt-% solution, followed by the addition of MMA. Then, the reaction mixture was heated to 88 °C, followed by the addition of Cu(I)TMEDA$_2$Br stock solution in anisole. The reaction scheme is displayed in **Figure 93**.

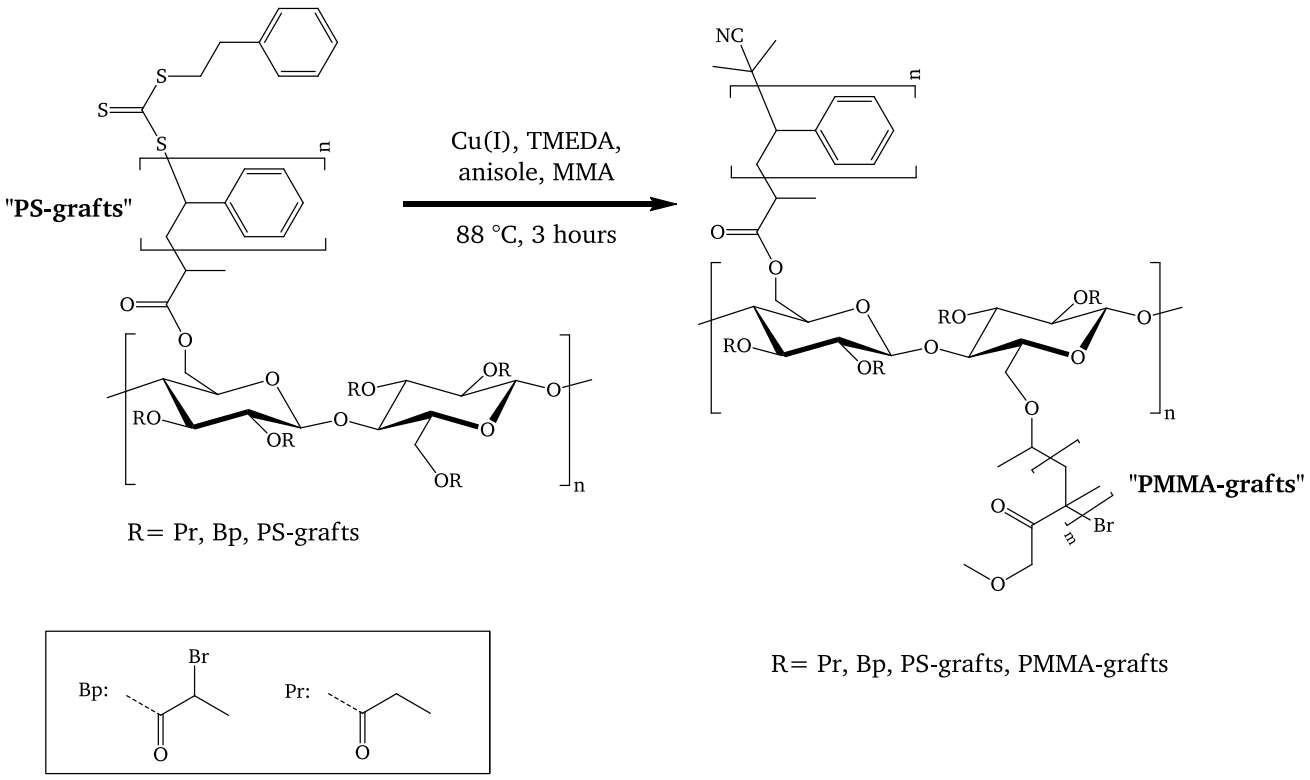

Figure 93. Reaction scheme of the synthesis of a mixed graft copolymer by consecutive ATRP reaction of a cellulose graft copolymer bearing 2-bromopropionyl ester functionalities as initiator groups.

After 3 hours reaction time, the polymer was isolated by removal of the copper complex through a basic aluminum oxide column followed by precipitation into methanol. The mass increase of the product after polymerization with MMA via ATRP proves that the polymerization took place under the applied conditions. After the polymerization, the product was analyzed by ^{1}H-NMR to proof the chemical identity and the relative amounts of PS and PMMA, as shown in **Figure 94**.

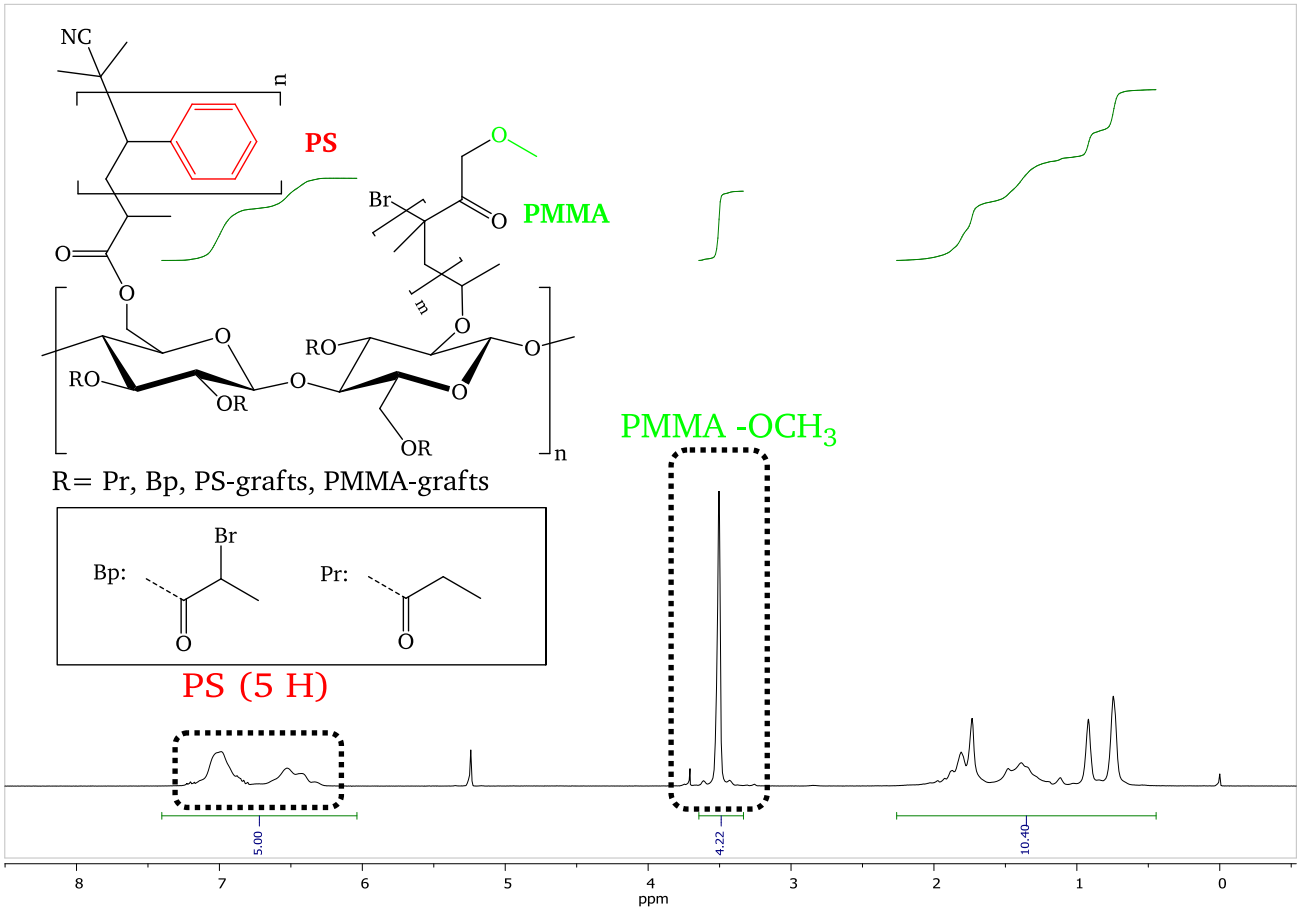

Figure 94. ^{1}H-NMR spectrum of cellulose mixed graft copolymer containing PS-grafts and PMMA-grafts (experiment MCC-CTA14-PS_13-PMMA_1). The ratio of the grafts was calculated from the corresponding proton signals of polystyrene and PMMA.

As inferred from the spectrum, proton signals originated from polystyrene as well as from PMMA can be identified and quantitatively analyzed. The aromatic proton signals from polystyrene at about 7 ppm were put in relation to the methyl ester protons from the PMMA grafts at a chemical shift of about 3.5 ppm. For the calculation of the graft ratio, it was considered that the precursor MCC-CTA14-PS_13 only contained 36 % polystyrene grafted onto the backbone of the cellulose polymer, and 64 % PS homopolymer (as explained earlier in **Figure 90**). Then, the ratio of PS and PMMA was determined to be 1:1.4. If we keep in mind that only 36 % of the polystyrene was grafted onto the cellulose, the molar ratio of monomer units of graft-PS/graft-PMMA would be 1:3.9. This finally leads to a total graft ratio of about 3,500 %. Additionally the product was analyzed by SEC for the analysis of the molar mass evolution, as presented in **Figure 95**.

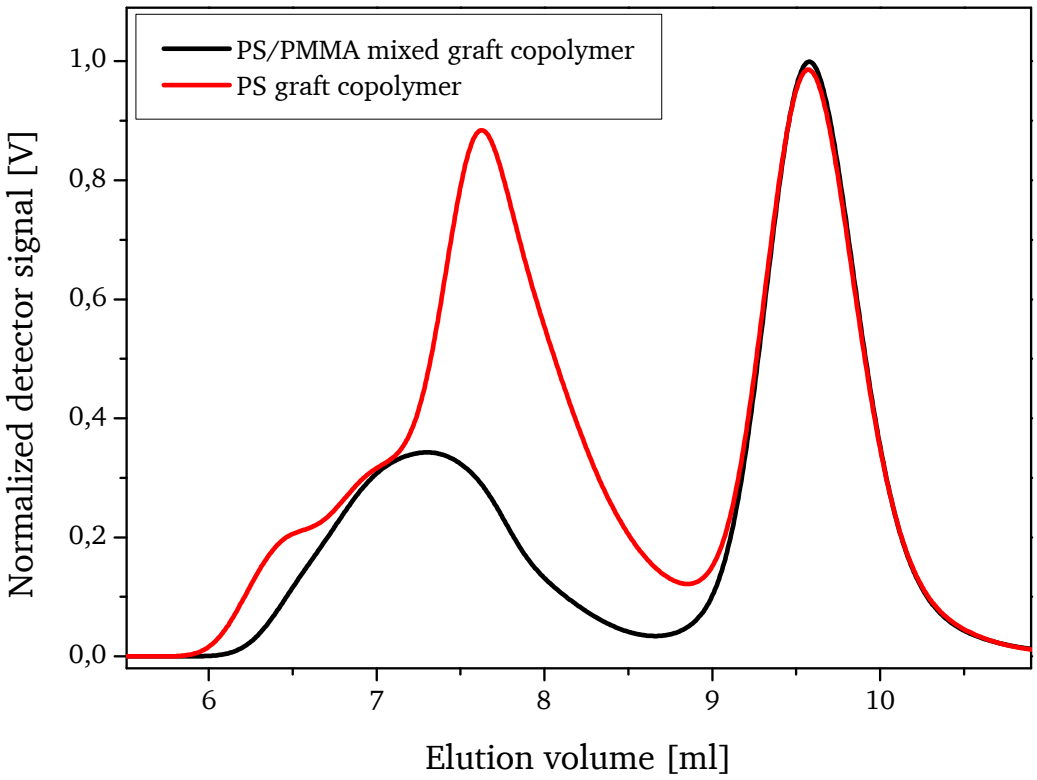

Figure 95. SEC traces of cellulose polystyrene graft copolymer and cellulose polystyrene polymethylmethacrylate mixed graft copolymer, measured in THF with UV-Vis detection. The homopolymer, which elutes at 8.7 ml to 10.5 ml, does not change in its distribution due to ATRP polymerization, thus proving that CTA-functionalities have been removed quantitatively in the prior step. The polystyrene graft copolymer, which elutes at about 6.0 ml to about 8.7 ml exhibits a significant change in the signal pattern and thus in its apparent molar mass distribution towards higher elution volumes and thus towards smaller apparent hydrodynamic radius.

As regarding for **Figure 95**, the signal of the cellulose graft copolymer changes its pattern, shifting its signal maximum towards higher elution volumes. Therefore the apparent hydrodynamic radius of the polymer was decreased, which does not agree with the assumption, that additional polymer grafts increase the steric demand of the graft copolymer in solution. Further analysis of the mixed graft copolymer was made by cleavage of the grafts by hydrolysis. For this a sample of the polymer was dissolved in THF, followed by the addition of potassium tert.-butanolate. After the reaction at room temperature, the polymer was isolated by precipitation and washing with methanol and subsequent drying at vacuum. The sample of hydrolyzed polymer grafts was insoluble in THF (unlike its precursor cellulose mixed graft copolymer), but it seemed to be well soluble in DMF. This is why the polymer was then further characterized by SEC analysis with DMF/LiCl as eluent. The elugram is shown in **Figure 96**; it shows that the broad signal of the graft copolymer at low elution volumes shifts towards higher elution volumes. This was considered an indication for the cleavage of the polymer grafts by the applied conditions. Molar mass and dispersity of the PMMA grafts are determined by use of a PMMA calibration. The number average molar mass was $M_n = 1.04*10^5$ and the dispersity was $Đ = 1.4$.

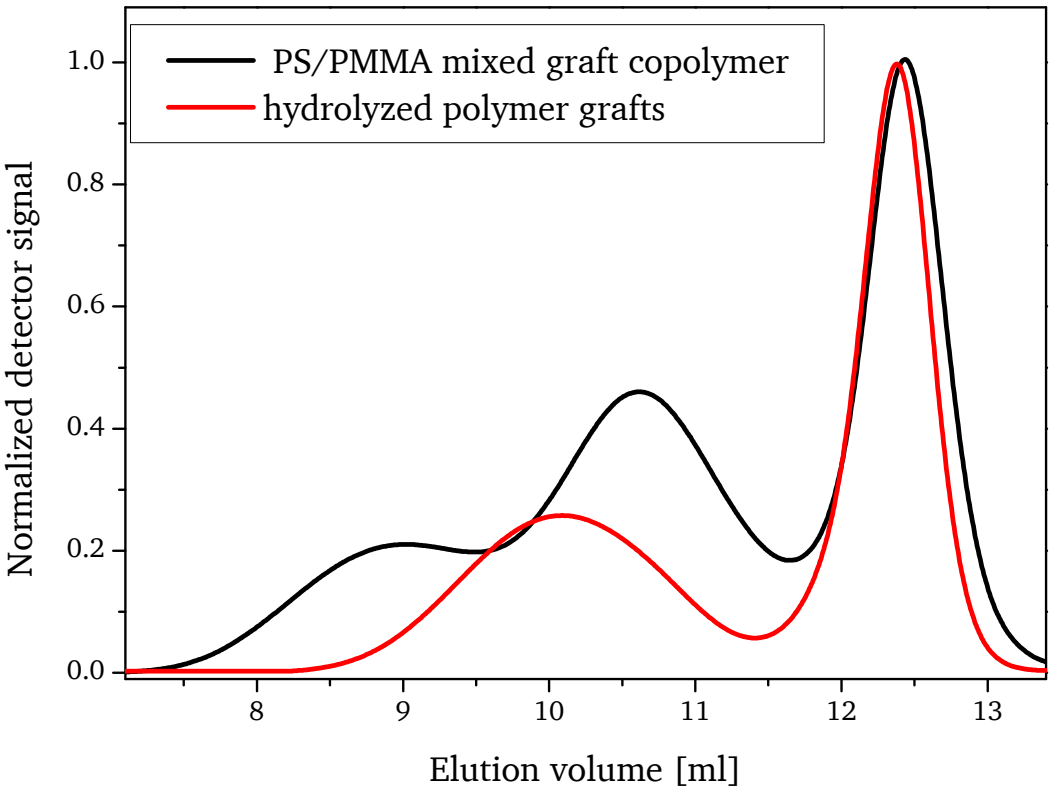

Figure 96. SEC traces of mixed graft polymer before and after cleavage of the polymer grafts. DMF/LiCl was used as eluent. Cellulose mixed graft copolymer "MCC-CTA14-PS_13-PMMA_1". The product was analyzed before (black) and after cleavage (red) of the grafts by hydrolysis. The elution volume of the linear polystyrene at 12.5 minutes did not change, therefore the PS is not affected by the hydrolysis conditions. The graft copolymer shows a change of the bimodal distribution towards a mono modal distribution.

As the product of the hydrolytic cleavage was insoluble in THF, we conclude that eventually the PMMA-grafts were hydrolyzed into the corresponding poly meth acrylic acid PMAA under the harsh reaction conditions during alkaline cleavage. Furthermore, the filtration of the DMF solution before analysis with SEC was not easy, indicating insoluble agglomerates. When the M_n for the PMMA-grafts (**Figure 96**, red curve at elution volumes of about 8 to 11.5 ml) was determined against PMMA standards, the value was significant higher than expected (100 kDa vs. 30 kDa expected), which also might originate from the different physical and chemical nature of PMMA/PMAA copolymer in comparison to the PMMA standards used for calibration. Therefore it is suggested, that these results should be considered as first successful proof of concept. It is emphasized that high graft ratios of the mixed graft copolymer and high initiation efficiencies of the precursor indicate a high potential for future syntheses of well-defined, complex polymer architectures based on cellulose. However, in order to control and to understand the system, further investigation will be necessary.

6.2. Synthesis by combination of “grafting-from” and “grafting-to”

The attachment of polyethylene glycol, known as pegylation, has been used on proteins and low molecular drugs in order to improve water solubility and bioavailability [89]. While being used in recent years for the modification of biotherapeutics, new applications of pegylated polysaccharides such as chitosan have been investigated for medical use [90]. As a simple concept study we finally addressed the question in this thesis, whether it is possible to transfer pegylation protocols to the synthesis of complex architectures based on cellulose. We started with the idea to synthesize cellulose graft copolymers, using PEG in a controlled fashion and chose protocols for regioselective modification of cellulose. The chemical structure of the target molecule is displayed in **Figure 97**.

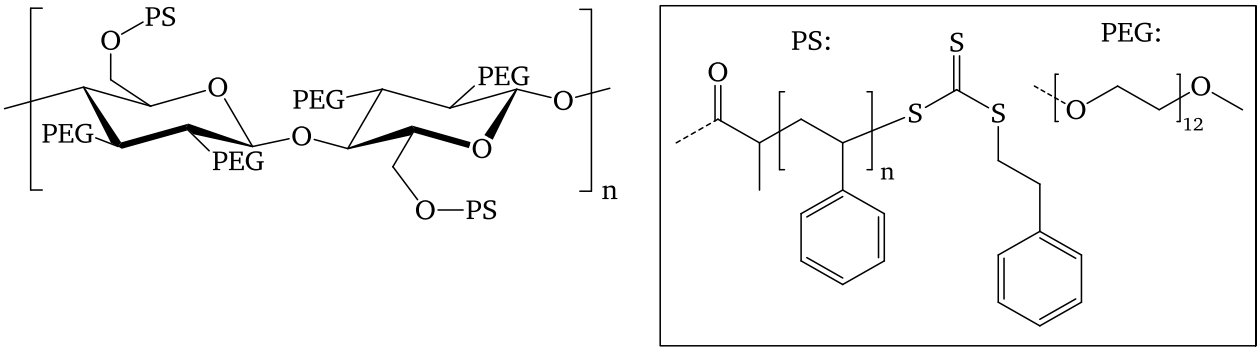

Figure 97. Chemical structure of the target macromolecules. Using protecting groups chemistry, we aimed for regioselective 2,3-*O*-PEGylated cellulose derivatives, carrying polystyrene grafts at the C-6 position.

After extensive study of the synthesis of these macromolecules we came to the conclusion, that the attachment of the PEG groups using etherification protocols lead to significant depolymerization of the cellulose backbone, regardless of the chosen reaction parameters. A detailed report concerning the synthesis and characterization of regioselective cellulose graft copolymers can be found in the appendix of this thesis.

Pegylated cellulose macro-CTA by esterification

The alternative strategy included the attachment of PEG onto cellulose under mild reaction conditions, which included the esterification of carboxyl-terminated PEG with cellulose, using CDI as activating agent. It should be mentioned that this approach excludes the use of protecting group chemistry with trityl chloride, since the reaction conditions for the removal of trityl groups also affects the ester functionalities. The target macromolecule is depicted in **Figure 98**.

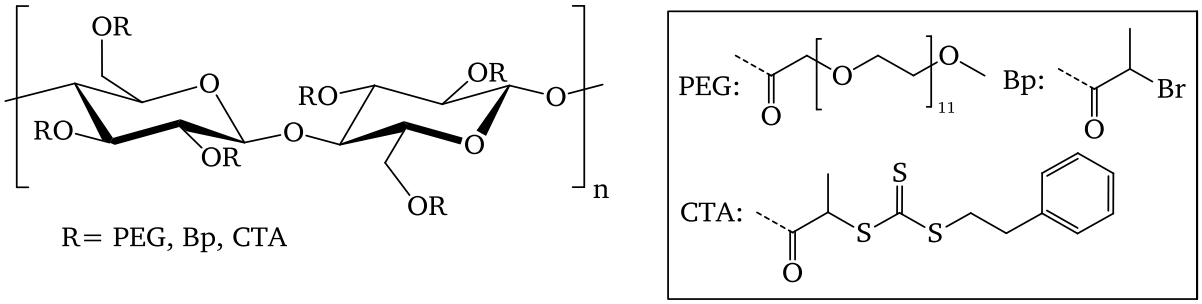

Figure 98. Target structure: statistically pegylated cellulose macro-CTA.

As inferred from the schematic targeted structure, the distribution of PEG groups and CTA functionalities within the repeating unit is not regioselective but statistically. As a consequence, the distribution pattern of CTA may vary between individual repeating units and thus along the cellulose chain. However, mild reaction conditions during the esterification process of the cellulose were considered a significant advantage over the etherification process because the focus was put on the prevention of depolymerization during the multi-step transformation of cellulose into cellulose macro-CTA.

Synthesis of carboxyl terminated poly(ethylene glycol) monomethyl ether (PEG550-COOH)

For the esterification process a carboxyl-functionalized poly(ethylene glycol) was needed. For this, PEG550-monomethyl ether was oxidized into its corresponding carboxylic acid using potassium permanganate and alkaline aqueous reaction conditions, as presented in **Figure 99**.

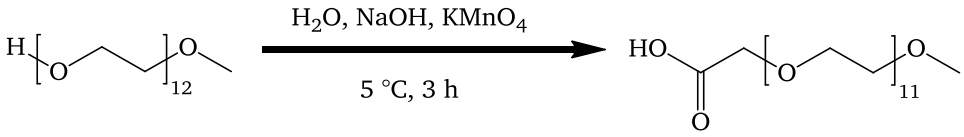

Figure 99. In order to oxidize the carbon atom carrying the hydroxyl functionality into a carboxyl functionality, the strong oxidation agent potassium permanganate was used.

The synthesis was adapted from an oxidation protocol for primary alcohols [91]. A strong temperature dependence on the product yield was observed. Best results were obtained when the reaction temperature was kept below 10 °C over the whole process. When the reaction was started at room temperature without external cooling, a temperature rise up to 40 °C was observed, resulting in yields below 30 %. By external cooling yields up to 78 % could be reached. The chemical identity and purity of the product was confirmed by ^{1}H-NMR spectroscopy.

Model experiment: pegylation via esterification using CDI as activation agent

The focus was put on the investigation of depolymerization of the cellulose backbone under the applied reaction conditions. For the experimental setup the same batch of regioselective tritylated cellulose (from experiment "MCC-Trt_2b") like prior experiments was chosen in order to have a direct comparison to earlier cellulose derivatives obtained by etherification. Besides this, 6-*O*-trityl cellulose has shown to be well soluble in a variety of organic solvents such as DMAc, therefore a convenient characterization with SEC before and after pegylation can be performed. As explained before, each repeating unit of 6-*O*-trityl cellulose offers two remaining hydroxyl functions for esterification, hence high DS(PEG) values may be theoretically achieved.

A model experiment was performed in order to validate the successful modification of cellulose with PEG550-COOH via esterification with the activation agent CDI. The carboxyl-functionalized poly(ethylene glycol) ("PEG550-COOH") was first activated with CDI and then attached onto cellulose via esterification, as presented in **Figure 100**.

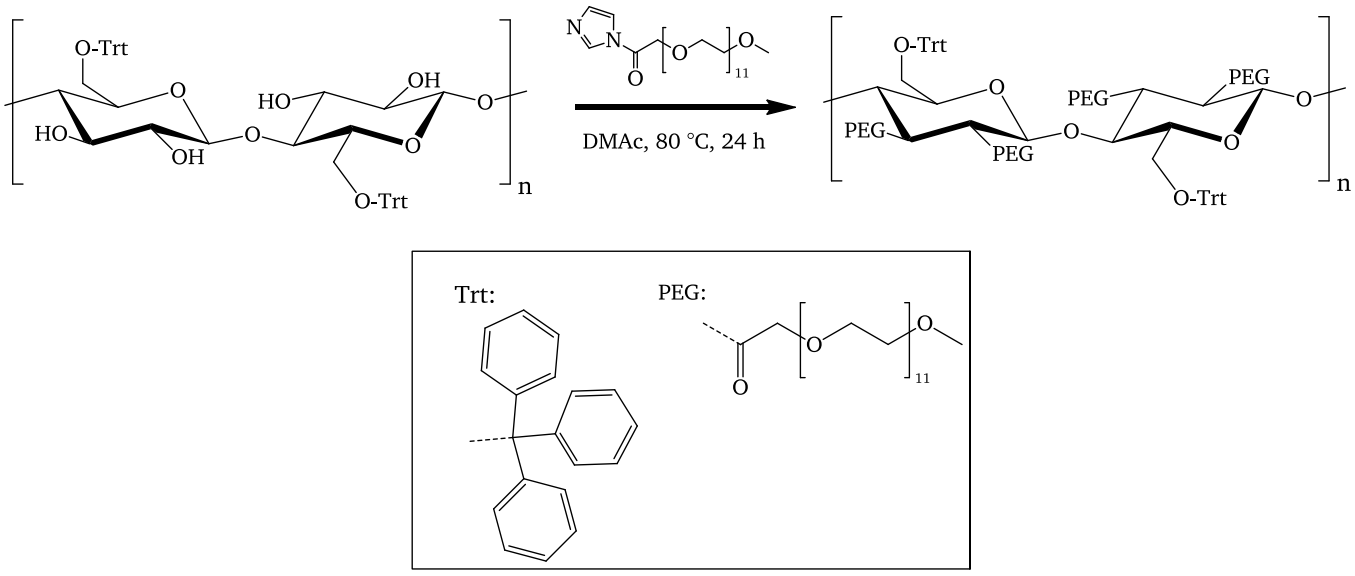

Figure 100. Reaction scheme of the pegylation of trityl cellulose via esterification.

In brief, the model experiment was conducted as follow: *N,N'*-carbonyldiimidazole was added to Schlenk-flask, followed by the addition of PEG55-COOH, diluted in water-free DMAc, under nitrogen counter flow and stirring. The reaction progress could be followed by the naked eye, since the reaction released CO_2, which could be seen as bubbles in the solution. After about 60 minutes, a solution of trityl cellulose in DMAc was added under stirring. The reaction mixture was heated to 80 °C and

continued for 24 hours. The product was isolated by precipitation in diethyl ether. As a qualitative proof of concept both, educt and product, were analyzed with SEC in DMF as eluent as shown in **Figure 101**.

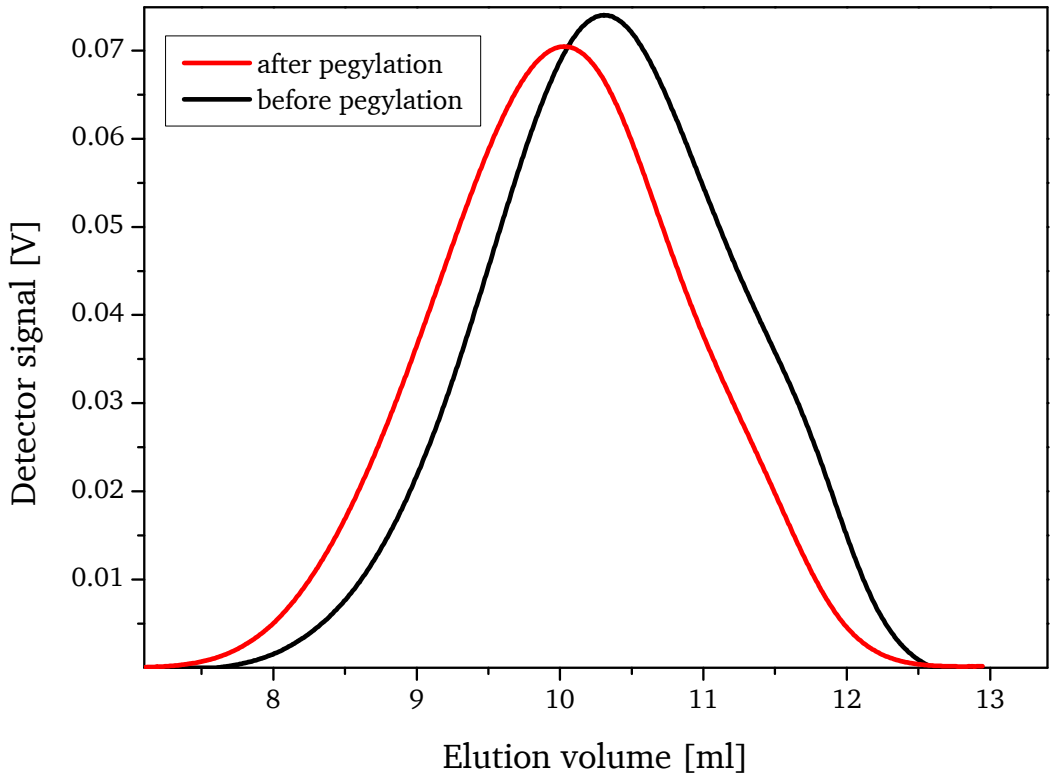

Figure 101. SEC traces of the polymer from the reference experiment for the CDI activated PEGylation of cellulose with PEG-COOH, measured in DMF/LiCl as eluent. Tritylated cellulose before (black) and after (red) pegylation.

The elution volume shifts slightly towards smaller values, indicating a slight increase in the hydrodynamic radius after pegylation. The result further indicates that significant depolymerization reactions during the pegylation process by carboxyl-functionalized PEG and esterification conditions can be neglected.

N,N'-carbonyldiimidazole (CDI) activated esterification of 2-bromopropionic acid with pegylated cellulose (experiment MCC-(PEG550-COOH_8)_2 (CDI)-Bp_1 (CDI))

We next turned our focus on the esterification of pure microcrystalline cellulose. In brief, after activation of PEG550-COOH with CDI in DMAc at room temperature for 60 minutes, a solution of MCC in DMAc/LiCl was added under nitrogen counter flow. The reaction time was set to 24 hours and a subsequent derivatization step was continued without isolation of the intermediate product, as displayed in **Figure 102**.

step 1: esterification of cellulose with PEG550-COOH:

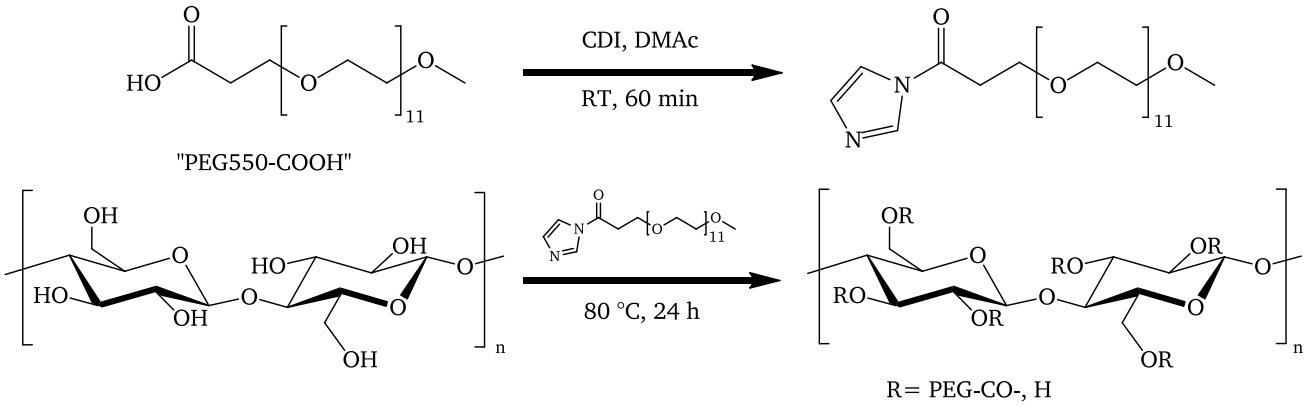

step 2: esterification of cellulose with 2-bromopropionic acid:

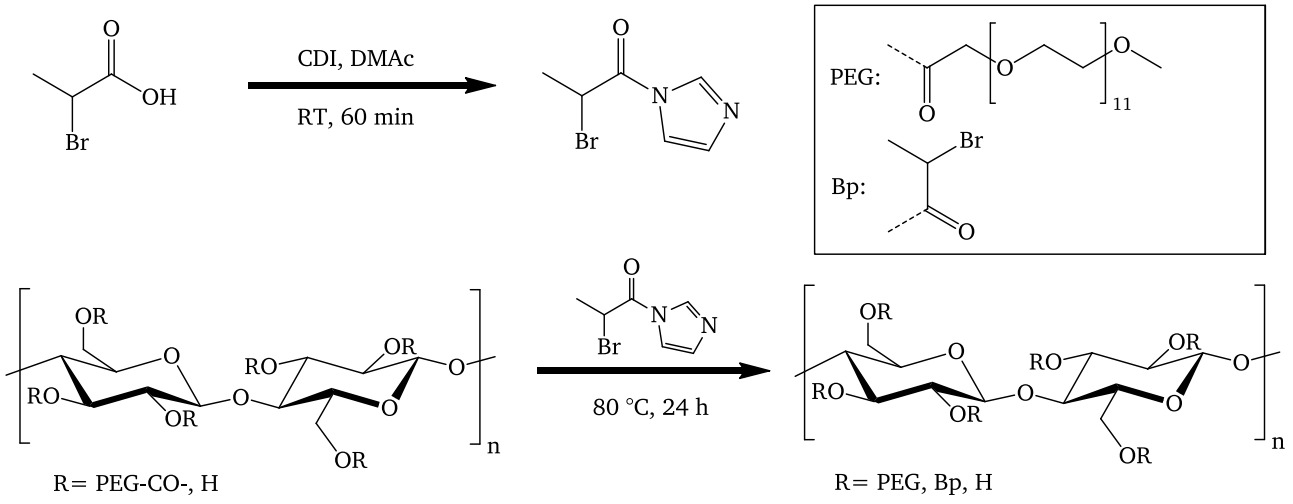

Figure 102. Reaction scheme for the esterification of cellulose with PEG-COOH and 2-bromopropionic acid using CDI and mild reaction conditions.

The idea behind this strategy was to avoid insolubility of the intermediate product, which is sometimes observed when partially substituted cellulose derivatives are isolated and dried under vacuum [80]. Furthermore no side reactions of the PEG550-COOH or its activated analogue were expected during the one-pot synthesis. In order to avoid steric hindrance during the derivatization, the bulky PEG550-COOH was first attached onto the cellulose backbone. Then the remaining hydroxyl functions of the cellulose were esterified with an excess of 2-bromopropionic acid under the same reaction conditions as in the first step. The polymer was isolated by precipitation of the reaction mixture in diethyl ether, followed by dissolution in chloroform and extraction with water. Purification was tedious because the chloroform and the aqueous phase turned into a foam-like emulsion and some water soluble reactants remained in the chloroform phase, requiring several extraction cycles. Centrifugation at 12 krpm helped to separate the phases. After extraction with diluted alkaline and acidic aqueous solutions the isolated product was dried and analyzed with ATR, ^{1}H-NMR and SEC. The ATR-IR spectrum (**Figure 103**) showed no absorption at 3000 - 3500 cm^{-1}, proving qualitatively the complete substitution of the cellulose OH-groups.

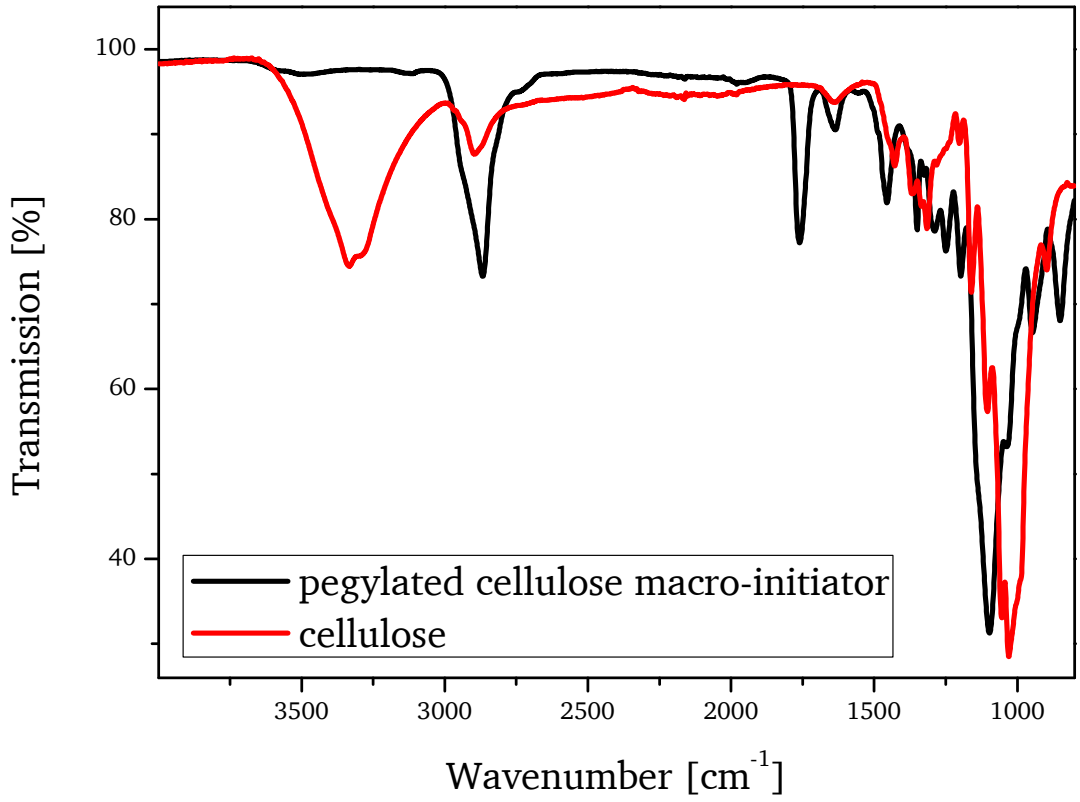

Figure 103. ATR-IR spectrum of the cellulose derivative after purification in comparison to unmodified MCC. Strong absorption is observed at 1700 cm^{-1}, indicating carbonyl moieties. No absorption can be seen at wave numbers above 3000 cm^{-1} (OH-bands of cellulose), therefore the cellulose derivative has been entirely substituted.

SEC analysis with THF as eluent was not possible due to a low solubility of the product in THF. The product was well soluble in polar solvents like DMSO, DMF and water. Furthermore we observed that after dissolution no insolubilities occurred when other solvents were added except for diethyl ether.
SEC analysis (**Figure 104**) in DMF/LiCl as eluent (with PMMA standards) showed high values of the average molar mass (M_n of about 100 kDa).

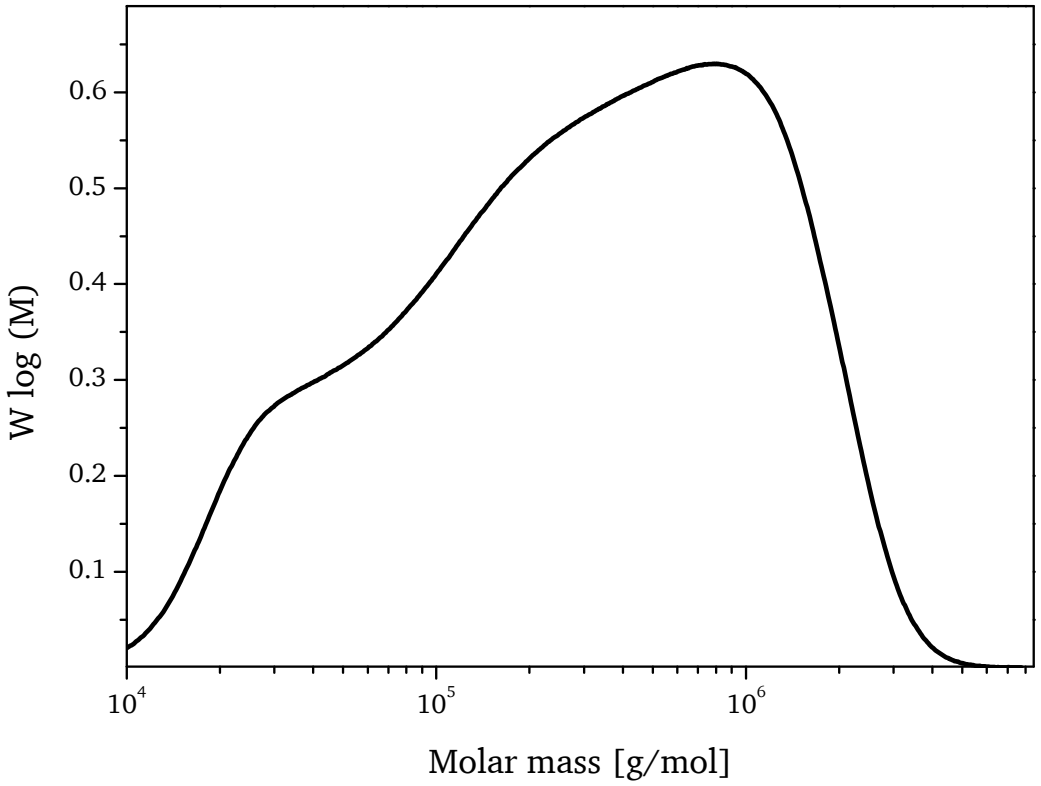

Figure 104. SEC traces of the cellulose derivative of after purification (DMF/LiCl with PMMA standards for calibration).

The DS values were determined quantitatively by ^{1}H-NMR analysis (**Figure 105**). The protons originated from the poly(ethylene glycol) grafts are observed at 3.5ppm and the protons from the CH_3-group of 2-bromo propionyl ester at 1.7 ppm. Since no residual OH-groups were observed in the analysis by ATR-IR spectroscopy, we assumed as complete substitution of all OH-groups, hence a total DS of 3. This allowed the determination of the DS values of PEG and Bp using the ratio of the integral intensities in the ^{1}H-NMR spectrum. We calculated a DS(PEG550) = 2.3±0.3 and DS(Bp) = 0.7±0.1. Note, a high relative standard error of about ±15 % results from the overlap of the PEG-proton signals with the cellulose backbone proton signals, because the broad and non-baseline separated signal showed a high deviation depending on the type of baseline correction and the choice of the integral borders.

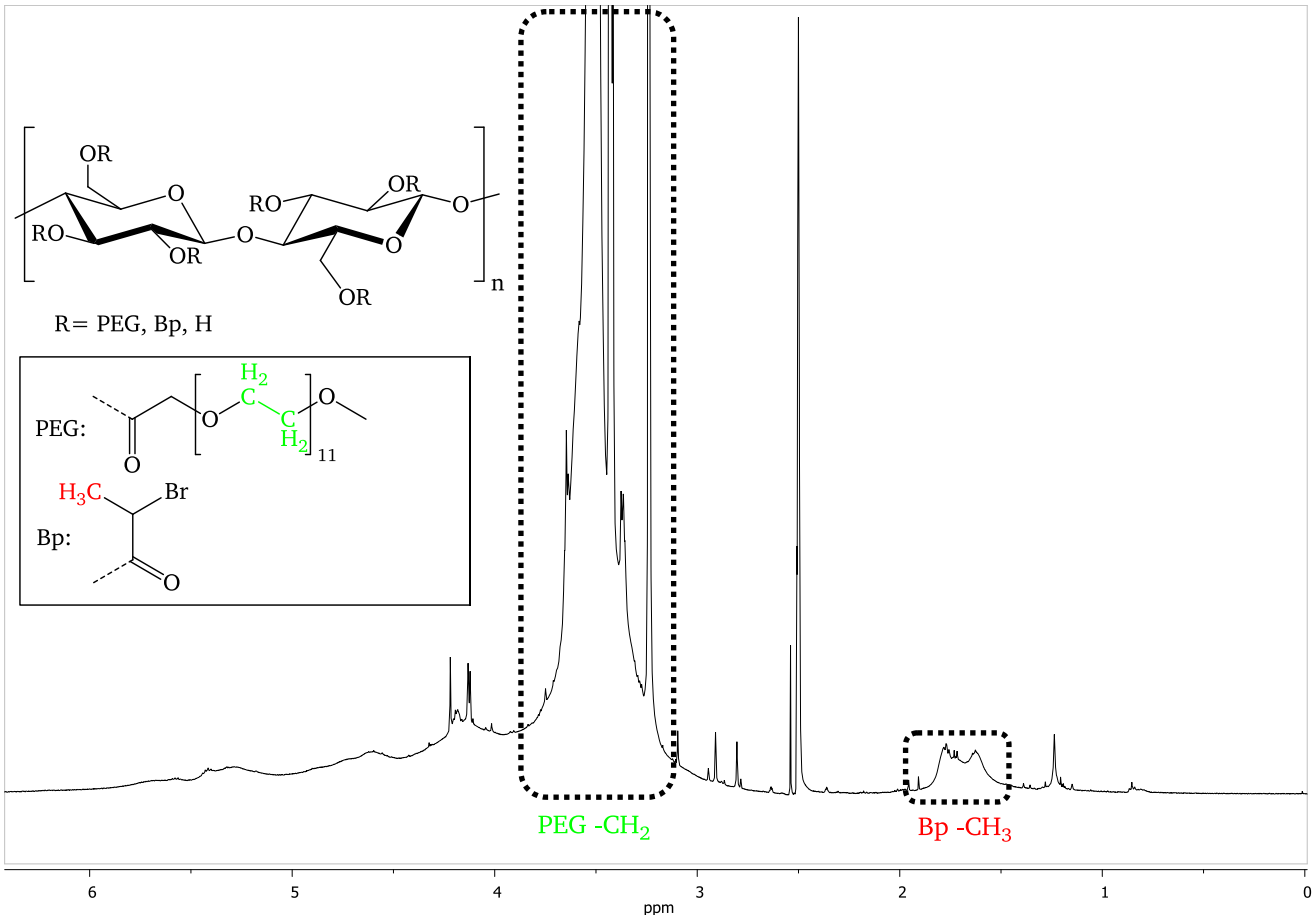

Figure 105. ^{1}H-NMR spectrum of the pegylated cellulose macro-initiator in d_6-DMSO. The relative integral signal intensities allowed the determination of the DS values.

As we were able to attach a large amount of PEG onto the cellulose and managed a complete substitution of the cellulose OH-groups, we can conclude that the chosen synthetic route allows the synthesis of cellulose derivatives bearing poly(ethylene glycol) grafts as well as 2-bromo propionyl functionalities, which may serve as initiator groups for ATRP reactions, in an efficient and controllable way. As we used only three equivalents of PEG-COOH with respect to the AGU of cellulose, we could reach a DS(PEG) of about 2.3, meaning that about 76 % of the applied PEG-COOH could be covalently attached onto the cellulose. By variation of the molar feed of PEG-COOH the DS(PEG) can be tuned depending on the targeted value.

Graft copolymerization of MMA with pegylated cellulose macro-initiator

Having already pegylated cellulose macro-initiators, we started with the graft copolymerization of MMA with ATRP because we assumed several advantages compared to the grafting by RAFT polymerization of styrene with pegylated cellulose macro-CTA. The reaction conditions are described in detail in **Figure 106**.

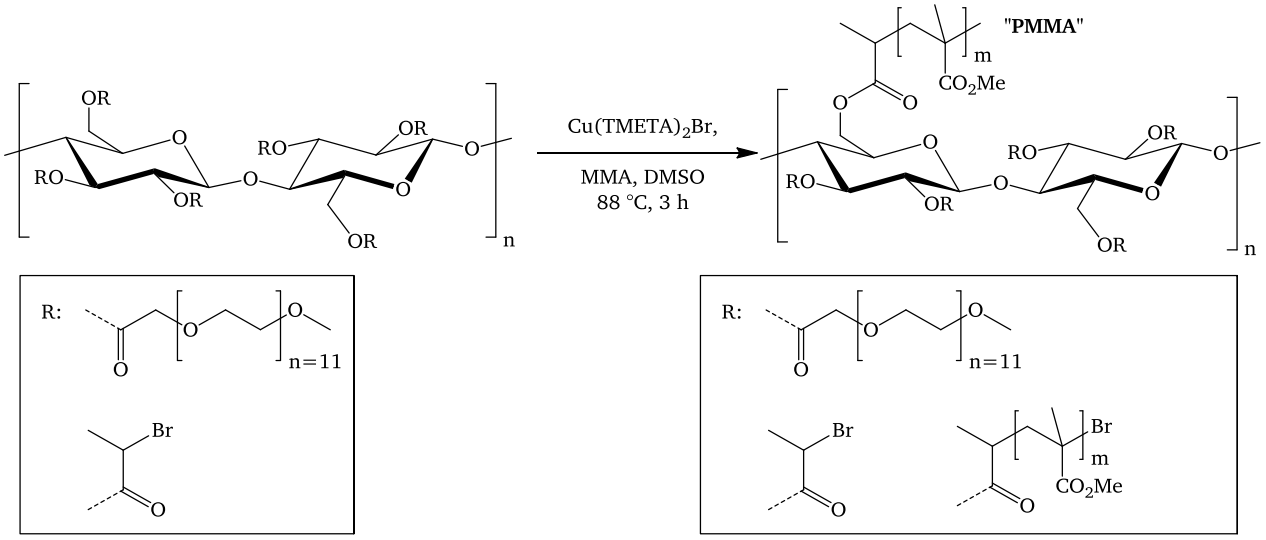

Figure 106. Schematic image of the ATRP reaction of MMA with pegylated cellulose macro-initiator, including all relevant reaction parameters such as reactants, temperature and polymerization time.

First, the cellulose macro-initiator showed a good solubility in DMSO but not in toluene. Polymerization of MMA in DMSO as solvent is well known, therefore the ATRP reaction could be performed according to standard protocols from literature, whereas the polymerization of styrene in DMSO would first require model reactions and investigation of the compatibility of monomer and solvent. Furthermore, using the ATRP reaction, no sacrificial initiator is needed, leading to a homopolymer-free sample, which simplifies workup and analysis of the product. Additionally the mass increase due to polymerization is a direct proof of polymer grafting and determination of grafting yield and initiation efficiency can be directly determined by the total mass of the product.

Graft copolymerization of MMA with cellulose macro-initiator was performed and the resulting polymers were characterized, as presented in the appendix. However the characterization by SEC and gravimetry had not been trivial; especially the SEC analysis left several open questions. In order to investigate the graft copolymerization process using cellulose macro-CTA, we continued with the use of styrene and RAFT polymerization, as presented in the next section.

Synthesis of pegylated cellulose macro-CTA

The synthesis of the cellulose macro-CTA was performed according to the procedure described in chapter 4.2.1. Pegylated cellulose with a DS(PEG) = 1.8 and DS(Bp) = 1.2 (from experiment MCC-(PEG550-COOH_7)_1 (CDI)-Bp_1 (CDI)) was dissolved in DMF and added slowly to the reaction mixtures, after the trithiocarboxylate was generated in-situ (**Figure 107**). The product was isolated by removal of solid K_3PO_4, followed by precipitation into diethyl ether. An unexpected low yield of about 26 % may result from partial solubility of the product in DMF/Et_2O mixtures.

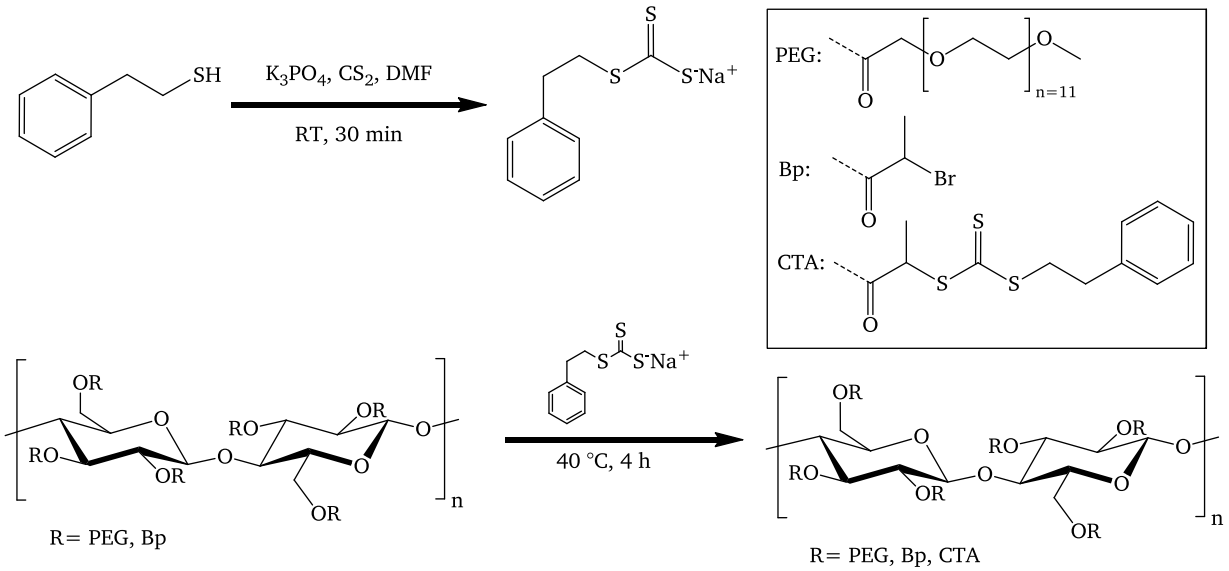

Figure 107. Reaction scheme of the partial transformation of 2-bromo functionalities into CTA groups.

It should be noted that the isolation of the product via precipitation was not trivial because the addition of more diethyl ether did not result in more precipitated product. This is why the diethyl ether was evaporated to yield a DMF solution containing all reactants. Then, several solvents from unpolar to very polar were tested for the precipitation of remaining product from the DMF solution. However no precipitation method was successful. Thus other methods for isolation (e.g. crystallization, column chromatography) may be investigated in future reports.

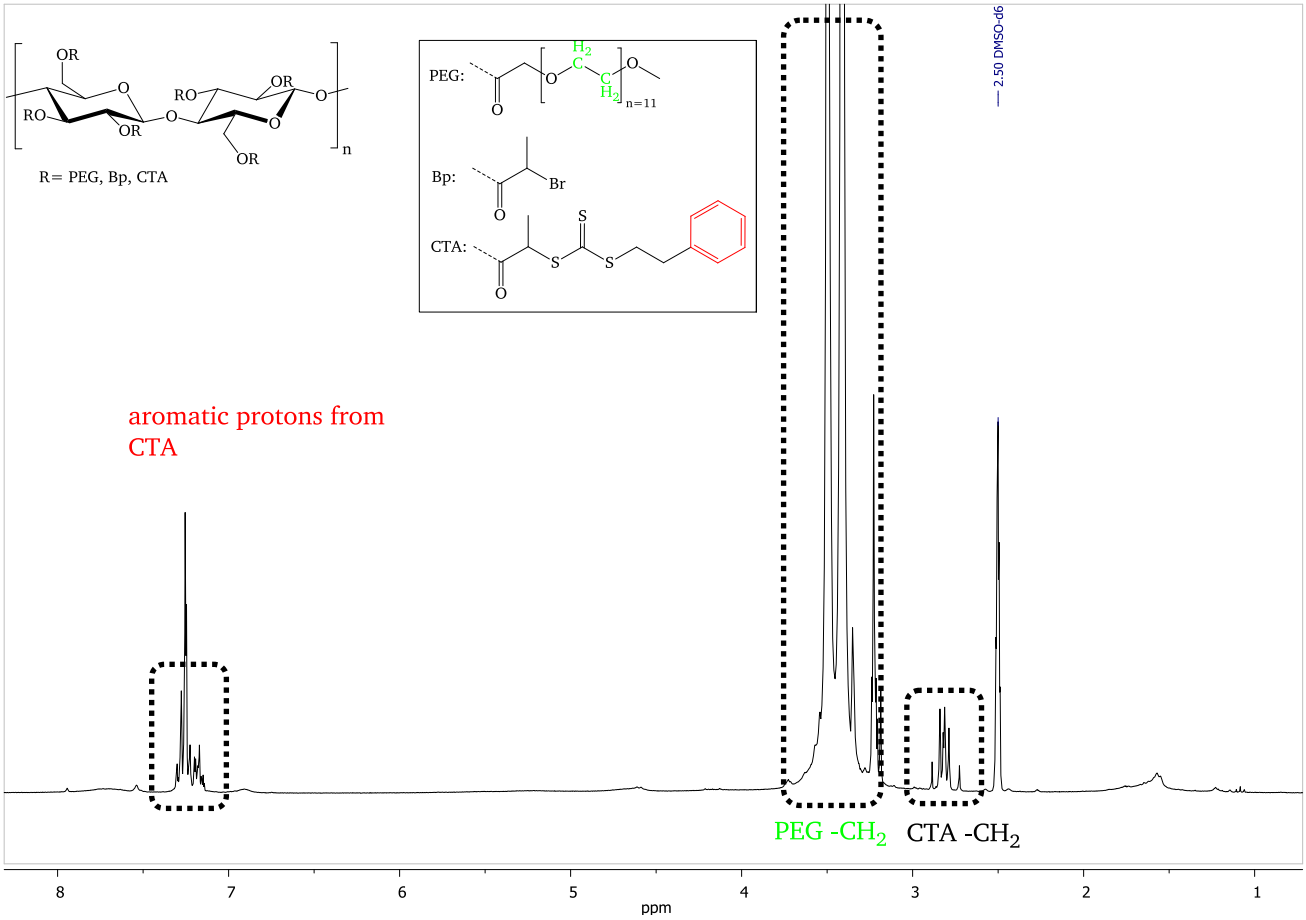

Figure 108. ^{1}H-NMR spectrum of cellulose macro-CTA "MCC-PEG550-CTA_4" in d_6-DMSO. The partial conversion of the bromine functionalities into CTA groups lead to two new signals at 7.3 ppm and at 2.8 ppm. The signals belong to the aromatic and the aliphatic protons of the phenyl ethyl moiety.

The product was analyzed with ^{1}H-NMR. DS values were calculated as before by comparison of the integers of the PEG proton signals with the aromatic protons. DS(PEG) = 1.8±0.3, DS(Bp) = 0.8±0.1, DS(CTA) = 0.4±0.1.

The product was soluble in DMF, DMSO and chloroform, but insoluble in THF, therefore SEC analysis was done with DMF/LiCl as eluent with PMMA calibration. It was also insoluble in toluene; therefore a subsequent graft copolymerization could not be performed in toluene, but required solvent mixtures. The pegylated cellulose macro-CTA was analyzed via SEC and then compared with its precursor substance, as shown in **Figure 109**. The almost identical distribution of the molecules before and after transformation into macro-CTA indicates that the reaction conditions don't cause depolymerization of the cellulose backbone.

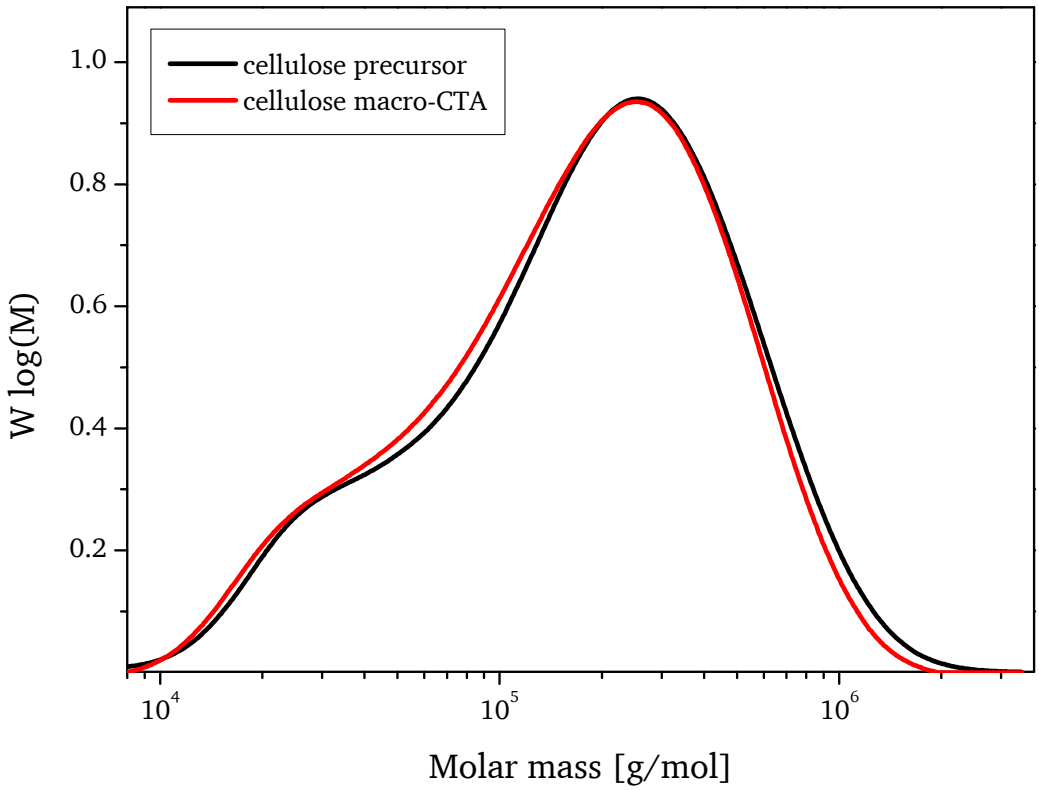

Figure 109. SEC traces of cellulose macro-CTA and its corresponding precursor cellulose derivative, measured in DMF/LiCl, calibrated against PMMA standards.

Furthermore, the cellulose macro-CTAs generated by strategy A (regioselective modification) and strategy B (statistical modification) (chapters 9.3 and 0) were compared using SEC in DMAc/LiCl as eluent, as shown in Figure 110. The M_{Peak} of MCC-PEG550-CTA1 (strategy A) is at about 20 kDa whereas the M_{Peak} value of MCC-PEG550-CTA4 (strategy B) is at about 200 kDa. This can be taken as a proof for the hypothesis, that mild esterification conditions keep cellulose chains intact, whereas etherification under alkaline conditions leads to a significant depolymerization of the cellulose macromolecules.

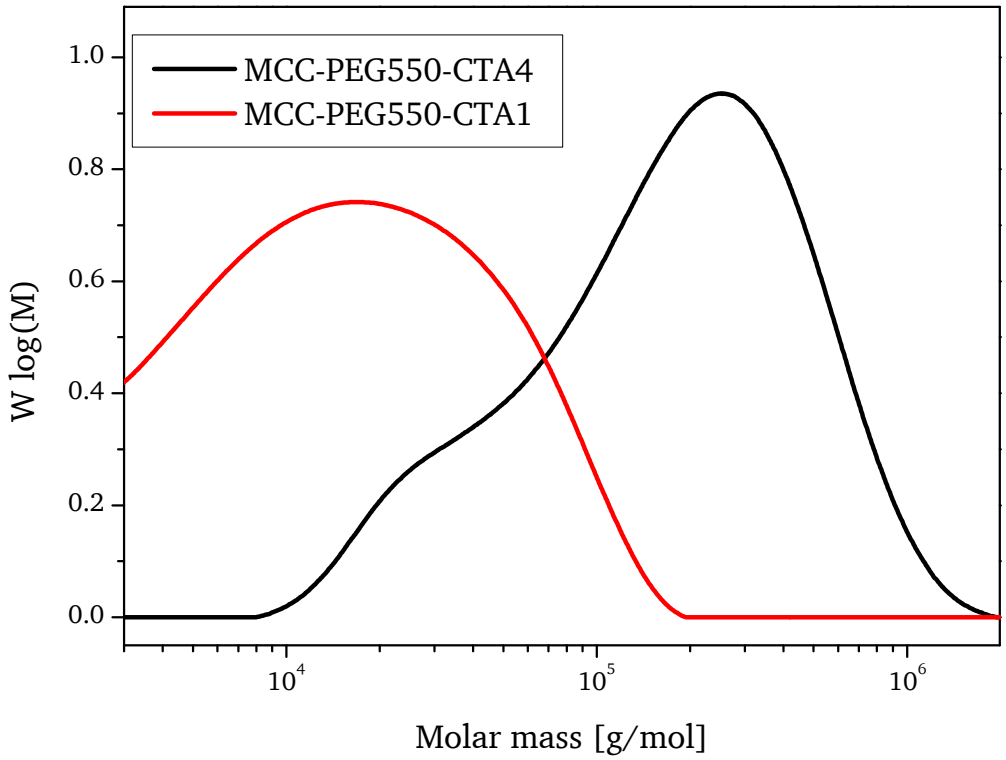

Figure 110. Analysis of the SEC traces of the pegylated cellulose macro-CTAs, synthesized with two different strategies. The eluent was DMF/LiCl, polymer samples were referenced against PMMA standards. The molar mass of cellulose macro-CTA "MCC-PEG550-CTA_1", which was synthesized by etherification and regioselective modification (strategy A) is much smaller than the molar mass of the cellulose macro-CTA, which has been synthesized in a non-regioselective fashion via esterification (strategy B).

Synthesis of cellulose mixed graft copolymers via RAFT

In a final step to obtain cellulose mixed graft polymers, we carried-out first RAFT polymerizations with the PEGylated macro-CTA, as shown in **Figure 111**.

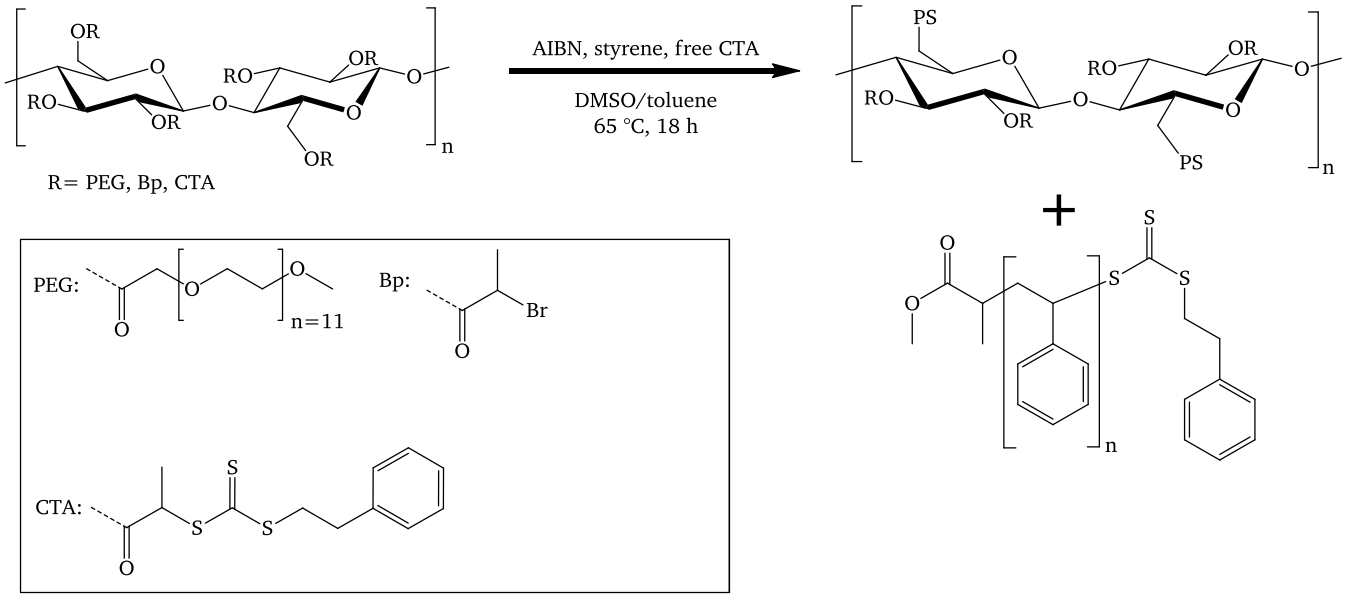

Figure 111. Synthesis of cellulose mixed graft copolymers. Due to solubility problems of the pegylated cellulose macro-CTA a small amount of DMSO had to be used.

The cellulose macro-CTA was dissolved in anhydrous DMSO. After complete dissolution, a mixture containing toluene, styrene, CTA and AIBN was added. After three freeze-pump-thaw cycles the reaction was initiated at 65 °C and run for 18 hours. After this time, the polymer was isolated by precipitation in methanol. Solubility tests showed that the polymer mixture was only partially soluble in THF; it was assumed that the graft copolymer was insoluble in THF just like the corresponding cellulose macro-CTA. Therefore two fractions were received by partial dissolution in THF: THF-soluble fraction and THF-insoluble fraction. Both fractions were analyzed with SEC using DMF/LiCl as eluent. As can be inferred from SEC analysis, the THF-soluble fraction consisted only of small macromolecules and was discarded. The THF-insoluble fraction which, was assumed to be graft copolymer, seemed to be mostly dissolved after mixing the polymer with DMF/LiCl. However, a fraction of fine dispersed particles seemed to remain, since a light cloudiness was observed by the naked eye. The polymer solution was not easily passed through a syringe filter, which was considered an indication for insoluble agglomerates in the solution. The SEC analysis of the THF-insoluble fraction is displayed in **Figure 112**.

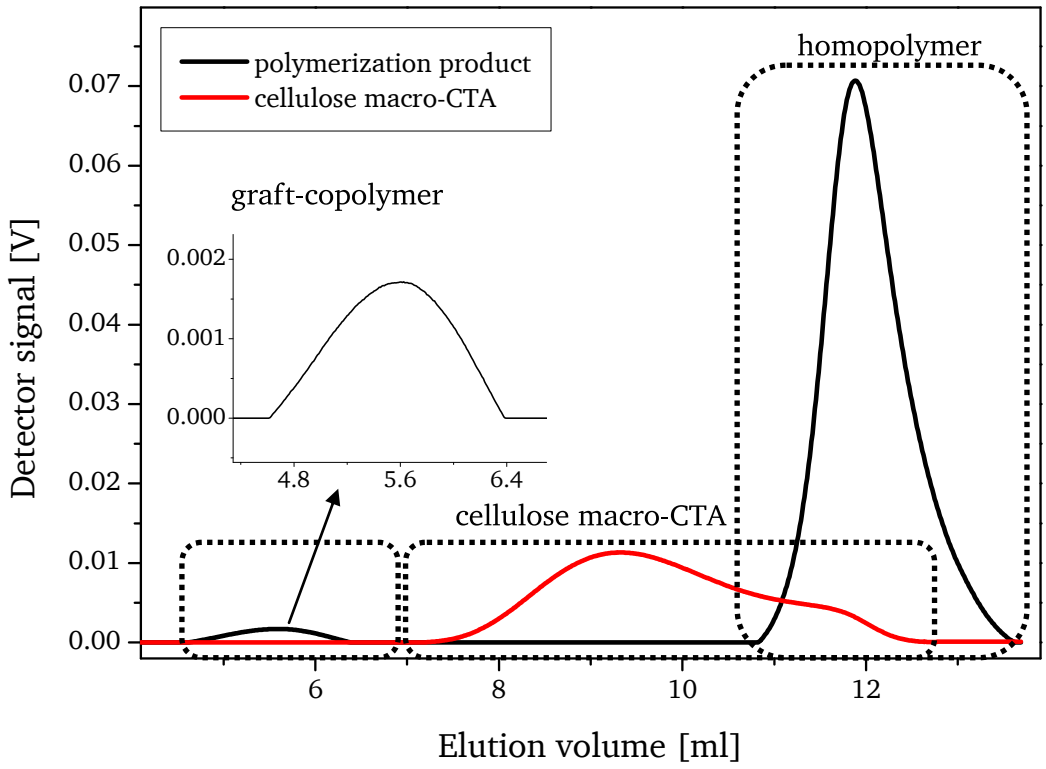

Figure 112. SEC traces of cellulose graft copolymer from experiment "MCC-PEG550-CTA_4-PS_1" and cellulose macro-CTA "MCC-PEG550-CTA4", using DMF/LiCl as eluent. The sample from the polymerization experiment shows a bimodal distribution, a signal originated from homopolymer and one signal from the graft copolymer (black line). The precursor, cellulose macro-CTA (red line) is also displayed for comparison.

The SEC traces of the crude product from the polymerization experiment show a bimodal distribution with a small signal at low elution volumes and one large signal at high elution volumes. This was considered an indication for a mixture containing graft copolymer with high molar mass (low elution volume) and homopolymer (high elution volume). When compared with the cellulose macro-CTA, a shift towards smaller elution volumes is observed, which also indicates a successful grafting reaction.

7. Summary

Since the first successful graft copolymerization experiments by Stenzel et al. [50] using an organo-soluble cellulose macro chain transfer agent (CTA), several approaches have been presented for the synthesis of well-defined cellulose graft copolymers using RAFT polymerization. However, limited solubility of cellulose and cellulose derivatives is still challenging during homogenous graft copolymerization. Limitation of the solubility reduces the amount of chemical available CTA groups on the cellulose and it is an important issue why various publications in this field report strong deviations between experimental and theoretic data regarding the amount of immobilized polymer grafts.

According to this, the goal of this thesis was to develop a "toolbox" where some of the most relevant aspects of the controlled design of cellulose graft copolymers using RAFT were investigated in detail, as follows:

- Excellent solubility of all precursor polymers and generated copolymers in typical organic solvents has to be provided.
- High graft ratios resulting from high graft density and large polymer grafts shall be accessible.
- For the reduction of termination reactions, the "CTA-shuttled R-group approach", as proposed by Axel Müller et al. [51], shall be transferred to the design of the cellulose graft copolymers.
- Optimization of the reaction conditions for the RAFT polymerization will be targeted to achieve a high level of control over the molecular structure of the copolymers.
- Convenient analytical methods for the cellulose graft copolymers are to be employed in order to investigate the reaction kinetics of cellulose macro-CTA and of free CTA.

As first steps, various synthesis strategies were pursued in this thesis in order to generate organo-soluble cellulose macro-CTAs. Due to difficulties with respect to the solubility of the polymers, existing literature protocols for esterification of MCC needed to be changed and cellulose was finally modified with the carboxyl-terminated RAFT agent 4-cyano-4-(phenylcarbonothioylthio)pentanoic acid (CPPA) by the use of the activation agent *N,N'*-carbonyldiimidazole (CDI). Esterification of residual OH-groups using propionic acid anhydride ensured solubility of the obtained derivative. The cellulose macro-CTAs prepared here, proved to be well-soluble in a variety of organic solvents, including DCM, $CHCl_3$, THF, toluene, DMF and styrene. As a consequence a large number of different polymerization reactions can thus be challenged.

First graft copolymerization experiments were successfully carried out using *N,N*-dimethylacrylamide (DMAA) monomer. Simple purification of the graft copolymer from the homopolymer PDMAA could be performed due to the good water solubility of the PDMAA homopolymer, whereas the cellulose graft

copolymer remained insoluble in water. Subsequent analysis of the pure graft copolymer with ^{1}H-NMR revealed only small amounts of grafted polymer. After a set of reference experiments, the origin of this problem was finally identified: it could be shown that side reactions of the CPPA with the activation agent CDI caused a partial conversion of CTA into non-reactive chemical species, limiting the success of the RAFT polymerization process.

As a result the strategy for the immobilization of the CTAs onto the cellulose was changed: instead of attaching a preformed RAFT agent via esterification, the CTAs on cellulose were successfully synthesized in a step-wise fashion by nucleophilic displacement reactions of bromo-isobutyro groups on cellulose with trithiocarboxylate, generating trithiocarbonates. First polymerization experiments showed excellent results in the control of the graft copolymerization process. However, this method exhibited limitations regarding the amount of immobilized CTA, which did not exceed a value of the degree of substitution (DS) of about 0.15. It was assumed that the steric demand of the 2-bromoisobutyro functionalities, where the bromine is attached on a tertiary carbon, was too high and thus had to be reduced. When 2-bromopropionyl modified cellulose was transformed into cellulose macro-CTA, an increase of the DS(CTA) value up to 0.6 was observed, depending on the reaction conditions. Higher DS values resulted in insoluble cellulose derivatives.
Graft copolymerization reactions using styrene monomer and cellulose macro-CTA were carried out with addition of free CTA (“shuttle approach”), showing very good control of the process. Note, without free CTA, polymerizations resulted in insufficient control and gel-formation. All polymerizations were monitored by ^{1}H-NMR and SEC at defined time intervals. By isolation and hydrolysis of the cellulose graft copolymers the kinetics of the formation of polymer grafts and free linear polymer were analyzed and compared. Very similar results of the molar mass of the polymer grafts in comparison to the free linear polystyrene in solution indicated similar reaction kinetics in solution as well as on the cellulose backbone. Hence, information for the molar mass of the grafted polystyrene could be conveniently obtained by measuring the molar mass of the free polymer, which showed a linear dependency on monomer conversion, proving the controlled fashion of the polymerization reaction (as proven by a large number of experiments). As a result, the molar mass could be well controlled by adjusting the monomer conversion. Analysis of the initiation efficiencies and graft ratios by SEC and gravimetric means, respectively, showed that initiation efficiencies and graft ratios depend on the reaction conditions chosen. For example, high ratios of [CTA]/[AIBN] lead to excellent control of the reaction as well as very high initiation efficiencies up to about 90 %, if not too high molar masses were targeted. Higher molar masses of the grafted polymers could of course be obtained. However, in such a case, a reduction in the initiation efficiency needs to be considered, due to a less controlled RAFT reaction, i.e. higher amounts of termination reactions. It was finally concluded that the development of a “toolbox” as part of the thesis provided the opportunity for the

design of versatile, tailor-made and well-defined cellulose-based graft copolymers. For this, future investigations in this area might focus on the design of functional cellulose graft copolymers by adaption of this system to the graft copolymerization of “smart” polymers that may undergo structural changes due to external stimuli. Furthermore, the investigation of the structure-property relationship of such brush-copolymer architectures will be in focus in future projects.

The next synthetic goal was to develop this above summarized concept further towards the synthesis of more complex cellulose-based polymer architectures. For this, a combination of RAFT technique with ATRP technique in two subsequent polymerization steps, using the same cellulosic material, was pursued. The reason for the choice of ATRP as second CRP technique was the fact, that the cellulose macro-CTAs already carried bromine functionalities due to the synthesis process (stepwise build-up of CTA on cellulose) and no further processing of the cellulose was necessary in order to perform ATRP. At first, cellulose graft copolymer was synthesized using styrene monomer, free CTA and cellulose macro-CTA. The CTA groups were then removed from the chain ends of the polystyrene grafts. In a consecutive step an ATRP reaction was used for a grafting process of methyl methacrylate. Characterization of the mixed graft copolymer was achieved by ^{1}H-NMR and SEC. ^{1}H-NMR clearly showed a successful a polymerization of MMA using the cellulose graft copolymer as ATRP initiator. Using the relative signal areas of polystyrene and PMMA, the total graft ratio (PS grafts and PMMA grafts) was estimated to about 3,500 %, meaning the mixed graft copolymer contained about 97 % polymer grafts and only 3 % cellulose. It should be noted, that this value is much higher than in any known work concerning cellulose-based graft copolymers to date, as inferred from a present literature screening, using web of science data base.
In contrast to the results from ^{1}H-NMR, SEC data did not show an increase in the apparent molar mass after the second graft copolymerization step, which was at first sight unexpected. A potential explanation for this finding might be a collapse of the polymer grafts, which decreases the hydrodynamic radius of the graft copolymer molecules. The latter hypothesis will be addressed in more detail using scattering techniques in future work.

A third part of the thesis targeted the design of mixed graft cellulose polymers using a combination of grafting-to and grafting-from approach. In brief, cellulose graft copolymers were targeted, where a part of the OH-groups were modified via grafting-to with poly(ethylene glycol) (PEG) moieties, and another part was modified by grafting-from with PMMA. In order to avoid significant depolymerization, which was observed in reference studies using regioselective grafting of PEG grafts onto cellulose by etherification, it was decided to use mild reaction conditions for PEGylation which are typically obtained when conducting esterification reactions with *N,N'*-carbonyldiimidazole (CDI) as activation agent. For this, statistical esterification of carboxyl-modified PEG and 2-bromopropionic acid

was conducted instead of the before-used protecting group chemistry with trityl-protected celluloses because of the incompatibility of ester functionalities with strong acidic reaction conditions, which are required during the deprotection step. All intermediate cellulose derivates were analyzed carefully using ^{1}H-NMR and SEC analysis. Finally a successful synthesis of PEGylated cellulose macro-CTA was achieved. Further investigation focused on the concept of synthesizing mixed grafts on cellulose by use of RAFT technique. After a first polymerization experiment the analytic results indicated successful grafting. However limitations in the solubility behavior and low graft ratios were still challenging. An alternative approach was pursued using ATRP technique for the graft copolymerization of MMA monomer with PEGylated cellulose macro-initiator without the addition of free initiator. The resulting mass increase of the product indicated a first proof of concept, whereas the chemical identity of the polymers was elucidated by ^{1}H-NMR analysis, showing additional signals originated from PMMA. Considering various review articles and other relevant publications in the field of cellulose-based graft copolymers using CRP techniques, this is the first time that the synthesis of such complex materials is presented. This is why these materials may be used as promising candidates for further investigation, such as to address a fundamental understanding of physical and chemical properties.

Concerning the RAFT polymerization of cellulose macro-CTA in homogenous media and mixed graft copolymers, future investigations will focus on understanding the morphology and the structure-property relationship of tailor-made cellulose graft copolymers. In particular, future analytic methods will include the following:

- AFM imaging: individual graft copolymer molecules may exhibit a worm like structure. This could be shown with AFM imaging of synthetic polymers by [63], but not for cellulose-based graft copolymers
- DSC analysis: dependence of thermal properties on graft-length and density
- DLS analysis: elucidating the “swollen” structure in solution

In order to pursue such interesting fundamental questions, the current thesis has laid down various opportunities to design such complex polymer architectures.

8. Experimental Part

8.1. Reagents and solvents

All solvents were distilled prior to use and kept under inert, anhydrous conditions. All solids were dried in a vacuum oven prior to use.

chemical	supplier
1,1-carbonyl diimidazole	Sigma Aldrich
1,4-dioxane	Roth, 99.9 %
1-ethyl-3-(3´-dimethylaminopropyl)-carbodiimide*HCl	Nova Biochem
2-bromopropionic acid	Alfa Aesar, 97 %
2-bromopropionic acid methyl ester	Merck Millipore, 98 %
2-propanol	Roth, >99.5 %
4-(dimethylamino)pyridine	Sigma Aldrich, ≥99%
4-cyano-4-(phenylcarbonothioylthio) pentanoic acid	Sigma Aldrich, 95 %
acetone for synthesis	Roth, >99.5 %
azo-bis (isobutyro nitrile)	Fluka Analytical, ≥ 98 %
bromoisobutyric acid, 2- (alpha-)	Sigma Aldrich, 98 %
bromopropionyl bromide, 2-	Sigma Aldrich 98 %
calcium carbonate	Grüssing GmbH
calcium chloride	Merck, 95 %
calcium hydride	Merck Millipore
carbon disulfide	VWR, >99 %
chloroform for synthesis	Roth, >99.5 %
dichloro methane	Roth, p.a.
diethyl ether	Sigma Aldrich, >99.5 %
dimethyl sulfoxide	Grüssing GmbH, 99 %
lithium chloride	Roth
magnesium sulphate	Grüssing GmbH, 99 %
methacrylic acid, stabilized	Merck Millipore
methanol, HPLC grade	Roth, 99 %
methyl 2-bromopropionate	Sigma Aldrich, 98 %
microcristalline cellulose, Avicel PH-101, DP_w =250	Fluka Analytical, ≥ 98 %
Molecular sieve 3A	Roth
Molecular sieve 4A	Alfa Aesar
N,N-diisopropylcarbodiimide	Sigma Aldrich, 99 %
N,N-dimethyl aminopyridine	Sigma Aldrich, 99 %
N,N-dimethylacetamide	Merck Millipore
N,N-dimethylformamide anhydrous	Alfa Aesar, >99.5 %
N,N-dimetylacrylamide	Sigma Aldrich, 99%
N-isopropylacrylamide	Sigma Aldrich, 97%
phenylethyl mercaptane	Sigma Aldrich, >99 %
poly(ethylene glycol) monomethylether 550	VWR
poly(ethylene glycol) monomethylether 550	VWR

potassium carbonate	OC shop
potassium hydroxide	AC shop
potassium iodide	Fluka Analytical, ≥ 98 %
potassium permanganate	OC shop
potassium phosphate tribasic	VWR, >95 %
potassium tert.-butoxide	Sigma Aldrich, 97 %
propionic acid anhydride	Merck Millipore, 98 %
pyridine	Roth, >99 %
sodium chloride	AC shop
sodium hydride	Sigma Aldrich
sodium hydroxide	AC shop
styrene	Merck Millipore, 99 %
thionyl chloride	Sigma Aldrich
toluene Chromasolv	Sigma Aldrich, 99,9%
triethylamine	OC shop, 99 %
triphenyl methyl chloride	Sigma Aldrich

8.2. Instrumental methods

Size exclusion chromatography (SEC)

THF as eluent:

Measurements were made at 30 °C with a flow rate of 1 ml/min with THF as eluent. Column setup: pre-column (PSS SDV) and column (PSS SDV linear M), pump (1050 HP), RI (1200 Agilent RID 35 Grad) and UV-Vis detector (1050 UV). Calibration: PS standards (PSS, Mainz, Germany).

DMF as eluent:

Measurements were made at 25 °C with a flow rate of 0.5 ml/min with DMF, containing LiCl (3 g/L) as eluent. Column setup: pre-column (GRAM 1000 A) and column (GRAM 1000A), pump (1200 Agilent iso.), RI (1200 Agilent RID 35 Grad). Calibration: PMMA standards (PSS, Mainz, Germany).

Elemental Analysis (EA)

The sulfur content of the cellulose macro-CTAs was analyzed with a Leco CS 600 elemental analyzer at the central institute for engineering, electronics and analytics (ZEA-3), Jülich, Germany. The DS(CTA) values were calculated from the sulfur content and compared with the data obtained from ^{1}H-NMR analysis.

Nuclear magnetic resonance (NMR)

Spectra were typically measured at 25 °C using a 300 MHz Bruker Avance II NMR spectrometer or a 500 MHz Bruker DRX 500 NMR spectrometer. The number of scans for ^{1}H-NMR typically varied between 32 and 512 and for ^{13}C-NMR between 128 and 10,000 scans. The chemical shifts were referenced to the deuterated solvent.

Attenuated total Reflection (ATR)

A Perkin Elmer Spectrum One FT-IR spectrometer was equipped with a Perkin Elmer ATR unit. Typically 10 scans were accumulated with a resolution of about 1 cm^{-1}.

Raman spectroscopy

Characterization with Raman spectroscopy was done with a Bruker Senterra Raman microscope by Krasimir Kantchev, working group of Prof. Vogel, TU Darmstadt. A 10 mW 785 nm laser light source with was used for excitation and a CCD was used for detection. Typically 60 scans were accumulated with an integration time of 10-20 seconds.

8.3. Synthesis

Dissolution of cellulose in DMAc/LiCl

A procedure described in literature [54] was applied to dissolve the MCC in a DMAc/LiCl mixture. A 500 ml Schlenk-flask was equipped with a septum and with a stirring bar and was heated under high vacuum in order to remove physisorbed water. MCC (10.2 g, 62.9 mmol) was suspended in 235 ml DMAC. This mixture was thermally treated at 140 °C for 60 minutes. The temperature was lowered to 100 °C and anhydrous LiCl (20.0 g, 472 mmol) was added under vigorous stirring and nitrogen counter flow. The reaction mixture was cooled down to ambient temperature within several hours by turning off the heater. The solution was kept at room temperature while stirring overnight, a clear solution was obtained.

Synthesis of cellulose macro-CTA based on dithioester CPPA (MCC-CPPA16-Pr)

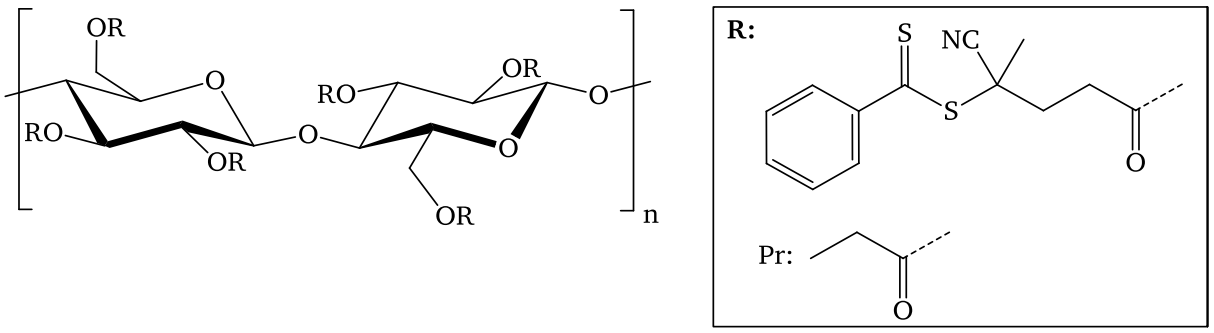

RAFT-Reagent CPPA (1.54 g, 5.53 mmol, 3.4 equiv.), CDI (0.67 g, 4.15 mmol, 4.5 equiv.) were dissolved in 20 ml anhydrous DMAc and stirred overnight at room temperature. In a second step MCC solution was added (5.85 g solution, 0.26 g MCC, 1.63 mmol, 1 equiv.) under stirring. The reaction mixture was stirred at 80 °C for 24 hours. The esterification was performed directly afterwards by adding a solution of propionic anhydride (6.0 ml), Triethylamine (6.0 ml), DMAP (20 mg) dissolved in 5ml DMAc to the reaction mixture. After stirring for 24 hours at 60 °C the product was purified by precipitation in methanol, washing and precipitation. Solvent was removed by evaporation in vacuo. Yield: 0.29 g (45 %). DS values determined by ^{1}H-NMR, molar mass per AGU was calculated by the DS values, apparent molar mass was determined by SEC with THF as eluent against PS standards.

Table 12. Analytic data of sample cellulose macro-CTA.

Sample	DS(CPPA)	DS(Pr)	M(AGU)	M_n	M_w	Đ
			[g/mol]	[kDa]	[kDa]	
MCC-CPPA16-Pr	0.31	2.69	394	52	106	2.0

Synthesis of cellulose-based PDMMA graft copolymer (MCC-CPPA16-Pr-PDMAA)

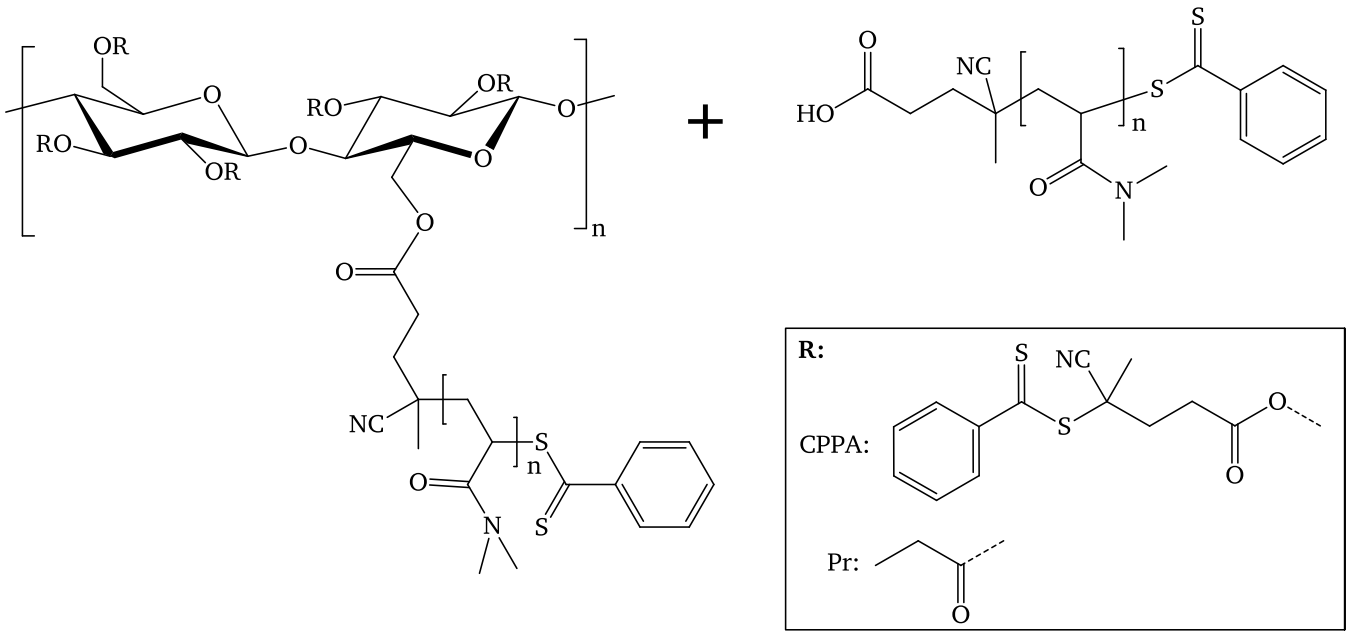

Cellulose macro-CTA (100 mg, 0.25 mmol, 1 equiv.) was stirred in 20 ml dry dioxane in a Schlenk-tube until complete dissolution occurred. Sacrificial initiator CPPA (71 mg, 0.25 mmol, 1 equiv.), initiator AIBN (20.8 mg, 0.13 mmol, 0.5 equiv.) and monomer DMAA (2.517 g, 2517 mmol, 100 equiv.) were added to the solution. The reaction mixture was degassed by freeze-pump-thaw method (three cycles). The reaction mixture was stirred for 18 hours at 65 °C. The polymer was precipitated and washed with diethyl ether. Homopolymer and graft copolymer were separated by partial dissolution in methanol. The soluble phase and the insoluble phase were separated. The polymer in the soluble phase was precipitated in diethyl ether. Both solid phases were dried by evaporation and analyzed by ^{1}H-NMR and SEC. The results are displayed in **Table 13**.

Table 13. Analytical data of the graft copolymerization of cellulose-CTA1 with DMAA.

Sample	M_n	M_w	Đ	N (DMAA) per AGU
	[kDa]	[kDa]		
graft copolymer	80	180	2.3	1.2
homo polymer	1.67	3.58	2.1	

Synthesis of cellulose polystyrene graft copolymer (MCC-CPPA16-Pr-PS_3)

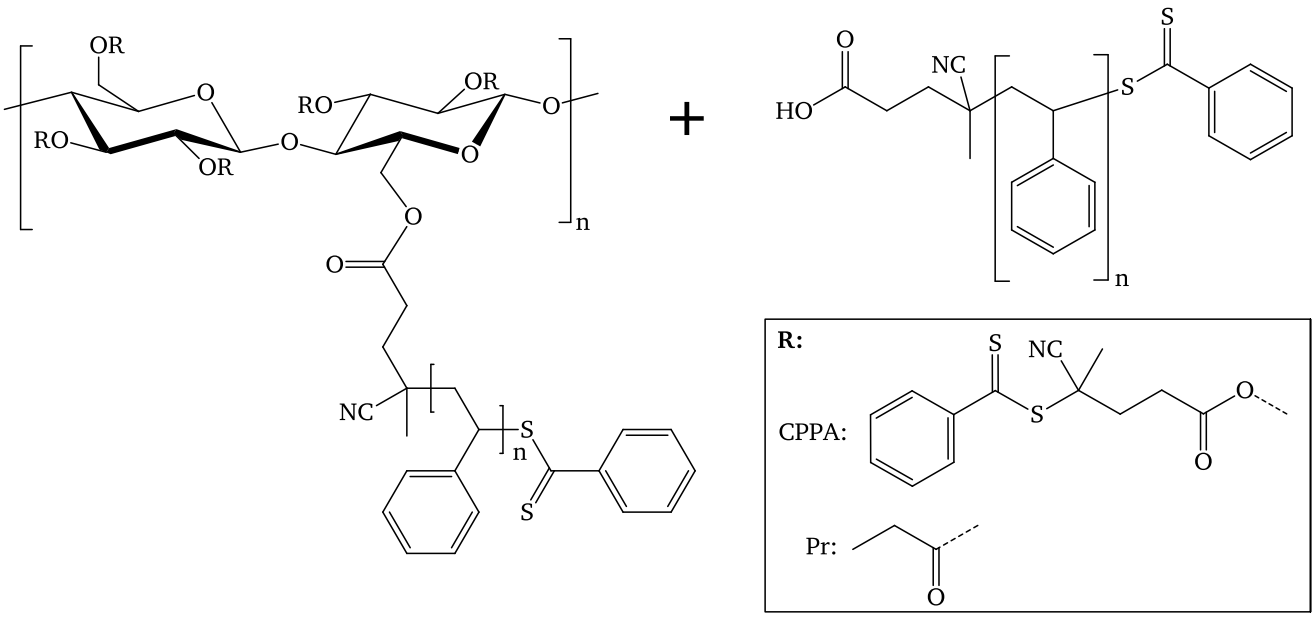

Cellulose macro-CTA (10 mg, 7.5 μmol CTA groups, 1 equiv.) was dissolved in 1 ml styrene. Stock solutions of free CTA and AIBN in styrene were prepared and corresponding amounts of CTA (2.1 mg, 7.5 μmol, 1 equiv.) and AIBN (0.147 mg, 0.9 μmol, 0.12 equiv.) were added to a Schlenk-tube. Styrene was added to yield an overall volume of 3 ml. The total amount of styrene was 2727 mg (26.18 mmol, 3500 equiv.) Oxygen was removed by three freeze-pump-thaw cycles. Polymerization was performed overnight (18 h) at 65 °C and was quenched by precipitation of the polymer into methanol and reprecipitation from THF into methanol. Yield 251 mg, conversion = 8.8 %.

Table 14. Comparison of cellulose graft copolymer with linear homopolymer.

Sample	M_n	M_w	Đ
	[kDa]	[kDa]	
graft copolymer	138	564	4.1
homopolymer	12.3	13.4	1.1

Synthesis of cellulose-bromoisobutyro ester (MCC-BiB3)

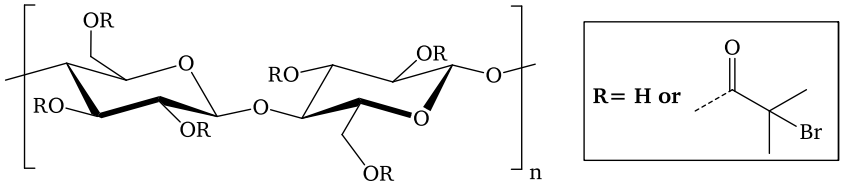

A solution of 4.3 w-% MCC in DMAc/LiCl (0.65 g, 4.0 mmol), DMAP (50 mg, 0.40 mmol) and pyridine (1.9 g, 24 mmol) were added to a Schlenk-flask and diluted with 10 ml dry DMAc. The reaction mixture was cooled with an ice bath and then bromoisobutyro bromide (5.5 g, 24 mmol) were diluted with 10 ml DMAc and added slowly to the reaction mixture. The ice bath was removed and the reaction mixture was stirred for 18 hours at room temperature. The product was isolated by precipitation of the reaction mixture into water and suspending in methanol. The product was dried at high vacuum to yield 1.5 g (78 %). The DS (BiB) = 2.2 was determined after propionylation.

It was soluble in acetone, DMF and DMSO but insoluble in unpolar solvents like $CHCl_3$, THF, toluene or ethyl acetate.

Synthesis of cellulose-bromoisobutyro/propionic mixed ester (MCC-BiB3-Pr)

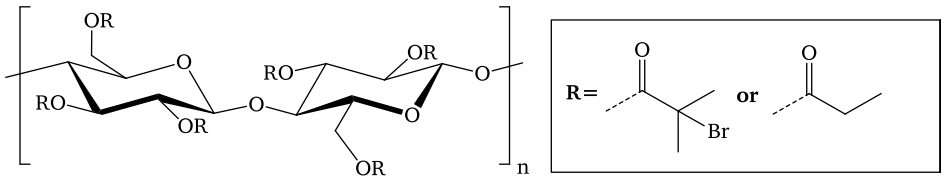

MCC-BiB (700 mg, 2.0 mmol) was dissolved in 10 ml anhydrous DMF and added to a 100 ml Schlenk-flask. DMAP (23 mg, 0.18 mmol), pyridine (3.7 g, 46 mmol) were added at room temperature while stirring. Then, propionic acid anhydride (6.0 g, 46 mmol) was added drop wise. The reaction mixture was heated and stirred for 24 hours at 60 °C. The product was purified by precipitation in MeOH/H_2O (1:1 vol/vol) with subsequent washings. The product was dried overnight at 30 °C in vacuum.
Yield: 0.56 g (54 %), DS(BpB) = 2.2 DS(Pr) = 0.8 (estimated by ^{1}H-NMR). The product was well-soluble in various polar and unpolar organic solvents like $CHCl_3$, THF or DMF.

^{1}H-NMR ($CDCl_3$): 1.0 (b.s., 3H, H-g), 1.7 (b.s., 3H, H-i), 2.3 (b.s., 2H, H-f), 3.3-5.2 (b.s., 7H, H-1 to H-6), 4.4 (b.s., 1H, H-h).

Synthesis of a cellulose macro-CTA based on cellulose-bromoisobutyro/propionic mixed ester (MCC-CTA_4)

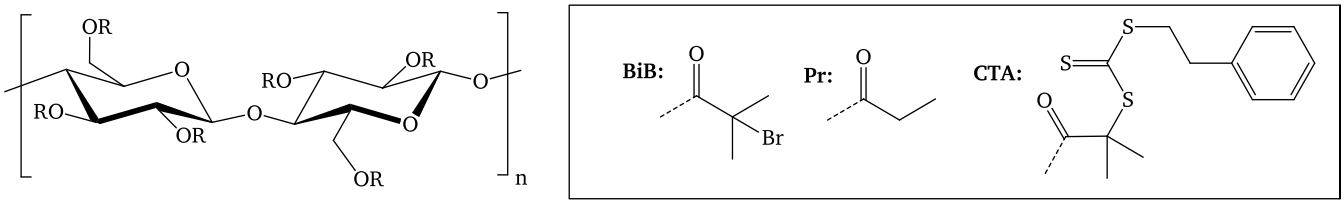

R= BiB, Pr, CTA

The trithiocarbonate functionality was produced in-situ by dilution of phenyl ethyl mercaptane (59 mg, 0.43 mmol) in 5 ml dry DMF, using a Schlenk-tube and N_2-inert gas. Fine grounded tribasic potassium phosphate (90 mg, 0.43 mmol) was added. The reaction mixture was stirred for 10 minutes at room temperature, than carbon disulfide (97 mg, 1.28 mmol) was added via a syringe through a septum. After stirring the mixture for 30 minutes the color turned bright yellow. Cellulose-bromoisobutyro/propionic mixed ester (200 mg, 0.38 mmol) was dissolved in 5 ml dry DMF and also added to the reaction mixture. After a reaction time of 4 hours at 40 °C the product was isolated by removal of the solid potassium phosphate with subsequent precipitation of the solution in methanol/water 1:1 and washing. The product was dried overnight at 50 °C in vacuo. Yield: 141 mg. The product was well soluble in a variety of organic solvents: styrene, toluene, $CHCl_3$, DMSO, DMF, and acetone.

Table 15. SEC analysis of the cellulose macro-CTA sample. Eluent: THF, calibration with PS standards.

Sample	M_n	M_w	Đ
	kDa	kDa	
MCC-CTA4	23	80	3.5

Synthesis of a cellulose polystyrene graft copolymer (MCC-CTA4-PS_1)

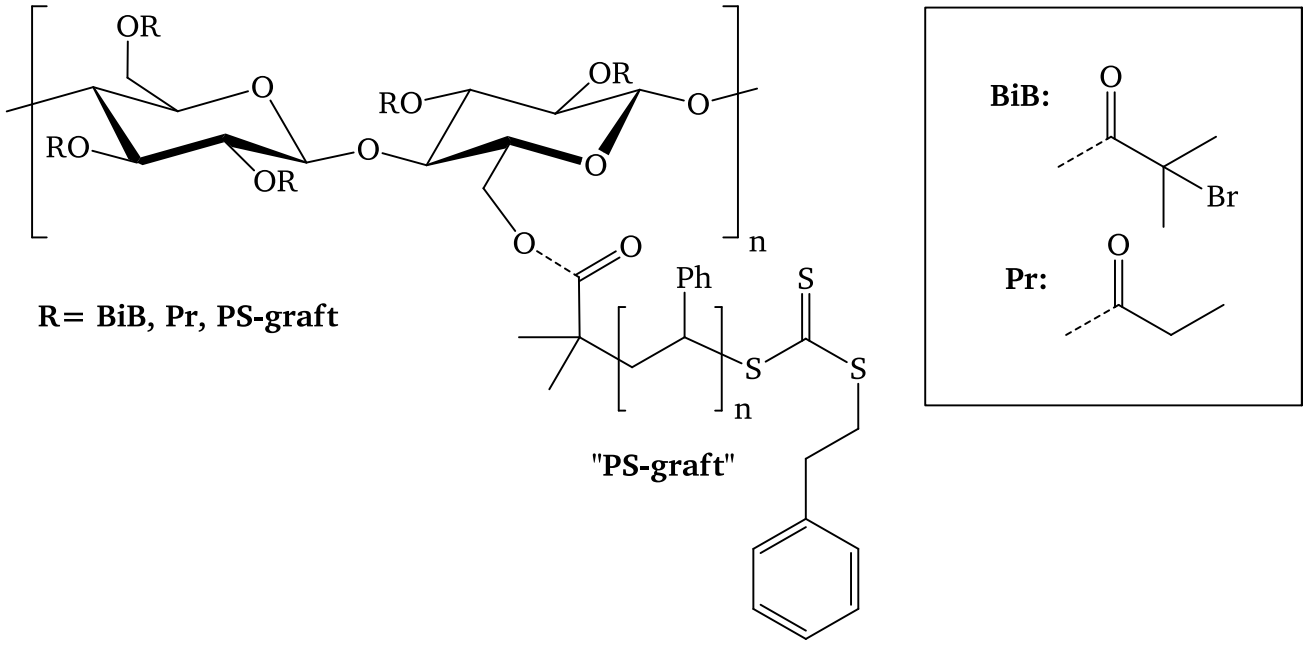

Cellulose-CTA (20 mg, 5 μmol CTA groups) was dissolved easily in 2 ml styrene. By use of stock solutions AIBN (0.15 mg, 0.9 μmol) and free CTA (4.5 mg, 15 μmol) was added. Styrene was added until the total volume of styrene was 3 ml (2.727 g, 26.18 mmol). All substances were added to a 15 ml Schlenk-tube. Oxygen was removed by three freeze-pump-thaw cycles. Polymerization was performed for 18 hours at 65 °C. The reaction was quenched by precipitation of the polymer into methanol and reprecipitation from THF into methanol and dried under vacuum to yield 260 mg product (20 mg cellulose-CTA + 240 mg polystyrene; monomer conversion = 8.1 %).

Table 16. SEC analysis of the cellulose macro-CTA sample. Eluent: THF, calibration with PS standards.

Sample	M_n	M_w	Đ
	kDa	kDa	
graft copolymer	128	320	2.5
homopolymer	11.5	12.8	1.1

Synthesis of cellulose-2-bromopropionyl ester (MCC-BpB4)

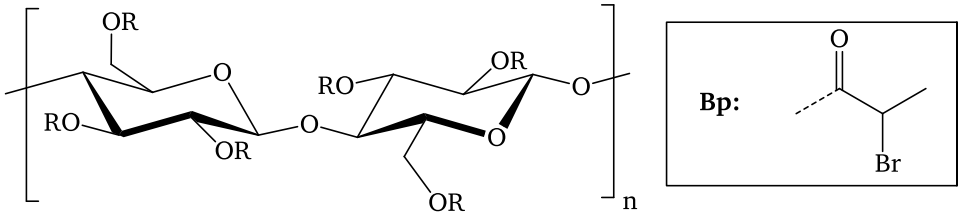

R= Bp, H

A 500 ml Schlenk-flask was filled with 151.5 g of MCC in DMAc/LiCl (3.3 w-% cellulose, 5 g, 30.84 mmol anhydroglucose units) and diluted with anhydrous DMAc (70 ml). pyridine (4.88 g, 61.67 mmol), DMAP (0.377 g, 3.08 mmol) were added. The Schlenk-flask was cooled with an ice bath, and then 2-Bromopropionic acid bromide, BpB (13.32 g, 61.67 mmol) was dissolved in DMAc (30 ml) and added drop wise through the septum. Note: If the concentration of BpB is too high or the addition too fast, the reaction mixture changes its color from pale yellow/brown to black, indicating degradation of the cellulose. The ice bath was removed and the reaction mixture was stirred at room temperature overnight (18 hours). The reaction mixture was poured slowly into 1,500 ml MeOH/H_20 (1:1 vol/vol) resulting in orange solid flake-like material. The product was washed several times with MeOH/H_20 (1:1 vol/vol) until the washing phase remained clear. The product was dried in vacuum at 30 °C overnight. 9.30 g (83 % yield) of pale orange solid material was collected. The DS(Bp) was 1.5 as determined by ^{1}H after propionylation, see next section for details. The product was well-soluble in DMF and DMSO.

Propionylation of cellulose 2-bromopropionyl ester (MCC-BpB4-Pr):

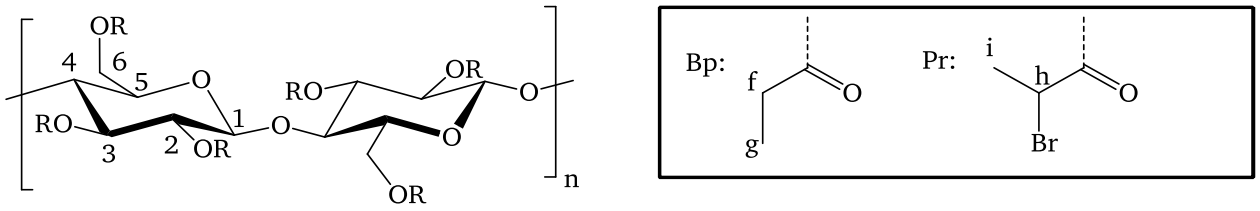

R= Bp, Pr

A sample of 2-bromo propionyl ester cellulose (MCC-BpB4) (9.3 g, 25.5 mmol) was dissolved in anhydrous DMF (250 ml) in a 500 ml Schlenk-flask to obtain an orange solution. DMAP (0.377 g, 3.08 mmol), pyridine (61.6 g, 771 mmol) were added at room temperature while stirring. Then, propionic acid anhydride (100.3 g, 771 mmol) was added drop wise. The reaction mixture was heated and stirred for 18 hours at 50 °C. The product was purified by precipitation in 1500 ml MeOH/H_2O (1:1 vol/vol) with subsequent washings. The product was dried overnight at 30 °C in vacuum. Yield: 10.2 g (73 %), DS(Bp) = 1.5 DS(Pr) = 1.5 (estimated by ^{1}H-NMR). The product was well-soluble in $CHCl_3$, DCM, acetone, THF and DMF.

^{1}H-NMR ($CDCl_3$): 1.0 (b.s., 3H, H-g), 1.7 (b.s., 3H, H-i), 2.3 (b.s., 2H, H-f), 3.3-5.2 (b.s., 7H, H-1 to H-6), 4.4 (b.s., 1H, H-h).

Table 17. SEC analysis of a 2-bromopropionyl cellulose sample. Eluent: THF, calibration with PS standards.

Sample	M_n	M_w	Đ
	kDa	kDa	
MCC-BpB4-Pr	18.3	40.7	2.2

Synthesis of cellulose macro-CTA based on cellulose 2-bromopropionyl/propionyl mixed ester with a DS(CTA) = 0.56 (MCC-CTA14)

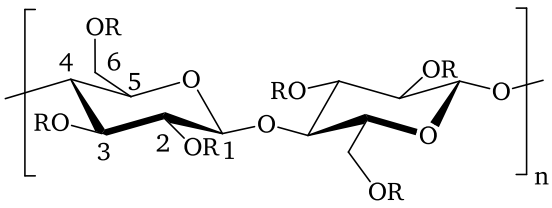

R= Bp, Pr, CTA

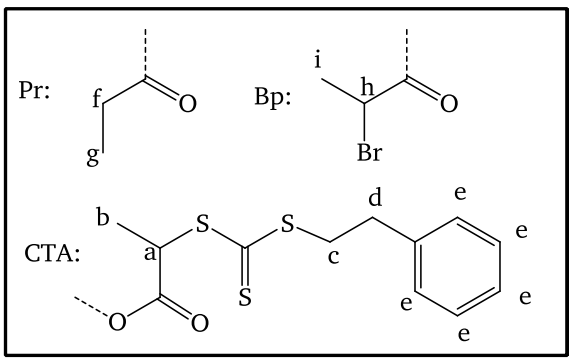

The synthetic route was adapted from literature [83]. In brief, anhydrous K_3PO_4 (467 mg, 2.20 mmol) was grinded and suspended in 50 ml anhydrous acetone in a 250 ml Schlenk-flask. Phenylethyl mercaptane (304 mg, 2.20 mmol) was added; the mixture was stirred for 10 minutes with subsequent addition of carbon disulfide (502 mg, 6.60 mmol). The solution turned to a bright yellow color within minutes. The reaction mixture was stirred for 30 minutes at room temperature. MCC-Bp-Pr (1.0 g, 2.2 mmol AGU) was dissolved in 50 ml acetone and added to the reaction mixture. The reaction mixture is stirred for 4 hours at 40 °C. The solid K_3PO_4 powder was removed by centrifugation to yield a clear solution. The reaction mixture was added drop wise in MeOH/H_2O (1:1 vol/vol), resulting in a very fine dispersion. Complete sedimentation of the solid was not possible by centrifugation (4.5 krpm for 15 minutes). The yields could be raised from less than 30 % to more than 90 % by use of small amounts of $CaCl_2$ as flocculation agent. After addition of $CaCl_2$ the particles flocculated within minutes and could be separated easily by centrifugation. The product was purified by several washing cycles with MeOH/H_2O. After drying in the vacuum oven overnight at room temperature 1.10 g (93.1 %) yellow powder was obtained. The DS(CTA) = 0.56 was calculated by ^{1}H-NMR and sulfur elemental analysis with good agreement of both methods. A comparison of the precursor substance MCC-BpB4-Pr and the product MCC-CTA with ^{1}H-NMR is displayed in the appendix.

^{1}H-NMR (CD_2Cl_2): 1.0 (b.s., 3H, H-g), 1.7 (b.s., 6H, H-b and H-i), 2.3 (b.s., 2H, H-f), 2.9 (b.s., 2H, H-c), 3.3-5.2 (b.s., 7H, H-1 to H-6), 3.6 (b.s., 2H, H-d), 4.4 (b.s., 1H, H-h), 4.8 (b.s., 1H, H-a) 7.0-7.8 (m, 5H, aromat.-H) ppm.

Table 18. SEC analysis of the cellulose macro-CTA sample. Eluent: THF, calibration with PS standards.

Sample	M_n	M_w	Đ
	kDa	kDa	
MCC-CTA14	20.7	47.8	2.3

Synthesis of RAFT reagent phenylethyl isopropionate methylester trithiocarbonate (PE-BpB-Me-TTC)

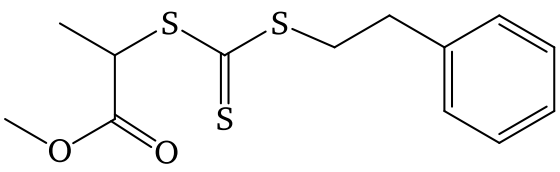

The free RAFT agent was prepared according to the literature [83], using phenylethyl mercaptane and 2-bromopropionic acid methyl ester as reactants. In brief: Phenylethyl mercaptane (858 mg, 6.21 mmol) was added to a dispersion of K_3PO_4 (1.32 g, 6.21 mmol) in dry acetone (20 ml). After 10 minutes of stirring CS_2 (1.42 g, 18.6 mmol) was added drop wise. The reaction mixture was stirred for another 30 minutes and the solution turned into bright yellow, followed by the addition of 2-bromopropionyl bromide (1.00 g, 6.21 mmol). After 4 hours of stirring at room temperature K_3PO_4 was removed by centrifugation, all solvent and reagents volatiles were removed by rotary evaporation to yield a viscous, orange liquid. Purification was done by flash column chromatography with n-hexane/ ethyl acetate 3:1 as eluent. Yield 1.39 g (74 %).

^{1}H-NMR (CD_2Cl_2): 1.7 (d, 3H, CH_3), 2.9 (t, 2H, CH_2), 3.6 (t, 2H, CH_2), 3.7 (s, 3H, OCH_3) 4.8 (q, 1H, CH) 7.0-7.8 (m, 5H, aromat.-H) ppm.

RAFT mediated polymerization of styrene with CTA „PE-BpB-Me-TTC“

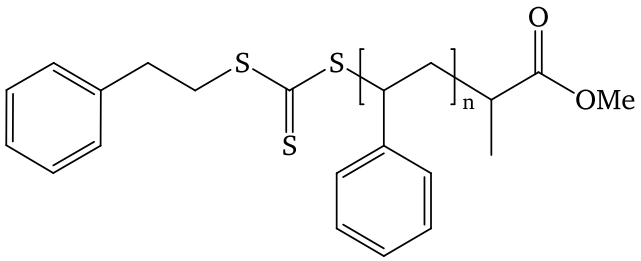

General procedure: AIBN (2.0 mg, 12 μmmol) and free CTA (18 mg, 60 μmol) were prepared as stock solutions and were added to a Schlenk-tube. Styrene (2.727 g, 26.18 mmol) and toluene was added to receive an overall volume of 6 ml. The reaction vessel was sealed with a septum and the reaction mixture was degassed by three pump-freeze-thaw cycles using argon as inert gas. The reaction vessels were placed in an oil bath at 65 °C, after 16 h, 22 h and 40 h samples were taken for analysis with argon flushed syringes. The monomer conversions were determined by ^{1}H-NMR analysis. Polymer samples were purified by precipitation of the reaction mixture into methanol with subsequent reprecipitation of the polymer from THF in methanol and analyzed with SEC.

RAFT polymerization of cellulose macro-CTA "MCC-CTA14" with styrene

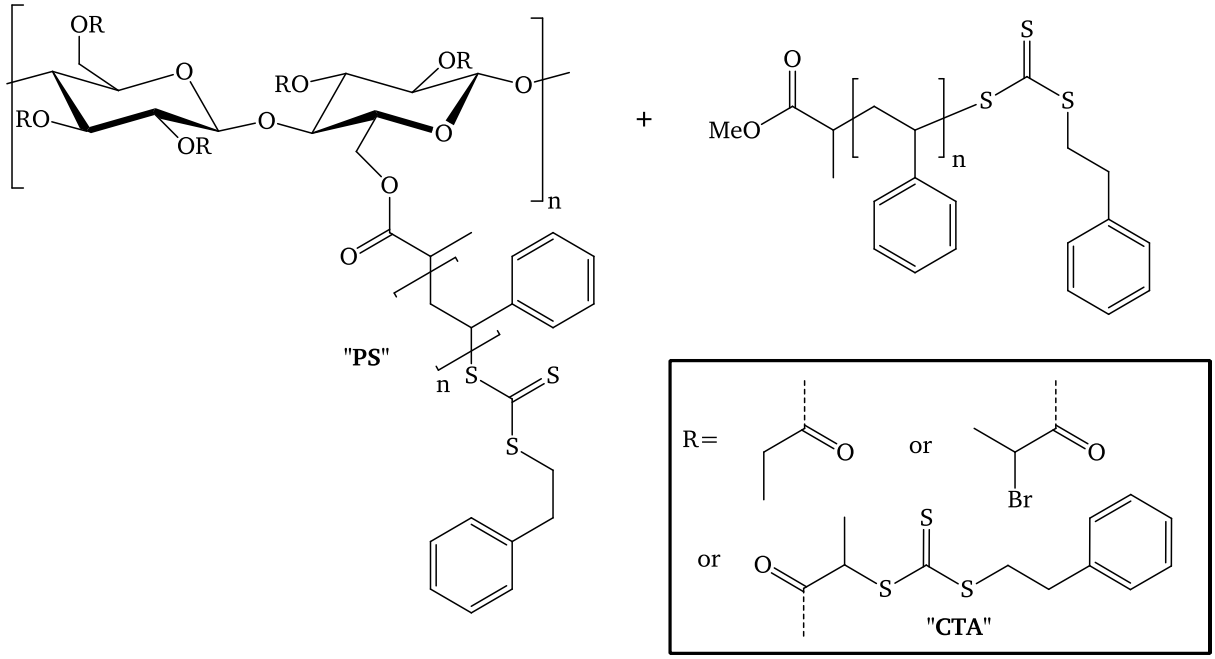

General procedure: Stock solutions of AIBN, free CTA and MCC-CTA in toluene (or in styrene for bulk polymerizations) were prepared separately. MCC-CTA was dissolved in toluene (styrene) within less than 20 minutes by ultrasonic treatment. For each individual set of experiments the overall concentration of CTA as well as the [styrene]/[CTA]/[AIBN] ratio was kept constant, whereas the ratio of CTA on cellulose to free CTA was varied. Defined amounts of all stock solutions were added to a Schlenk-tube. The reaction vessel was sealed with a septum and the reaction mixture was degassed by three pump-freeze-thaw cycles using argon as inert gas. The reaction vessels were placed in an oil bath at 65 °C, aliquots of the reaction mixture (300 μL) were taken with argon flushed syringes in defined time intervals, and the monomer conversion was determined by ^{1}H-NMR analysis (for details see appendix). Polymer samples were purified by precipitation of the reaction mixture into methanol with subsequent reprecipitation of the polymer from THF in methanol.

For isolation of cellulose-graft-polystyrene from free polystyrene, typically about 400 mg of a mixture of linear polymer and graft-polymer, respectively, are dissolved in 4 ml THF and precipitated into 40 ml diethyl ether. While the cellulose graft copolymer turned-out to be insoluble in this solvent and thus precipitates, the linear PS homopolymer stays in solution, and can be conveniently separated. The latter procedure was repeated twice to yield graft-polymer with a purity of >90 % as confirmed by SEC. By evaporation of diethyl ether from the organic liquid phase followed by precipitation into methanol the corresponding polystyrene homopolymer could be isolated as well.

Cleavage of polystyrene grafts from the cellulose backbone

General procedure: 100 mg of purified cellulose-graft-polystyrene was dissolved in 2 ml of THF with subsequent addition of 100 mg potassium tert.-butanolate. The solution was stirred at room temperature for 60 minutes which was found to be sufficient to cleave-off the polymer chains from the polysaccharide backbone. Cleaved polymer grafts were isolated by precipitation into methanol with subsequent washing using water and methanol, drying in a vacuum oven at room temperature (yield: 46 mg).

Removal of the terminal CTA-groups on a cellulose graft copolymer (MCC-CTA14-PS13)

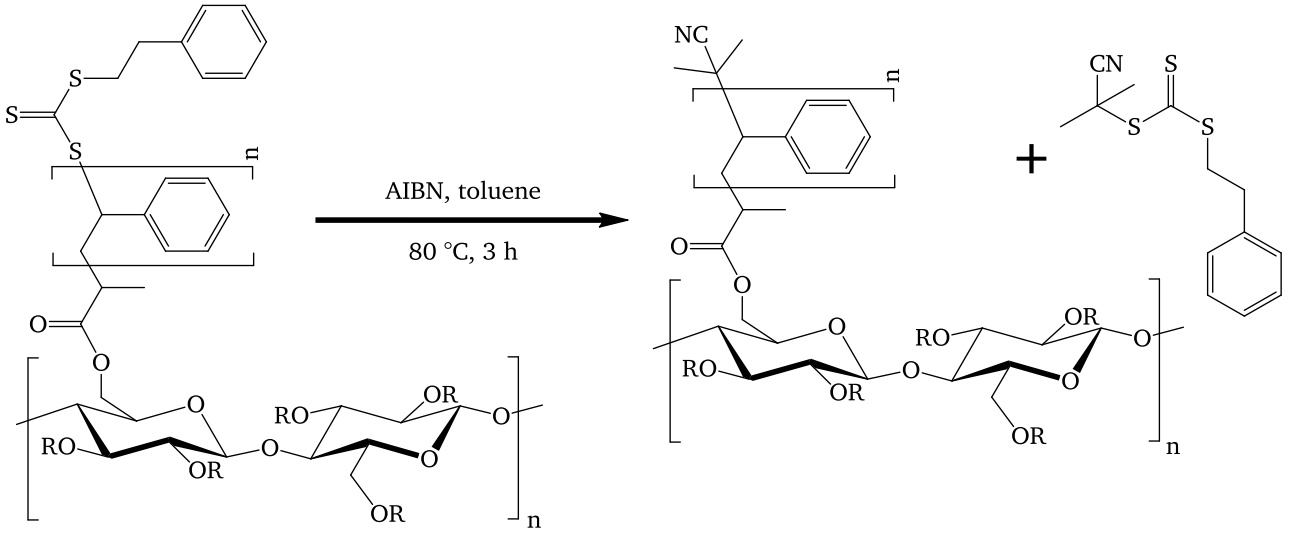

Reaction conditions were adopted from Perrier et al [88]. 1.0 g of the yellow graft copolymer and 0.5 g AIBN were dissolved in toluene and added to a reaction vessel. The reaction mixture was stirred at 80 °C for three hours; the polymer was isolated by precipitation in MeOH, dissolved in THF and again precipitated in MeOH, followed by drying. Yield: 600 mg of a white solid.

Table 19. SEC analysis of the cellulose graft copolymer. Eluent: THF, calibration with PS standards.

Sample	M_n	M_w	Đ
	kDa	kDa	
graft copolymer	123	188	1.5
homopolymer	8.1	9.6	1.2

Synthesis of polyethylene glycol-550-monomethylether tosylate (PEG550-Tosylate)

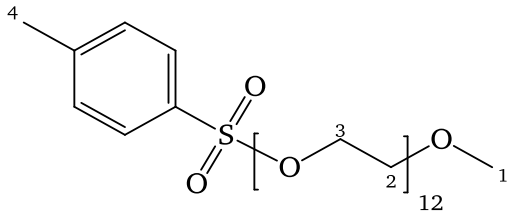

The synthesis was performed as described by Cowie and Coworkers [92]. PEG550-Monomethylether (100 g, 182 mmol) was added to a 500 ml round bottom flask and diluted with 40 ml pyridine and 100 ml dry dichloromethane under nitrogen atmosphere. The mixture was stirred and cooled with an ice bath to keep the reaction temperature below 5 °C. Tosyl chloride (52 g, 273 mmol) was suspended in 100 ml dichloromethane and was added slowly within 15 minutes. The reaction mixture was stirred for another 4 hours, than it was stirred for 24 hours at room temperature. The product was isolated with the following procedure: dilution with 300 ml CH_2Cl_2, followed by washing of the organic phase with water, 0.1 N HCl, saturated $NaHCO_3$ solution and finally with saturated brine. The organic phase was dried with $MgSO_4$ and solvent was removed. The remaining high viscous, colorless liquid was further dried at vacuum overnight to yield 75.5 g (58 %). Purity was analyzed by the signal ratio of protons H-4 and PEG-backbone protons H-2 and H-3 (89 %).

^{1}H-NMR ($CDCl_3$): 2.3 (s, 3 H, H-4), 3.2 (s, 3 H, H-1), 3.3-3.6 (m, 48 H, H-2 and H-3), 7.0-7.8 (m, 4 H, aromat.-H) ppm.

Synthesis of polyethylene glycol-550-monomethylether iodide

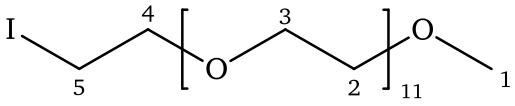

The synthesis was performed as described by Cowie and coworkers [92]. PEG550-Tosylate (75.5 g, 89 % purity, 95 mmol) was dissolved in 600 ml anhydrous acetone under nitrogen atmosphere. Potassium iodide (71 g, 430 mmol) was added and the reaction mixture was stirred for 24 hours under reflux. Isolation of the product: Removal of the acetone, dissolution of the reaction mixture in chloroform followed by subsequent washing with water, 0.3 N $Na_2S_2O_3$ solution, saturated $NaHCO_3$ solution and finally twice with water. The solution was dried with $MgSO_4$ and solvent was removed.

The remaining high viscous, yellow liquid was further dried at vacuum overnight to yield 63 g (≈100 %).

The purity was analyzed with ^{1}H-NMR (>98 %), where traces of tosylate groups remained in the product.

^{1}H-NMR ($CDCl_3$): 3.2 (t, 2H, H-5), 3.3 (s, 3H, H-1), 3.4-3.8 (m, 44H, H-2 and H-3), 3.7 (t, 2H, H-4) ppm.

Synthesis of 6-*O*-(triphenylmethyl) cellulose

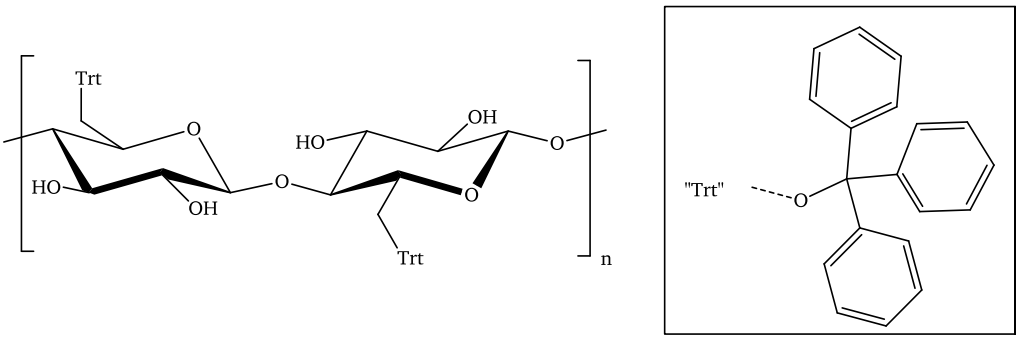

The procedure was adopted from literature [55]. 198 g of a solution of DMAc/LiCl containing 2.02 w-% MCC (4.0 g, 24.67 mmol) was added to a 500 ml Schlenk-flask under nitrogen atmosphere. Half of the total amount of TEA (triethylamine) (75 g, 75 mmol) and Trt-Cl (trityl chloride) (17.4 g, 62.5 mmol) were added under nitrogen counter flow. The reaction mixture was stirred for 24 hours at 70 °C, than the second portion of triethylamine and trityl chloride were added, followed by another 24 hours stirring at 70 °C. The product was isolated by precipitation in 1.5 L methanol. The pale, light brown flocculates were dissolved in 300 ml THF and precipitated in 1.5 L methanol again. The product was dried in vacuo at 30 °C overnight. Yield: 8.6 g (86 %)

Table 20. SEC analysis of trityl cellulose.. Eluent: THF, calibration with PS standards.

Sample	M_n	M_w	Đ
	kDa	kDa	
MCC-Trt2b	35	80	2.3

Synthesis of 2,3-*O*-(polyethylene glycol-550-monomethylether)-6-*O*-(triphenylmethyl) cellulose

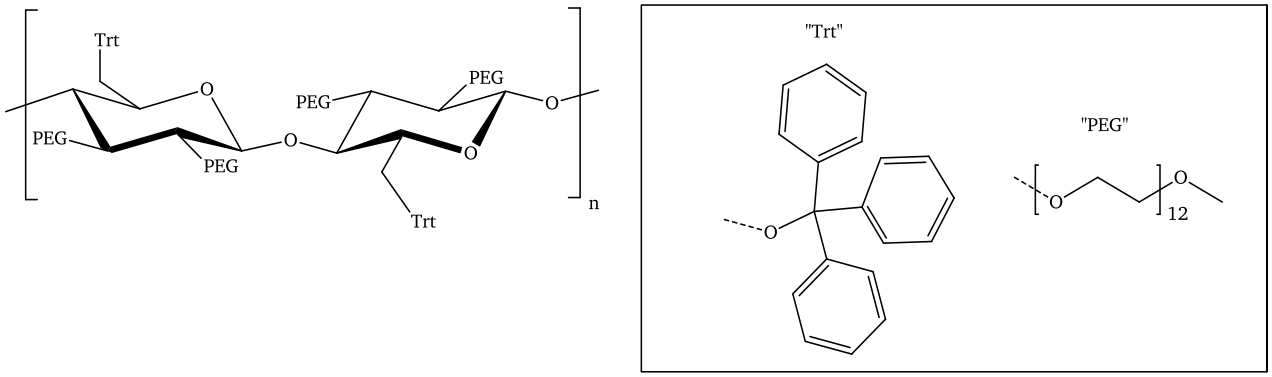

The procedure was adapted from Cowie and coworkers [92]. For synthesis MCC-Trt (0.5 g, 1.2 mmol) was dissolved in 60 ml DMSO. Than fine powdered NaOH (1.25 g, 31 mmol) and 0.5 ml water were added. The reaction mixture was stirred for 60 minutes at room temperature, than PEG550-iodide (16.5 g, 25 mmol) was dissolved in 40 ml DMSO and added to the reaction mixture. The reaction was continued for 18 hours at 70 °C under stirring. The product was isolated by precipitation into diethyl ether, the sticky solid was dissolved in $CHCl_3$, followed by washing with water, 0.1 N HCl, saturated $NaHCO_3$ and brine. The organic phase was dried with $MgSO_4$ followed by precipitation in diethyl ether. Dissolution and reprecipitation was repeated another 2 times. The product was dried in vacuo at 30 °C overnight to get 1.3 g of a brown sticky substance, which was analyzed with ^{1}H-NMR. This allowed the determination of the DS values of the product. For this, the relative abundance of aromatic protons (trityl moieties) was compared with the protons from the PEG550 backbone.

^{1}H-NMR (DMSO): 3.3-3.75 (m, 48 H, PEG550), 6.8-7.6 (m, 15 H) ppm.

DS(PEG550)≈ 1.6

DS(Trt) = 1

Table 21. SEC analysis of 2,3-PEG-6-tritylcellulose.. Eluent: THF, calibration with PS standards.

Sample	M_n	M_w	Đ
	kDa	kDa	
MCC-Trt2b-PEG550_1	4.2	5.5	1.3

Synthesis of 2,3-*O*-(polyethylene glycol-550-monomethylether) cellulose by removal of the trityl protection groups (MCC-PEG550)

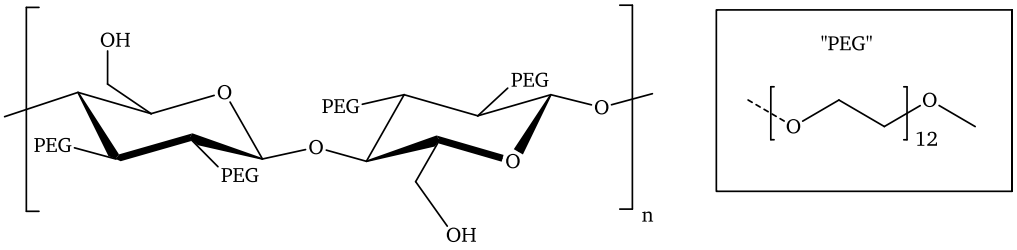

Deprotection of the trityl moieties with TFA (trifluoroacetic acid) and TES (tetra ethyl silane) could not be repeated from literature successfully. Therefore an alternative method was tested, but there was no synthetic protocol available. For this MCC-Trt-PEG550 (the product from the prior step; 1.3 g) was dissolved in $CHCl_3$ and cooled with an ice bath. Then, 5 ml of a solution containing HBr in glacial acetic acid (35 w-%) were added slowly under stirring. The ice bath was removed and the reaction mixture was stirred for another 5 minutes and then the product was isolated by precipitation in diethyl ether and careful washing in diethyl ether. The Product was dried in vacuo at 30 °C overnight. Yield: 0.9 g. Determination of the DS values was not possible; however the successful removal of the trityl moieties was confirmed by ^{1}H-NMR and with ATR-IR spectroscopy.

Table 22. SEC analysis of 2,3-*O*-PEG-cellulose.. Eluent: THF, calibration with PS standards.

Sample	M_n	M_w	Đ
	kDa	kDa	
MCC-Trt2b-PEG550_1_1	2.1	4.2	2.0

Synthesis of 2,3-*O*-(polyethylene glycol-550-monomethylether)-6-*O*-(2-bromopropionyl)-cellulose (MCC-PEG550-BpB)

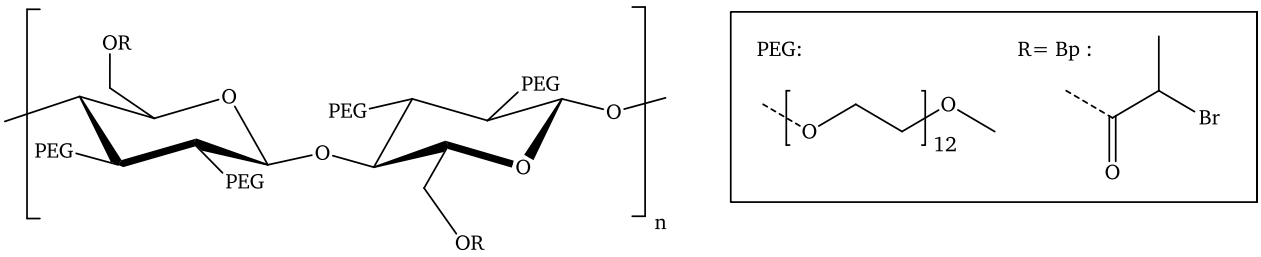

Esterification of the remaining hydroxyl functions on the cellulose with 2-bromopropionyl functionalities was done by use of 2-bromopropionyl anhydride instead of the corresponding acid bromide. For this 15 ml dry DMF, 5 ml pyridine and DMAP (0.15 g, 1.24 mmol) were added to a Schlenk-tube under nitrogen flow. Then 2-bromopropionyl bromide (5.35 g, 24.8 mmol) and 2-bromopropionic acid (4.74 g, 31 mmol) were added. After stirring for two hours at room temperature MCC-PEG550 (0.9 g), dissolved in 10 ml dry DMF, was added. The reaction mixture was stirred for 18 hours at 60 °C. The product was isolated by precipitation in diethyl ether followed by dissolution in $CHCl_3$ and extraction with water (three times) with subsequent drying with MgSO4 of the organic phase, followed removal of $CHCl_3$. Yield: 0.9 g. Analysis with ^{1}H-NMR clearly showed the existence of PEG protons as well as 2-bromopropionyl protons, but precise determination of the DS values was not possible since the PEG protons strongly dominate the spectrum, leaving only a relative small signal from the 2-bromopropionyl moieties.

^{1}H-NMR (300 MHz, CDCl3): 1.68 (d, 3 H), 3.49-3.69 (m, 48 H), 4.38 4.46 (q, 1 H) ppm.

Table 23. SEC analysis of 2,3-*O*-PEG-6-*O*-Bp-cellulose.. Eluent: THF, calibration with PS standards.

Sample	M_n	M_w	Đ
	kDa	kDa	
MCC-Trt2b-PEG550_1_1-BpB_1	1.0	1.2	1.2

Synthesis of 2,3-*O*-(poly(ethylene glycol) 550 monomethyl ether)-6-*O*-(CTA)-cellulose (MCC-PEG550-CTA1)

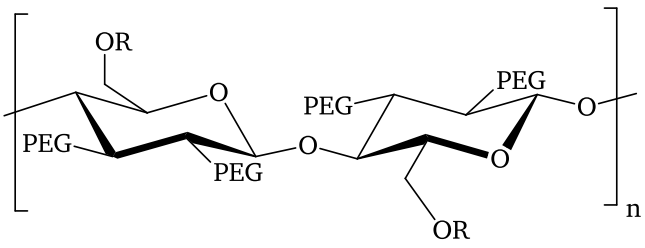

R= Bp, CTA

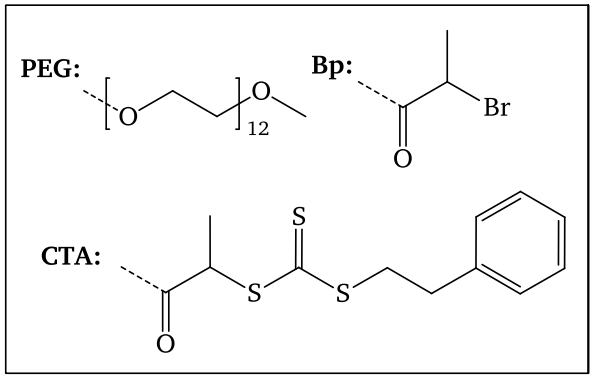

Phenylethyl mercaptane (43 mg, 0.31 mmol) was added to a suspension of K_3PO_4 (66 mg, 0.31 mmol) in 5 ml dry DMF. The solution was stirred for 10 minutes, then CS_2 (0.71 mg, 0.93 mmol) was added with a syringe. The reaction mixture was stirred for another 30 minutes, and then MCC-PEG550-BpB (0.90 g) was dissolved in 5 ml DMF and was added to the reaction mixture. The reaction proceeded for another 4 hours at 40 °C.

K_3PO_4 was removed by centrifugation; the product was isolated by precipitation in diethyl ether, dissolution in acetone with re precipitation in diethyl ether. The product was dried overnight in vacuo at 30 °C to yield 0.29 g product. The DS(CTA) = 1.2 was roughly estimated from the ratio of aromatic protons, PEG backbone protons and Bp protons in the ^{1}H-NMR spectrum (a complete modification of the cellulose, thus a DS(total) = 3 was assumed for this estimation).

^{1}H-NMR (300 MHz, CD_2Cl_2): 1.68-1.70 (d, 3 H), 3.49-3.69 (m, 48 H), 7.22-7.37 (m, 5 H) ppm.

Table 24. SEC analysis of 2,3-*O*-PEG-6-*O*-CTA cellulose.. Eluent: THF, calibration with PS standards.

Sample	M_n	M_w	Đ
	kDa	kDa	
MCC-PEG550-CTA1	0.5	0.7	1.4

Synthesis of 2,3-*O*-(poly(ethylene glycol) 550 monomethyl ether)-6-*O*-(CTA)-cellulose-polystyrene graft copolymer (MCC-PEG550-CTA1-*g*-PS)

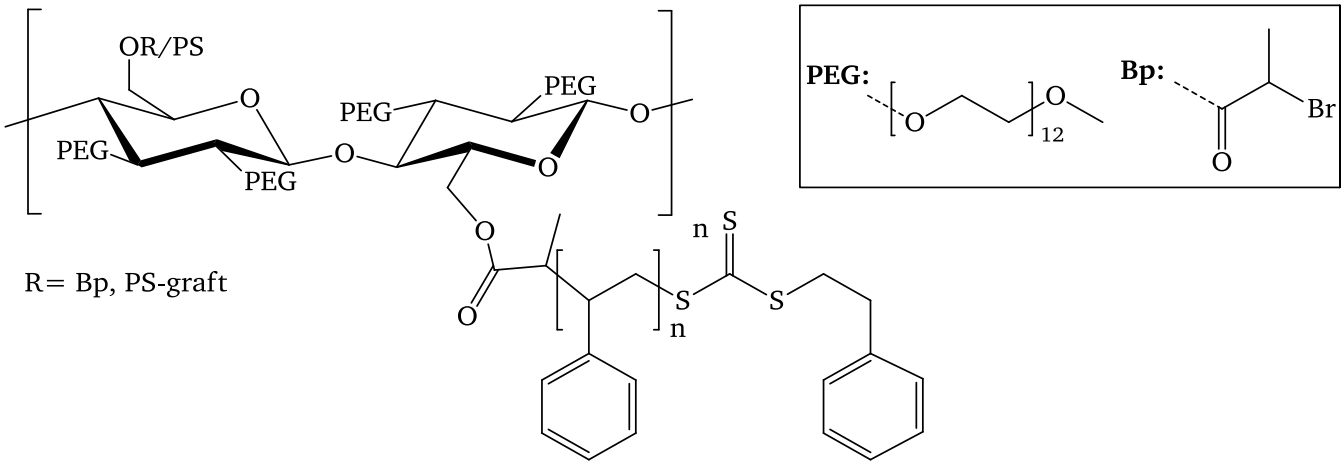

"**PS-graft**"

Cellulose-PEG550-CTA1 (6 mg, 4 μmol CTA groups), free CTA (MeBpB-Me-TTC) (5.4 mg, 18 μmol), AIBN (5.0 mg, 30 μmol), styrene (2.83 g, 35.9 mmol) were dissolved in 10 ml dry THF. After degassing with three pump-freeze-thaw cycles the polymerization was performed for three hours at 65 °C. The polymer was isolated by precipitation in diethyl ether to yield 1.2 g product (42 %).

Synthesis of 2,3-*O*-(poly(ethylene glycol) 550 monomethyl ether)-6-*O*-(CTA)-cellulose-poly NiPAM graft copolymer (MCC-PEG550-CTA1-*g*-PNiPAM)

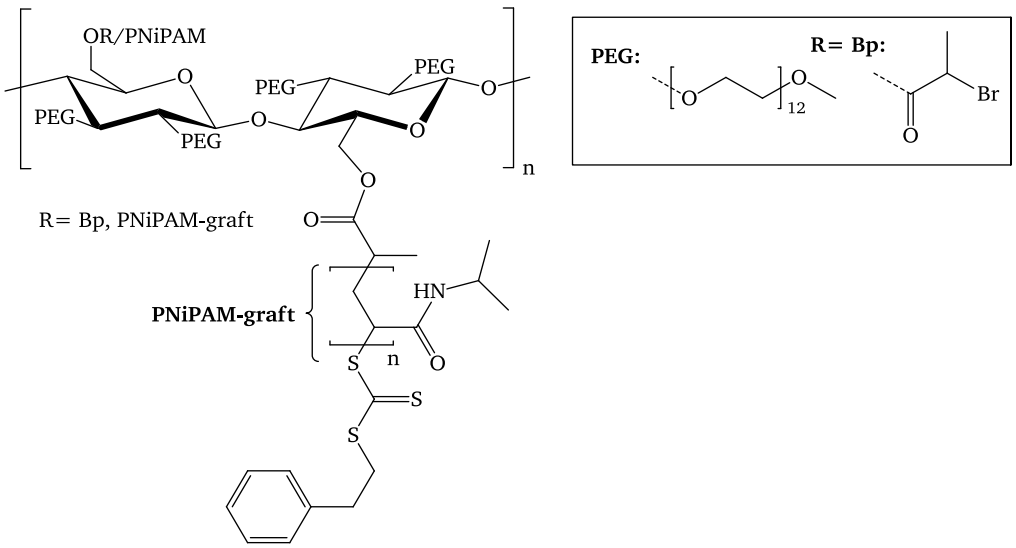

Cellulose-PEG550-CTA1 (44 mg, 40 μmol CTA groups), free CTA (MeBpB-Me-TTC) (36 mg, 120 μmol), AIBN (3.3 mg, 20 μmol), NiPAM (5.660 g, 50 mmol) were dissolved in 20 ml dry DMF. After degassing with three pump-freeze-thaw cycles the polymerization was performed for three hours at 60 °C. The polymer was isolated by precipitation in diethyl ether to yield 4.2 g product (74 % yield).

Synthesis of (poly(ethylene glycol) 550 monomethylether) carboxylic acid (PEG550-COOH)

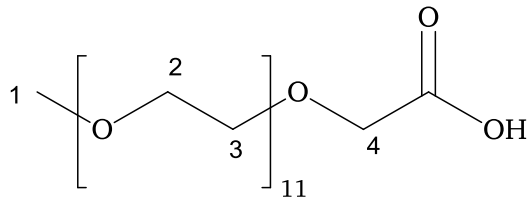

Solid NaOH pellets (34.9 g, 873 mmol) were dissolved in 700 ml water while stirring and cooling with an ice bath. PEG550-monomethyl ether (80.0 g, 145 mmol) was added followed by the addition of solid $KMnO_4$ (138 g, 873 mmol) in portions of 20 g while stirring and cooling. The initial purple color turns quickly green and finally black and the mixture heats up. Therefore the temperature of the reaction mixture was checked in intervals and was kept all the time below 10 °C. After the addition of the last portion $KMnO_4$ the mixture was stirred for a total reaction time of 4 hours. The black solid was removed by cold filtration, the solution was cooled again with an ice bath and concentrated HCl was added slowly until a pH of about 8-9 was reached and more of the black solid was generated. The solid was filtered off; unreacted PEG550-monomethyl ether was removed by extraction with $CHCl_3$ (3 times with 300 ml each). Chloroform was recovered by distillation. 2N HCl was used to lower the pH of the aqueous phase to about 2-3, the color changed to light purple. Then solid Na_2SO_3 was added under stirring until the aqueous phase became clear. Product was isolated by extraction with $CHCl_3$ (3 times with 300 ml each), followed by extraction of the organic phase with brine. The organic phase was dried with $MgSO_4$ and chloroform was removed by distillation to yield 63.9 (78 %) product. The Product was only well soluble in polar solvents like DMSO, DMF and water. When dissolved in DMSO, the solution showed miscibility with many other organic solvents without precipitation, except for very unpolar solvents like diethyl ether, hexane or toluene.

^{1}H-NMR (300 MHz, $CDCl_3$): 3.3 (s, 3 H, H-1), 3.5-3.8 (m, 44 H, H-2 and H-3), 4.1 (s, 2 H, H-4) ppm.

Synthesis of (poly(ethylene glycol) 550 monomethyl ether)/2-bromopropionyl cellulose mixed ester (MCC-(PEG550-COOH_8)_2 (CDI) –Bp_1 (CDI))

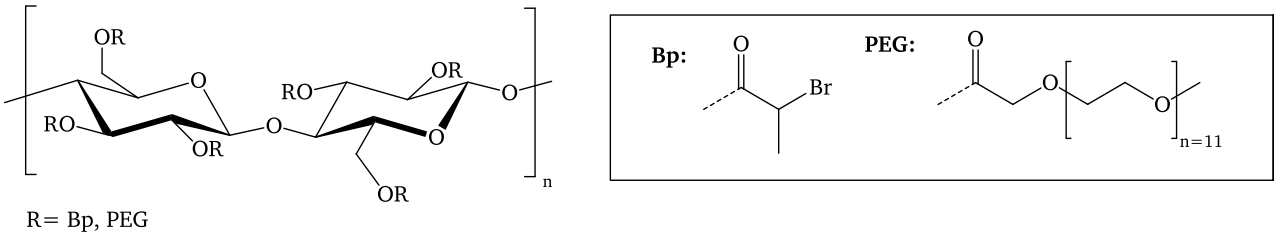

R= Bp, PEG

Activation agent CDI (1.50 g, 9.25 mmol) was added to a dry 100 ml Schlenk-flask equipped with a stirring bar. Then PEG55-COOH, diluted in 15ml dry DMAc was added under nitrogen counter flow. The flask was sealed with a septum and a balloon for pressure release. Intensive generation of gas was observed for about 10 minutes. The reactions mixture was stirred for another 60 minutes at room temperature than 14 g of a solution DMAc/LiCl containing 3.57 w-% cellulose (500 mg, 3.08 mmol) were added and again generation of gas was observed. The reaction mixture was then stirred for 24 hours at 80 °C. Further modification was performed without isolation of this (intermediate) product.
The next step was the activation of 2-bromopropionic acid (2.36 g, 15.4 mmol) with CDI (2.50 g, 15.4 mmol) in 10 ml DMAc. This solution was then added to the reaction mixture with the cellulose intermediate, followed by another 24 hours stirring at 80 °C. The product was isolated by precipitation of the reaction mixture in diethyl ether, followed by dissolution of the crude product in $CHCl_3$. The organic phase was washed twice in saturated $NaHCO_3$, twice with 0.1N HCl and twice water. The washing procedure lead every time to an emulsion, therefore centrifugation at 12 krpm was used to separate the organic and the aqueous phase, but every time a foam like substance was observed at the inter-phase. Each time the organic phase and the foam were separated from the aqueous phase. Finally, the organic phase and the foam were dried with $MgSO_4$. Chloroform was removed by distillation, the resulting brown, sticky polymer was dried at high vacuum to receive 1.60 g (34 % yield) product.

^{1}H-NMR (300 MHz, DMSO-d6): 1.68 (b.s., 3 H), 3.0-4.3 (m, 51 H) ppm.
DS(PEG550-COOH) = 2.5; DS(BpB) = 0.5

Table 25.

Sample	M_n	M_w	Đ
	kDa	kDa	
MCC-(PEG550-COOH_8)_2 (CDI) –Bp_1 (CDI))	96	277	2.9

Synthesis of (poly(ethylene glycol) 550 monomethyl ether)/2-bromopropionyl cellulose mixed ester (MCC-PEG550-CTA_4)

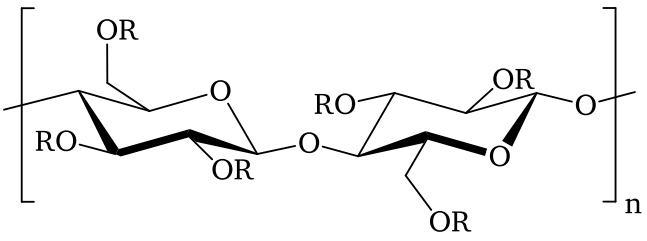

R= CTA, Bp, PEG

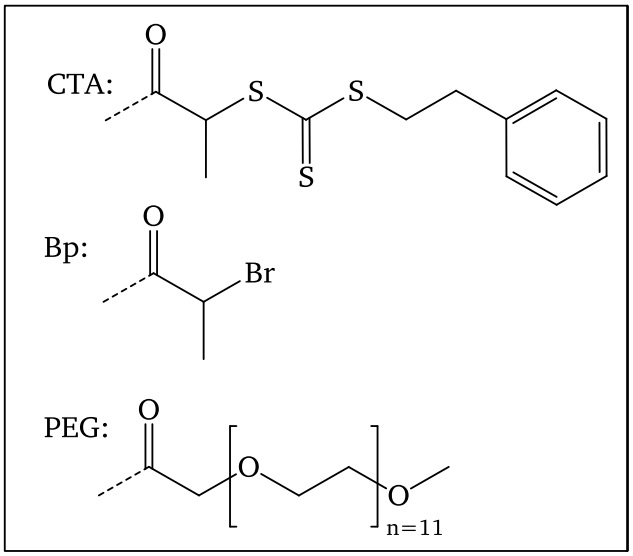

A cellulose mixed ester, which had been synthesized according to the procedure described in but with a different educt ratios, with a DS(PEG) = 1.8 and a DS(BpB) = 1.2 was transferred into a cellulose CTA. For this MCC-PEG550-BpB (500 mg, 0.38 mmol AGU) was dissolved in 5 ml dry DMF. K_3PO_4 was suspended separately in 5ml dry DMF, phenylethyl mercaptane (106 mg, 0.77 mmol) was added and stirred for 10 minutes. Then CS_2 (175 mg, 2.30 mmol) were added and the mixture was stirred for 30 minutes at room temperature. The dissolved cellulose was added and the reaction mixture was stirred for 4 hours at 40 °C. Purification of the product was performed by removal of solid K_3PO_4 and subsequent precipitation in diethyl ether to yield 135 mg (26 %) product after drying. The DS(CTA) = 0.4 was estimated by ^{1}H-NMR.

^{1}H-NMR (300 MHz, DMSO-d6): 1.68 (b.s., 3 H), 2.81 (m, 2 H), 3.0-4.3 (m, 51 H), 7.25 (m, 5 H) ppm.
DS(PEG550-COOH) = 1.8 ; DS(BpB) = 0.8 ; DS(CTA)= 0.4
M(AGU) ≈ 1400 g/mol

Table 26. SEC analysis. Eluent: DMF/LiCl, calibration with PMMA standards.

Sample	M_n	M_w	Đ
	kDa	kDa	
MCC-PEG550-CTA_4	88.6	253	2.9

Graft copolymerization of cellulose PEG macro-CTA (MCC-PEG550-CTA_4-PS_1)

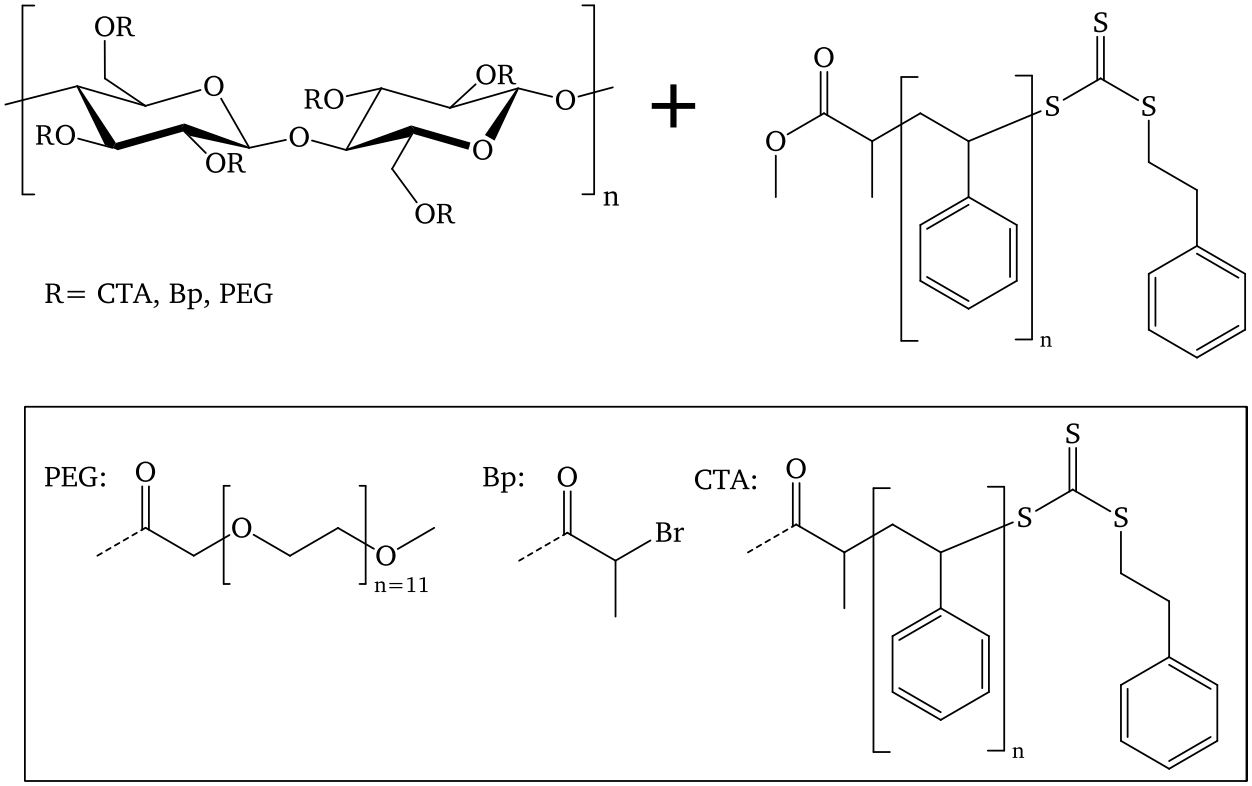

Cellulose macro-CTA (40 mg, 27 μmol) was dissolved in 0.5ml anhydrous DMSO. After complete dissolution 2.5 ml toluene, styrene (2.73 g, 26.2 mmol), free CTA (16.2 mg, 54 μmol) and AIBN (2 mg, 12 μmol) were added. After three freeze-pump-thaw cycles the reaction was started at 65 °C for 18 hours. Polymer was isolated by precipitation in methanol. Homopolymer was removed by dissolution in THF, where insoluble graft copolymer was separated from the THF-soluble homopolymer. Both product fractions were analyzed with SEC (eluent: DMF/LiCl, RI-detection).

Table 27. SEC analysis. Eluent: DMF/LiCl, calibration with PMMA standards.

Sample	M_n	M_w	Đ
	kDa	kDa	
graft copolymer	926	1260	1.4
homopolymer	12.2	17.9	1.5

Graft copolymerization via ATRP technique using cellulose macro-initiator (MCC-BpB4-Pr-PMMA_1 (ATRP))

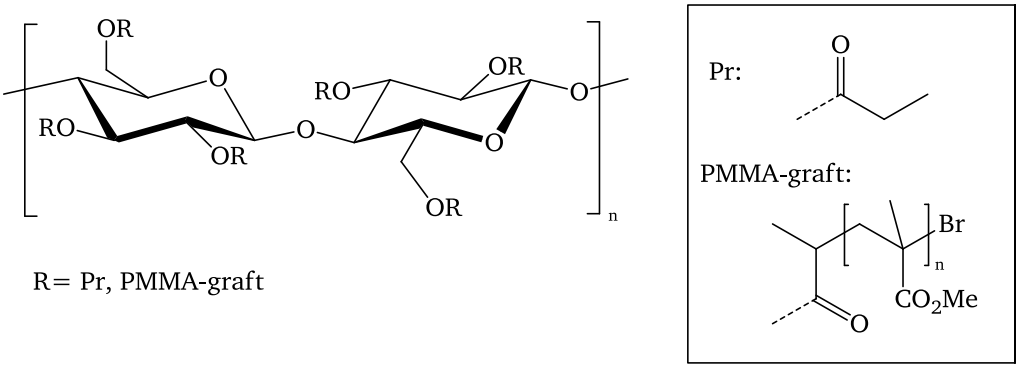

Cellulose macro-Initiator (50 mg, 0.109 mmol) was dissolved in 3.5 ml anisole, followed by the addition of MMA (3.25 g, 32.5 mmol). The reaction mixture was heated to 88 °C, then 1 ml 0.2 N Cu(I)TMEDA$_2$Br stock solution in anisole. After 3 hours the reaction mixture was quenched by cooling and precipitation into methanol to yield 560 mg product.

Table 28. SEC analysis. Eluent: DMF/LiCl, calibration with PMMA standards.

Sample	M_n	M_w	Đ
	kDa	kDa	
MCC-BpB4-Pr-PMMA_1(ATRP)	272	1100	4.0

Graft copolymerization via ATRP technique using cellulose macro-initiator with additional free initiator (MCC-BpB4-Pr-PMMA_2 (ATRP))

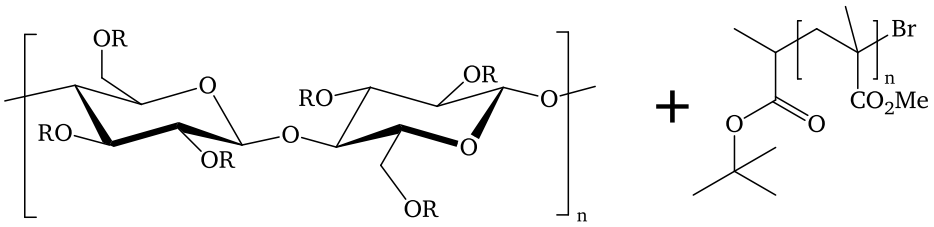

R= Pr, PMMA-graft

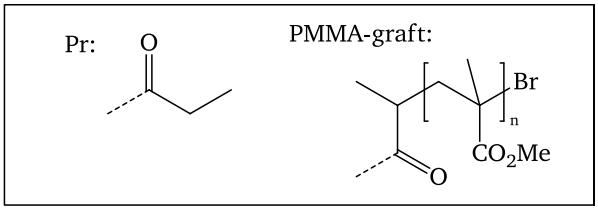

2-bromopropionyl functionalized cellulose mixed ester (MCC-BpB4-Pr) (50 mg, 0.109 mmol) was dissolved in 3.5 ml anisole, followed by the addition of 10 μl tBbib and MMA (3.25 g, 32.5 mmol). The reaction mixture was heated to 88 °C, then 1 ml 0.2N Cu(I)TMEDA$_2$Br stock solution in anisole. After 3 hours the reaction mixture was quenched by cooling and precipitation into methanol to yield 840 mg product.

Table 29. SEC analysis. Eluent: THF, calibration with PS standards.

Sample	M_n	M_w	Đ
	kDa	kDa	
graft copolymer	76.7	116	1.5
homopolymer	79.7	93.8	1.2

Graft copolymerization of pegylated cellulose macro-initiator with ATRP (MCC-PEG550-COOH_8)_2-Bp_1 (CDI) – PMMA_1)

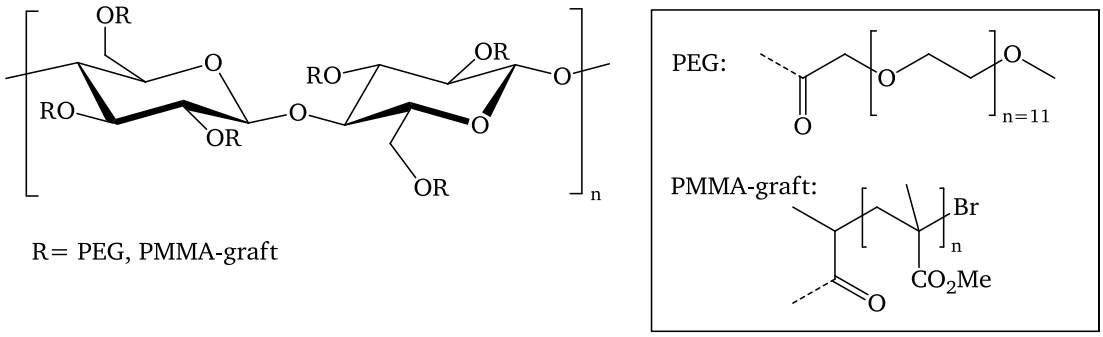

Pegylated cellulose macro-initiator was provided as 14 wt-% stock solution in DMSO. 1.0 g of solution (containing 140 mg macro-initiator with total 45 μmol Br), 900 mg MMA and 0.6 ml anisole were mixed and degassed. After heating the mixture to 88 °C, 0.5 ml 0.2 N Cu(I)TMEDA$_2$Br stock solution in anisole was added. After 3 hours the reaction mixture was quenched by cooling and precipitation into methanol. Yield 460 mg of a blue solid. SEC analysis revealed a multimodal signal of the graft copolymer with a M_n of about 90 kDa, which was therefore not quantified against PMMA calibration.

Synthesis of PS/PMMA mixed grafts:

Graft copolymerization of PS-grafted cellulose macro-initiator with ATRP (experiment "MCC-CTA14-PS_13-RAFT entfernt-PMMA_1")

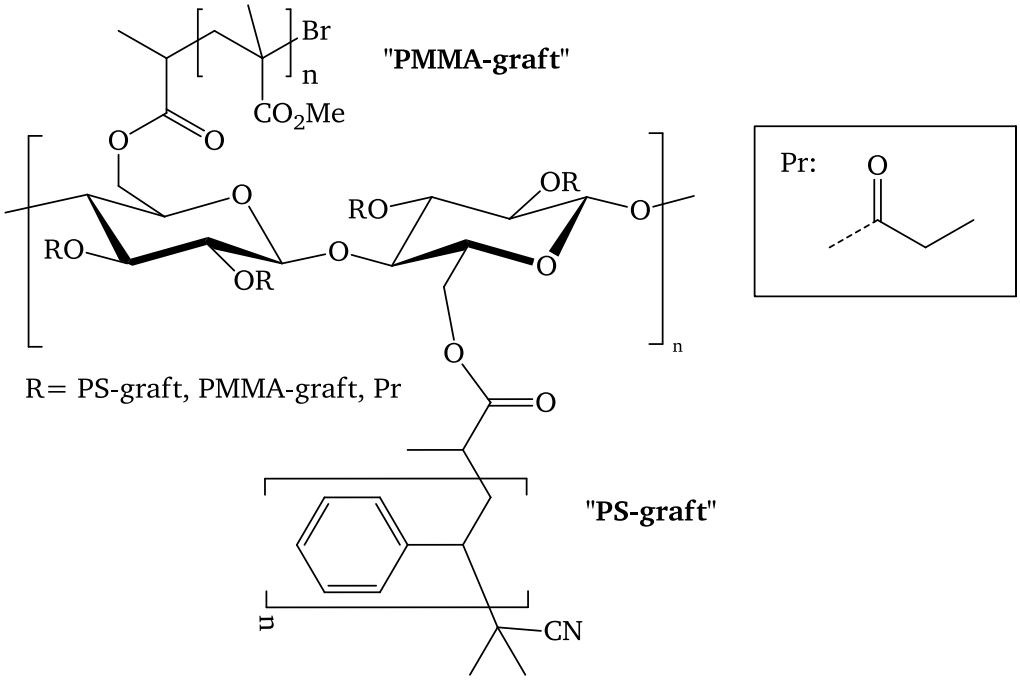

Cellulose-polystyrene graft copolymer (250 mg, containing 25 μmol Br) was dissolved in 2 ml anisole and 920 mg MMA and then the reaction mixture was heated to 88 °C, followed by the addition of 0.25 ml 0.2N Cu(I)TMEDA$_2$Br stock solution in anisole. After 3 hours reaction time, the polymer was isolated by precipitation into methanol. Yield was not determined. The relative amounts of PS and PMMA were determined with ^{1}H-NMR.

Table 30. SEC analysis. Eluent: DMF/LiCl, calibration with PMMA standards.

Sample	M_n	M_w	Đ
	kDa	kDa	
graft copolymer	87.3	201	2.3
homopolymer	8.3	10	1.2

9. Appendix

9.1. Graft copolymerization of cellulose macro-CTA ("MCC-CPPA16-Pr") with DMAA

As explained in the following section, graft copolymerizations using DMAA and cellulose macro-CTA were performed. After the analysis of the graft copolymers the author decided to use styrene as model monomer instead of DMAA, as presented in chapter 4.1.

Model experiment: polymerization of DMAA with free CPPA

Prior to the graft copolymerization, the reaction conditions were investigated with a model polymerization of free RAFT agent CPPA with monomer DMAA, as schematically shown in **Figure 113**.

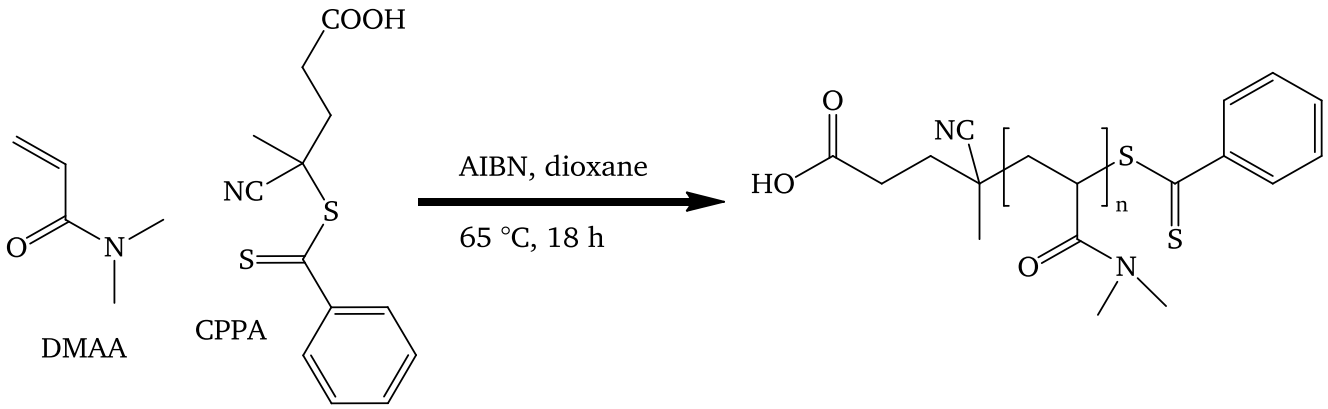

Figure 113. Reaction conditions for the RAFT polymerization of DMAA.

The reaction was performed in anhydrous dioxane at 65 °C for 18 hours. After the reaction, the polymer was purified by precipitation in Et_2O. Analysis with SEC revealed a $M_n = 1.4*10^3$ and a Đ of 1.1, which indicates a good control over the polymerization process. Since the model experiment was successful, further experiments for the synthesis of graft copolymers were performed under identical reaction conditions (concentration of reactants, temperature).

Synthesis of cellulose-PDMAA graft copolymers

RAFT polymerization of DMAA using CPPA as CTA was performed successfully, thus graft copolymerization of cellulose macro-CTA with PDMAA was performed by the addition of one molar equivalent of CPPA-groups immobilized on cellulose macro-CTA, as presented in **Figure 114**.

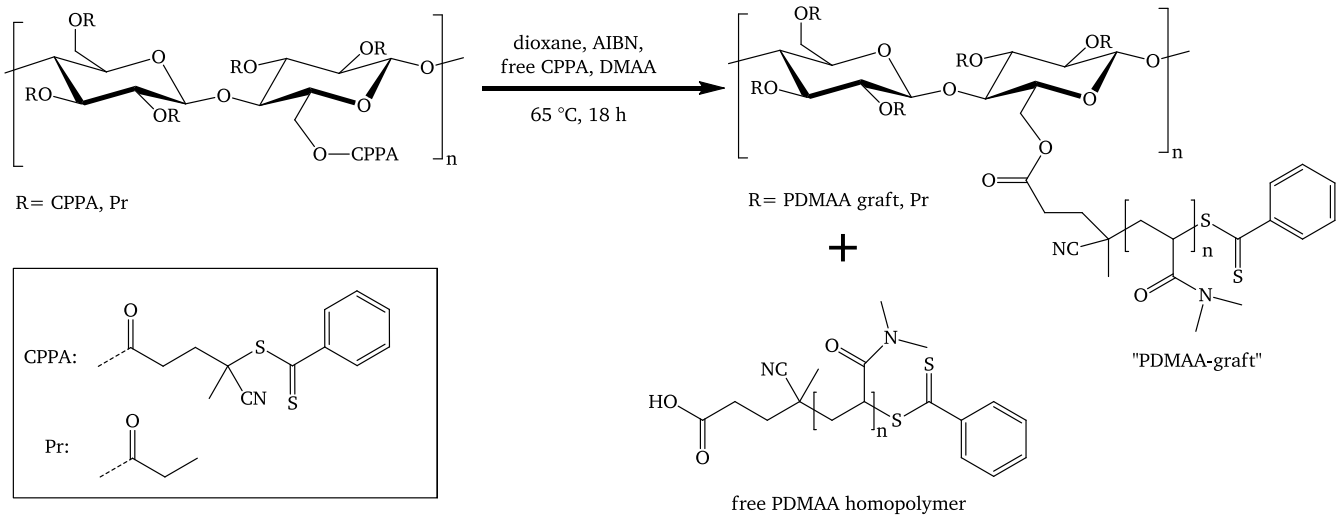

Figure 114. Reaction conditions for the graft copolymerization using cellulose macro-CTA, free CTA and DMAA monomer. Note: The CPPA functionality displayed in the scheme is on located at the 6-O position for illustration purpose; in reality only a statistically distribution is obtained.

After a reaction time of 18 hours, the reaction was stopped by cooling. Then, the polymer mixture containing graft copolymer and homopolymer were isolated by precipitation in diethyl ether. Both polymer species could be well separated by partial dissolution of the crude product in methanol, where PDMAA homopolymer was soluble and graft copolymer remained insoluble. The cellulose graft copolymer was analyzed by ^{1}H-NMR (**Figure 115**). This allowed the determination of the amount of PDMAA attached to the cellulose backbone and therefore the average DP of the PDMAA grafts was estimated.

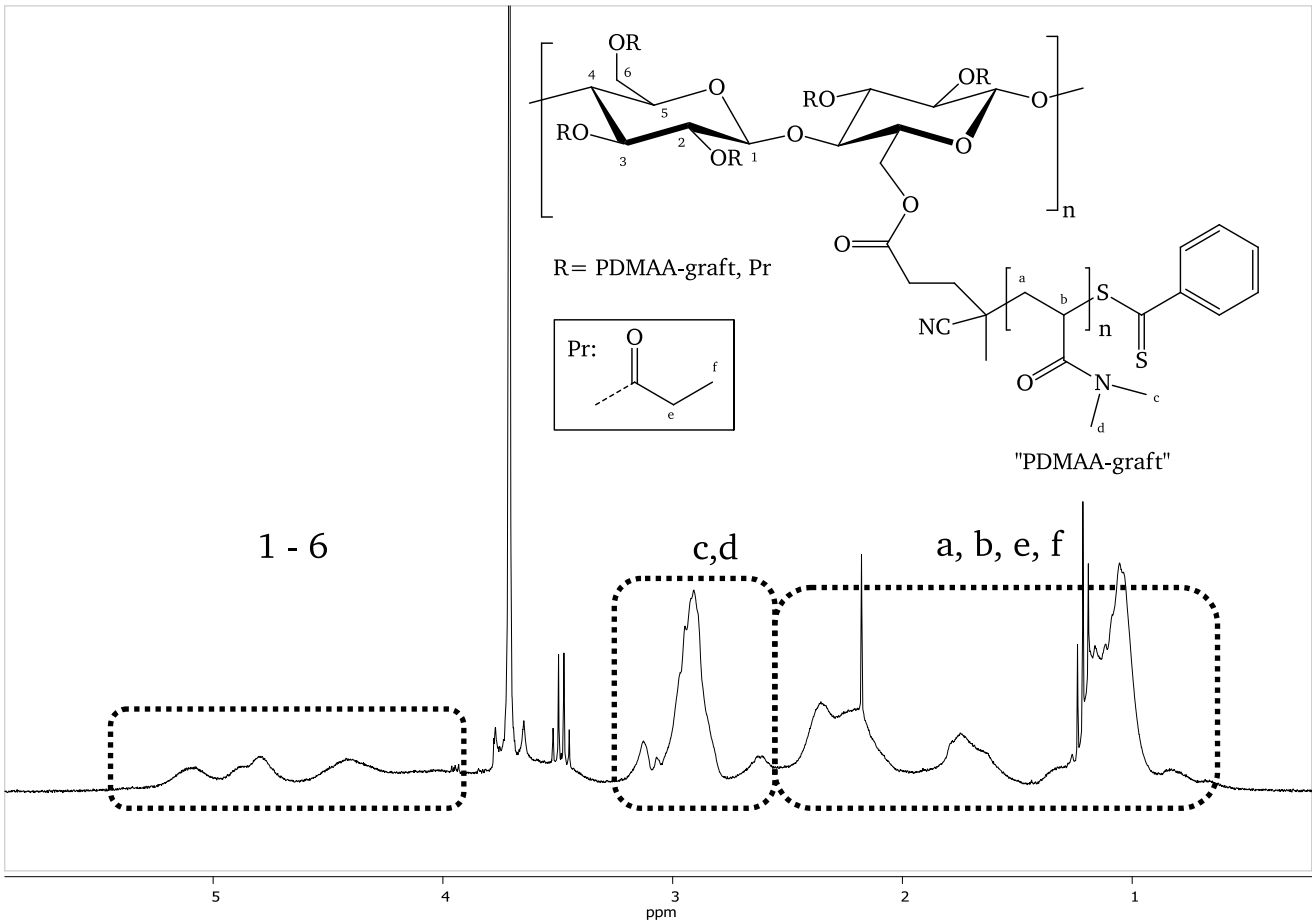

Figure 115. ^{1}H-NMR spectrum of the isolated cellulose graft copolymer (experiment "MCC-CTA16-Pr-PDMAA_1").

The polymer/cellulose-ratio of the product was estimated by the relative integral intensities of the proton signals. The signal of the cellulose backbone between 3.5-5.5 ppm corresponds to 7 protons, whereas the PDMAA CH_3-proton signal at 3.0 ppm corresponds to 6 protons. It should be noted, that the protons from the cellulose backbone appear as a very broad signal and additional overlapping signals from remaining impurities are visible. Hence, the ratio of polymer grafts can only be considered a rough estimation. The ratio was estimated at 1.2 DMAA units per each AGU. Since the DS(CTA) was 0.3, each PDMAA chain has 4 units (DP = 4). The data was compared to the theoretical values. With a applied ratio [DMAA]/[CTA] = 50:1 and a monomer conversion of 40 % the PDMAA chains should have a DP of about 20. Therefore the calculated DP deviates significantly from the experimental DP, indicating limitations in the polymerization process. The results were further validated by SEC analysis with THF as eluent (**Figure 116**). The elugram reveals two different molar mass distributions for homopolymer and graft copolymer. The molar mass distribution was then determined by calibration against polystyrene standards and THF as eluent. The graft copolymer showed a molar mass increase from originally 52 kDa for the cellulose macro-CTA to 80 kDa due to the increased apparent hydrodynamic radius from the polymer grafts. However, the number average molar mass of the linear homopolymer was determined as 1.67 kDa, having a signal maximum at 6 kDa and broad distribution

with a low molecular mass shoulder. This was also considered as an indication for a non-trivial control of the polymerization process. In order to exclude experimental errors, the graft copolymerization was repeated under the same conditions with fresh dried solvent; however the outcome of this repetition resulted in the same experimental observations.

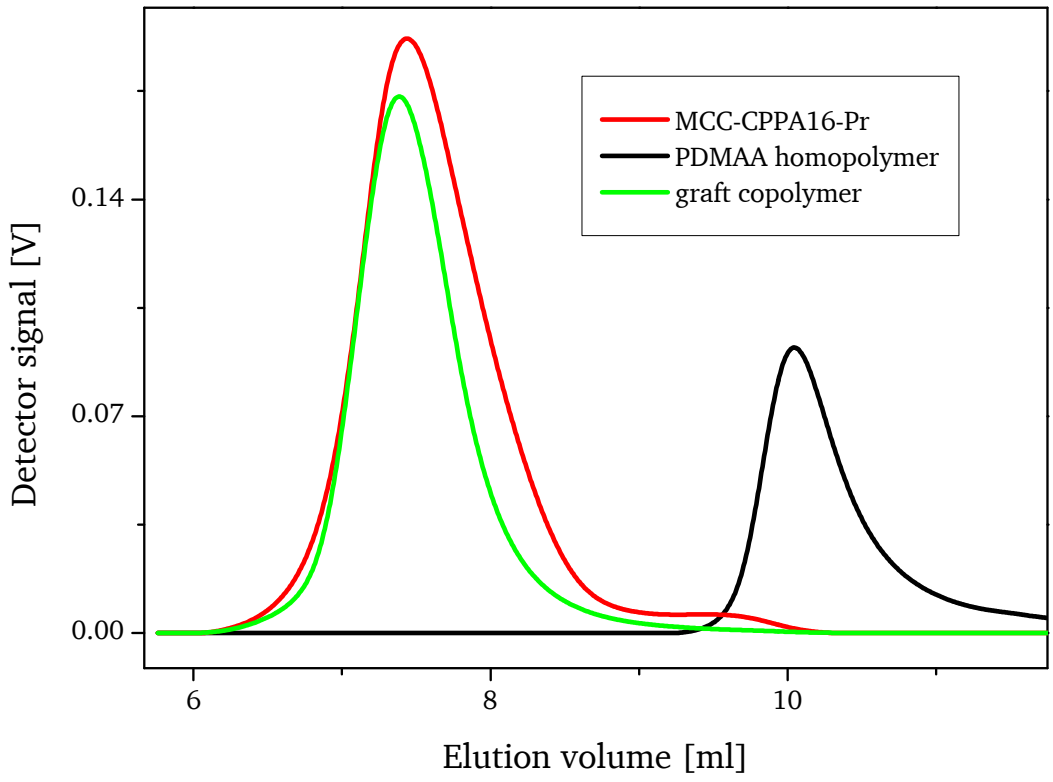

Figure 116. SEC traces of cellulose macro-CTA (MCC-CPPA16-Pr), isolated cellulose graft copolymer and isolated linear homopolymer, measured in THF as eluent. The small shift of graft copolymer towards smaller elution volumes may be considered an indication for successful polymer grafting on cellulose macro-CTA.

Although control of the molar mass of attached PDMAA was limited, these first experiments were a successful proof of concept for the copolymerization of cellulose macro-CTAs with monomer, since the cellulose macro-CTA showed an increase in the apparent molar mass and ^{1}H-NMR analysis revealed the relative amount of PDMAA attached to the cellulose backbone. However, due to some significant deviation of the experimental data from the theoretical values, further investigations needed to be performed. The decision was made to change the model monomer from DMAA to styrene, because styrene was considered an ideal candidate for analysis due to commercially available poly styrene standards for SEC analysis. Furthermore the author aimed for the optimization of the reaction conditions towards larger polymer grafts, allowing the synthesis of graft copolymers with high graft ratios.

9.2. Theoretical considerations of the molecular structure of the cellulose graft copolymers

When discussing the polymeric architecture of the graft copolymers, which have been presented within this work, it comes to the debate if these structures can be defined as brush copolymer or comb polymer. For the following discussion of the definition we use the simplified model of tethered polymer chains attached on a substrate, as shown in **Figure 117**.

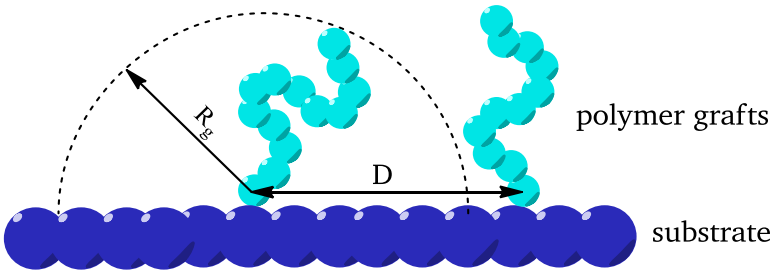

Figure 117. Schematic image of polymer chains tethered to a substrate. The average distance between to grafts is denoted as D, whereas R_g is defined as the radius of gyration.

A schematic image of "brush polymers" and "mushroom polymers" is displayed in **Figure 118**. If individual polymer grafts are too far away from each other, they are not capable of physical interactions. In this case, the polymers are in a "mushroom regime".

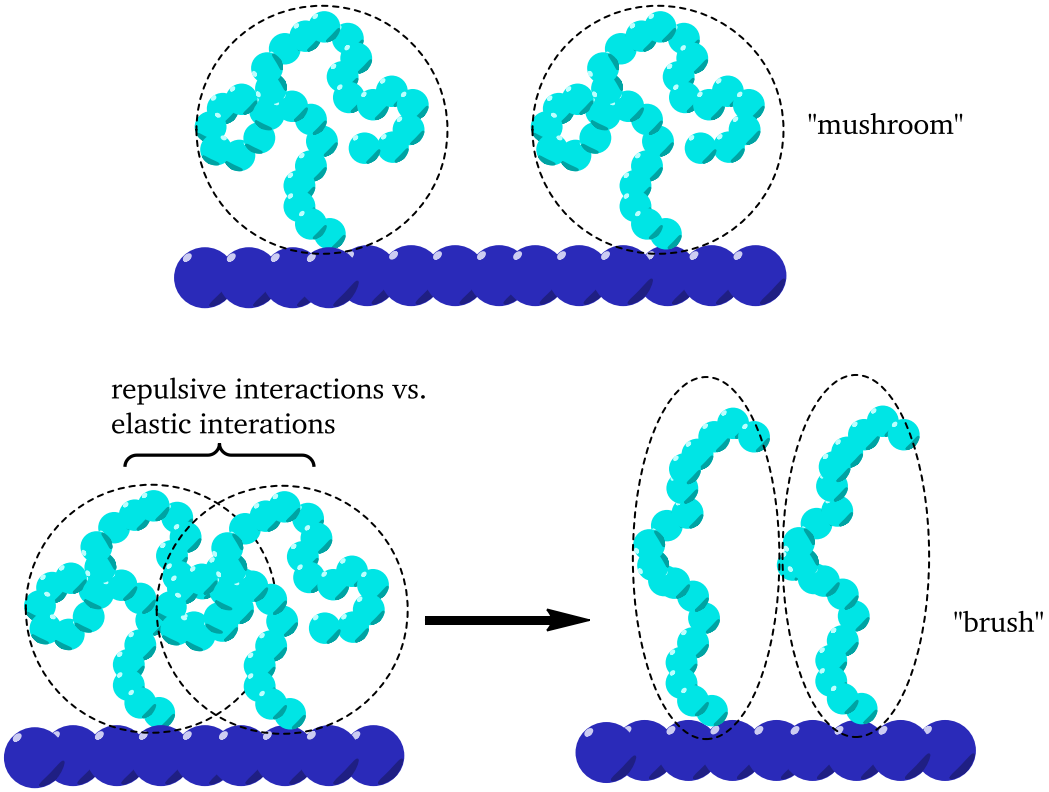

Figure 118. Schematic image of polymer grafts tethered onto a substrate. Top: the radius of gyration R_g is smaller than the distance between the two grafts. Bottom: R_g is higher than the distance of the two grafts, resulting in repulsive interactions which lead to the stretching of the polymer grafts.

The radius of gyration of a flexible polymer chain in a good solvent can be estimated by the following equation [93]:

$$R_g = a * \sqrt{N} \tag{37}$$

Where N is the number of segments and a is the size of each segment.

The structure of polymer grafts on a substrate can be defined by the average distance between the attachments points, or alternatively, by the grafting density σ:

$$\sigma = \frac{1}{D^2} \tag{38}$$

According to Binder et al. [93], the transition of a polymer with a "mushroom" structure into a "brush" can be estimated by the following equation:

$$\sigma > \sigma^* \tag{39}$$

With the characteristic length σ^*:

$$\sigma^* = \left(a * \sqrt{N}\right)^{-2} \tag{40}$$

By combination of equation (38) and equation (40) in equation (39) it can be concluded that the polymeric architecture is a polymer brush if:

$$R_g > D \tag{41}$$

For the calculation of R_g and D, an average size of 0.25 nm for a monomer unit of styrene is assumed. Furthermore an average molar mass of 10 kDa is assumed, since all graft copolymers presented in this work had larger polymer chains, i.e. the calculation is valid for all graft copolymers in this work.

Estimation of R_g:

$$R_g = 0.25\ \text{nm} * \sqrt{100} = 2.5\ nm \tag{42}$$

The average distance D between two polymer grafts was estimated by the average distance between two CTA groups, which can be calculated by the DS(CTA) and the estimated size of a anhydroglucose repeating unit. The DS(CTA) of 0.54 for cellulose macro-CTA "MCC-CTA14" is provided in chapter

4.2.2. The size of an AGU of about 0.5 nm was estimated by the dimension of crystal structure of cellulose II, as provided by Klemm et al. [28]

$$D = \frac{1}{DS(CTA)} * a\ (AGU) = \frac{1}{0.54} * 0.5\ nm\ \approx 1\ nm \tag{43}$$

Comparison of R_g with D shows, that the radius of gyration of an individual polymer graft is higher than the average distance between two grafting points. From this calculation we assume that the polymer grafts overlap, leading to repulsion and stretching of polymer grafts away from the cellulose backbone.

Since we used a low average molar mass of 10 kDa for the calculation, we can consider all graft copolymers which have been presented in this work can be considered as polymer brushes. As a consequence of having polymer brush architecture, the cellulose graft copolymers may be interesting candidates for future structural investigations. For example, these structures might exhibit a "worm-like" structure when analyzed with AFM, as it has already been shown for fully synthetic graft copolymers [94].

9.3. Synthesis of regioselective-modified mixed graft copolymers

Regioselective synthesis of 2,3-*O* substituted cellulose has been reported by Kondo and Gray [95]. A general description of the process is shown in **Figure 119**.

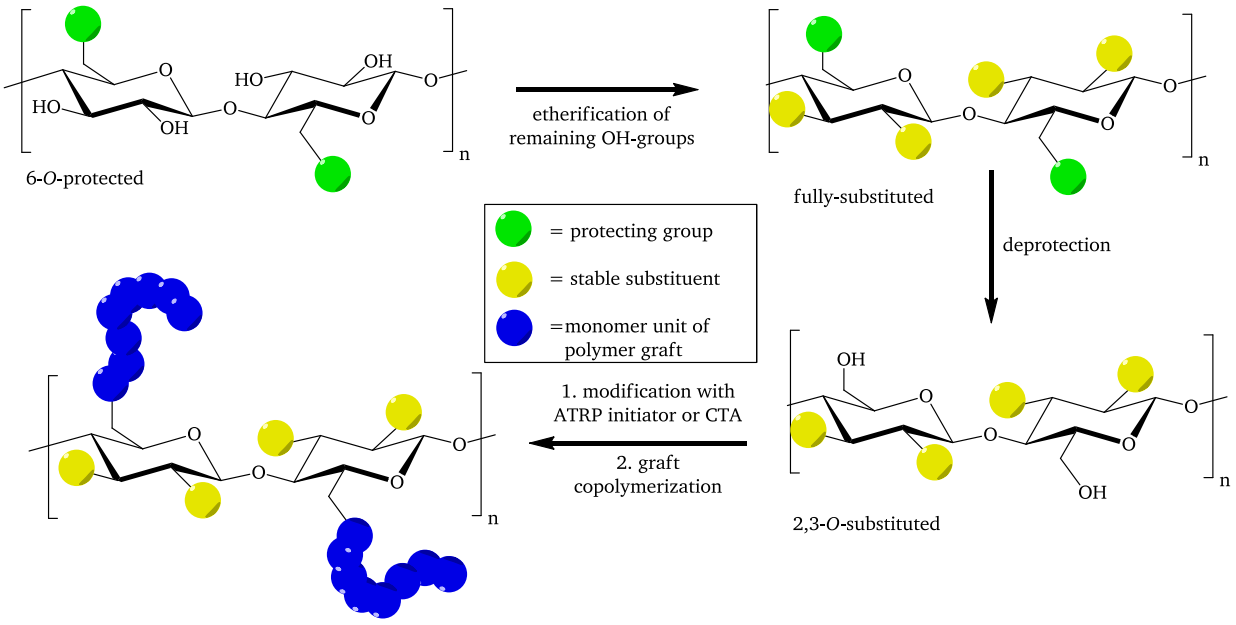

Figure 119. Procedure of 6-*O* regioselective protecting group chemistry on cellulose, allowing the synthesis of regioselective modified cellulose mixed graft copolymers.

This particular substitution pattern can be obtained by first blocking the 6-*O* position with a trityl moiety. The 6-*O*-tritylcellulose is soluble in organic solvents, thus homogenous reaction conditions can be applied. In a subsequent step, remaining hydroxyl moieties on the cellulose are to be modified, to yield a fully substituted cellulose derivative. The protecting groups are then removed and the released hydroxyl groups are then further processed. Note: substitution of the 2,3-*O* positions is typically performed as etherification because the subsequent deprotection step requires strong acidic conditions, which are incompatible with ester functionalities.

Synthesis of 6-*O*-(triphenylmethyl) cellulose by regioselective protection of the 6-*O* position with trityl chloride

In a first step we followed the regioselective modification of the 6-*O* position of the anhydroglucose repeating units by use of trityl chloride is well described in literature [96]. The synthesis procedure was further optimized Fenn et al. [55], and the reaction conditions are displayed in **Figure 120**.

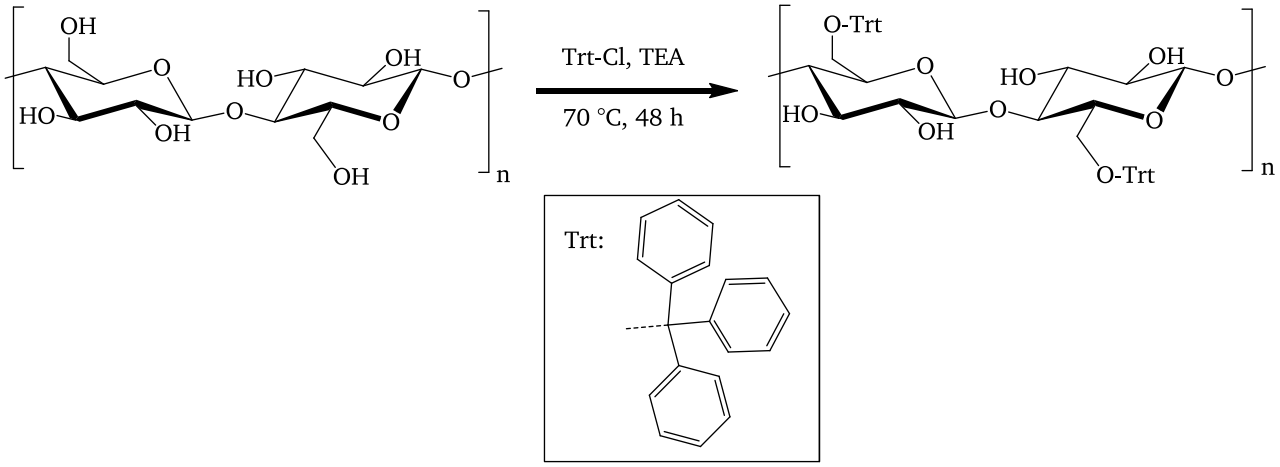

Figure 120. Reaction scheme with the typical reaction condition applied for the synthesis of regioselective protected trityl cellulose.

For the synthesis trityl chloride and triethyl amine were added to a solution of cellulose in DMAc/LiCl in two portions; the first half in the beginning of the reaction time and the second half after 24 hours. After a total reaction time of 48 hours at 70 °C, the product was isolated by precipitation in methanol, followed by washing with methanol and drying of the polymer under vacuum. The product was found to be well soluble in DMF, DMSO and THF, which allowed further synthesis to be conducted in homogenous reaction conditions. Characterization with ^{1}H-NMR resulted in a spectrum with broad signals; therefore a small fraction of material was further processed by propionylation to yield a well-resolved ^{1}H-NMR, as shown in **Figure 121**. The DS(Trt) = 1 was calculated, indicating a complete protection of the 6-OH groups.

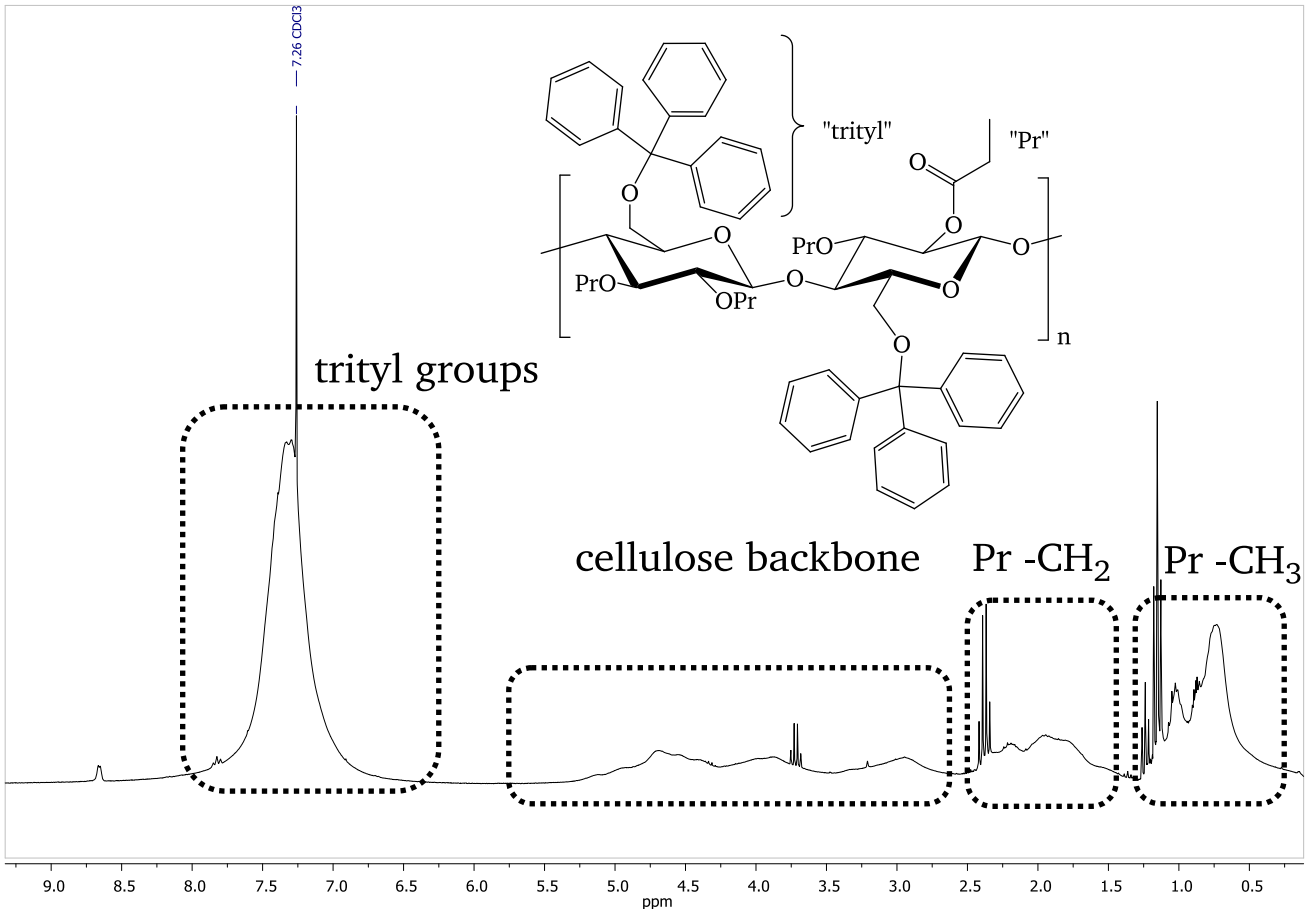

Figure 121. Exemplary spectrum of propionylated trityl cellulose, dissolved in $CDCl_3$. Note, the sharp signals at about 1.2, 2.4 and 3.7 ppm originate from remaining traces of solvents, which could not be completely removed. However, the DS values for trityl moieties could be determined by the relative integral signal intensities of the cellulose backbone (2.5 ppm to about 5.0 ppm) and aromatic trityl protons at about 7.3 ppm.

Synthesis of 6-*O*-(triphenylmethyl)-2,3-*O*-(poly(ethylene glycol) monomethyl ether) cellulose by etherification with poly(ethylene glycol) monomethyl ether iodide using sodium hydride and tetrabutyl ammonium iodide

After attachment of the trityl group to the hydroxyl group at the C-6 position of the cellulose polymer, in a second step the C-2 and C-3 OH groups were to be modified. For this, first approaches were performed under reaction conditions described by Cowie et al. [97]. According to the synthetic protocol, the reaction mixture is stirred for 4 days at room temperature, leading to highly substituted products. In contrast our first tests at room temperature showed very low DS values for PEG. It was assumed, that higher reaction temperatures were needed. Further experiments were thus made under reflux (66 °C) in THF for 24 hours.

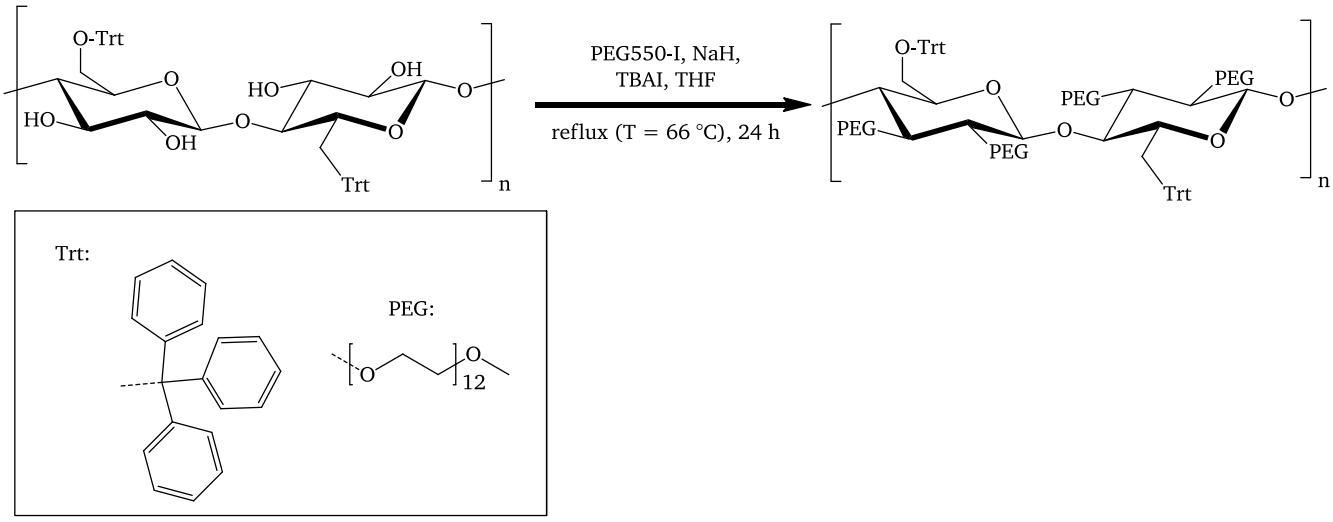

Figure 122. Reaction scheme for the etherification of trityl cellulose with asymmetric poly(ethylene glycol) monomethyl ether iodide.

After the reaction, the pegylated cellulose was isolated by precipitation of the reaction mixture into methanol. However purification was not trivial because the product formed stable suspensions in methanol, which only could be separated by use of high-speed centrifugation. Then all solvent was removed by evaporation at high vacuum, leading to a sticky, brown substance. Using analysis with ^{1}H-NMR, we could determine a DS(PEG) of about 1.2. This means that not all OH-groups at position C-2/C-3 had been modified accordingly. The reaction was therefore repeated with higher molar ratios of PEG iodide and longer reaction time; however it was not possible to gain higher DS values this way. Since a (almost) complete DS(PEG) of about 2 was desired, other reaction conditions for the pegylation of cellulose were to be evaluated and are described in the following subsection.

Synthesis of 6-*O*-(triphenylmethyl)-2,3-*O*-(poly(ethylene glycol) monomethyl ether) cellulose by etherification with poly(ethylene glycol) monomethyl ether iodide using sodium hydroxide

In order to increase the amount of PEG groups on cellulose, we next followed a synthesis protocol from Kadla et al. [92]. For this, NaOH as base was suspended in a solution of tritylated cellulose in water free DMSO, as shown in **Figure 123**.

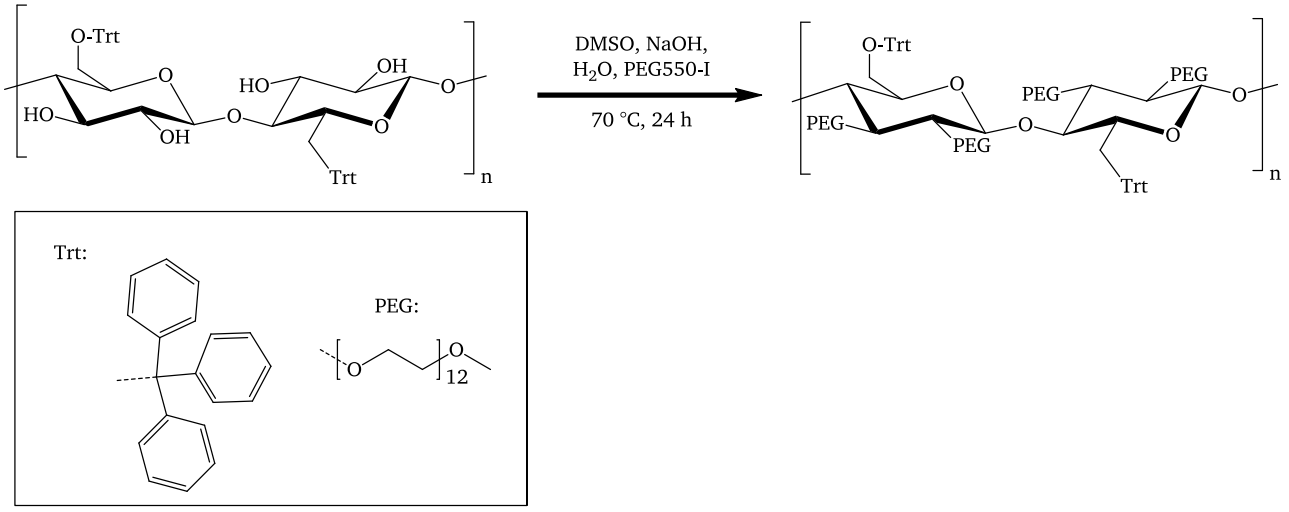

Figure 123. Reaction conditions for the PEGylation of cellulose, according to Kadla et al [92].

After reaction for 24 hours at 70 °C and precipitation of the product in diethyl ether, a sticky brown solid was obtained. DS value of PEG was estimated by ^{1}H-NMR to be about 0.4. It was suggested by Andreas Koschella (working group of Prof. Thomas Heinze, University of Jena) [98], that traces of water should dissolve the suspended NaOH partially, leading to strong basic reaction conditions, which facilitates the etherification process. We followed this procedure; the resulting pegylated cellulose derivative was purified by precipitation in diethyl ether and re-precipitation from THF into diethyl ether. The isolated product was then characterized by ^{1}H-NMR (**Figure 124**). For the quantification of the relative amount of PEG groups attached to the cellulose backbone we used the relative integral signal intensity of the trityl protons (DS(Trt) = 1.15 H per trityl group) and the PEG protons (48 H per PEG substituent). Using the modified method, presented here, DS(PEG) values up to 2.0 were obtained.

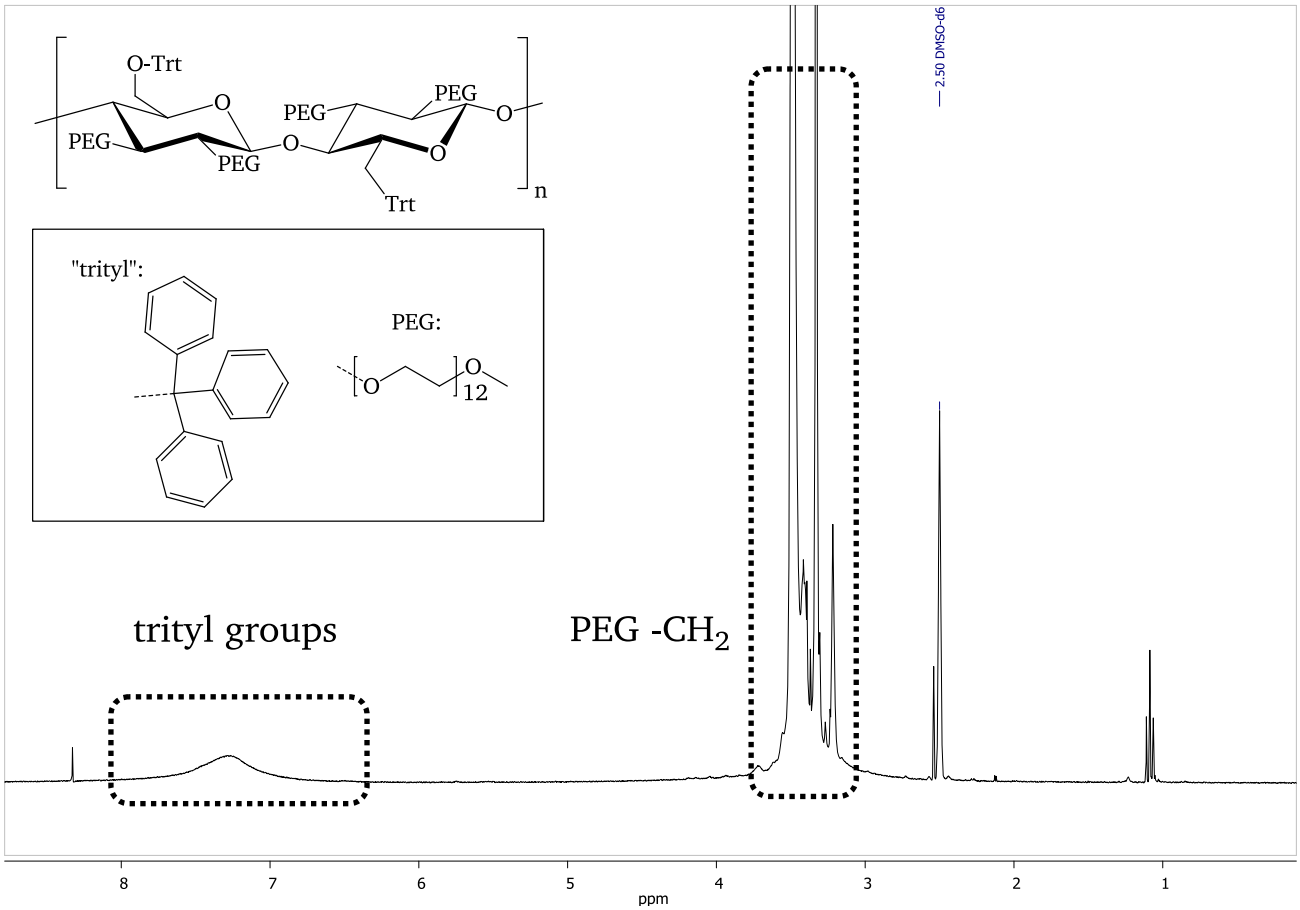

Figure 124. Typical example of a ^{1}H-NMR spectrum (in d_6-DMSO) of pegylated trityl cellulose. The proton signals at 7.3 originate from the trityl moieties whereas the protons of the PEG groups at 3.7 ppm clearly overlap with the cellulose backbone protons.

Synthesis of 2,3-*O*-(poly(ethylene glycol) monomethyl ether) cellulose

After substitution of the 2,3-OH functionalities of the cellulose with PEG, the trityl protection groups had to be removed. Several attempts of deprotection were based on protocols from literature with concentrated hydrochloric acid [99] or with trifloro acetic acid/ tetra ethyl silane [100]. However, none of these methods resulted in quantitative removal of the trityl moieties as inferred from ^{1}H-NMR. Finally we followed a procedure (displayed in **Figure 125**) that was suggested by Andreas Koschella, University of Jena [98].

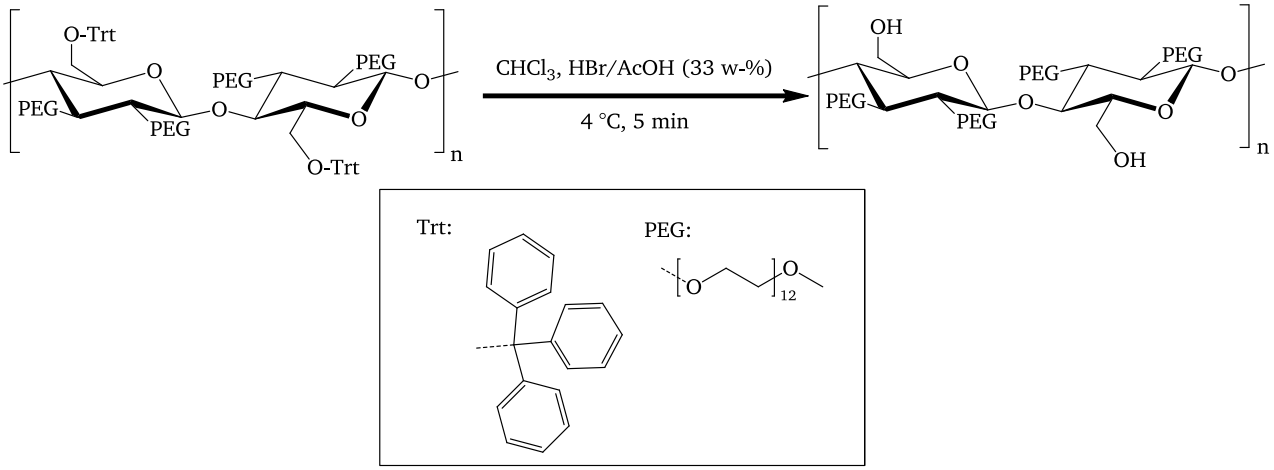

Figure 125. Deprotection of the 6-OH group by detritylation under strong acidic reaction conditions.

In brief, the tritylated cellulose was dissolved in $CHCl_3$, cooled to about 4 °C and HBr in acetic acid was added. When adding the acid to the solution, the reaction mixture turned to a milky color, indicating precipitation of the cellulose material. The product was then purified by washing with diethyl ether. Complete removal of the trityl moieties could be verified by ^{1}H-NMR, where no aromatic protons could be detected after removal of the trityl groups (**Figure 126**). Additional analysis with ATR-IR spectroscopy validated the complete removal of trityl moieties.

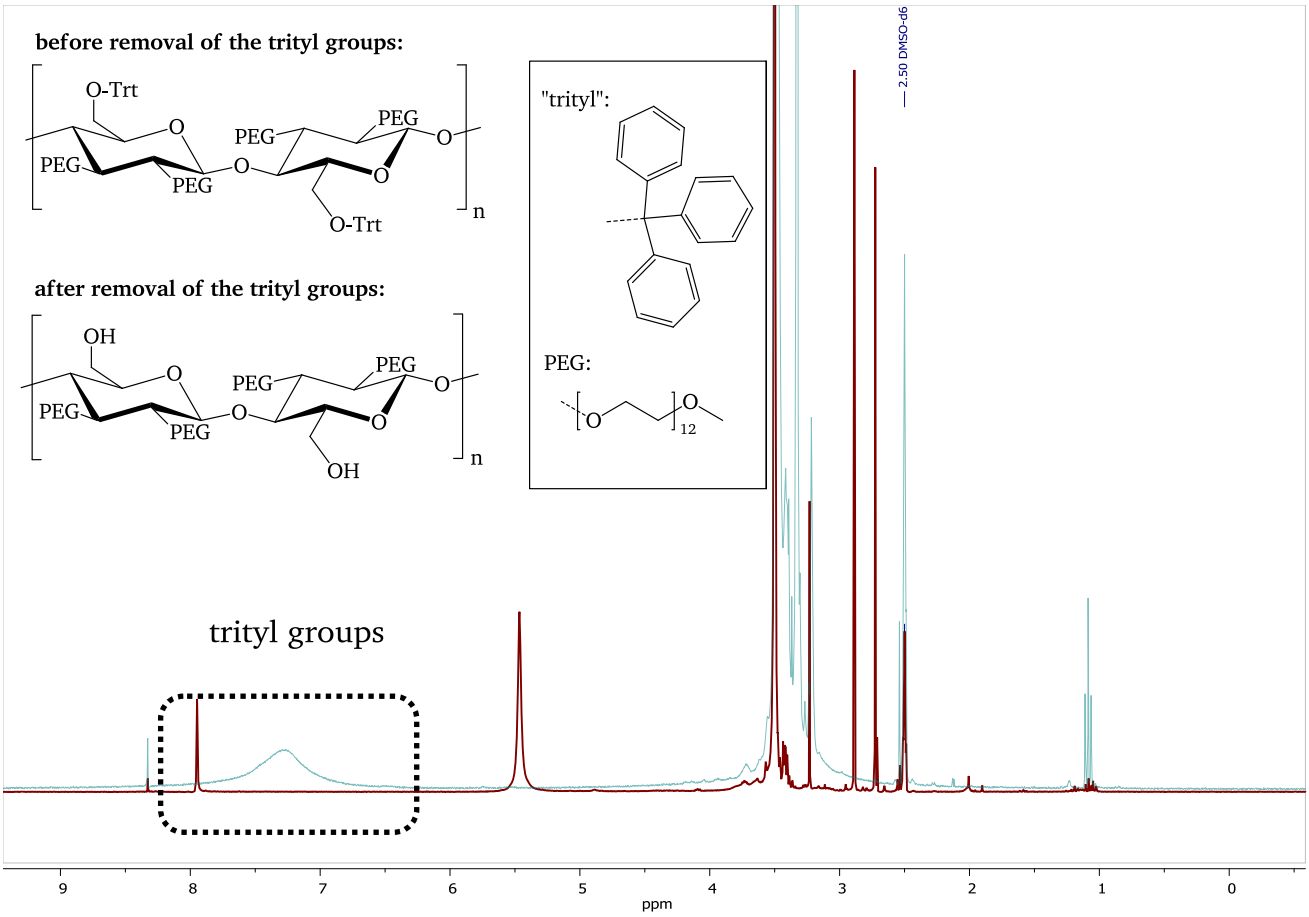

Figure 126. ^{1}H-NMR spectrum of tritylated PEG-cellulose before and after deprotection of the trityl groups with HBr/AcOH. Proton signals at 7-8 ppm originate from the trityl group. No remaining signal after deprotection proves successful removal of the trityl moieties.

Synthesis of 6-*O*-(2-bromopropionyl)-2,3-(poly(ethylene glycol) monomethyl ether) cellulose by esterification with 2-bromopropionyl bromide

After successful pegylation of the C-2/C-3 OH-groups, esterification of the remaining hydroxyl groups of the cellulose C-6 position with 2-bromopropoinyl moieties was performed using 2-bromopropionic acid anhydride (**Figure 127**). The anhydride was generated in-situ by addition of 2-bromopropionyl bromide to small excess of 2-bromo propionic acid and then the reaction was performed at a temperature of 60 °C.

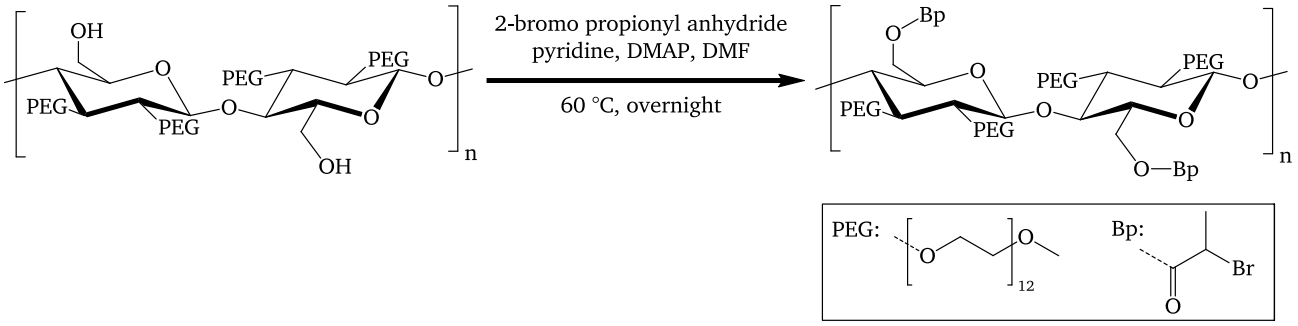

Figure 127. Modification of 2,3-*O*-pegylated cellulose with 2-bromopropionyl ester groups.

After reaction overnight the product was isolated and analyzed with ^{1}H-NMR (**Figure 128**). The signal at about 3.7 ppm originates from the PEG-protons whereas the signal at about 1.8 ppm originates from the 2-bromopropionyl protons. We then determined the relative integral signal intensities of the 2-bromopropionyl protons and poly(ethylene glycol) protons. The corresponding DS values were estimated from these integers to be about DS(PEG) = 1.7±0.3 and DS(Bp) = 1.3±0.3, assuming a DS(total) of about 3. However these DS values should be considered a rough estimation since the PEG protons clearly dominate the spectrum and thus errors in the estimation are high. Nevertheless, a functionalized group useful to initiate an ATRP reaction or if further modified a RAFT reaction, could be successfully isolated.

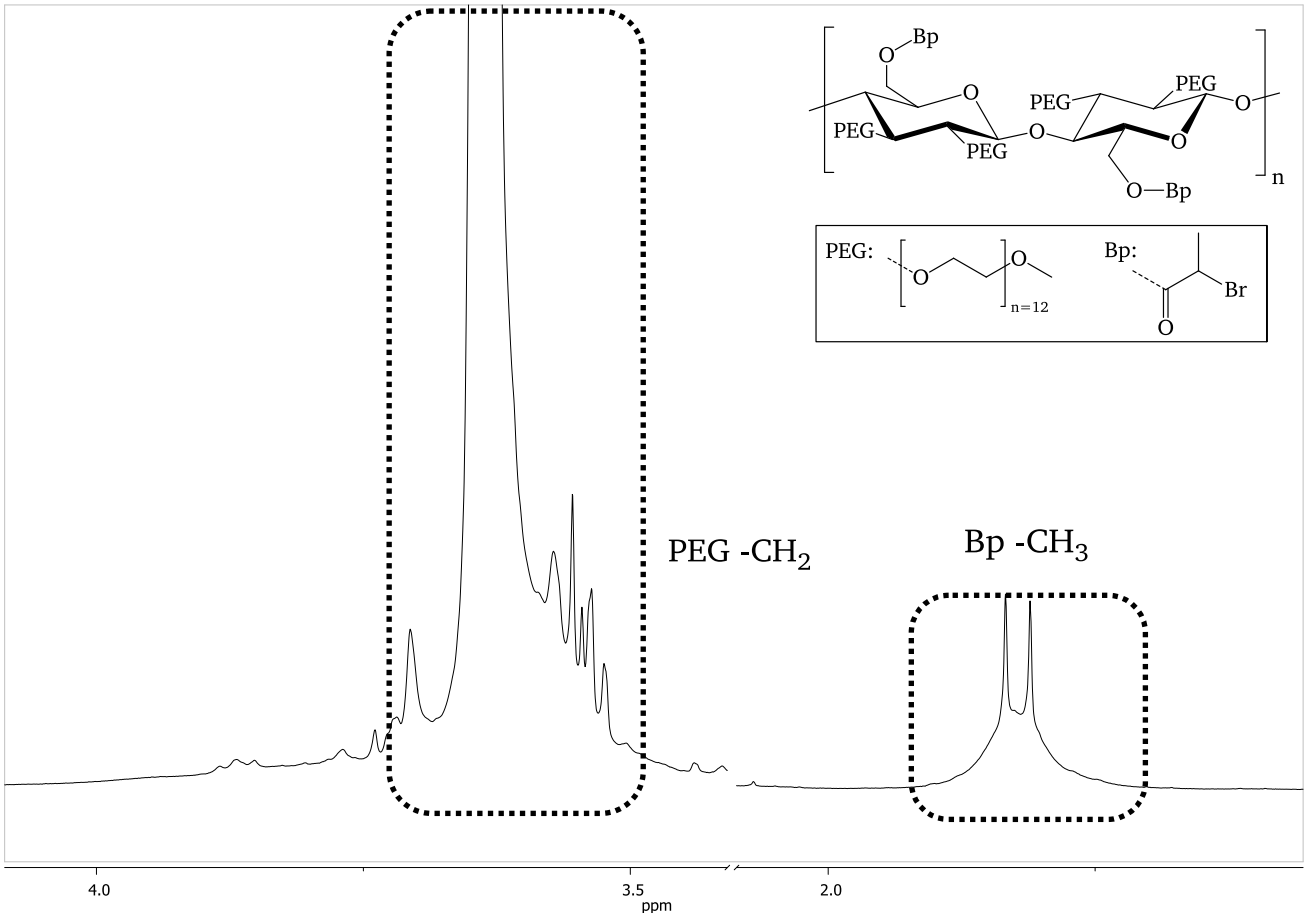

Figure 128. [1]H-NMR spectrum of a cellulose derivative containing poly(ethylene glycol) and 2-bromo propionyl moieties. Every PEG group contains 51 protons; therefore the PEG signal clearly dominates the spectrum, leading to small signals for the 2-bromopropionyl moieties.

Synthesis of pegylated cellulose macro-CTA

In the next step, the pegylated and C-6 functionalized cellulose was converted into the corresponding macro-CTA. The reaction conditions were adapted from O'Reilly et al. [83] and are displayed in **Figure 129**.

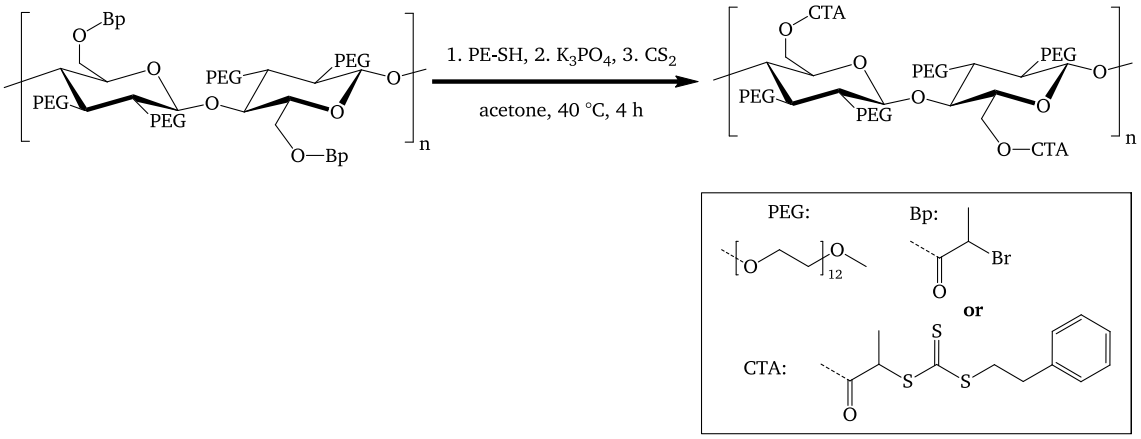

Figure 129. Partial transformation of 2-bromine functionalities into CTA groups.

As can be inferred from **Figure 130**, the 2-bromo propionyl moieties were to be transformed into trithiocarbonates. For this phenyl ethyl mercaptane (PE-SH) was mixed with carbon disulfide under alkaline conditions using K_3PO_4 as base. The progress of the formation of trithio carboxylate intermediate could be followed by the naked eye, since the initially clear solution turns to an intensive yellow color. Then, a solution of the cellulose derivative in dry acetone was added, the reaction continued for four hours at 40 °C. The solid K_3PO_4 was removed by centrifugation; the cellulose was purified by precipitation in diethyl ether with subsequent reprecipitation from acetone into diethyl ether. The DS(CTA) was determined by analysis of the polymer with ^{1}H-NMR (**Figure 130**). By comparison of the aromatic protons from the CTA with the PEG protons a DS(CTA) = 1.4±0.3 was calculated, which is within the experimental error in the order of the initial DS value of the Bp-functionalities on cellulose (DS(Bp) = 1.3), indicating a complete transformation of the bromine functionalities into the corresponding CTA.

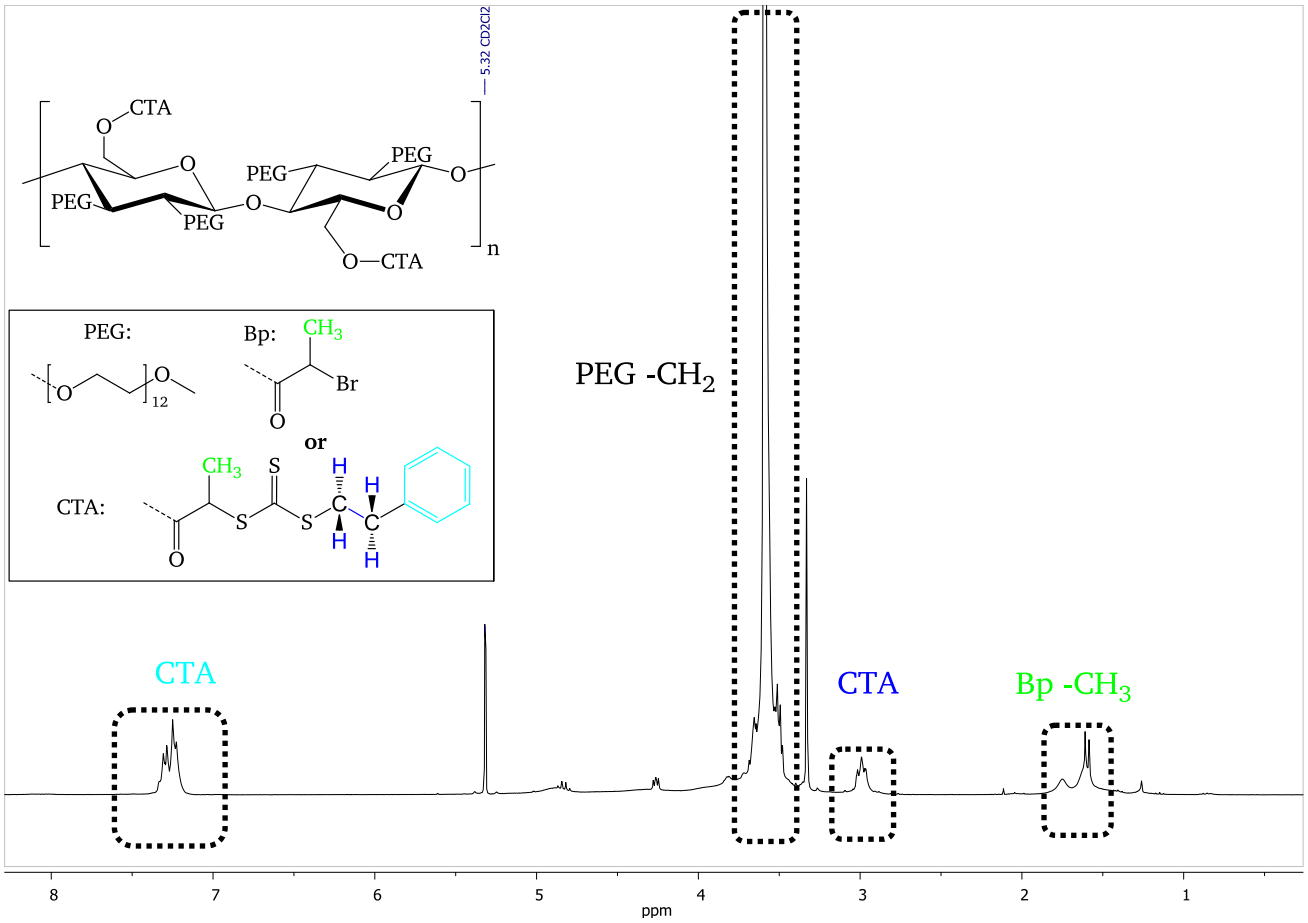

Figure 130. ^{1}H-NMR spectrum of a cellulose derivative containing poly(ethylene glycol) as well as CTA functionalities. The proton signal of the PEG substituents at 3.7 ppm and the aromatic protons from the CTA at 7.3 ppm can clearly be seen, indication successful transformation of 2-bromopropionyl moieties into CTA groups.

Synthesis of cellulose mixed graft copolymers

It was next attempted to generate cellulose mixed graft copolymers by RAFT polymerization of the pegylated cellulose macro CTA with styrene as model monomer, as shown in **Figure 131**. After the reaction the polymer was precipitated into methanol. Graft copolymer and homopolymer were separated by fractional precipitation with THF and diethyl ether.

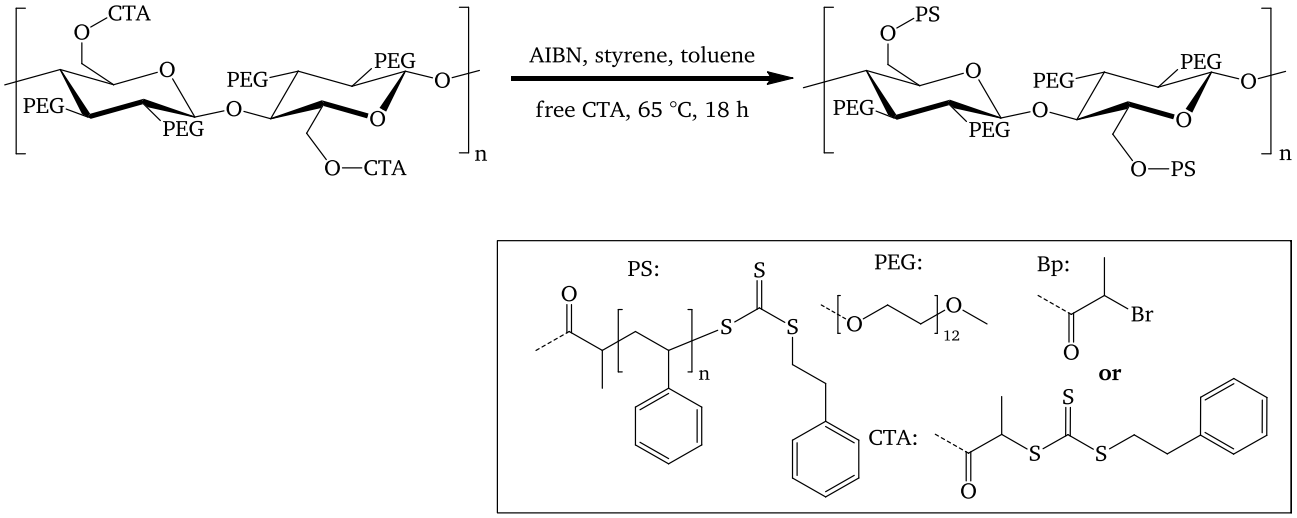

Figure 131. Synthesis of cellulose mixed graft copolymer having poly(ethylene glycol) grafts and polystyrene grafts.

Polymer samples of the crude product, graft copolymer linear homopolymer were analyzed with SEC; the results are displayed in **Figure 132**. A bimodal distribution with two distinct signals (one for the homopolymer and one for the graft copolymer) was expected. But instead an almost monomodal signal with a shoulder at low elution volumes was observed. Further analysis of the separated homopolymer and graft copolymer indicated that the shoulder in the signal originates from the graft copolymer.

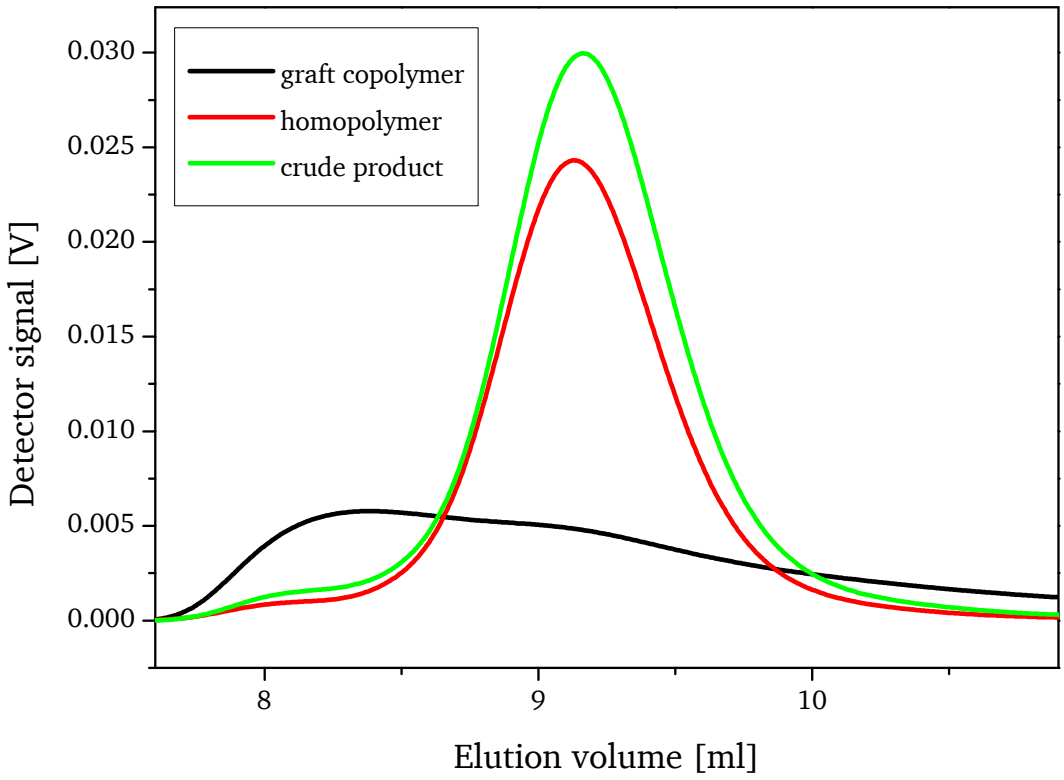

Figure 132. SEC traces of product fractions from experiment MCC-PEG550-CTA1-PS_1 in THF eluent. The analysis of the crude product (green) only shows the homopolymer signal with a small shoulder at low elution volumes. Homopolymer (red) and graft copolymer (black) were separated by fractional precipitation. The homopolymer shows similar signal shape like the crude product, the graft copolymer shows a very broad distribution with a signal maximum at low elution volumes.

The experiment was repeated in order to exclude experimental errors, but showed the same results (MCC-PEG550-CTA1-PS_2). We investigated origin of this phenomenon. This included the analysis of all cellulose precursors with SEC, as shown in **Figure 133**. The largest decrease in the apparent molar mass occurred during the pegylation step. Although these obtained molar masses are not absolute values due to the different chemical nature in comparison of the polystyrene standards, these results may be considered as indication for a significant degradation of the cellulose backbone under the strong alkaline reaction conditions during etherification.

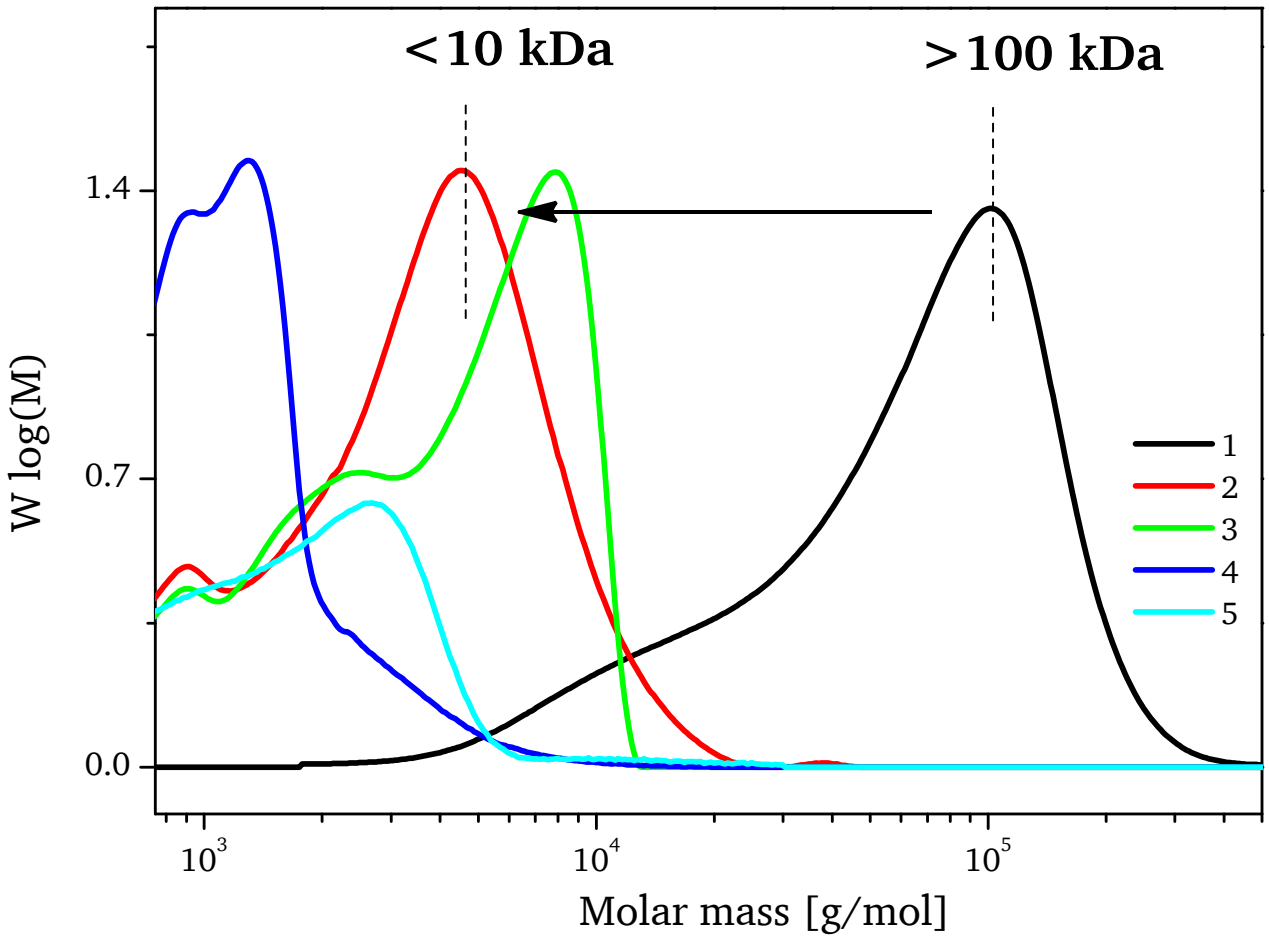

Figure 133. SEC analysis (THF/ PS standards) of all cellulose intermediate products. Cellulose after tritylation (1), after pegylation (2), after detritylation (3), after 2-bromopropionylation (4), after conversion into CTA (5). The pegylation of the cellulose has the largest relative impact on the apparent molar mass. The curve maximum is reduced from >100 kDa to <10 kDa.

Conclusion:

The attachment of PEG onto the cellulose backbone via etherification and strong alkaline reaction conditions has a significant effect on the depolymerization of the cellulose backbone. Here it is pointed out, that these results are in contrast to prior publications regarding pegylated celluloses, where degradation effects are not mentioned or neglected [92, 95, 97]. However, publications concerning methylation of cellulose clearly show depolymerization due to hydrolysis [101]. Degradation may be circumvented by use of mild reaction conditions such as the activation of carboxyl-functionalized PEG derivatives with CDI. However this procedure requires different methods and carboxyl-functionalized polyethylene glycol, as presented in chapter 0.

9.4. Synthesis of cellulose mixed grafts via ATRP

The graft copolymerization was performed via an ATRP reaction with MMA as monomer and DMSO as solvent. Starting with about 140 mg of pegylated cellulose macro-initiator (carrying 45 μmol of bromine functionalities), 460 mg of graft copolymer was obtained. The reaction scheme is shown in **Figure 134**.

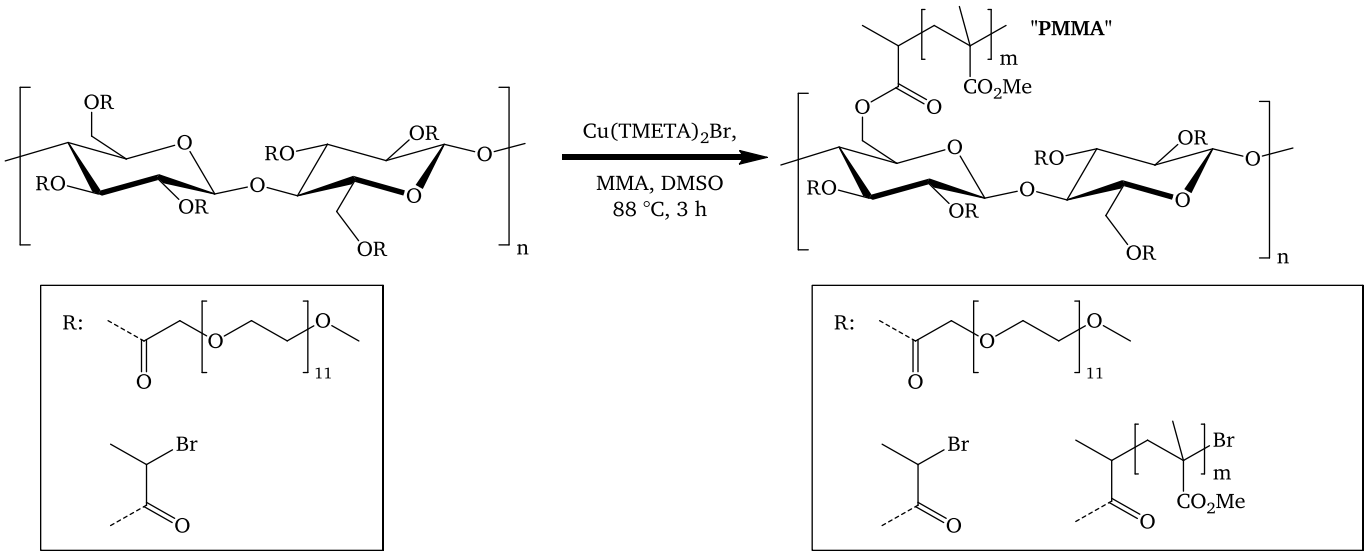

Figure 134. Reaction scheme of the ATRP mediated graft copolymerization, using pegylated macro-initiator and MMA as monomer.

Since no additional "free" initiator was added, we conclude that the polymerization took only place on the cellulose macro-initiator, leading to a graft ratio of about 230 %. The initiation efficiency is estimated by the amount of initiating groups multiplied with the average molar mass of each individual graft. For this, the polymer grafts were cleaved by hydrolysis and analyzed by SEC in DMF/LiCl as eluent. Note: When preparing the polymer sample for GPC, we realized some insoluble residues which clogged the syringe filter, thus we like to point out, to evaluate this result carefully. When comparing the polymer grafts with linear PMMA standards, we obtain PMMA polymer grafts with a $M_n \approx 30$ kDa (see **Figure 135)**. Having 45 μmol initiator groups should lead ideally to the same amount of polymer grafts. Having a M_n of about 30,000 g/mol, the total mass of the polymer grafts would be 1.35 g, compared to the graft mass of 320 mg. From this ratio, we can estimate a graft efficiency of about 24 %. Further validation of the grafting-process was done by SEC: cellulose macro-initiator and graft copolymer were analyzed via SEC in DMF/LiCl as eluent, as shown in **Figure 135.**

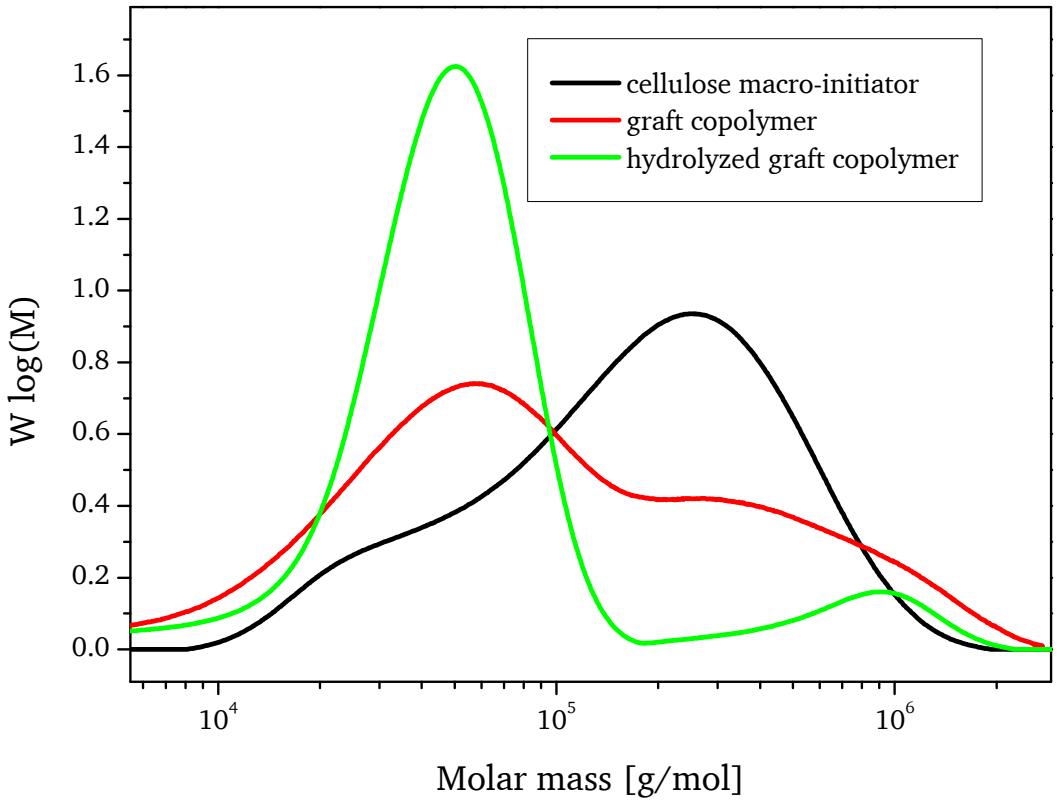

Figure 135. Molar mass distribution of cellulose precursor, cellulose mixed graft copolymer and polymer grafts, obtained by SEC in DMF/LiCl as eluent. Comparison of the molar mass distributions of pegylated cellulose macro-initiator (black line) and mixed graft copolymer (red line) indicate a decrease in the apparent molar mass.

Comparison of cellulose macro-initiator with the graft copolymer showed a bimodal distribution, showing a significant decrease in the apparent average molar mass. Thus PMMA grafting could not be confirmed by an increase in apparent average molar mass.

We conclude that in a first set of experiments successful grafting of PMMA from pegylated cellulose macro-initiator was conducted. To our best knowledge, there is no evidence that such a complex structure based on cellulose has been presented in literature before. A mass increase of the cellulosic product after the polymerization reaction was observed, which proves successful grafting. A graft efficiency of 24 % may be considered a good value to start; nonetheless the process should be rather considered a proof-of concept, leaving some potential for optimization. Also the analytic strategy using hydrolytic cleavage of the PMMA grafts followed by SEC analysis needs to be further improved. The alkaline cleavage process interfered with the ester groups of PMMA, thus the synthetic procedure could be improved by grafting of polymers with higher chemical stability such as polystyrene instead of PMMA. Furthermore alternative polymer analytics such as dynamic laser scattering or SEC-MALLS could give more reliable information about the graft copolymers

10. References

1. S. Thomas, D.D., C. Christophe, *Handbook of Biopolymer-Based Materials: From Blends and Composites to Gels and Complex Networks*. 2013: Wiley-VCH Verlag GmbH & Co. KGaA.
2. Kalia, S., *Cellulose Fibers: Bio- and Nano-Polymer Composites*. 2011: Springer-Verlag Berlin Heidelberg 2011.
3. D. Klemm, H.P.S., T. Heinze, *Biopolymers*. Vol. 6. 2002: Wiley VCH.
4. Dumas, J.-B., *Rapport sur un mémoire de M. Payen, relatif à la composition de la matière ligneuse.* Comptes rendus, 1839. **8**: p. 51-53.
5. Klemm, D., et al., *Cellulose: Fascinating Biopolymer and Sustainable Raw Material.* Angewandte Chemie International Edition, 2005. **44**(22): p. 3358-3393.
6. Luckachan, G.E. and C.K.S. Pillai, *Biodegradable Polymers- A Review on Recent Trends and Emerging Perspectives.* Journal of Polymers and the Environment, 2011. **19**(3): p. 637-676.
7. Bugnicourt, E., et al., *Polyhydroxyalkanoate (PHA): Review of synthesis, characteristics, processing and potential applications in packaging.* eXPRESS Polymer Letters, 2014. **8**: p. 791-808.
8. Lenz, R.W. and R.H. Marchessault, *Bacterial Polyesters: Biosynthesis, Biodegradable Plastics and Biotechnology.* Biomacromolecules, 2005. **6**(1): p. 1-8.
9. Jawaid, M. and H.P.S. Abdul Khalil, *Cellulosic/synthetic fibre reinforced polymer hybrid composites: A review.* Carbohydrate Polymers, 2011. **86**(1): p. 1-18.
10. Narayan, R., et al., *Cellulose Graft Copolymers for Potential Adhesive Applications*, in *Adhesives from Renewable Resources*. 1989, American Chemical Society. p. 337-354.
11. Siro, I. and D. Plackett, *Microfibrillated cellulose and new nanocomposite materials: a review.* Cellulose, 2010. **17**(3): p. 459-494.
12. Crini, G., *Recent developments in polysaccharide-based materials used as adsorbents in wastewater treatment.* Progress in Polymer Science, 2005. **30**(1): p. 38-70.
13. Qiu, X. and S. Hu, *"Smart" Materials Based on Cellulose: A Review of the Preparations, Properties, and Applications.* Materials, 2013. **6**(3): p. 738.
14. Carlmark, A., E. Larsson, and E. Malmström, *Grafting of cellulose by ring-opening polymerisation – A review.* European Polymer Journal, 2012. **48**(10): p. 1646-1659.
15. O'Connell, D.W., C. Birkinshaw, and T.F. O'Dwyer, *Heavy metal adsorbents prepared from the modification of cellulose: A review.* Bioresource Technology, 2008. **99**(15): p. 6709-6724.
16. Saheb, D.N. and J. Jog, *Natural fiber polymer composites: a review.* Advances in polymer technology, 1999. **18**(4): p. 351-363.
17. Roy, D., et al., *Cellulose modification by polymer grafting: a review.* Chemical Society Reviews, 2009. **38**(7).
18. Tizzotti, M., et al., *Modification of Polysaccharides Through Controlled/Living Radical Polymerization Grafting—Towards the Generation of High Performance Hybrids.* Macromolecular Rapid Communications, 2010. **31**(20): p. 1751-1772.
19. Malmstrom, E. and A. Carlmark, *Controlled grafting of cellulose fibres - an outlook beyond paper and cardboard.* Polymer Chemistry, 2012.
20. Kang, H., R. Liu, and Y. Huang, *Graft modification of cellulose: Methods, properties and applications.* Polymer, 2015. **70**: p. A1-A16.
21. Hiltunen, M., et al., *Cellulose-g-PDMAam copolymers by controlled radical polymerization in homogeneous medium and their aqueous solution properties.* European Polymer Journal, 2012. **48**(1): p. 136-145.
22. Majoinen, J., et al., *Polyelectrolyte Brushes Grafted from Cellulose Nanocrystals Using Cu-Mediated Surface-Initiated Controlled Radical Polymerization.* Biomacromolecules, 2011. **12**(8): p. 2997-3006.
23. Sui, X., et al., *Synthesis of Cellulose-graft-Poly(N,N-dimethylamino-2-ethyl methacrylate) Copolymers via Homogeneous ATRP and Their Aggregates in Aqueous Media.* Biomacromolecules, 2008. **9**(10): p. 2615-2620.

24. Yan, L. and K. Ishihara, *Graft copolymerization of 2-methacryloyloxyethyl phosphorylcholine to cellulose in homogeneous media using atom transfer radical polymerization for providing new hemocompatible coating materials.* Journal of Polymer Science Part A: Polymer Chemistry, 2008. **46**(10): p. 3306-3313.
25. Chang, F., et al., *Modification of Cellulose by Using Atom Transfer Radical Polymerization and Ring-Opening Polymerization.* Polym. J, 2008. **40**(12): p. 1170-1179.
26. Hufendiek, A., et al., *Temperature Responsive Cellulose-graft-Copolymers via Cellulose Functionalization in an Ionic Liquid and RAFT Polymerization.* Biomacromolecules, 2014.
27. Lin, C., et al., *RAFT synthesis of cellulose-g-polymethylmethacrylate copolymer in an ionic liquid.* Journal of Applied Polymer Science, 2013. **127**(6): p. 4840-4849.
28. D. Klemm, B.P., T. Heinze, U. Heinze, W. Wagenknecht, *Comprehensive Cellulose Chemistry*. 1998: Wiley-VCH.
29. Nicolae, A., G.-L. Radu, and N. Belc, *Effect of sodium carboxymethyl cellulose on gluten-free dough rheology.* Journal of Food Engineering, 2016. **168**: p. 16-19.
30. Dan, J., et al., *Microcrystalline cellulose-carboxymethyl cellulose sodium as an effective dispersant for drug nanocrystals: A case study.* Carbohydrate Polymers, 2016. **136**: p. 499-506.
31. Naderi, A., et al., *Microfluidized carboxymethyl cellulose modified pulp: a nanofibrillated cellulose system with some attractive properties.* Cellulose, 2015. **22**(2): p. 1159-1173.
32. Milovanovic, S., et al., *Application of cellulose acetate for controlled release of thymol.* Carbohydrate Polymers, 2016. **147**: p. 344-353.
33. SHI, D., et al., *Convenient fabrication of carboxymethyl cellulose electrospun nanofibers functionalized with silver nanoparticles.* Cellulose, 2016. **23**(3): p. 1899-1909.
34. Yang, Z.-Y., et al., *The transparency and mechanical properties of cellulose acetate nanocomposites using cellulose nanowhiskers as fillers.* Cellulose, 2013. **20**(1): p. 159-168.
35. Liebert, T.F., T.J. Heinze, and K.J. Edgar, *Cellulose Solvents: For Analysis, Shaping and Chemical Modification*. ACS Symposium Series. Vol. 1033. 2010: American Chemical Society. 0.
36. Heinze, T., K. Schwikal, and S. Barthel, *Ionic Liquids as Reaction Medium in Cellulose Functionalization.* Macromolecular Bioscience, 2005. **5**(6): p. 520-525.
37. El Seoud, O.A., et al., *Applications of Ionic Liquids in Carbohydrate Chemistry: A Window of Opportunities.* Biomacromolecules, 2007. **8**(9): p. 2629-2647.
38. Heinze, T. and M. Nagel, *Study about the efficiency of esterification of cellulose under homogeneous condition: dependence on the chain length and solvent.* Lenziger Berichte, 2012. **90**: p. 85-92.
39. Heinze, T., Liebert, T, Koschella A *Esterification of Polysaccharides*. 2006: Springer Berlin Heidelberg.
40. Müllner, M., *Dissertation: Template-Directed Synthesis of One-Dimensional Hybrid Nanostructures from Cylindrical Polymer Brushes*. 2012.
41. Hebeish, A., M.I. Khalil, and M.H. El-Rafie, *Graft copolymerisation of vinyl monomers on modified cottons. VII. Grafting by chain transfer.* Die Angewandte Makromolekulare Chemie, 1974. **37**(1): p. 149-160.
42. Koenig, H.S. and C.W. Roberts, *Vinylbenzyl ethers of cellulose. Preparation and polymerization.* Journal of Applied Polymer Science, 1974. **18**(3): p. 651-666.
43. Hansson, S., et al., *Grafting Efficiency of Synthetic Polymers onto Biomaterials: A Comparative Study of Grafting-from versus Grafting-to.* Biomacromolecules, 2013. **14**(1): p. 64-74.
44. Samal, R.K., P.K. Sahoo, and H.S. Samantaray, *Graft copolymerization of cellulose, cellulose derivatives and lignocellulose*
Journal of Macromolecular Science, Part C: Polymer Reviews, 1986. **26**(1): p. 81-141.
45. Sarmad, G.G.a.S., *Polysaccharide Based Graft Copolymers*. 2013: Springer-Verlag Berlin.
46. Krzysztof Matyjaszewski, A.H.E.M., *Controlled and Living Polymerizations: From Mechanisms to Applications*. 2009: Wiley-VCH.
47. Kwak, Y. and K. Matyjaszewski, *ARGET ATRP of methyl methacrylate in the presence of nitrogen-based ligands as reducing agents.* Polymer International, 2009. **58**(3): p. 242-247.

48. Meng, T., et al., *Graft copolymers prepared by atom transfer radical polymerization (ATRP) from cellulose.* Polymer, 2009. **50**(2): p. 447-454.
49. Raus, V., et al., *Cellulose-based graft copolymers with controlled architecture prepared in a homogeneous phase.* Journal of Polymer Science Part A: Polymer Chemistry, 2011. **49**(20): p. 4353-4367.
50. Stenzel, M.H., T.P. Davis, and A.G. Fane, *Honeycomb structured porous films prepared from carbohydrate based polymers synthesized via the RAFT process.* Journal of Materials Chemistry, 2003. **13**(9): p. 2090-2097.
51. Zheng, Z., J. Ling, and A.H.E. Müller, *Revival of the R-Group Approach: A "CTA-shuttled" Grafting from Approach for Well-Defined Cylindrical Polymer Brushes via RAFT Polymerization.* Macromolecular Rapid Communications, 2014. **35**(2): p. 234-241.
52. Semsarilar, M., V. Ladmiral, and S. Perrier, *Synthesis of a cellulose supported chain transfer agent and its application to RAFT polymerization.* Journal of Polymer Science Part A: Polymer Chemistry, 2010. **48**(19): p. 4361-4365.
53. Mccormick, C.L. and D.K. Lichatowich, *Homogeneous Solution Reactions of Cellulose, Chitin, and Other Polysaccharides to Produce Controlled-Activity Pesticide Systems.* Journal of Polymer Science Part C-Polymer Letters, 1979. **17**(8): p. 479-484.
54. Rahn, K., et al., *Homogeneous synthesis of cellulose p-toluenesulfonates in N,N-dimethylacetamide/LiCl solvent system.* Die Angewandte Makromolekulare Chemie, 1996. **238**(1): p. 143-163.
55. Fenn, D., *Regioselektives Strukturdesign von Celluloseethern: Synthese, Chemie, Struktur-Eigenschafts-Beziehungen.* 2010.
56. Fox, S.C., et al., *Regioselective Esterification and Etherification of Cellulose: A Review.* Biomacromolecules, 2011. **12**(6): p. 1956-1972.
57. Iwata, T., et al., *Preparation and n.m.r. assignments of cellulose mixed esters regioselectively substituted by acetyl and propanoyl groups.* Carbohydrate Research, 1992. **224**(0): p. 277-283.
58. Koschella, A., T. Heinze, and D. Klemm, *First synthesis of 3-O-functionalized cellulose ethers via 2,6-di-O-protected silyl cellulose.* Macromolecular Bioscience, 2001. **1**(1): p. 49-54.
59. Chiefari, J., et al., *Living Free-Radical Polymerization by Reversible Addition−Fragmentation Chain Transfer: The RAFT Process.* Macromolecules, 1998. **31**(16): p. 5559-5562.
60. Keddie, D.J., *A guide to the synthesis of block copolymers using reversible-addition fragmentation chain transfer (RAFT) polymerization.* Chemical Society Reviews, 2014. **43**(2): p. 496-505.
61. Moad, G., E. Rizzardo, and S.H. Thang, *Living Radical Polymerization by the RAFT Process.* Australian Journal of Chemistry, 2005. **58**(6): p. 379-410.
62. Barner-Kowollik, C., et al., *Mechanism and kinetics of dithiobenzoate-mediated RAFT polymerization. I. The current situation.* Journal of Polymer Science Part A: Polymer Chemistry, 2006. **44**(20): p. 5809-5831.
63. Kwak, Y., A. Goto, and T. Fukuda, *Rate retardation in reversible addition-fragmentation chain transfer (RAFT) polymerization: Further evidence for cross-termination producing 3-arm star chain.* Macromolecules, 2004. **37**(4): p. 1219-1225.
64. Ting, S.R.S., T.P. Davis, and P.B. Zetterlund, *Retardation in RAFT Polymerization: Does Cross-Termination Occur with Short Radicals Only?* Macromolecules, 2011. **44**(11): p. 4187-4193.
65. Chernikova, E.V., et al., *The role of termination reactions of radical intermediates in reversible addition-fragmentation chain-transfer polymerization.* Polymer Science Series C, 2015. **57**(1): p. 94-109.
66. Ranieri, K., et al., *Direct Access to Dithiobenzoate RAFT Agent Fragmentation Rate Coefficients by ESR Spin-Trapping.* Macromolecular Rapid Communications, 2014. **35**(23): p. 2023-2028.
67. Sidoruk, A., M. Buback, and W. Meiser, *Kinetics of Dithiobenzoate-Mediated Methyl Methacrylate Polymerization.* Macromolecular Chemistry and Physics, 2013. **214**(15): p. 1738-1748.
68. Thomas, D.B., et al., *Hydrolytic Susceptibility of Dithioester Chain Transfer Agents and Implications in Aqueous RAFT Polymerizations†.* Macromolecules, 2004. **37**(5): p. 1735-1741.
69. Robert J. Young, P.A.L., *Introduction to Polymers, Third Edition*. 2011: CRC Press. 688.

70. Barner-Kowollik, C., et al., *Kinetic Investigations of Reversible Addition Fragmentation Chain Transfer Polymerizations: Cumyl Phenyldithioacetate Mediated Homopolymerizations of Styrene and Methyl Methacrylate.* Macromolecules, 2001. **34**(22): p. 7849-7857.
71. Ott, M.W., et al., *Cellulose-graft-polystyrene bottle-brush copolymers by homogeneous RAFT polymerization of soluble cellulose macro-CTAs and "CTA-shuttled" R-group approach.* Polymer. **98**(Special Issue: Polymer Brushes): p. 505-515.
72. Tatsuki Kitayama, K.H., *NMR Spectroscopy of Polymers* 2004: Springer-Verlag Berlin Heidelberg 228.
73. Coustet, M.E. and M.S. Cortizo, *Functionalization of styrenic polymer through acylation and grafting under microwave energy.* Polym J, 2011. **43**(3): p. 265-271.
74. Strube, O.I., et al., *New Functional Block Copolymers via RAFT Polymerization and Polymer-Analogous Reaction.* Macromolecular Chemistry and Physics, 2012. **213**(12): p. 1274-1284.
75. Lynne, *Simplification of the synthesis of the raft agent 2-(2-cyanopropyl)-dithiobenzoate.* Journal of the Serbian Chemical Society, 2010.
76. Hofle, G., W. Steglich, and H. Vorbruggen, *4-Dialkylaminopyridines as Acylation Catalysts .4. 4-Dialkylaminopyridines as Highly Active Acylation Catalysts.* Angewandte Chemie-International Edition in English, 1978. **17**(8): p. 569-570.
77. Barsbay, M., et al., *RAFT-mediated polymerization and grafting of sodium 4-styrenesulfonate from cellulose initiated via γ-radiation.* Polymer, 2009. **50**(4): p. 973-982.
78. Stenzel, M.H. and T.P. Davis, *Star polymer synthesis using trithiocarbonate functional β-cyclodextrin cores (reversible addition–fragmentation chain-transfer polymerization).* Journal of Polymer Science Part A: Polymer Chemistry, 2002. **40**(24): p. 4498-4512.
79. Liebert, T.F. and T. Heinze, *Tailored Cellulose Esters: Synthesis and Structure Determination.* Biomacromolecules, 2004. **6**(1): p. 333-340.
80. Hussain, M.A., T. Liebert, and T. Heinze, *Acylation of cellulose with N,N '-carbonvldiimidazole-activated acids in the novel solvent dimethyl sulfoxide/tetrabutylammonium fluoride.* Macromolecular Rapid Communications, 2004. **25**(9): p. 916-920.
81. Perrier, S., et al., *Versatile Chain Transfer Agents for Reversible Addition Fragmentation Chain Transfer (RAFT) Polymerization to Synthesize Functional Polymeric Architectures.* Macromolecules, 2004. **37**(8): p. 2709-2717.
82. Roy, D., J.T. Guthrie, and S. Perrier, *Graft polymerization: Grafting poly(styrene) from cellulose via reversible addition-fragmentation chain transfer (RAFT) polymerization.* Macromolecules, 2005. **38**(25): p. 10363-10372.
83. Skey, J. and R.K. O'Reilly, *Facile one pot synthesis of a range of reversible addition-fragmentation chain transfer (RAFT) agents.* Chemical Communications, 2008(35): p. 4183-4185.
84. Moad, G., et al., *Kinetics and Mechanism of RAFT Polymerization*, in *Advances in Controlled/Living Radical Polymerization*. 2003, American Chemical Society. p. 520-535.
85. Li, C., et al., *A versatile method to prepare RAFT agent anchored substrates and the preparation of PMMA grafted nanoparticles.* Macromolecules, 2006. **39**(9): p. 3175-3183.
86. Bernaerts, K.V. and F.E. Du Prez, *Dual/heterofunctional initiators for the combination of mechanistically distinct polymerization techniques.* Progress in Polymer Science, 2006. **31**(8): p. 671-722.
87. Zhang, W., et al., *SET-RAFT Polymerization of Progargyl Methacrylate and a One-Pot/One-Step Preparation of Side-chain Functionalized Polymers via Combination of SET-RAFT and Click Chemistry.* Macromolecular Rapid Communications, 2010. **31**(15): p. 1354-1358.
88. Perrier, S., P. Takolpuckdee, and C.A. Mars, *Reversible Addition−Fragmentation Chain Transfer Polymerization: End Group Modification for Functionalized Polymers and Chain Transfer Agent Recovery.* Macromolecules, 2005. **38**(6): p. 2033-2036.
89. Giorgi, M.E., R. Agusti, and R.M. de Lederkremer, *Carbohydrate PEGylation, an approach to improve pharmacological potency.* Beilstein Journal of Organic Chemistry, 2014. **10**: p. 1433-1444.
90. Casettari, L., et al., *PEGylated chitosan derivatives: Synthesis, characterizations and pharmaceutical applications.* Progress in Polymer Science, 2012. **37**(5): p. 659-685.

91. M., T.G.F., *Oxidation of Primary Alcohols to Carboxylic Acids- A Guide to Current Common Practice* Vol. 2. 2007: Springer Verlag.
92. Yue, Z. and J.M.G. Cowie, *Preparation and Chiroptical Properties of a Regioselectively Substituted Cellulose Ether with PEO Side Chains.* Macromolecules, 2002. **35**(17): p. 6572-6577.
93. Binder, K. and A. Milchev, *Polymer brushes on flat and curved surfaces: How computer simulations can help to test theories and to interpret experiments.* Journal of Polymer Science Part B: Polymer Physics, 2012. **50**(22): p. 1515-1555.
94. Nese, A., et al., *Synthesis of Amphiphilic Poly(N-vinylpyrrolidone)-b-poly(vinyl acetate) Molecular Bottlebrushes.* ACS Macro Letters, 2012. **1**(1): p. 227-231.
95. Kondo, T. and D.G. Gray, *The Preparation of O-Methyl-Celluloses and O-Ethyl-Celluloses Having Controlled Distribution of Substituents.* Carbohydrate Research, 1991. **220**: p. 173-183.
96. Clode, D.M. and D. Horton, *Synthesis of the 6-aldehydo derivative of cellulose, and a mass-spectrometric method for determining position and degree of substitution by carbonyl groups in oxidized polysaccharides.* Carbohydrate Research, 1971. **19**(3): p. 329-337.
97. Bar-Nir, B.B. and J.F. Kadla, *Synthesis and structural characterization of 3-O-ethylene glycol functionalized cellulose derivatives.* Carbohydrate Polymers, 2009. **76**(1): p. 60-67.
98. *personal communication.*
99. Klemm, D., et al., *New approaches to advanced polymers by selective cellulose functionalization.* Acta Polymerica, 1997. **48**(8): p. 277-297.
100. MacCoss, M. and D.J. Cameron, *Facile detritylation of nucleoside derivatives by using trifluoroacetic acid.* Carbohydrate Research, 1978. **60**(1): p. 206-209.
101. Nakagawa, A., et al., *Synthesis of Diblock Methylcellulose Derivatives with Regioselective Functionalization Patterns.* Journal of Polymer Science Part a-Polymer Chemistry, 2011. **49**(23): p. 4964-4976.

11. Zusammenfassung

Seit den ersten erfolgreichen Pfropfcopolymerisationsexperimenten unter Verwendung organolöslicher Cellulose Makro-Kettentransferagenzien (CTA) von Stenzel et al. [50] wurden verschiedene Lösungsansätze für die Herstellung von gut definierten Cellulosepfropfcopolymeren mittels reversibler Additions-Fragmentierungs-Kettentransfer (RAFT)-Polymerisationstechnik publiziert. Hierbei ist jedoch die eingeschränkte Löslichkeit der Cellulosederivate bei der homogenen Pfropfcopolymerisation nach wie vor eine Herausforderung. Die Einschränkungen der Löslichkeit vermindern die Anzahl an chemisch verfügbaren CTA Funktionalitäten an der Cellulose und sind daher ein wichtiger Grund dafür, dass zahlreiche Veröffentlichungen in diesem Bereich starke Abweichungen zwischen den experimentellen und den theoretischen Werten in Bezug auf die Menge an immobilisierten Polymerpfropfen schildern.

Daher ist die Zielsetzung der hier präsentierten Arbeit die Entwicklung eines Baukastens, mit dessen Hilfe die folgenden Aspekte bezüglich der gesteuerten Gestaltung von Cellulose Pfropfcopolymeren näher untersucht werden sollten:

- Ausgezeichnetes Lösungsverhalten in üblichen organischen Lösungsmitteln der Cellulosevorprodukte und der Pfropfcopolymere soll gewährleistet werden
- Hohe Pfropfverhältnisse, resultierend aus hoher Pfropfdichte und großen Polymerpfropfen, sollen erreicht werden
- Zur Verminderung von Abbruchreaktionen soll der „CTA-vermittelte R-Gruppen Ansatz“, welcher von Alex Müller et al. publiziert wurde [51], auf die Gestaltung von Cellulose Pfropfcopolymeren angepasst werden.
- Durch Optimierung der Reaktionsbedingungen bei der Durchführung von RAFT Polymerisationen soll ein hoher Grad an Steuerung bezüglich der molekularen Struktur der Copolymer erzielt werden.
- Geeignete analytischer Methoden sollen zur Untersuchung von Pfropfcopolymeren und der Polymerisationskinetik von Cellulose Makro-CTA und freiem CTA angewandt werden.

Als erste Schritte wurden verschiedene Synthesestrategien bei der Entwicklung organolöslicher Cellulose Makro-CTAs verfolgt. Auf Grund von Schwierigkeiten bezüglich des Löslichkeitsverhaltens der Polymere wurden eigene Synthesevorschriften entwickelt beziehungsweise bestehende Synthesevorschriften entscheidend verändert. Letztendlich konnte gezeigt werden, dass der verwendete, Carbonsäure-funktionalisierte CTA 4-cyano-4-(phenylcarbonothioylthio)pentansäure (CPPA) mit dem Aktivierungsagenz *N,N*‘-Carbonyldiimidazol (CDI) an Cellulose angebunden werden kann. Ferner wurden verbleibende OH-Funktionalitäten mittels Propionsäureanhydrid verestert, was eine gute Löslichkeit der Cellulose Makro-CTAs in organischen Lösungsmitteln gewährleisten sollte. Die auf diese Weise hergestellten Cellulose Makro-CTAs zeigten sich gut Löslich in DCM, $CHCl_3$, THF,

Toluol, DMF oder Styrol. Dies ermöglicht die Untersuchung einer Vielzahl an verschiedenen Polymerisationsreaktionen.

Erste Pfropfcopolymerisationsexperimente wurden mit dem Monomer *N,N*-Dimethylacrylamid (DMAA) durchgeführt. Einfache Auftrennung von Pfropfcopolymer und Homopolymer PDMAA wurde durch das unterschiedliche Löslichkeitsverhalten in Wasser ermöglicht, da das Homopolymer im Gegensatz zum Pfropfcopolymer sehr gut wasserlöslich ist. Darauf folgende Analysen vom Pfropfcopolymer mittels ^{1}H-NMR zeigten jedoch nur geringe Mengen an Polymerpfropfen. Nach einer Reihe an Referenzexperimenten konnte schließlich der Ursprung des Problems gefunden werden: Es konnte gezeigt werden, dass Nebenreaktionen vom CPPA mit den Aktivierungsagenz CDI zu einer zumindest teilweisen Umsetzung vom CTA in eine unreaktive Spezies führte, welches dann den Erfolg der RAFT Polymerisation einschränkte.
Daher musste die Synthesestrategie für die Verknüpfung von CTA an die Cellulose verändert werden: Anstelle der Anbindung eines CTAs mittels Veresterung wurden nachfolgend CTA-Gruppen auf der Cellulose in einer mehrstufigen Umsetzung aufgebaut, indem die 2-Bromoisobuttersäure-Gruppen an der modifizierten Cellulose mit Trithiocarboxylaten mittels S_N-Reaktionen in die entsprechenden Trithiocarbonate überführt wurden. Erste Versuche zeigten ausgezeichnete Ergebnisse bezüglich der Steuerung des Pfropfcopolymerisations-prozesses. Allerdings zeigte diese Methode Einschränkungen in der Menge an anzubindendem CTA, welcher nicht über einen Substitutionsgrad (DS) von 0.15 hinaus kam. Es wurde angenommen, dass der sterische Anspruch des tertiären Kohlenstoffatoms an den 2-Bromoisobutro-Gruppen hierfür verantwortlich war und daher reduziert werden sollte. In darauf folgenden Experimenten mittels 2-Bromopropionyl-modifizierter Cellulose konnte der DS(CTA) durch Anpassung der Reaktionsbedingungen auf bis zu 0,6 erhöht werden. Allerdings wurden beim Versuch, höhere DS(CTA) Werte zu erreichen unlösliche Cellulosederivate erhalten.
Darauf folgende Pfropfcopolymerisationsversuche mit Styrol Monomer, Cellulose Makro-CTA und freiem CTA („CTA-vermittelter R-Gruppen Ansatz“) zeigten ausgezeichnete Steuerbarkeit des Prozesses. Hierbei sei darauf hingewiesen, dass Polymerisationen ohne Zugabe an freiem CTA in ungenügender Steuerbarkeit und Gelbildung resultierten.
Mittels Isolation und Hydrolyse der Cellulose-Pfropfcopolymere wurde die Kinetik des Polymerpfropfenwachstums mit der Polymerisationskinetik von freiem, linearem Polymer analysiert und verglichen. Hierbei zeigten sich große Ähnlichkeiten in Bezug auf die Molmasse der Polymerpfropfen und der linearen Homopolymere, was eine ähnliche Reaktionskinetik vermuten lässt. Aus diesem Grund konnte in darauf folgenden Experimenten die Molmassen der Polymerpfropfen anhand der Molmassen des linearen Homopolymers bestimmt werden, ohne dafür jeweils das Pfropfcopolymer isolieren und hydrolysieren zu müssen. Die Homopolymere zeigten in einer Vielzahl an Versuchen eine lineare Abhängigkeit der Molmassen mit dem Monomerumsatz, was eine gute

Steuerbarkeit der Polymerisationsreaktion nahelegt und eine Einstellung der Molmasse mit dem Monomerumsatz ermöglicht. Darauf folgende Analysen mittels GPC und Gravimetrie zeigten eine Abhängigkeit der Initiierungseffizienz und des Pfropfverhältnisses von den gewählten Reaktionsbedingungen. Beispielsweise sorgten hohe [CTA]/[AIBN] Verhältnisse für eine ausgezeichnete Steuerbarkeit der Reaktion und hohe Werte der Initiierungseffizienz von bis zu 90 %, wenn nicht sehr hohe Molmassen erreicht werden sollen. Selbstverständlich könnten auch höhere Molmassen erzielt werden, wobei in diesem Fall eine Verminderung der Initiierungseffizient aufgrund von vermehrten Abbruchreaktionen unvermeidbar ist. Letztendlich wurde aus den genannten Ergebnissen geschlussfolgert, dass die Entwicklung des „Werkzeugkastens“ im Rahmen dieser Arbeit die künftige Möglichkeit bietet, eine Vielzahl an gut definierten, maßgeschneiderten Pfropfcopolymeren auf Basis von Cellulose herstellen zu können. Daher könnten sich zukünftigen Untersuchungen beispielsweise auf die Entwicklung von funktionellen Pfropfcopolymeren konzentrieren, indem das Cellulose Makro-CTA-System angepasst wird auf die Pfropfcopolymerisation von „intelligenten“ Polymeren, welche auf äußere Reize mit strukturellen Änderungen reagieren. Des Weiteren wird im Rahmen zukünftiger Projekte die Untersuchung der Struktur-Eigenschaftsbeziehung derartiger „Bürstenpolymer“-Strukturen im Mittelpunkt stehen.

Das darauf folgende Ziel war die Weiterentwicklung von Cellulose Pfropfcopolymeren in Richtung Polymerarchitekturen höherer Komplexität. Dafür wurde die RAFT Polymerisationstechnik mit ATRP in zwei aufeinanderfolgenden Schritten unter Verwendung des gleichen Ausgangsmaterials miteinander kombiniert. Die Entscheidung fiel gezielt auf die ATRP-Technik im zweiten Schritt, da die Cellulose Makro-CTAs aufgrund des Syntheseprozesses über Bromofunktionalitäten verfügen und daher ohne weitere Modifikation direkt für die ATRP Reaktion verwendet werden können. Die Synthese erfolgte schrittweise, beginnend mit der Pfropfcopolymerisation von Styrol mit Cellulose Makro-CTA, gefolgt von der Abspaltung der CTA-Funktionalitäten an den Enden der Polymerpfropfen. Die Analyse mit ^{1}H-NMR und GPC zeigte eindeutig die erfolgreiche Anbringung der Polystyrolpfropfen an die Cellulose. Im Folgeschritt wurden PMMA-Pfropfen mittels ATRP-Technik auf die Cellulose angebracht. Mittels ^{1}H-NMR und GPC wurde die chemische und strukturelle Identität der Polymere untersucht. Hierbei belegten die ^{1}H-NMR-Daten eindeutig die erfolgte Polymerisation von MMA mittels ATRP Reaktion an die Bromofunktionalitäten des Cellulose Pfropfcopolymers. Anhand der relativen Integralintensitäten von Polystyrol und PMMA wurde das totale Pfropfverhältnis von Polymer zu Cellulose Makro-CTA von rund 3.500 % bestimmt, was bedeutet, dass das gemischte Pfropfcopolymere zu rund 97% aus Polymerpfropfen und nur zu 3 % aus Cellulose besteht. Es wird darauf hingewiesen, dass dieser Wert um ein Vielfaches höher ist als sämtliche publizierten Werte auf dem Gebiet der cellulose-basierten Pfropfcopolymere, wie eine Literaturrecherche mittels „Web of Science“ darlegen konnte. Allerdings zeigte die Analyse des Polymers mit GPC eine Zunahme des Elutionsvolumens, was mit einer Abnahme des apparenten hydrodynamischen Radius und damit der Molmasse einhergeht. Dieses Resultat stand

in Kontrast zu den ^{1}H-NMR Daten, die die erfolgreiche Pfropfcopolymerisation belegen. Eine Theorie, welche beide Befunde in Einklang bringt, wäre, dass nach der Anbringung weiterer Polymerpfropfen mittel ATRP die Polymerpfropfen zusammenfallen, was zu einer Abnahme des apparenten hydrodynamischen Radius bei gleichzeitiger Zunahme der Molmasse zur Folge hätte. Diese Hypothese wird im Rahmen zukünftiger Arbeiten mittels Streuungstechniken untersucht.

Der dritte Teil dieser Arbeit beschäftigte sich mit der Synthese von cellulosebasierten, gemischten Pfropfcopolymeren durch die Kombination eines „grafting-to“ mit einem „grafting-from“ Ansatz. Hierfür sollten Cellulose Pfropfcopolymere hergestellt werden, welche bereits an einem Teil der OH-Gruppen Polyethylenglykol-Ketten aufwiesen und an dem anderen Teil ein synthetisches Polymer wie PS oder PMMA. Um erhebliche Depolymerisationsprozesse zu unterbinden, welche in vorhergehenden Untersuchungen beobachtet werden konnten, wurden für darauf folgende Synthesen ausschließlich milde Reaktionsbedingungen gewählt. Dies wäre beispielsweise bei Veresterungsreaktionen mit Hilfe von *N,N*-Carbonyldiimidazol gewährleistet. Diese Syntheseroute unter Verwendung von 2-Bromopropionsäure kann jedoch nicht regioselektiv durchgeführt werden, da die Schutzgruppenchemie mittels Tritylgruppen einen Entschützungsschritt unter stark sauren Bedingung erfordert, welche inkompatibel mit den Esterfunktionalitäten sind. Schließlich gelang die Synthese von PEGlyiertem Cellulose Makro-CTA, wobei entlang der Syntheseroute die Intermediate stets mittels ^{1}H-NMR und GPC analysiert wurden. Daraufhin wurde das Konzept der Mischpfropfen-Synthese mittels RAFT-Technik weiter verfolgt. Nach einer Polymerisation konnte eine erfolgreiche Pfropfanbindung mittels GPC gezeigt werden, wobei sich jedoch Agglomerierung der Mischpfropfcopolymere und niedrige Pfropfverhältnisse als Schwierigkeiten herausstellten. Diese sollten mittels ATRP-Technik umgangen werden. In der darauffolgenden Synthese konnten wir qualitativ die Kompatibilität der verwendeten PEGylierten Cellulose Makro-Initiatoren mit der ATRP-Reaktion mit MMA ohne Zugabe an freiem Initiator nachweisen. Diese Ergebnisse wurden als erster erfolgreicher Ansatz zum Beweis des Synthesekonzeptes gedeutet. Nach Recherche und unter Beachtung verschiedener Übersichtsartikel und relevanter Publikationen in dem Bereich der cellulose-basierten Pfropfcopolymeren mittels kontrollierter radikalischer Polymerisation wurde geschlussfolgert, dass über die Synthese eines derart komplexen Materials zum ersten Mal berichtet wird. Daher könnten diese Materialen als ideale Kandidaten in zukünftigen Untersuchungen für das grundlegende Verständnis von physikalischen und chemischen Eigenschaften dienen.

Bezüglich der RAFT Polymerisation von Cellulose Makro-CTAs in homogenen Reaktionen und Mischpfropfpolymeren können zukünftig Untersuchungen der Morphologie und von Struktur-Eigenschafts-Beziehungen von maßgeschneiderten Cellulosepfropfcopolymeren durchgeführt werden. Insbesondere folgende analytische Methoden werden hierfür zukünftig in Betracht gezogen:

- Rasterkraftmikroskopie: Untersuchung von einzelnen Pfropfcopolymeren, ob diese eine wurmartige Struktur aufweisen. Dieses Phänomen konnte bereits bei vollsynthetischen Polymeren nachgewiesen werden [63], jedoch nicht für cellulose-basierte Systeme.

- DSC Analyse: Abhängigkeit der thermischen Eigenschaften von Pfropfgröße oder Pfropfdichte

- DLS Analyse: Ergründen der „gequollenen“ Struktur in Lösung

Die vorgelegte Arbeit bietet verschiedene künftige Möglichkeiten um derartige komplexe Polymerarchitekturen zu gestalten und um interessante grundlegende Fragestellungen zu verfolgen.

Marcus W. Ott
Margaretenstraße 21
63225 Langen

07.11.2016

Erklärung

Ich erkläre hiermit, dass ich meine Dissertation selbstständig und nur mit den angegebenen Hilfsmitteln angefertigt habe.

_____

Marcus W. Ott

Marcus W. Ott
Margaretenstraße 21
63225 Langen

07.11.2016

Erklärung

Ich erkläre hiermit, noch keinen Promotionsversuch unternommen zu haben.

_____

Marcus W. Ott

Lebenslauf

Dipl.-Ing. Ott, Marcus Werner
Margaretenstraße 21
63225 Langen

Geburtsdatum: 29.07.1984

Geburtsort: Langen, Hessen

Bildungsweg

08/1995 – 06/2004	Dreieichschule Langen, Gymnasium
10/2004 – 03/2012	Studium an der TU Darmstadt Studiengang Diplom Chemie
09/2011 – 03/2012	Diplomarbeit im AK von Prof. Markus Biesalski zum Thema *„Polymerisationen auf Filterpapieren mit Hilfe von Cellulosefaser-immobilisierten Monomeren und grafting-through-Verfahren“*
04/2012 - 09/2012	wissenschaftlicher Mitarbeiter im AK von Prof. Markus Biesalski
10/2012 – 12/2016	Promotion am Ernst-Berl-Institut für Technische und Makromolekulare Chemie der Technischen Universität Darmstadt in der Arbeitsgruppe von Prof. Dr. Markus Biesalski.